Loughborough University
Institutional Repository

Experimental and mumerical analysis of deformation of low-density thermally bonded nonwovens

This item was submitted to Loughborough University's Institutional Repository by the/an author.

Additional Information:

- A Doctoral Thesis. Submitted in partial fulfillment of the requirements for the award of Doctor of Philosophy of Loughborough University.

Metadata Record: https://dspace.lboro.ac.uk/2134/6175

Publisher: © Xiaonan Hou

Please cite the published version.

EXPERIMENTAL AND NUMERCIAL ANALYSIS OF DEFORMATION OF LOW-DENSITY THERMALLY BONDED NONWOVENS

By

Xiaonan Hou

A DOCTORAL THESIS SUBMITTED IN PARTICAL FULFILMENT OF THE REQUIREMENTS FOR THE AWARD OF DOCTOR OF PHILOSOPHY OF LOUGHBOROUGH UNIVERSITY

Jan 2010

Abstract

Nonwoven materials are engineered fabrics, produced by bonding constituent fibres together by mechanical, thermal or chemical means. Such a technology has a great potential to produce material for specific purposes. It is therefore crucial to develop right products with requested properties. This requires a good understanding of the macro and micro behaviours of nonwoven products. In last 40 years, many efforts have been made by researchers to understand the performance of nonwoven materials. One of the main research challenges on the way to this understanding is to link the properties of fibres and the fabric's random fibrous microstructure to the mechanisms of overall material's deformation. The purpose of this research is to study experimentally and numerically the deformation mechanisms of a low-density thermally bonded nonwoven fabric (fibre: Polypropylene; density: 20 gsm).

The study started with tensile experiments for the nonwoven material. Specimens with varying dimensions and shapes were tested to investigate the size-dependent deformation mechanisms of the material. Based on obtained results, representative dimensions for the material are determined and used in other experimental and numerical studies. Then standard tensile tests were performed coupled with image analysis. Analysis of the obtained results, allowed the tensile behaviour of the nonwoven material to be determined, the initial study of the effects of material's nonuniform microstructure was also implemented.

Based on the experimental results obtained from tensile tests, continuous finite-element models were developed to simulate the material properties of the nonwoven material for its two principle directions: machine direction (MD) and cross direction (CD). Due to the continuous nature of the models, they were only used to establish the mechanical behaviour of the material by treating it as a two-component composite. The effects of bond points, which are a stiffer component within the material, were analysed.

I

Due to the limitations of the continuous FE models, experimental studies were performed focused on the material's microstructure. The latter was detected using an x-ray Micro CT system and an ARAMIS optical strain analysis system. According to the obtained images, the nonwoven fabric is a three-component material. The effects of material's microstructure on stress/strain distributions in the deformed material were studied using advanced image analysis techniques. Based on the experimental results, a new stress calculation method was suggested to substitute the traditional approach, which is not suitable for the analysis of the low density nonwoven material. Then, the fibres' orientation distribution and material properties of single fibres were measured due to their significant effects on overall mechanical properties.

Finally, discontinuous finite-element models were developed accounting for on the material's three-component structure. The models emphasised the effects of the nonuniform and discontinuous microstructure of the material. Mechanical properties of fibres, the density of fibrous network, the fibres' orientation distribution and the arrangement of bond points were used as input parameters for the models, representing features of the material's microstructure. With the use of the developed discontinuous models, the effects of material's microstructure on deformation mechanisms of the low-density nonwoven material were analysed.

Keywords: Nonwovens; Low Density; Anisotropic Behaviour; Nonuniformity; Random Microstructure; Deformation Mechanism; Finite Element Analysis

Acknowledgements

First, I am deeply indebted to Loughborough University, UK, for offering me the great opportunity to have my first step in academy.

I wish to express my sincerest appreciations to my supervisors Prof. Vadim. V. Silberschmidt and Prof. Memis Acar for their help, guidance, encouragement and, particularly, patience during my PhD studies.

I also would like to thank the most skilled technician, Mr. Andy Sandaver, for his suggestions for, and help with, for experimental studies.

I also grateful to be one of the members of the Mechanics of Advanced Materials Reaearch Group; its activities extended my knowledge and inspired my research.

The research was strongly supported by the Nonwoven Cooperative Research Centre (NCRC) of North Carolina State University, USA, and I am grateful for the specimens and knowledge generously shared. Especially, I would like to thank Prof. Behnam Pourdeyhimi, for his kindest assistance during IAB meeting.

Finally, thanks must go to my parents for their unlimited support, love and sacrifice. I owe them too much.

Table of Contents

Table of Figures

List of Tables

Chapter 1 Introduction

Nonwoven materials are engineered fabrics, which are produced by bonding the constituent fibres together by mechanical, thermal or chemical means. Because of the low energy cost, high productivity and environmentally friendly processes, the market of the nonwoven products continue to grow rapidly, and they are widely used in various aspects of social life, from personal care products to automotive parts. According to the figures released by European Disposables and Nonwovens Association (EDANA), the global nonwoven productions reached 5.1 million tonnes in 2006, which is an increase of 23.1% from 2003. One of the main market segments of this industry is the low-density nonwoven materials, which are usually used in hygiene and medical applications, and account for 36 % in terms of volume. However, with the development of manufacturing technology for nonwoven, the consumer industry continues demanding better mechanical properties. On the another hand, as a kind of artificial material, nonwovens still have a great potential to be improved for more specific purposes. It is therefore crucial to understand the effect of material's microstructure on the overall properties of nonwovens; it could help the industry to improve their mechanical properties by optimising respective manufacturing processes. Moreover, the manufacturing industry also tries to study the material using expensive, time-consuming trial-and-error methods. Hence, it is necessary to develop theoretical and computational tools for the nonwoven materials both to have opportunity to study them and to optimize the manufacturing processes.

Besides requests by industry, the unique material properties make the nonwoven fabrics an interesting and challenging material to study. Actually, within the last 50 years, many efforts have been made to study the material properties of fibrous structures by investigating various materials, e.g., paper, textiles, nonwovens and composites. According to those studies, nonwoven fabrics can be described as anisotropic, nonhomogeneous, discontinuous and highly non-linear materials (Petterson, D.R. and Backer, S. 1963, Hearle, J.W.S. and Stevenson, P.J. 1963, Russell 2007).

1

The anisotropic material properties of the nonwovens are linked to the character of random fibre orientations, especially along two principle directions of the material: machine direction (MD) and cross direction (CD). Significant differences in the material properties and the deformation mechanism are demonstrated by tensile tests for these two directions (Figure 1.1). All these characteristics of nonwoven fabrics make their mechanical behaviour, in particular their tensile behaviour, very complicated. It is affected by tension, shear, compression and damage coupling modes. Although it is well known that the mechanical properties of nonwovens are anisotropic, the deformation mechanisms of the nonwoven fabrics in different directions and the effects of material's microstructure are still not understood sufficiently.
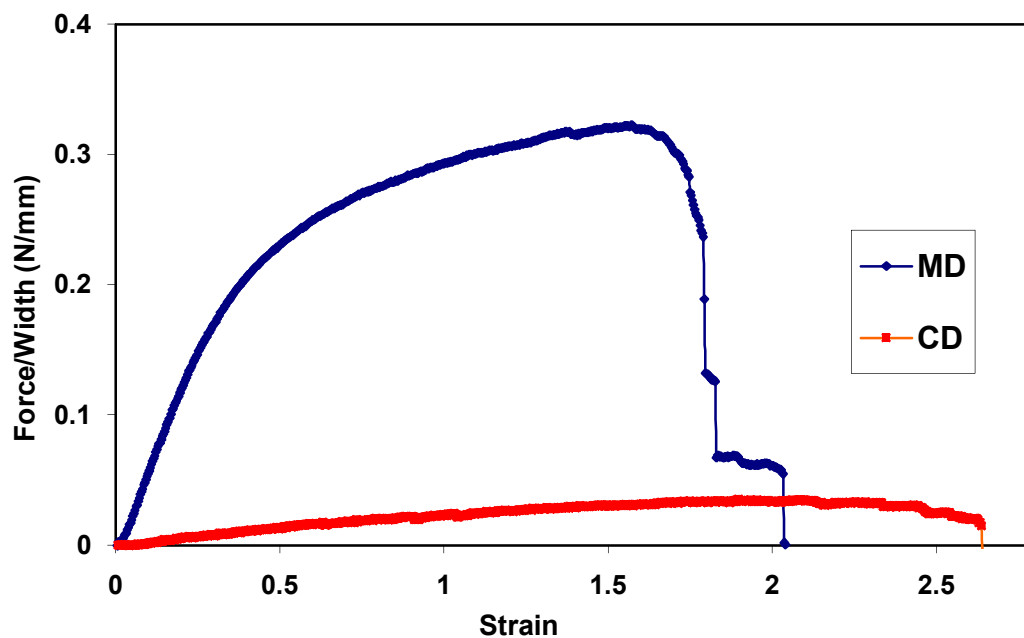
Figure 1.1: Different tensile behaviours of thermally bonded nonwoven fabric in MD and CD

Nonwoven materials are basically formed by randomly arranged fibres. Due to the manufacturing process, the microstructure of the material is discontinuous and nonuniform as shown in Figure 1.2. This unique microstructure causes nonuniform distributions of stresses and strains in the deformed material and affects its deformation mechanisms. Besides, when the nonwoven fabrics achieve large strain levels in extension, their cross-sectional area and volume change significantly due to the effect of lateral contraction. It makes the analysis of the deformation and fracture

mechanisms of the nonwoven material even more complicated. Moreover, the non-linear material behaviour of nonwoven material is another challenging problem. Due to the complex microstructure of the material, the non-linearity of nonwoven material could be caused by both the material non-linearity of fibres and the geometry non-linearity of the discontinuous and nonuniform microstructure.

1 mm
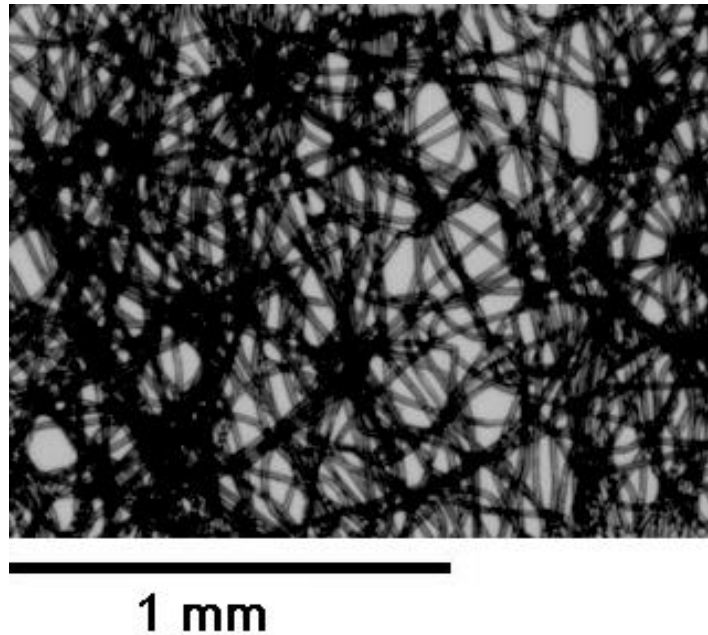
Figure 1.2: Discontinuous microstructure of low-density nonwoven material

Since the microstructure of the nonwoven material affects its performance significantly, there is an obvious need to investigate the material's microstructure, in order to develop a theory of deformation for nonwoven materials.

The mechanical properties of nonwoven materials are determined by their microstructure, fibre properties and bonding features. From Backer and Pettersion's pioneering work (Backer, S. and Petterson, D. R. 1960), researchers have used considerable efforts to develop a theory to describe the unique material. Basically, there are two most popular theories at present, and most of the researches are based on them. One is the orthotropic theory, which is used to predict directly the properties of a thermally bonded nonwoven at the macroscopic level (Kim 2004a). Some researchers also use a classic orthotropic theory to model spun-bonded nonwovens (Bais-Singh, S., Biggers, S.B.JR. and Goswami, B.C. 1998, Bais-Singh, S. and Goswami, B.C. 1998). The theory treats nonwoven materials as a layer system, using

3

the laminate composite theory and assumes a unique orientation for every layer of fibres. Another theoretical description of the material is based mainly on a "cell theory": the nonwoven fabric is divided into cells and each cell has the features of fabrics' microstructure (Kim, H.S. and Pourdeyhimi, B. 2000, Kim 2004b, Limem, S. and Warner, S.B. 2005, Mueller, D.H. and Kochmann, M. 2004, Liao, Adanur 1997). However, these methods only reveal part of the real deformation mechanisms of thermally bonded nonwoven material due to the use of periodic boundary conditions, which cannot describe the nonuniformity of the nonwoven fabrics adequately. Therefore, to explore the deformation mechanism of nonwoven materials, the research should be carried out at both micro-scale and macro-scale of the material and investigate the effect of real features of the material's discontinuous and nonuniform microstructure. Moreover, due to complex microstructure of the material, which is hard to investigate experimentally, the material should be studied both experimentally and numerically.

1.1 Motive and objectives of research

In last decades, although a significant progress has been achieved in describing the mechanical behaviour of nonwovens, there are still some unresolved problems in this area. Both industry and academy are interested in better understanding of the effects of its discontinuous and nonuniform microstructure. An appropriate model could allow the industry to improve their products by optimising the microstructure of the material. Moreover, novel research methods and theory will benefit academic studies, focusing on new engineered materials with complicated microstructures. Therefore, the overall aim of this project is to investigate a low-density thermally bonded nonwoven fabric experimentally and numerically in order to develop a good theoretical description of the deformation mechanism of the material. To achieve the aim of the project, its major objectives are formulated in the following way:

1. To investigate the tensile behaviour of the low-density thermally bonded nonwoven material at macro-scale. To establish the effects of dimensions and shape of specimens on the mechanical properties of the nonwoven material.

2. To investigate the features of microstructure of the low-density thermally bonded nonwoven material. To determine the effects of the material's microstructure on its mechanical properties.

3. To develop continuous FE models to describe the mechanical behaviour of the nonwoven material by introducing is macroscopic features.

4. To develop discontinuous FE models by taking account for the features of the microstructure of the nonwoven material to simulate its mechanical properties.

5. To summarise deformation mechanism of the low-density thermally bonded nonwoven material according to the results of experimental and numerical studies.

1.2 Methodology of research

The research proposes to explore the mechanical properties of the low-density thermally bonded nonwoven material by analysing the effects of the material's discontinuous and nonuniform microstructure. The research consists of two main parts: experimental studies and computational modelling. A flowchart in Figure 1.3 summarises the methodology.

At macro-scale, the experiments will be carried out to investigate the tensile behaviour of the nonwoven material. Specimens with different dimensions will be used to explore the shape- and size-dependent tensile behaviour of the material. The deformation process in the experiments will be studied with a high-speed camera and thermal analysis system, which could provide information on a non-uniformed tensile behaviour of the material.

Then, continuous FE models will be developed based on the macro-scale experimental studies. The models will treat the material as a two-phase (fibrous network and bonded areas) composite material and the classic theory for composites will be used to describe the material behaviour. The results will be used to assess the

capability of the theory to describe the low-density nonwoven material, which have been successfully used to simulate nonwoven material with a higher density. And the simulation results will also be used to analyse the effect of bonded areas, which are stiffer than the fibrous network, on the overall material properties.

Besides the researches at macro-scale, the features of the microstructure of the nonwoven material will be investigated. Optical and electron microscopy will be used to capture the material's microstructure for both undeformed and deformed specimens. The obtained images will be analysed using the image analysis software and program. The orientation distribution function (ODF) of the nonwoven material will be determined. The effects of the discontinuous and nonuniform microstructure on deformation mechanisms of the material will be estimated.

Based on the understanding of the effects of the material's microstructure and the results of continuous models, discontinuous FE models will be developed to simulate the tensile behaviour of the nonwoven material by introducing the features of the discontinuous and nonuniform microstructure of the material into them. Due to the complex microstructure of the material, the geometric part will be generated according to orientation distribution of fibres using a special program. And the discontinuous FE models will be built up by editing the input files directly. Using those, effects of the fibres' orientation distribution and arrangement of bond points will be explored.

Finally, the characteristic deformation mechanism of the low-density thermally bonded nonwoven material will be summarised according to the results of experimental studies and numerical simulations.
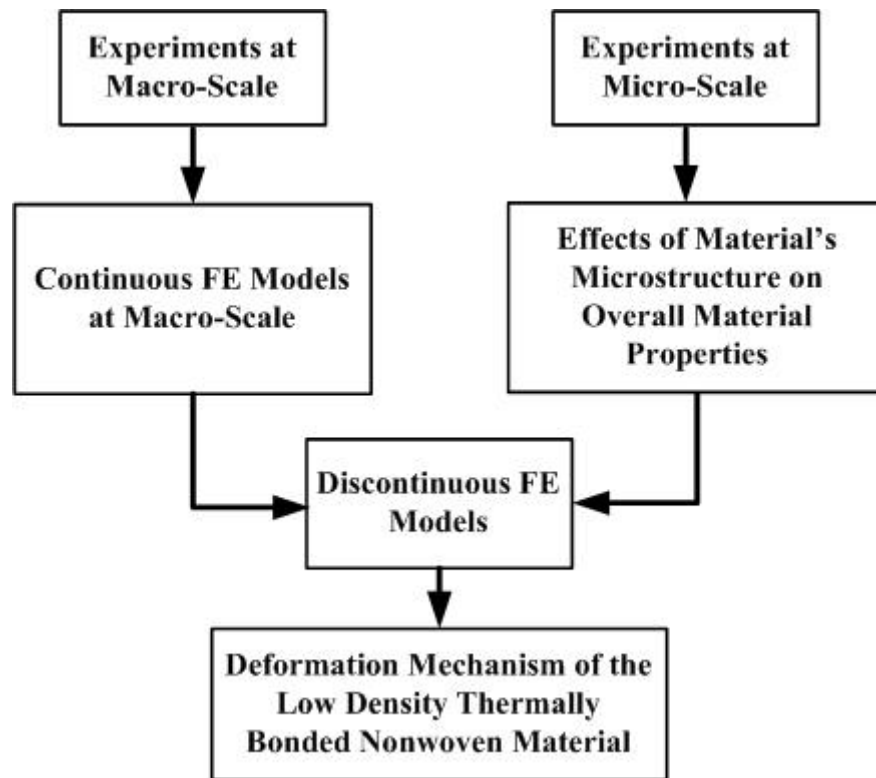
Figure 1.3: Flow chart of overall methodology

1.3 Outline of thesis

The thesis contains eight chapters; the outline of the chapters is as follows:

- Chapter 1 provides a general background of the study of nonwoven materials from the view point both of industry and academy. The motive, objectives and methodology of the research are presented.

- Chapters 2 comprise the introduction of nonwoven materials and the review of previous studies related to this research. First, it focuses on the review of definition of nonwoven materials and the existing theories about their mechanical properties. Then, numerical models are demonstrated, which are used to describe the material behaviours of the nonwovens. The advantages and limitations of the existing models are discussed.

- Chapter 3 presents the experimental studies, focused on the mechanical properties of the low-density nonwoven material. Size-dependent mechanical properties of the nonwoven material are discussed.

- Chapter 4 reports the development of continuous FE models, which account for the feature of the nonwoven material at macro-scale.

- Chapter 5 presents the investigation of the microstructure of the low-density nonwoven material. Various image analysis methods are presented, and the effects of the material's microstructure on the overall mechanical properties are estimated.

- Chapter 6 deals with development of discontinuous FE models. The models are developed by introducing the features of the material's microstructure. Based on the models, the effects of material properties of fibres, the orientation distribution of fibres and arrangement of bond points on the overall mechanical properties are discussed.

- Chapter 7 summarises the major findings of the research. The deformation mechanisms of the low-density thermally bonded nonwoven material are analysed by taking account for the effects of material's microstructure. The future works is suggested based on results of the present research.

Chapter 2 Nonwoven Material

2.1 Introduction of nonwoven material

Nonwoven fabrics are engineered fabrics, which are widely used in various aspects of human life. In last 50 years, the nonwoven industry developed really fast by implementing new technical innovations. Nonwoven fabrics start to become a broad concept. Therefore, the definition of nonwoven fabrics has long been a cause for argument and discussion. According to the definition of British Standard, "a nonwoven is a manufactured sheet, web or batt of directionally or randomly orientated fibres, bonded by friction and/or cohesion and/or adhesion, excluding paper and products which are woven, knitted, tufted, stitch-bonded incorporating binding yarns or filaments, or felted by wet-milling, whether or not additionally needled. And the fibres may be of natural or man-made origin. They may be staple or continuous filaments or be formed *in situ*" (British Standards, 1992)

2.1.1 Manufacturing process

The manufacturing process of nonwoven fabrics is a complex mechanical and chemical process. The basic raw materials for nonwovens are polymers, and their material properties change with respect to different process conditions such as webbing mechanisms, bonding techniques, manufacturing rates and temperatures. Therefore, various manufacturing processes affect the material properties of nonwoven fabrics in different ways.

Although there are many techniques, which are used for manufacturing nonwoven fabrics, there are four principle steps in the nonwovens manufacturing technologies (Batra, S.K. and Davis, H. 1999).

1 Preparation: this step involves preparing the raw material for the next stage of the production.

9

2 Web formations: this step refers to the process or methodology that converts staple fibres or filaments into a two-dimensional or three-dimensional web assembly (batt), which is the precursor for the final fabric. Its structure and compositions strongly influences the dimensions, structure and properties of the final fabric (Russell 2007). During this process, the arrangement of fibres, specifically the fibre orientation, is resolved. Therefore, the uniformity and anisotropy of eventual nonwoven fabric is determined solely during this process (Purdy 1983, Russell 2007). Other critical fabric parameters influenced at this stage are the unfinished product weight and manufactured width.

The universal processes of web formation are the carding technology and the airlay technology. The carding technology produces parallel-laid webs, or, in conjunction with cross-lappers, cross-laid webs. And the airlay technology transports fibres by means of air and reputedly provides a more randomized fibre arrangement in the resulting web.

3 Bonding: this step is the one to give final integrity to the web. There are three main methods to bond a fibre web: mechanical bonding, adhesive bonding and thermal bonding. The degree of bonding is a primary factor in determining fabric's mechanical properties (particularly strength), porosity, flexibility, softness, and density (loft, thickness)(Russell 2007). And there are various techniques used by the industry, which are presented in Table 2.1.

Mechanical Bonding	Adhesive Bonding	Thermal Bonding
Felting Needlepunching Hydroentanglement Stith bonding	Spray Saturation Print Collapsible foam	Calendar Through-air Impingement IR radiation Ultrasonic

Table 2.1: Bonding techniques (Batra 1998)

4 Finishing: this step follows bonding. If the bonded web is not in its final form corresponding to the end product, it may require additional processing steps to give it the desired aesthetics or appearance, physical and mechanical properties and

additional functional properties. For example, the nonwoven can be made conductive, flame retardant, water repellent, antistatic, breathable, coated, printed on and so on. There are mechanical and chemical finishing methods for achieving different end products (Albrecht, Fuchs et al. 2003).

The definition of nonwoven material is generalized, because there are many types of products and they share characteristics not only with textiles but also with paper and plastic products. Therefore, it is reasonable to classify the materials and give more specific definitions.

2.1.2 Classification

To classify the nonwoven materials, one of the convenient ways is according to their manufacturing principles. Hence, nonwoven materials can be classified as mechanically bonded nonwoven textiles, adhesively bonded nonwoven textiles, and thermally bonded nonwoven textiles.

- The mechanically bonded nonwovens are pliable and porous planar products made from textile elements by reinforcing these with fibres belonging to the original system by extraneous bonding threads (Krčma 1962).

- The adhesively or chemically bonded nonwovens are pliable and porous planar products made from textile elements by binding these with adhesives (Krčma 1962).

- The thermally bonded nonwovens are manufactured by interlocking the fibres through the use of heat energy employing the thermoplastic properties of synthetic fibres such as polypropylene. The heat in the process softens the surface of the fibre. At the bond point, fibres in contact with each other will form strong bonds, which hold the fabric together.

2.1.3 Raw materials

There are two main types of fibres -natural and man-made- that are used for the manufacturing of nonwoven materials. Both the extrinsic and intrinsic properties of the fibres based on their outward and inner structure affect the properties of nonwoven fabrics. Alongside thermal and chemical properties of the fibres, their geometry (the fibre length, fibre cross-section, volume and surface characteristics) and mechanical properties (tensile strength, the break length, elongation properties, elasticity and plasticity) are the fundamental factors in the research of mechanical properties of nonwoven fabrics (Krčma,1962), which are determined by the macromolecular structure and dimensional parameters.

Nowadays, nonwoven materials are mainly produced form man-made fibres, accounting for over 90% of total output. There are numerous fibres in applications such as polypropylene, polyethylene, PET, nylon, rayon, aramids, glass, acetate, biconponents, blends and copolymers, etc. Two most popular ones are polypropylene and polyesters. And polypropylene holds 63% of the world usage (Russell 2007). Moreover, short fibre (staple) and long continuous fibre behave differently.

2.2 Properties of nonwoven fabrics

The main factors of nonwoven fabrics, which affect the material properties and manufacturing process are (Russell 2007, Krčma 1962):

1. Geometrical properties;
2. Mechanical properties of fibres;
3. Physico-chemical properties;
4. Chemical properties;
5. Physiological properties.

Geometrical and mechanical properties of fibres are the essential factors for the mechanical properties of nonwovens.

2.2.1 Geometrical properties

To some extent, the structure of the nonwoven determines its mechanical properties. The core factors of nonwovens are:

a) Fibre length and crimp.

b) Fabric dimensions and variation: dimensions (length, width, thickness, and weight per unit area), dimensional stability, density and thickness uniformity.

c) Fibre alignment: fibre orientation distribution.

d) Bond points: bonding type, shape, size, bonding area, bonding density, bond strength, bond point distribution, geometrical arrangement, the degree of freedom of fibre movement within the bond points, interface properties between a binder and fibre and surface properties of bond points.

e) Porous structural parameters: fabric porosity, pore size, pore size distribution, pore shape.

2.2.2 Mechanical properties

The mechanical properties of the nonwovens are important factors with regard to the end-use properties of the final products. Many researchers have been done to study the following basic mechanical behaviours:

a) Compression and compression recovery.

b) Tension (The Young's modulus, tenacity strength and elasticity, elastic recovery, work of rupture).

c) Bending and shear rigidity.

d) Tear resistance

Also, the burst strength, crease resistance, abrasion, frictional properties (smoothness, roughness, friction coefficient), energy absorption of nonwoven are other important mechanical properties for the specific functionality.

2.3 Application of nonwoven materials

The nonwoven materials are engineered to provide specific functions to ensure fitness for purpose, and the properties of the nonwovens also could be combined to create the required functionality, with achieving a profitable balance between the expected product life and cost (Russell 2007). With development of manufacturing techniques for the nonwoven industry, the materials are widely used in various aspects of social life. Some end uses of nonwovens nowadays are given in Table 2.2.

Personal care products	Clothing, footwear, baggage	Absorbent hygiene products	Agriculture and horticulture	Industry	Household	Medical and healthcare
Absorbent hygiene products; wipes, shin care; depilatory strips, etc.	Interlinings; disposable underwear; shoe components; bag components; bonding agent; composition and (wash) care labels, etc.	Baby diapers; feminine hygiene products; incontinence products, etc.	Crop covers; plant protection; seed blankets; weed control fabrics; greenhouse shading, root control bags, biodegradable plant pots; capillary matting; landscape fabric, etc.	Abrasive; automotive; building; cable wrapping; civil engineering; cleaning, soil/water cleansing; coating substrates; composites; conveyor belts; electric/electronics; filtration; graphic arts; packaging; protective clothing, etc.	Abrasives; bed linen; blinds/curtains; carpet/carpet backing; covering and separation material; detergent pouches/fabric softener sheets; flooring; furniture/upholstery; mops; table linen; tea and coffee bags; wall-covering; wipes, etc.	Surgical caps and masks; drapes, wraps and packs, sponges, dressings and wipes; contamination control gowns; examination gowns; lab coats; isolation gowns; transdermal drug delivery; shrouds; underpads; procedure packs; heat packs; ostomy bag liners; fixation tapes; incubator mattress; sterilisation wraps; wound care; cold/heat packs; drug delivery etc.

Table 2.2: Application of nonwoven materials (edana 2008)

14

2.4 Thermally bonded nonwovens

Thermal bonding is one of the most widely used bonding technologies in the nonwovens industry. The viability of this technology is rooted in the price advantage obtained by lower energy costs. It is used extensively in spunbond, meltblown, air-lay, and wet-lay manufacturing as well as with carded-web formation technologies (Mishakov, V. Slutsker, G. and Stalevich, A. 2006, Michielsen, S., Pourdeyhimi, B., and Desai, P. 2006). Generally, only fibres with thermoplastic characteristic or with blends containing them that are not intended to soften or low on heating can be used in thermally boning process (Russell 2007). And the stronger fibres make stronger textile structures when all other factors are the same. But still there are plenty of types of fibres in practice: polypropylene (PP), polyesters (PES), nylons, polyethylene (PE), vinyon and sheath-core bicomponents involving PE/PP, PP/PES, copolymers of PES, etc (Batra 1998). For bicomponent fibres, the non-binder component (core) is referred to as the base fibre component, and the binder component (sheath) normally ranges from 5-50% on weight of fibre depending on the physical property requirements of the final product (Russell 2007). Compared to other bonding processes, the advantages of thermally bonded nonwovens are:

1. High economic efficiency as compared to chemical bonding, because the thermally bonding process slightly use the binder agents and need less energy (Chand, Bhat et al. 2001).
2. Generally, the manufacturing systems are cheaper than those for other processes.
3. The process can be used for the thick web, and the bonding affect is designable.
4. The material is recyclable, which is good for environment, since it is possible to use pure polymer fibres in the process.
5. The fibre properties are controllable, so there are opportunities to produce nonwovens with different functions (flame-residence, high bulk and resilience nonwovens, heat-insulating nonwovens, etc.)

2.4.1 Manufacturing process of thermally bonded nonwovens

As it is described in Section 2.1.1, four principle processes are necessary to manufacture nonwoven material. To produce thermally bonded nonwovens, the bonding processes are specified as following (Pourmohammadi 2007):

1. Compressing and heating the web to partially melt in the crystalline region;
2. Bonding the web to from the newly released chain segments across the fibre-fibre interface;
3. Cooling the bonded web to re-solidify it and to trap the chain segments that diffused across the fibre-fibre interface.

There are several thermal bonding technologies, which are predominantly used in industry, and discussed below.

Through-air thermal bonding makes bulkier and heavy-weight products by the overall bonding of a web containing low melting fibres. The hot air flows through holes in a plenum positioned just above the nonwoven. And negative pressure or suction, pulls the air through the open conveyor apron that supports the nonwoven as it passes through the oven. Binders are necessary to help the bonding such as crystalline binder fibres, bi-component binder fibres, and powders (Kamath, M.G., Dahiya, A. and Hegde, R.R. 2004, Batra, S.K. and Davis, H. 1999). For this technique, it is important and challenging to control the temperature and air flow. To avoid any undesirable change in web thickness, it is essential that the web is quickly heated to the melting temperature and the air flow is reduced. And actually, the high air speed cause thinner web and high fabric strength, due to forming more inter-fibre bond points (Russell 2007).

Another process -ultrasonic bonding- is based on conversion of electromagnetic energy into mechanical energy, which takes place when the molecules of the fibres held under a patterned roller are excited by high frequency energy, which produces internal heating and softening of fibres. In the process, a fibrous web is compacted between an embossed patterned roller and an ultrasonic tool (horn). The horn is vibrated at a high frequency in the range of 20-40 kHz and hammers the web (Russell 2007). The contacts between ultrasonic horn and the web implement a limited

pressure on web surface within a brief time with a high frequency about 20,000 cycles/s. Energy is therefore transferred to restricted areas in the web to induce thermal bonding as the mechanical energy applied to the fibres is converted into heat (Russell 2007).Then the web is bonded. Since this bonding method causes self-bonding of fibres, one advantage of this technique is that no binder is necessary for manufacturing (Kamath, M.G., Dahiya, A. and Hegde, R.R. 2004).

The third process is that infrared (IR) bonding relies on the radiation type of heat transfer. IR emitting heaters are used to radiate electro-magnetic energy in part of IR wave length rage (approximately 760-10000 μm), which then translates to heat in the receiving material. IR radiation cannot penetrate deep into the structure of the web, and it is not economical to be used in area bonding for thinner webs. Therefore, IR boding is used largely as method of "glazing" the surface of thick nonwovens, and "stabilizing" needlepunched geotextiles and roofing felts (Batra 1998).

Hot calendar bonding is the most frequently used method for thermal bonding in the industry. Calendaring (shown in Figure 2.1) uses heat and high pressure applied through rollers to weld the fibre webs together at speed. For point bonding, one of these rolls has an engraved pattern on its surface that leads to fibre-to-fibre bonding locally at the points of the intersection of the engraved pattern with the smooth roll (Bhat, Malkan 2002). Both of the rollers are heated internally, and the temperatures determine the level of bonding besides the other factors such as nip pressure, throughput speed and web parameters (basis weight, fibre type, fibre mass linear density and blend level).
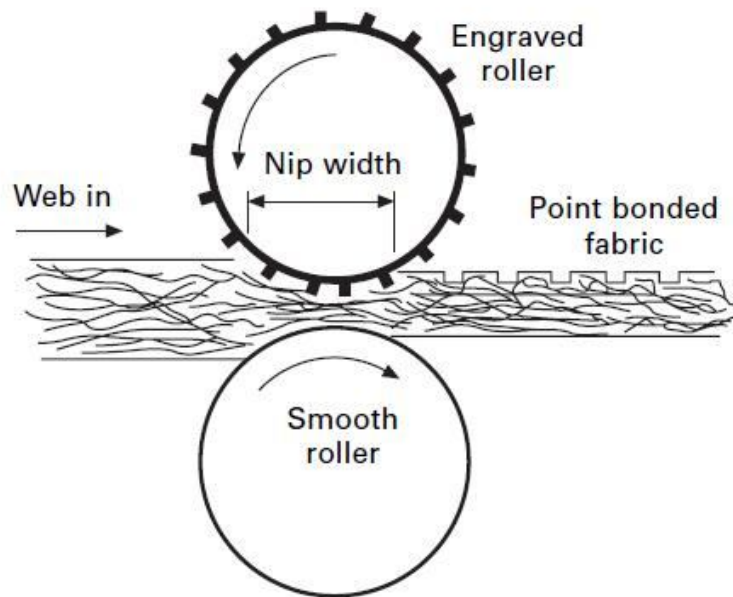
Figure 2.1: Typical thermal point bonding roller arrangement (Russell 2007)

As well known, the manufacturing process determines the material properties of nonwoven. Before bonding can occur, a web must be formed. During this process, different fibre orientation distribution functions (ODF) are produced by different web formatting processes. The ODF indicates the material's anisotropy, different deformation mechanisms, and the subsequent failure modes (Kim 2004b, Michielsen, S., Pourdeyhimi, B., and Desai, P. 2006, Pourdeyhimi, B. and Ramanathan, R 1996, Liao, Adanur 1999b). When the web passed through the hot calendar rolls, the web is compressed and heated. During this process, a minimal pressure is required at the nip, especially for thin nonwovens. The pressure brings fibre to fibre contact, which affects the heat transfer to and then through the web. Beyond the minimal pressure, the bonding pressure appears to have little or no effect on fabric performance (Michielsen, S., Pourdeyhimi, B., and Desai, P. 2006). The bonding temperature determines the structure of the single fibre and the bond points. Only the fibres located under the bond-points heat up significantly, and the bridging fibres are slightly changed in the morphology (Wang, Michielsen 2002, Kim, Pourdeyhimi et al. 2002). In bonding areas, the heat is not only due to the heat conduction from the rolls to the fabric but also due to the thermal input, which is a deformation induced heating process (Warner 1989, Anderassen, Myhre et al. 1995). And within the bond points,

18

the fibres are not completely melted to a film-like structure, but flattened (Figure 2.2). That means the temperature must be adjusted to avoid complete fibre melting and film formation for obtaining fabrics with high strength and good softness (Russell 2007). As extensively studied, the effect of bonding temperature on fabric physical properties is important and complicated. For tensile behaviour, with the increase of bonding temperature up to a certain points, the tensile properties of the fabric increase due to the formation of a well-developed bonding structure. But further increase in bonding temperature causes reduction of the tensile properties, which is attributed by losing the fibre integrity and formation of film-like spots as well as the reduction in load transfer from fibres to the bond points (Haoming, Bhat 2003, Kwok, Crane et al. 1988). This kind of over bonding also leads to a sudden rupture under tensile load at the bond points. The shear modulus and bending rigidity of calendar bonded fabric are also increased by increasing the bonding temperature (Kim, Pourdeyhimi et al. 2001).
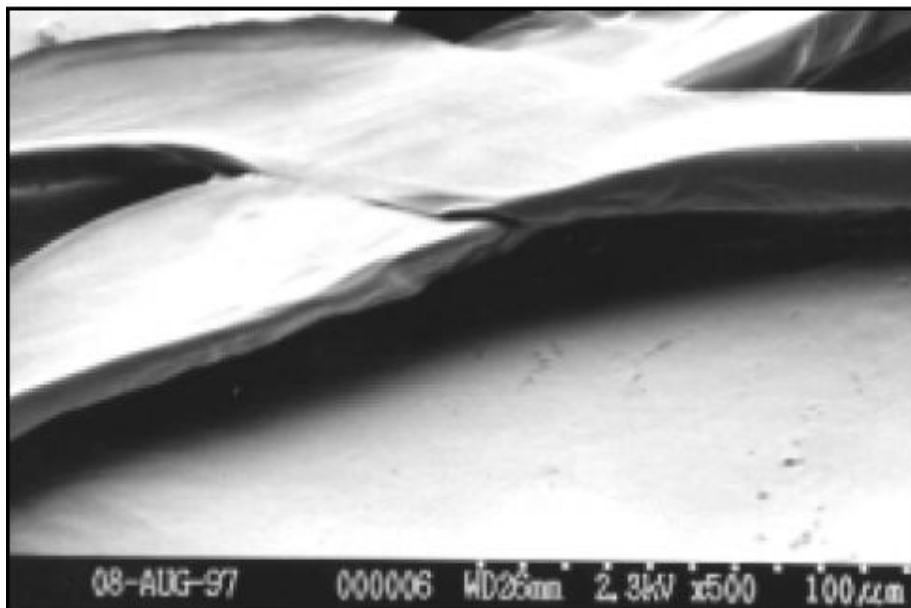
Figure 2.2: Flattened fibres bonded by hot calendar (Chidambaram, Davis et al. 2000)

2.4.2 Characterisation of thermally boned nonwoven fabrics

Because of the low cost of energy, environmentally friendly and good economic efficiency of thermal bonding, the technique is widely used nowadays. A better understanding of thermally bonded nonwovens is requested. The important nonwoven fabric properties include: mechanical properties, fluid handling properties, physical

properties, chemical properties and application specific performance (Russell 2007). One of the challenging works is to study the mechanical properties of the thermally bonded nonwoven, due to its unique and complicated structure.

2.4.3 Geometrical properties

As shown in Figure 2.3, the thermally bonded nonwoven fabric includes two components: a fibrous web and bond points. And the mechanical properties of the material depend on its structure and the interactions between its components. Normally, the nonwoven fabric is anisotropic; the material properties in its two principle directions are different. The machine direction (MD) is the longitudinal direction within the plane of the fabric that is in the direction, in which the fabric is being produced by the machine (Batra, Thompson et al. 2002).The cross direction (CD) is the direction perpendicular to the machine direction. In the industry, a direction ratio (MD/CD) of tensile strength is commonly used to describe the anisotropy of the material.
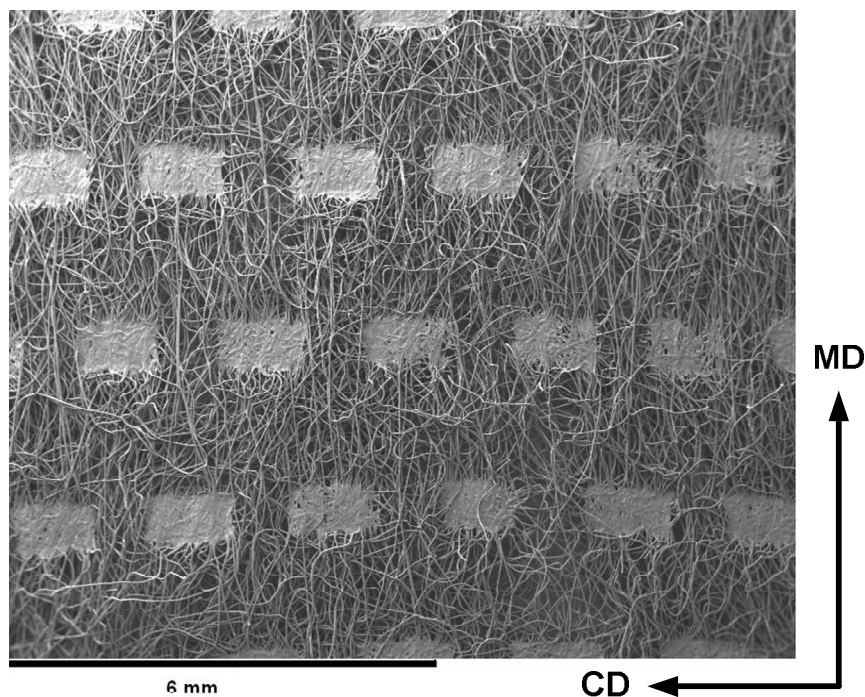
Figure 2.3: A typical structure of thermally bonded nonwoven fabric

2.4.4 Fibres for thermally boned nonwovens

Polymer fibre is the raw material of nonwovens. For thermally bonded nonwoven fabrics, the fibres form both fibrous network and bond points after manufacturing processes. The randomly arranged bridging fibres form fibrous network. And the bond points are formed by heated and compressed fibres. Therefore, it is essential to understand the properties of fibres. The most foundational geometry properties of fibre are its stiffness, dimensions and crimp. Generally, stiffer fibres make stiffer fabric. Moreover, for a given areal density, the fabric strength increase with a decrease in fibre diameter, and increases up to a limiting value as the fibre length increase (Shimalla, Whitwell 1976). For the fibres within the bond points, the birefringence (molecular orientation) of the fibres are reduced compared to the original bridging fibres, due to the bonding process (Chidambaram, Davis et al. 2000, Shimalla, Whitwell 1976, Dharmadhikary, Davis et al. 1999). The phenomena lead to a large decline in the fibre modulus in the bonded points, and affect mechanical properties of the overall nonwoven fabric.

As shown in Figure 2.3, fibres within the nonwoven fabric are crimped. The degree of curvature of fibres affects the deformation mechanisms of the fabric (Petterson, D.R. and Backer, S. 1963, Backer, S. and Petterson, D. R. 1960, Hearle, J.W.S. and Ozsanlav, V. 1979). Therefore, some researches have been done to investigate the degree and distribution of fibre curl by introducing a curl factor (Petterson, D.R. and Backer, S. 1963, Adanur, S. and Liao, T. 1999, Rawal 2006).

2.4.5 Orientation distribution function (ODF)

Due to the manufacturing process, the fibres in a nonwoven fabric are rarely completely randomly orientated, rather, individual fibres are aligned in various directions mostly in-plane. In 1952, Cox' introduced the conception of "distribution function" in his famous model for paper to describe the fibre orientation in fibrous assembly (Cox 1952). Then dealing with the ODF (orientation distribution function) became a common way to nearly all the researchers in that field because it is not only describes the structure of nonwovens but also determines, to a great extent, the deformation mechanism and mechanical failure of the material (Michielsen, S., Pourdeyhimi, B., and Desai, P. 2006).

Although the fibre segment orientation in a nonwoven is potentially in any three-dimensional direction (Figure 2.4), the measurement of fibre alignment in three dimensions is complex and expensive (Russell 2007, Gilmore, Davis et al. 1993). And due to the nature of nonwoven fabric, which is a kind of thin material, researchers usually simplify a three dimensional problem as a two dimensional structure. If a three dimensional structure is required, the structure may be a combination of two-dimensional layers (Bais-Singh, S., Biggers, S.B.JR. and Goswami, B.C. 1998). In some model, the layers are connected by fibres orientated perpendicular to the layers (Mao, Russell 2003).
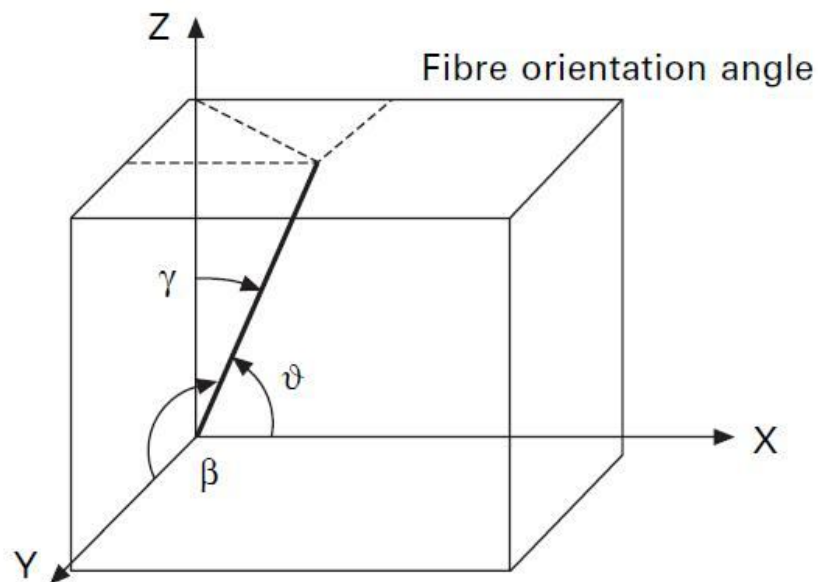
Figure 2.4: Fibre orientation angle in nonwoven fabric in three dimensions (Russell 2007, Mao, Russell 2003).

In two dimensions, the ODF of the fabric is usually presented as the distribution of fibre orientation angle, which is defined as the relative directional position of individual fibres in the structure relative to the machine direction as shown in Figure 2.5.
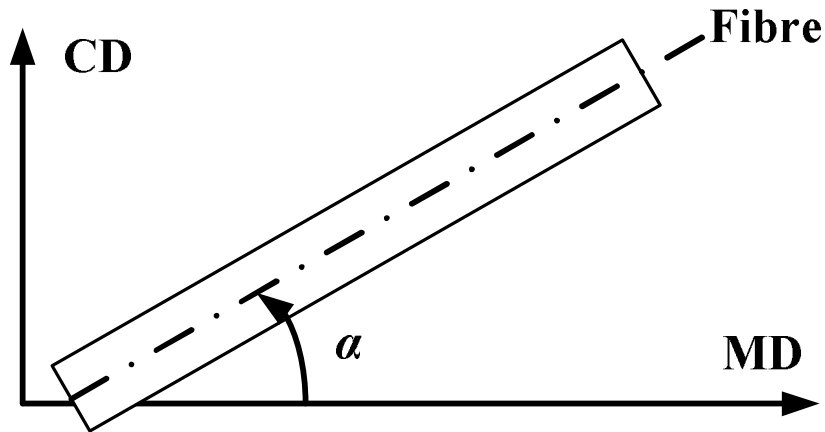
Figure 2.5: Fibre orientation and orientation angle (Russell 2007)

To measure the orientation distribution of fibres, many efforts have been done. In 1963, Hearle and Stevenson suggested a method to determine the orientation from the directional phenomena of dichroism and birefiringence (Hearle, J.W.S. and Stevenson, P.J. 1963). Later, with the development of imaging devices and computation tools, the ODF start to be measured directly from optical microscopic image (Xu, B. and Ting, Y. 1995). At present, photomicrographs of fabric taken with a scanning electron microscope are normally used to determine the orientation distribution of nonwovens. In 1979, Hearle and Ozsanlav expressed the ODF in term of powers of the cosine function (Hearle, J.W.S. and Ozsanlav, V. 1979, Rawal 2006). Xu and Ting presented their software, which could compute the ODF based on the image obtained by a CCD camera (Xu, B. and Ting, Y. 1995). Pourdeyhimi and Ramanathan (1996) computed ODF using engineering software and developed an image model to simulate the fibre arrangement of nonwovens (Pourdeyhimi, B. and Ramanathan, R 1996). Then Pourdeyhimi introduced the Fourier transform method in his paper in 1997, which is one of the most popular methods to obtain the ODF (Figure 2.6) nowadays (Pourdeyhimi, B., Dent, R. and Davis, H. 1997, Pourdeyhimi, Dent et al. 1999). In 2002, Ghassemieh and Acar implement the Hough transform to estimated the ODF of nonwoven fabric and compared the method with FFT (fast Fourier transform) (Ghassemieh, Acar et al. 2002a, Ghassemieh, Acar et al. 2002b, Ghassemieh, E., Versteeg, H.K. and Acar, M. 2001).

23
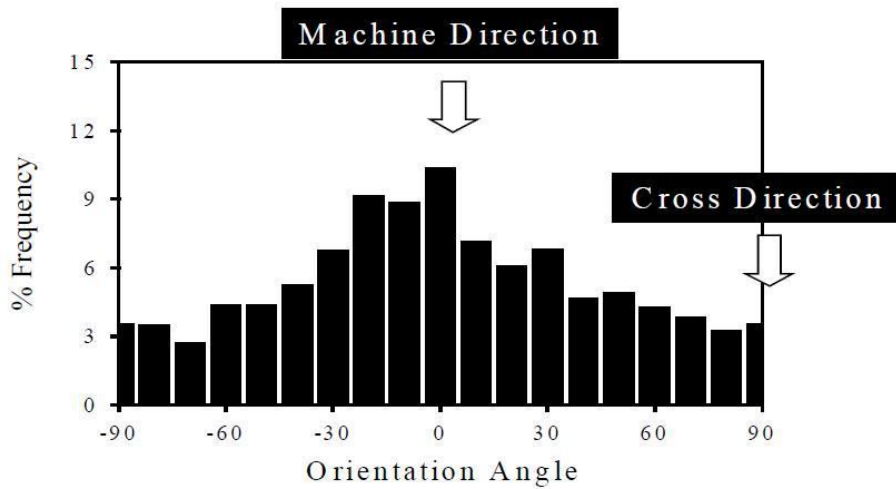
Figure 2.6: Typical fibre orientation distribution function (Kim, H.S. and Pourdeyhimi, B. 2000)

Fourier Transform:

Fourier analysis is used as an indirect method to estimate the fibre orientation distribution by most researchers. The Fourier transform decomposes an image from its spatial domain of intensities into frequency domain with appropriate magnitude and phase values. Then the frequency can be depicted as an image where the gray scale intensities present the magnitudes of the various frequency components (Wood 1990). A higher rate of the change in gray scale intensity will be reflected in higher amplitudes (Ghassemieh, E., Versteeg, H.K. and Acar, M. 2001). In two dimensions, the corresponding direct Fourier transform is given as:

$$F(u,v) = f(x,y)e^{-2\pi i(xu+yv)}dxdy \quad , \tag{2.1}$$

where $f(x,y)$ is the image and $F(u,v)$ is its transform, u refers to the frequency along the x direction and v represents the frequency along the y direction (Pourdeyhimi, B., Dent, R. and Davis, H. 1997, Ghassemieh, Acar et al. 2002b).

In the analysis of nonwoven materials, the Fourier transform is used to determine the rate at which the intensity transition occurs in a given direction in the image. Thus, if fibres are predominantly oriented in a given direction of the fabric, the spatial frequencies in that direction will be low and the spatial frequencies in the

24

perpendicular direction will be high (Pourdeyhimi, B., Dent, R. and Davis, H. 1997). Hence, the fibre orientation distribution can be computed according to this property of the Fourier transform.

Hough transforms:

The Hough transform (HT) is an effective method for object detection in an image directly. The classical HT is usually used for the detection of regular lines, especially for straight lines. The basic concept involved in locating lines by the HT is point-line duality (Davies 2005). And the main process is to transform a line in the Cartesian space to a point in a parametric space (Xu, Yu 1997). To represent a straight line the most common equation is the polar form, which is convenient to describe the lines parallel to y axis in Cartesian space (Ghassemieh, Acar et al. 2002b). It is given as:

$$\rho = x\cos\theta + y\sin\theta , \tag{2.2}$$

where ρ is the normal distance from the origin, and θ is the angle of the normal line with respect to the x axis. This transformation produces a sinusoidal curve in the $\theta - \rho$ parameter space for a point (x, y), and converts a line into a point (θ, ρ) in the $\theta - \rho$ space. In this way, a set of collinear points in the images space generates a family of sinusoidal curves in the $\theta - \rho$ space, which cross each other at point $P(\theta, \rho)$. Therefore, point P in $\theta - \rho$ space is representing a straight line L in the image.

Simulation:

To validate the method of measuring ODF, Xu and Yu generated images by straight lines with designed fibre orientations (Xu, Yu 1997). But before their publication, in 1996 Pourdeyhimi and Ramanathan presented their image simulation using S-random and μ-random approaches, which could simulate both continuous and discontinuous nonwoven network according to ODF. Later the improved model was used in a mechanical model to simulate the deformation process of nonwovens (Pourdeyhimi, B. and Ramanathan, R 1996, Kim, H.S. and Pourdeyhimi, B. 2001b).

Figure 2.7 shows the two scheme of simulation. μ-randomness is used to simulate a continuous-fibre assembly. The method defines a line by the perpendicular random

distance *d* from a fixed reference point *O* (centre point), *α* is the angular position, which is chosen according to ODF. I-randomness is used to simulate the staple fibre assembly. To define a line, a point *P* is chosen at random by its *x* and *y* coordinates to make sure it lies in a plane, which is larger than the image by length *l*. Then, an angular position *α* is selected depending on ODF, and a line is drawn with length *l* (Pourdeyhimi, B. and Ramanathan, R 1996, Kim, H.S. and Pourdeyhimi, B. 2001a, Suh, Chun et al. 2010).

(a)   (b)
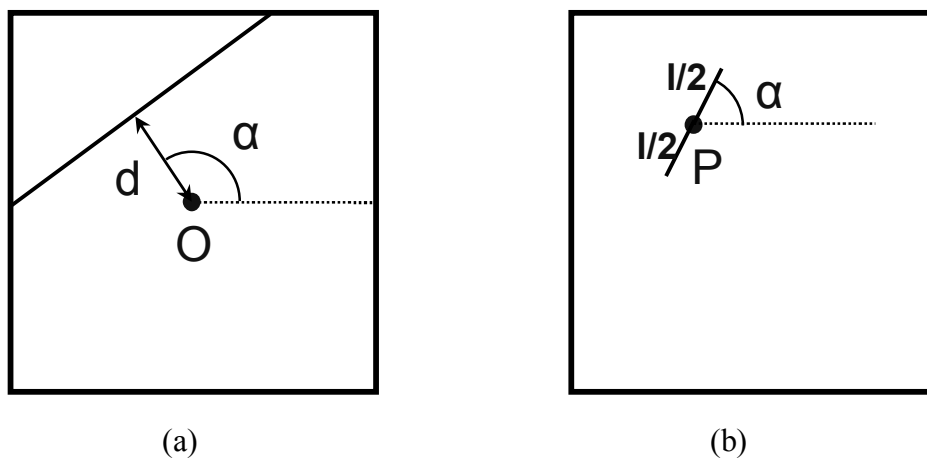
Figure 2.7: Procedures of image simulation: a) μ- randomness, continuous fibres; b) I-randomness, staple fibres

2.4.6 Bond points

The technique of thermal bonging involves the use of heat and often pressure to soften and then fuse or weld fibres together without inducting melting. The bond points have properties distinct from those of bridging fibres due to the bonding process, and affect the mechanical properties of the fabric significantly as one of its two basic components. It is known that increasing the bonding temperature up to a certain point increases the tensile properties of the fabric due to the formation of a well-developed bonding structure. A further increase in the bonding temperature reduces the birefringence (molecular orientation) of the fibres within the binding area, as well as the tensile properties of the fabric (Russell 2007, Michielsen, S., Pourdeyhimi, B., and Desai, P. 2006, Fedorova, Verenich et al. 2007). The properties of bridging fibres at locations farther than 30-40 microns from the bond edge are unchanged during the bonging process (Fedorova, Verenich et al. 2007). The parameters of a thermally bonded fabric are also influenced by the pattern and size of the engraved surface on

the embossed calendar roller. Figure 2.8 shows a typical engraved surface on the embossed calendar roller. But only limited research has been performed to understand the effect of bond area and bond size (Bhat, Jangala et al. 2004). According to the experiments, the tensile strength and tear strength increase with the increase in the bond area and size (Bhat, Jangala et al. 2004).
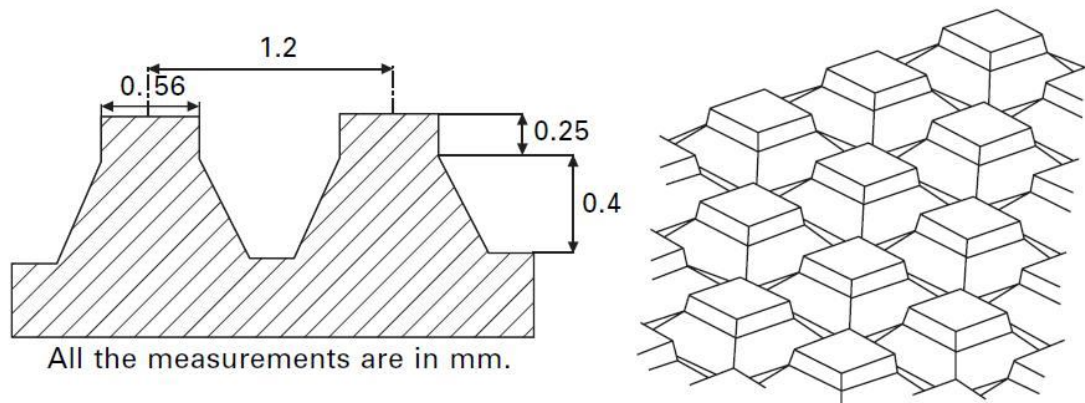
Figure 2.8: Typical engraved roller with 22% bonding area and 60 bond points/cm^2 (Mao, Russell et al. 2007b)

2.5 Mechanical properties of nonwoven materials

With the extension of applications of nonwoven products, the material is requested to possess better mechanical properties than before. Moreover, the complex microstructure of the nonwoven materials makes its mechanical properties really challenging and interesting to be explored. Therefore, researchers have made many efforts in last fifty years to find a proper way to describe the mechanical properties of nonwoven materials. As fundamental mechanical behaviours, compression and tension are widely studied. However, still no really successful work has been done to estimate the material's deformation and failure mechanisms.

2.5.1 Compression and tension

Compression

One of the pioneer works in the analysis of the compression of fibre assemblies is C. M. Van Wyk's model. His theory simplified the fibre mass as a system of bending

units, which are the elements of fibres between adjacent contacts with other fibres (Van Wyk 1946). And the fibre bending is considered to be the only process of importance in fibre deformation. So the crimp, slippage, extension, friction and reorientation of fibres were neglected and the fibre elements were treated as random.

The work provided the relation between pressure and the volume of fibre assembly in the following form:

$$p = \frac{KEm^3}{\rho^3}(\frac{1}{v^3} - \frac{1}{v_o^3}), \qquad (2.3)$$

where K is a constant determined by the structure of the fibre mass, E is the Young's modulus of the fibre, v_0 is a constant corresponding to the fibre-mass volume at zero pressure, ρ is the density of the fibre, m is the mass of fibres, and v is the volume of the fibre mass under pressure p (Van Wyk 1946, Krucinska, I., Jalmuzna, I. and Zurek, W. 2004).

Besides ignoring some structure parameters in its assumptions, the theory overestimates the observed stress by as much as 48-120 times without any parametric adjustment (Komori, T., Itoh, M. and Takaku, A. 1992).

Later, some researchers tried to introduce more fibre characteristics into the Wyk's model. Matsuo extended it, taking into account fibre curl, orientation, slippage and the hysteresis factor (Matsuo 1968). Dunlop analysed the effect of the slippage factor, acoustic emission, dynamic bulk modulus and stress-strain hysteresis in compression of fibre masses (Dunlop 1983). According to his work, the hysteresis is independent of the rate of compression (Beil, N.B. and Roberts, W.W. 2002b); he also introduced several models to describe the behaviour, although none of them were capable of accounting any viscoelastic or time-dependent behaviour. His work was more focused on the behaviour of fibres assemblies but not the fibres themselves (Dunlop 1983), and Lee and Lee (1985) introduced the anisotropic initial modulus and Poisson's ratio in to the analysis (Komori, T., Itoh, M. and Takaku, A. 1992). Later, Canaby and Pan (1989) developed their analysis with incorporating the effect of friction and slippage at fibre contacts, and elucidated the hysteresis in the compression-recovery loop. Beil

and Roberts at first created a single fibre model with mechanical properties, and then the motions of several interacting fibres were computed based on interactions. They compared the results with those by Wyk, proving that slippage and friction have a strong effect on the resistance to compression of an assembly (Beil, N.B. and Roberts, W.W. 2002b, Beil, N.B. and Roberts, W.W. 2002a). Later, they improved their model with adding the effect of hysteresis, crimp, and orientation (Beil, N.B. and Roberts, W.W. 2002b).

The energy method is used as an approach that differs from the above theories. On the basis of the minimum energy principle, Lee, Carnby and Tandon (1990), used a circularly curved beam in place of the straight beam in the Wyk's theory. That means they can examine the effects caused by the structure parameters, such as fibre crimp, the distribution of lengths and curl, which are difficult to study using traditional ways. Komori and Itoh (1992) developed the model of Lee-Carnady-Tandon (1978) and considered the dependence of the mean free fibre length on direction (Komori, T., Itoh, M. and Takaku, A. 1992, Komori, T. and Makishima, K. 1978), and pointed out that the directional dispersion in the elemental beam length might play a role that cannot be ignored. To improve their theory, they also investigated the contact between fibres, which was assumed to be ideal overlapping in most of former works (Komori, T. and Itoh, M. 1994).

Jacob, *et al.* (2003) presented a new plan in their annual report of the National Textile Centre, which model the compressive behaviour of fibre assemblies using the lattice or spring network (Jacob, K.I., McDowell, D., Tech, G., Aneja, A.P. and Corporation, D. 2003). It was supposed to incorporate large deformation and nonlinear paramters of fibres. A similar study has been done by Krucinska *et al.*; they developed a rheological model by treating the nonwoven material as an elastic/viscoplastic material (Kim 2004a, Krucinska, I., Jalmuzna, I. and Zurek, W. 2004).

The latest works trend to use finite element analysis as a tool to study the fibres assembly. Ostoja-Starzewski developed a lattice models in 2002 and Engelmayr and Sacks (2006) used a representative volume element (RVE) as the basic element in their analysis in 2006 (Ostoja-Starzewski 2002b, Engelmayr Jr, G.C. and Sacks, M.S. 2006).

The researches on compression behaviour of a fibrous mass basically introduce information on the characteristics of microstructure of the materials and summarise the important factors, which are worth to be concerned in other researches. In those theories, several basic properties were brought forward, which significantly affect the mechanical properties of nonwoven materials: the fibre length, fibre diameter, crimping, friction, fibre slippage and hysteresis.

Hyperesis and Friction

The hyperesis and friction characteristics are important factors in both compression and tension behaviours of nonwoven materials. And they depend on the properties of fibres and their assembly.

In his research, Wyk discussed the relationship between the hysteresis and the effect of friction, although he did not introduce that factor in his compression model. He claimed that friction may be one of the factors, which result in the hysteresis, but it should not be the only one. And the frictional effect may be constant or proportional to the inverse cube of the volume (Van Wyk 1946).

Dunlop stated the relationship between the fibre-slippage and the hysteresis by observing compression – release cycling of fibre masses in a compression cell. The hysteresis indicates the dissipation of energy and may be mainly attributed to frictional losses (Dunlop 1983).

In 2002, Beil and Roberts developed their compression theory based on a single-fibre model, which is different from the previous work dealing with the behaviour of fibres' assemblies. And then they successfully developed a model for describing the compression behaviour including the information both on fibres and the structure of assembly. Especially, their model considered both static and kinetic friction between fibres, and described the changeable friction coefficient and viscoelastic behaviour of fibre assemblies (Bhat, Malkan 2002, Beil, N.B. and Roberts, W.W. 2002b, Beil, N.B. and Roberts, W.W. 2002a).

Figure 2.9 shows that their model is composed of the following elements: parallel springs with stiffness C_1 and C_2 determining elasticity, a Newtonian damper set up in

series with one of the springs, representing stress relaxation, since it is parallel to another spring, (it also represents delayed elasticity), and a frictional element with changeable characteristics depending on deformation under compression, representing plastic deformation.
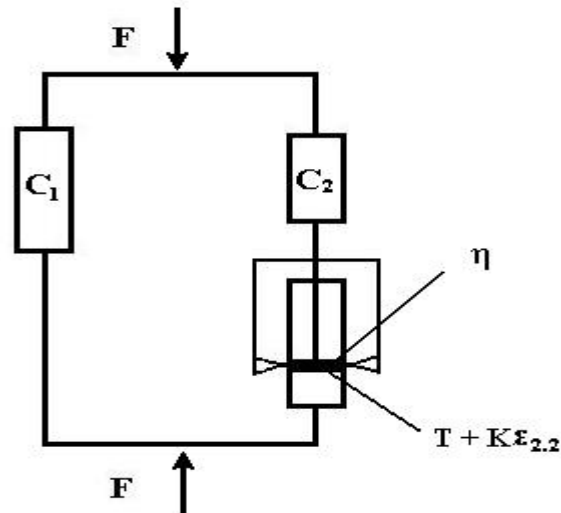
Figure 2.9: Modified rheological model (Krucinska, I., Jalmuzna, I. and Zurek, W. 2004)

The following equation corresponds to their model, which is for a practical use:

$$F = Cut - Au[t - t_0 + \tau(1 - e^{t - t_0 / \tau})], \tag{2.4}$$

where

$A = \left(\dfrac{C_2^2}{C_2 + K}\right)$ and $\tau = \dfrac{\eta}{C_2 + K}$, F is the compression force, C is the total stiffness of the model, u is a constant according to the Hookean spring 2, and control the movement of the piston, t_0 is the time to reach the limit of proportionality.

<u>Tension</u>

One of the pioneering works in this area is a fibre web theory which was developed for paper but also accommodate the broad mechanical design requirements of nonwovens. And most of the current researches of nonwoven material are based on this theory, which is the well known Cox's model. It provides an analytical derivation of the in-plane compliance of a mat of infinitely long fibres, laid in a plane according

to a Fourier series-type probability density function (Cox 1952, Ostoja-Starzewski, M. and Stahl, D.C. 2000):

$$\pi f(\theta) = 1 + a_1 \cos 2\theta + a_2 \cos 4\theta + a_3 \cos 6\theta + ... + a_n \cos 2n\theta + ... \quad , \tag{2.5}$$

Here, θ is the angle a fibre makes with respect to the *x*-axis and it must be between zero and π. The x and y axes are referred to as the machine direction (MD) and cross direction (CD), respectively. And the model assumes that each fibre is straight and propagates throughout the whole material body, and it can be loaded only at its end. The flexural stiffness of a single fibre is considered to be negligible, so that the fibre can transmit loads only in tension and the loading applied at the edges or free surfaces of the material is assumed to match this condition (Cox 1952). Generally, the Cox's model can predict the effective Young's moduli but cannot describe the shear modulus, both for isotropic and orthotropic system. Besides, it did not consider local nonuniformities and nonlinear behaviours of the fibres or the fabric.

The orthotropic theory and fibre-web theory of a nonwoven material was reported by Becker and Petterson (Petterson, D.R. and Backer, S. 1963, Backer, S. and Petterson, D. R. 1960). To determine the applicability of the orthotropic theory to a nonwoven material, they obtained the constants from the principle-direction tensile tests and simultaneous measurements of the materials Poisson's ratio. Then they predicted the strain-stress relationships of the material for any direction by developing a relationship between the global coordinates and local coordinates of the material.

In the model, a rectangular nonwoven fabric is treated as an orthotropic material with symmetry axes *L* and *T*. The length of the fabric lies parallel to the direction y which makes an angle θ to the *L* direction. And *x-y* is a Cartesian coordinate system in the plane of material. The material stress-stain relationships in the *x-y* coordinate system are (Petterson, D.R. and Backer, S. 1963):

$$\varepsilon_y = c_{11}\sigma_y, \tag{2.6}$$

$$\varepsilon_x = c_{12}\sigma_y, \tag{2.7}$$

$$\gamma_{yx} = c_{31}\sigma_y, \tag{2.8}$$

where

$$c_{11} = \frac{\varepsilon_y}{\sigma_y} = \frac{1}{E_y} = \frac{cos^4\,\theta}{E_L} + \frac{sin^4\,\theta}{E_T} + \left[\frac{1}{G_{LT}} - \frac{2v_{LT}}{E_L}\right] sin^2\,\theta\,cos^2\,\theta\ , \qquad (2.9)$$

$$c_{21} = \frac{\varepsilon_x}{\sigma_y} = -\frac{v_{yx}}{E_y} = -\frac{v_{LT}}{E_L} + \left[\frac{1}{E_L} + \frac{1}{E_T} + \frac{2v_{LT}}{E_L} - \frac{1}{G_{LT}}\right] \times sin^2\,\theta\,cos^2\,\theta\ , \qquad (2.10)$$

$$c_{31} = \frac{\gamma_{yz}}{\sigma_y} = \left[\frac{1}{G_{LT}} - \frac{2v_{LT}}{E_L} - \frac{2}{E_L}\right] sin\,\theta\,cos^3\,\theta - \left[\frac{1}{G_{LT}} - \frac{2v_{LT}}{E_L} - \frac{2}{E_T}\right] sin^3\,\theta\,cos\,\theta\ . \qquad (2.11)$$

E_L is the elastic modulus in L direction , E_T is the elastic modulus in T direction; v_{LT} is the contraction ratio between contractive strain in the T direction and the positive strain in the tensioned L direction; G_{LT} is the shear modulus in the LT plane and γ_{LT} is the shear strain.

There are two essential problems in this theory. One is the Poisson's ratio v_{TL} , the calculated values of which have more than 10% difference with the measured values. And another one is the shear modulus G_{xy} in the global coordinates which is difficult to measure directly. In their research, they preferred experimental data to calculated, which involve a big error.

To predict the elastic behaviour of uniform nonwoven structures, Becker and Petterson also established a fibre-web theory. It assumes that the bonding strength exceeds the rupture strength of the fibres, the fibres are straight and fibre properties are uniformly distributed in the fabric. The fabric is considered to be subjected to a longitudinal strain (Petterson, D.R. and Backer, S. 1963, Backer, S. and Petterson, D. R. 1960, Kim, H.S. and Pourdeyhimi, B. 2001a).

The relationship between fabric strain ε_y and the strain ε_β of a fibre lying at an angle β to the direction y is shown to be

$$\varepsilon_\beta = \varepsilon_y (cos^2\,\beta - \gamma_{xy}\,sin^2\,\beta)\ , \qquad (2.12)$$

where γ_{xy} is the contraction ratio for the x-y plane (Backer, S. and Petterson, D. R. 1960).

Considering the orientation distribution of fibres in the nonwoven, the stress contributed by all fibres to the fabric in y-direction is

$$\sigma_y = E_f \varepsilon_y \int_{-\pi/2}^{+\pi/2} \left[cos^2\,\beta - \gamma_{xy}\,sin^2\,\beta\right] cos^2\,\beta f(\beta)d\beta \ , \tag{2.13}$$

where σ_y is the fabric stress in the y-direction; E_f is the fibre modulus; $f(\beta)$ is the distribution function of the fibres.

Then if loading is uniaxial in the y-direction and no fibre buckling is considered, the stiffness of the fabric in y-direction is:

$$E_y = E_f \int_{-\pi/2}^{+\pi/2} \left[cos^4 - cos^2\,\beta\,sin^2\,\beta \times \frac{\int_{-\pi/2}^{+\pi/2} sin^2\,\beta\,cos^2\,\beta f(\beta)d\beta}{\int_{-\tau/2}^{+\pi/2} sin^4\,\beta f(\beta)d\beta}\right] f(\beta)d\beta \ . \tag{2.14}$$

The initial fibre-web theory is definitely not mature and has several problems. The Poisson's ratio is one of the factors, which cannot be described in this theory properly. And their implicit assumption, which uses one fabric web to represent the whole fabric, cannot describe the nonuniformity (mass, fibre diameter and orientation, local density) of nonwovens.

Immediately, one improvement to the fibre-web theory is that Petterson described the tensile behaviour in two different situations, which are small-strain theory and large-stain theory. In the small-strain theory, the second-order effects of the deformation are ignored as well as the lateral contraction of the specimen. In large-strain theory, all the factors neglected in the small-strain theory are included. But the Poisson's ratio of the material is measured in the middle area of the specimen, which cannot represent other areas of the material.

After the Becker and Petterson's foundational work, many researches tried to improve the theories and to describe the relationship between the fabric structure and its

mechanical performance. Hearle and Stevenson introduced the effect of a fibre curl into the Pentterson's model by identifying a curl factor c (Shaffer 1964)

$$c = \frac{g}{k},$$ (2.15)

where g is the length of fibre segment and k is the length of the chord of the fibre.

In 1979, Hearle and Ozsanlav developed a model to represent the structure of bonded –fibre fabrics, which consists of curled fibre and binder segments (Hearle, J.W.S. and Ozsanlav, V. 1979). This was the first work, which introduced the effect of binder deformation. Crindstaff and Hansen (1986) developed a numerical model to obtain a stress-strain curve of point-bonded fabrics. But it does not include information on the web structure, such as the ODF and fabric strength mechanism (Grindstaff, T.H. and Hansen, S.M. 1986).

To link the structural parameters of a nonwoven material and the deformation mode, Kim and Pourdeyhimi investigated (2000) the effect of ODF and bond points of point-bonded nonwovens (Kim, H.S. and Pourdeyhimi, B. 2000). Their group reported about a particular device (Figure 2.10) for *in situ* monitoring of changes in the structure of the nonwoven fabric during its deformation. The system can acquire current images of the samples under the tensile tests. Therefore, the structure's geometry and its deformation parameters, such as the orientation distribution function of fibres, bond-region strain, unit cell strain, shear deformation of the unit cell, etc. are measured under tension. From tests and observations, they found that different ODFs resulted in different fibre reorientation modes, and the bond shape and properties affected the failure modes of the fabric. Different structural details also led to different shear deformations along the preferred orientation of fibres. And as shown in Figure 2.11, the tensile strain in the machine direction produced a significant lateral compression of bond points. In the cross direction, the reposition of bond points and reorientation of fibres tend to occur towards the direction with relative ease. And different deformation mechanisms affect deformation of the bond point itself (Kim, H.S. and Pourdeyhimi, B. 2001b, Kim, H.S. and Pourdeyhimi, B. 2001c, Kim, H.S., Pourdeyhimi, B. and Abhiraman, A.S. 2001).
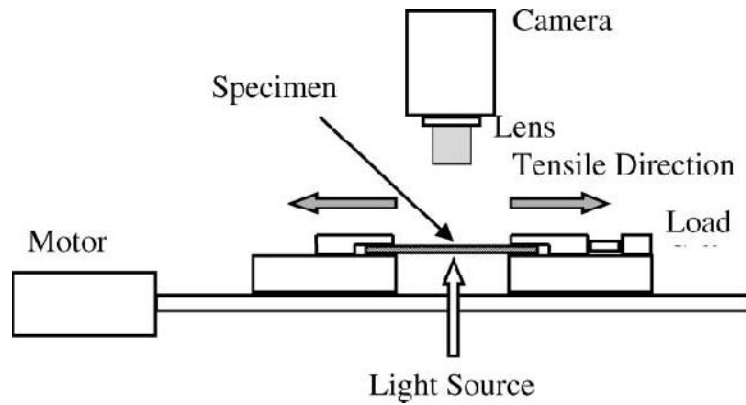
Figure 2.10: Set up used to characterise structural changes in nonwovens during load deformation experiments (Kim, H.S., Pourdeyhimi, B. and Abhiraman, A.S. 2001)
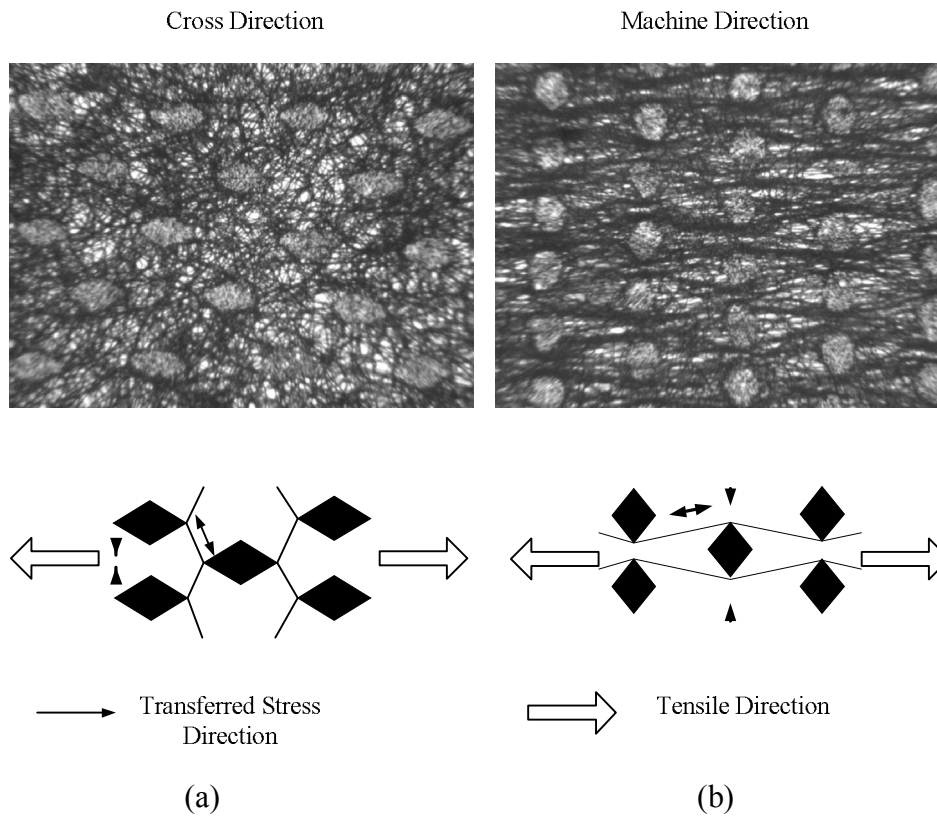
Figure 2.11: Images captured at 50% fabric tensile strain, with fabrics tested in the cross direction (a) and machine direction (b) (Kim, H.S. and Pourdeyhimi, B. 2000).

The image and mechanical performance theory was developed later. The model is the extension of the Mi-Batra model, which is one of web theories. (Kim, H.S. and

Pourdeyhimi, B. 2001b). The basic theory is shown in Figure 2.12. When the web is deformed, the extension of a fibre segment is described as

$$(l_0 + \Delta l)^2 = (y_0 + \Delta y)^2 + (x_0 + \Delta x + \tan\Delta\gamma.((y_0 + \Delta y)))^2 \ , \tag{2.16}$$

where Δl is the elongation of the fibre, Δx and Δy are the elongation in MD and CD respectively, and $\Delta\gamma$ is the shear strain in the web cell.
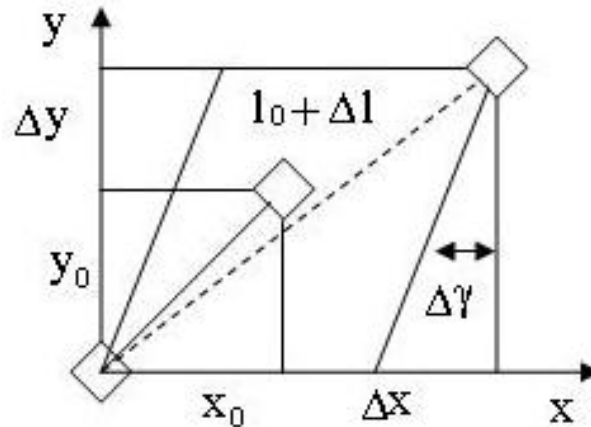
Figure 2.12: Incremental deformation of web (Kim, H.S. and Pourdeyhimi, B. 2001a).

Kim (2004) reported the development of the orthotropic theory for predicting the in-plane strain-stress relations for a nonwoven fabric using the orthotropic theory (Kim 2004a). A different approach to that in the Backer and Petterson's model was used. It allows the attainment of more meaningful compliance constants for nonwovens without the need for the ambiguous measurement of the Poisson's ratio. The polynomial regression analysis based on the transformation rule is used to predict the mechanical properties. The shear modulus is measured with the Kawabata Evaluation System (KES). The orthotropic strain-stress relationship is

$$\begin{Bmatrix} \varepsilon_1 \\ \varepsilon_2 \\ \gamma_{12} \end{Bmatrix} = \begin{bmatrix} S_{11} & S_{12} & 0 \\ S_{12} & S_{22} & 0 \\ 0 & 0 & S_{44} \end{bmatrix} \begin{Bmatrix} \sigma_1 \\ \sigma_2 \\ \tau_{12} \end{Bmatrix} \ , \tag{2.17}$$

The tensile modulus at an arbitrary direction is given for planar orthotropic structures, which is computed by regression analysis method:

$$\frac{1}{E_X(\theta)} = S_{11}(\theta) = S_{11} \cos^4\theta + S_{22} \sin^4\theta + 2S_{12} \cos^2\theta \sin^2\theta + 4S_{44} \cos^2\theta \sin^2\theta$$

, (2.18)

$$= C_1 + C_2 \sin^2\theta + C_3 \sin^4\theta$$

where

$$C_1 = S_{11} \ ,$$ (2.19)

$$C_2 = -2S_{11} + 2S_{12} + S_{44} \ ,$$ (2.20)

$$C_3 = S_{11} + S_{22} - 2S_{12} - S_{44} \ .$$ (2.21)

The "layer theory" is one of the important improvements to the orthotropic theory for the nonwoven materials. In 1995 Bais-Singh and Goswami presented their theory, which assumes that the nonwoven web is made up of a number of layers of fibres. In each layer, fibres are straight lines aligned in the same direction, as shown in Figure 2.13. So the fibre orientation distribution can be represented by the layer system (Bais-Singh, S. and Goswami, B.C. 1995). In this theory, the fibres cannot transmit load when in compression. And the extensional stiffness of layers, which are perpendicular to the fibre direction and the shear stiffness parallel to the fibre direction, are almost negligible. In 1998, they improved the model by introducing the effect of fibre buckling and material nonlinearity (Bais-Singh, S., Biggers, S.B.JR. and Goswami, B.C. 1998). By using finite element analysis, the model can predict the variation of Poisson's ratio with longitudinal strains, which cannot be achieved by most of the present models.
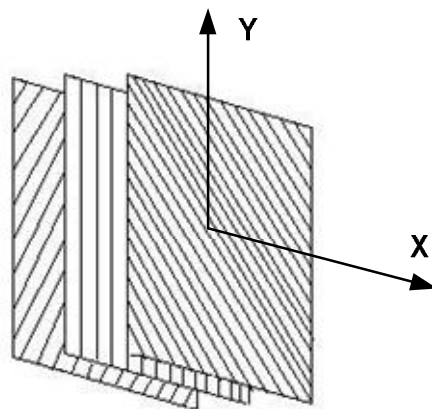
Figure 2.13: Layered structure of a typical unit cell

In 1997, Liao and Adanur published their FE model, which combined the ideas of "cell units" and "layer theory" (Liao, Adanur 1997). The model assumes that the nonwoven fabric is composed of a finite number of discrete cells, which are finite elements in the model. Each element has a different structure and property. And within each element, the fabric is made up of a number of fibre layers, within each layer the fibres are arranged according to the measured ODF, and the layers are connected by fibres orientated perpendicular to the layer plane (Figure 2.14) (Liao, Adanur 1999b).
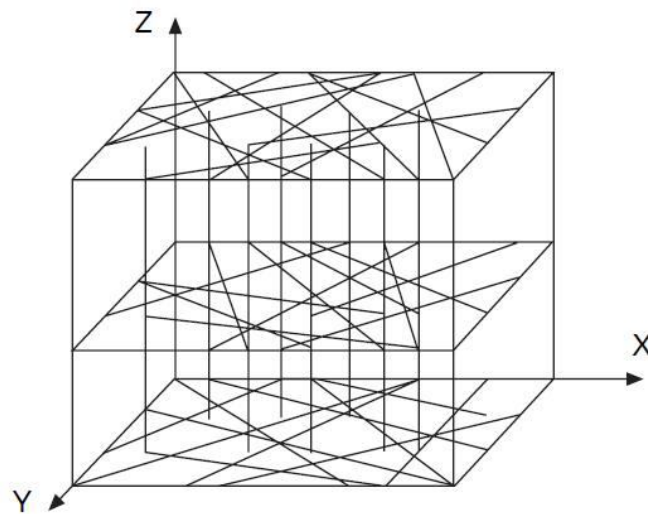
Figure 2.14: Example of a simplified three-dimensional nonwoven structure (Russell 2007, Liao, Adanur 1997)

2.5.2 Deformation mechanism and failure mechanism of nonwoven material
Deformation and failure

Although many studies have been done to investigate the mechanical properties of nonwoven materials, only few of them investigate a deformation mechanism of these materials. In 2000, Kim and Pourdeyhimi published the work on characterization of structural changes in a nonwoven fabric during a load-deformation experiment using a specially designed device (results are shown in Figure 2.10) (Kim, H.S. and Pourdeyhimi, B. 2000). They described the reorientation of fibres in specimens during the deformation. When CD samples were tested, the dominant orientation angle was between the machine direction and the loading direction. Large deformation, which is influenced by the structure reorientation and bond strain, occurs in the direction of

extension (Kim, H.S. and Pourdeyhimi, B. 2001c, Kim, H.S., Pourdeyhimi, B. and Abhiraman, A.S. 2001, Kim, H.S., Pourdeyhimi, B. and Abhiraman, A.S. 2001). However, when the MD samples are tested, because the loading direction is the one coinciding with the material's preferred orientation, the effect of deformation is primarily due to the increase in the preferably oriented fibres. The effect of bond points also indicates that their different properties result in different mechanisms of failure and affect the mechanical properties of the whole fabric.

One of other important characteristics of the deformation mechanism of nonwovens is the shear strain generated along the preferred direction of the fabric under uniaxial extension. The preferred direction is determined by the structure of the fibrous network, e.g. the fibre orientation distribution function and the shape and arrangement of bond points. But in the Kim's later study, the tensile behaviour of thermally bonded nonwoven materials is more complicated. It is governed by a different load transfer mechanism, which is affected by tension, shearing and compression modes of constituent fibres, and results from the tensile load and simultaneous lateral contraction (Kim 2004b).

If the oriented nonwoven samples, which have the maximum of the orientation distribution function in one direction, are subjected to shear deformation at positive and negative angles, tension will be dominant for positive and compression for negative angle to the preferred direction of constituent fibres (Kim 2004a).

In Figure 2.15, the preferred orientation of the nonwoven material is the machine direction (0º), and under the tensile strain, shear strain is generated alongside with the tensile strain according to the preferred orientation of fibres and the angles of the samples. Therefore, at negative angles, an in-plane compressive force would be generated along the lateral side of the sample. And the compression force results in fibre bending, bulking or the fabric bulking. For a positive angle, a tensile force would be generated along the lateral side of sample. But for the whole sample, it is easy and safe to assume, that in a nonwoven material's specimen with the symmetrical orientation distribution with regard to the test direction, both positive and negative shear strains will be generated at the same rate, and the overall shear strain generated in the fabric specimen will be zero (Bais-Singh, S., Biggers, S.B.JR. and

Goswami, B.C. 1998). In the asymmetric case, the mechanism will be more complicated according to the bonding type and the ODF.
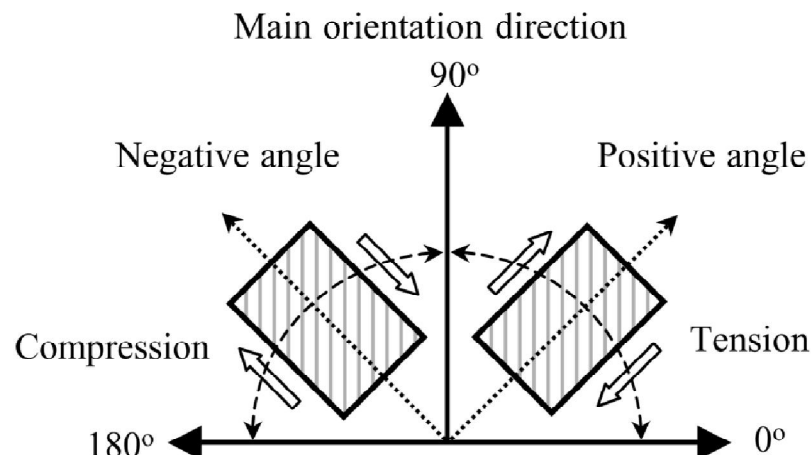
Figure 2.15: Schematic diagram of shear deformation for negative and positive angle directions (Kim 2004a).

The results of failure of nonwovens shows different load transfer mechanisms due to shear stress along the initially preferred direction in the fibre ODF, in the cases where the two directions are either parallel or normal to each other (Figure 2.16) (Kim 2004b). In more detail, the failure is generally initiated at the bonded/nonbonded interfaces at higher bonding temperatures (Kim, H.S., Pourdeyhimi, B. and Abhiraman, A.S. 2001). Basically, this failure analysis stays at macro-scale. There are also failure analyses based on the material features at micro-scale. There are two main possible mechanisms for the failure of nonwoven fabrics in tensile deformation: (1) fracture at the bond perimeter, (2) degeneration of the bonds, followed by fibre fracture (Michielsen, S., Pourdeyhimi, B., and Desai, P. 2006, Anderassen, Myhre et al. 1995). When the bond points are well bonded or over-bonded, the fabric usually fractures at the bond periphery, because the fibres in these areas experience a complex thermal and mechanical process during bonding, and their strength decreases due to the reduction of their birefringence (Fedorova, Verenich et al. 2007). When the bond point is not properly bonded, which could be due to lower pressure or low temperature, the fabric tends to fracture by disintegration of bond points (Michielsen, S., Pourdeyhimi, B., and Desai, P. 2006).

0 °(MD)   34°   90°(CD)
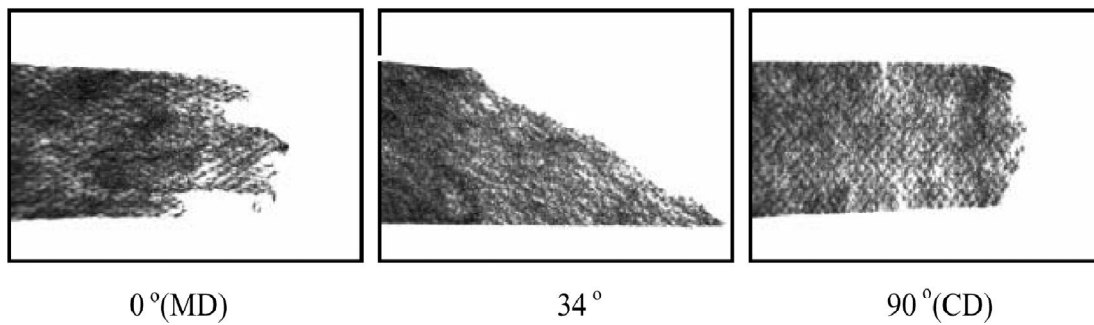
Figure 2.16: Rupture images of nonwovens for various directions of applied macroscopic tensile load (Kim 2004b)

Initial nonlinear deformation

As well known, material nonlinearity stems from two main sources: material nonlinearity and geometric nonlinearity. For nonwoven material, besides the nonlinearity caused by the nonlinear material properties of fibres and bond points, the discontinuous microstructure and characteristics of fibres also lead the overall fabric to perform nonlinearly. In a tensile test, the nonwoven material behaves nonlinearly before its linear performance; this is called initial nonlinearity. This phenomenon is unique compared to typical solid materials. Generally, many factors affect the nonlinear behaviour of nonwoven materials, especially the properties of fibres and the structural parameters of the fibrous network.

One of the important factors is the fibre curl. Figure 2.17 shows a fibre layer consisting of fibres with different levels of curl. In this case, when the fibre layer is extended, only some of the fibres with a low curl level sustain the strain and are the main carrier of the load, while the fibres with a high curl level keep their curled state (Adanur, S. and Liao, T. 1999). As the figure reveals, the different curl levels determine the different tensile performance. At the initial stage of the deformation this feature leads to a nonlinear behaviour of the material.
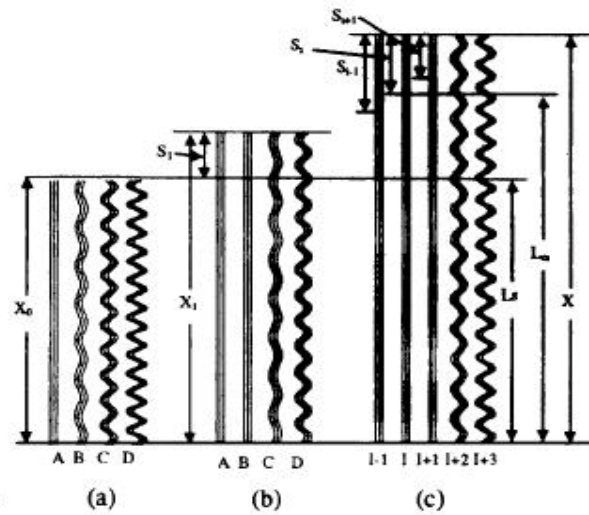
Figure 2.17: Schematics of extension fibres of with different curls: (a) first step, (b) second step, (c) general case (Adanur, S. and Liao, T. 1999).

Among other factors, which cause the nonlinear behaviour, is the bi-linear strain-stress relationship of fibres at the initial stage of the extension (Bais-Singh, S., Biggers, S.B.JR. and Goswami, B.C. 1998, Bais-Singh, S. and Goswami, B.C. 1998). As shown in Figure 2.18, at this stage the initial linear behaviour happens when the fibre strain ε_1 is below a tensile yield strain ε_y, and when the strain is beyond that level, the tensile behaviour transmits to another linear behaviour. Besides the buckling behaviour was also includes in the model by determining a critical negative strain ε_c.
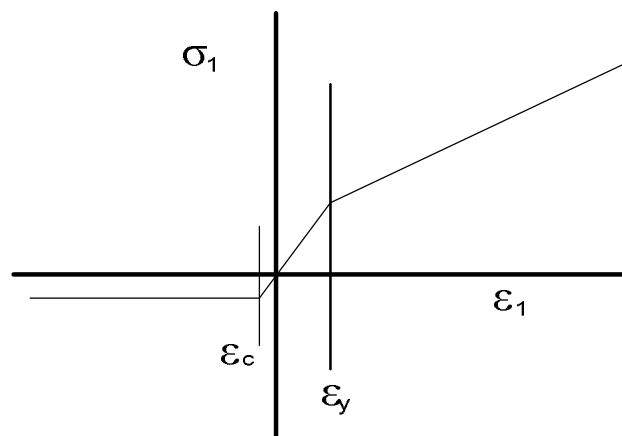
Figure 2.18: Assumed strain-stress relationship of fibre layer in FEA model (Bais-Singh, S., Biggers, S.B.JR. and Goswami, B.C. 1998).

Recently, in 2005, Limen and Warner also described fibre buckling as the result of tensile tests of their PP filaments. But in their model, they only introduced the bi-linear behaviour but not the fibre buckling (Limem, S. and Warner, S.B. 2005). In 2006, researchers studied the nonwovens as a viscoelastic material (Mishakov, V. Slutsker, G. and Stalevich, A. 2006); Rawal used a series of an ideal elastic spring and an ideal viscous dashpot to represent fibre segment and bond points of thermally bonded nonwoven material in his model (Rawal 2006).

2.6 Numerical simulation of thermally bonded nonwoven materials

Various researchers have done many efforts to describe the mechanical properties of nonwoven materials. However, most of the works have been done using experimental methods. Due to the complicated microstructure of the nonwoven material, researchers start to realise the limitation of the experiments and try to use numerical methods to investigate the material. This section focuses on the numerical methods, which have potential to describe the mechanical properties of nonwoven materials. Moreover, the advantage and limitation of existing models are discussed.

2.6.1 Classic theory for composite material

As well known, the thermally bonded nonwoven material is composed of two components: thermally bonded points and a fibrous network. The two-phase structure is similar as composites materials. As the stiffer component of the nonwoven material, bond points are important to the overall material performance. They determine different deformation and failure mechanisms of the nonwoven material. Therefore, their effect cannot be ignored nor can they be simply treated as a rigid body. To include the material properties of bond points into a numerical model, the classic theory for composite material could be used for reference. A composite is a material made from two or more physically different constituents, each of which largely retains its original structure and identity (Oxford English Dictionary). Composite materials are widely used nowadays, and their theory is well developed. Mechanical properties of composites vary with their structure; the composites can be homogenous, heterogeneous, layered, orthotropic and anisotropic. Actually, for a thermally-bonded nonwoven material, to some extent, it is possible to find some common features with

composites with regard to the structure and mechanical properties. For example, the orthotropic theory was the one widely used in the researches of both nonwoven and composite materials. Figure 2.19 shows a geometric model for a fibre-reinforced composite material, which can be confusing due to a structure similar to thermally bonded nonwoven materials.
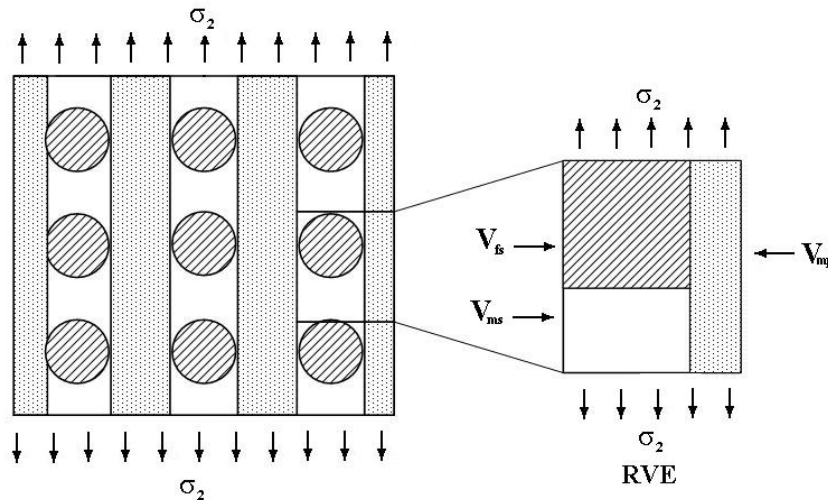
Figure 2.19: Idealization of geometry for combined series and parallel model of composite (Daniel, I.M. and Ishai, O. 2006).

To describe the combination model as shown in Figure 2.13 Shaffer developed his model in 1964, which became one of the classic approaches (Shaffer 1964).

$$E_2 = E_m V_{mp} + E_{2s}(1 - V_{mp}),$$ (2.22)

where E_{2s} is the modulus of the series portion of the element given by

$$E_{2s} = \frac{E_{2f} E_m}{E_m V_{fs} + E_{2f} V_{ms}},$$ (2.23)

and

V_{mp} is an overall volume ratio of parallel matrix columns,

V_{fs}, V_{ms} are fibre and matrix volume ratios of series portion, respectively.

Another solution was developed by Halpin-Tsai in 1967 (Daniel, I.M. and Ishai, O. 2006). The modulus is

45

$$E_2 = \frac{E_m(1 + \xi\eta V_f)}{1 - \eta V_f} \quad , \tag{2.24}$$

where

$$\eta = \frac{E_{2f} - E_m}{E_{2f} + \xi E_m} \quad , \tag{2.25}$$

The parameter ξ is obtained from an experimental value of E_2 as a curve-fitting parameter. Usually, it is assumed that ξ=1 for hexagonal arrays and ξ=2 for square arrays.

Another evidence, which proves that composite materials could share some features with nonwoven materials, is the Cox's model. It is not only used by researchers of nonwovens but also treated as a classic theory by composite researchers. Figure 2.20 shows a RVE geometry before and after deformation. Using the Cox's theory, researchers analysed the shear and axial fibre stresses in the element (Cox 1952, Daniel, I.M. and Ishai, O. 2006). And the average stress of the composite RVE is

$$\sigma_1 = V_f \overline{\sigma_{1f}} \_ V_m \overline{\sigma_m} = [V_f E_{1f}(1 - \frac{\tan(\beta l/2)}{\beta l/2} + V_m E_m]\varepsilon_1 \quad , \tag{2.26}$$

where

$$\beta^2 = \frac{n^2}{r^2}, \tag{2.27}$$

$$n^2 = \frac{2G_m}{E_{1f} \log(r_0/r)}, \tag{2.28}$$

V_f is the volume ratio of fibres,

V_m is the volume ratio of matrix,

$\overline{\sigma_{1f}}$ is the average fibre stress,

$\overline{\sigma_m}$ is the average matrix stress,

E_{1f} is the modulus of fibre in x direction,

E_m is the modulus of matrix,

G_m is the shear modulus of matrix,

r_0 is the radius, which is related to the fibre radius and the fibre volume ratio :

$$r_0 = \frac{r}{\sqrt{V_f}} \quad , \tag{2.29}$$

r is the radius of a fibre,

l is the length of a fibre.

Before deformation
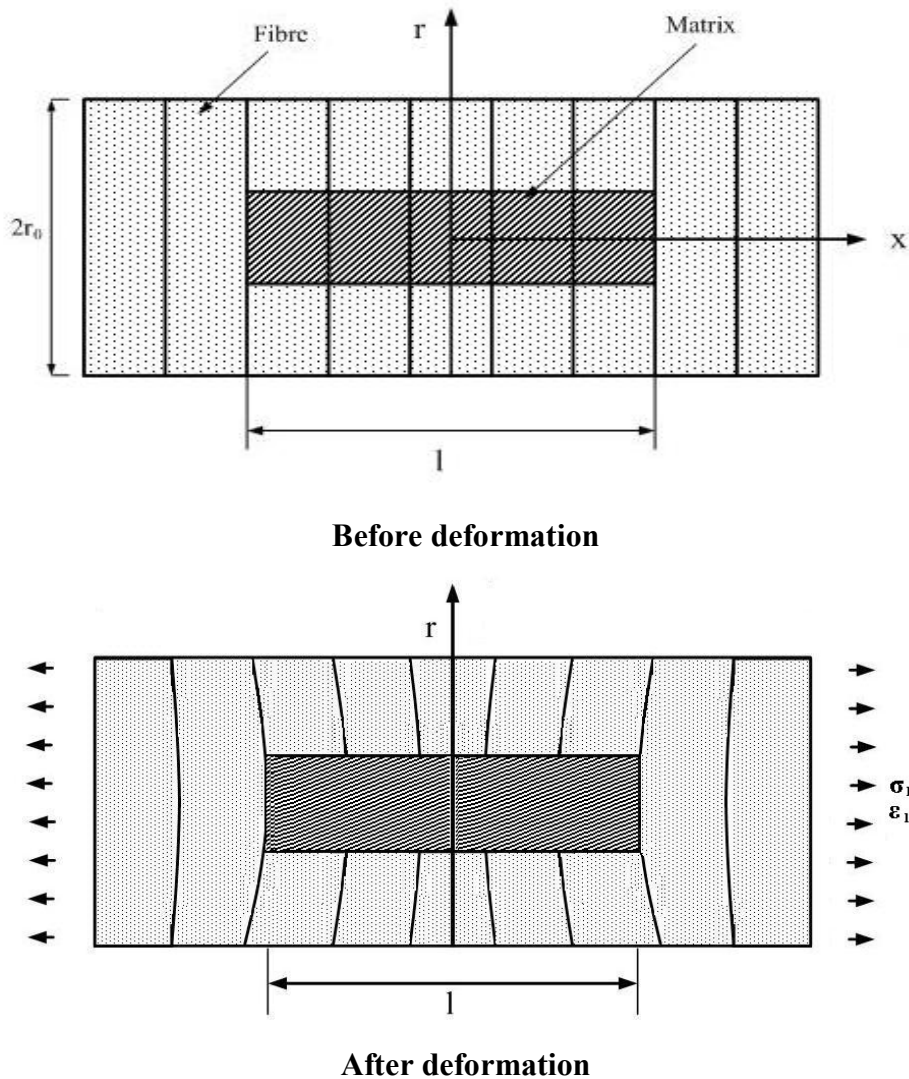
After deformation

Figure 2.20: Representative column element before and after deformation (Daniel, I.M. and Ishai, O. 2006)

Besides this similarity with regard to structure, composite materials also could provide a mature sight into basic parameters of nonwovens like the fibre length distribution, measurement of the Poisson's ratio and shear modulus and so on

(Petterson, D.R. and Backer, S. 1963, Hine, P.J., Lusti, H.R. and Gusev, A.A. 2002, Böhm 2004).

2.6.2 Lattice model

A lattice (or spring network) model is a physical model that is defined on a lattice, as opposed to the continuum of space (Ostoja-Starzewski 2002a). The method is originally used to represent nonhomogeneous media. A mechanical lattice model typically consists of sites, which are connected to nearest neighbours by either springs, trusses or beams (Rinaldi, Krajcinovic et al. 2008). Due to the nature of lattice models, which are suitable to describe heterogeneous random structures and anisotropic material properties, a few researchers start to use the method to represent fibrous networks. One of such works is that by Britton and Sampson (1983) who developed a model to simulate the nonwoven material, which is built by spring-like fibre segments (Figure 2.21) (Britton, Sampson 1983). Later, they started to describe plastic deformation by introducing bond breaking (Britton, Sampson 1984a, Britton, Sampson 1984b).
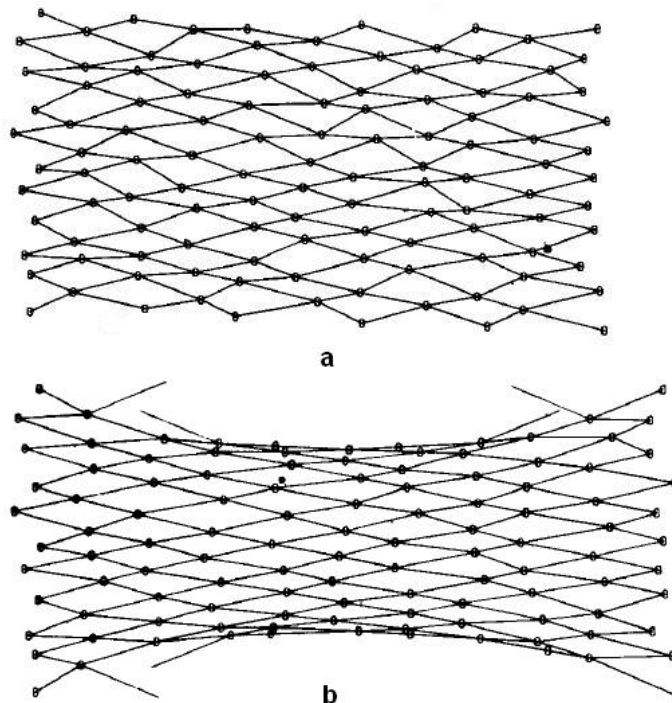
Figure 2.21: Computational model of nonwoven material (Britton, Sampson 1984a): (a): undeformed model; (b): deformed model with 10 % strain

2.6.3 Finite element analysis

To predict the mechanical behaviour of nonwoven materials, researchers have tried various approaches of numerical analysis. Recently, there has been a trend to describe the material using finite element analysis, which brings satisfactory solutions to other heterogeneous materials such as composite materials.

The finite element method is an analytical tool that subdivides an object into very small but finite-size elements. The method is endowed with three basic features. First, a domain of the system is represented as a collection of geometrically simple subdomains, called *finite element*. Second, over each finite element, the unknown variables are approximated by a linear combination of algebraic polynomials and undetermined parameters, and algebraic rations among the parameters are obtained by satisfying the governing equations, often in a weighted-integral sense, over each element. The undetermined parameters represent the values of the unknown variables at a finite number of preselected points, called *nodes*, in the element. Third, the algebraic relations from all elements are assembled using continuity and equilibrium considerations (Reddy 2004). With the fast development during last fifty years, the method is widely used for solving engineering problems such as: stress and vibration, heat transfer, fluid and electromagnetic. A typical analysis using the finite element technique requires the following information:

1. Nodal point spatial locations (geometry);
2. Elements connecting the nodal points;
3. Mass properties;
4. Boundary conditions or restraints;
5. Loading or forcing function details;
6. Analysis options.
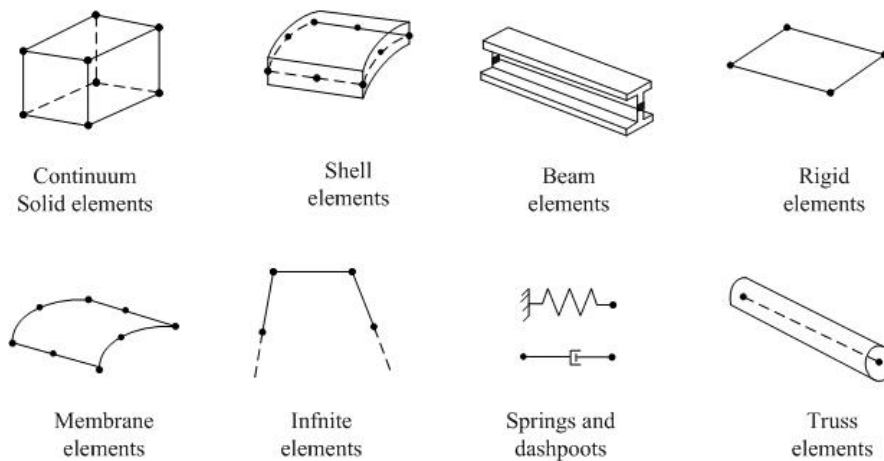
Figure 2.22: Commonly used finite elements (ABAQUS 2001)

Based on the concept above the analysis procedures of FEA are similar to each other. As an example, consider that a loaded structure requires analysis. The first step of any finite element analysis is to divide the actual geometry of the structure using finite elements. A variety of element shapes may be used (Figure 2.22), and different element shapes may be employed in the same solution region (Huebner, Dewhirst et al. 2001). The elements are joined together at *nodes*. The grids combined with nodes and finite elements are the *meshes*. The mesh contains the information about the material properties of a structure, which can characterize the structure when it is loaded. The number and type of elements depends on the anticipated stress distribution, so the node density could be different in different areas. When the problem has been divided into the discrete elements, the governing equations for each element are calculated and then assembled to give system equations that describe the behaviour of the body as a whole (Huebner, Dewhirst et al. 2001, Champion 1992, Desai, Kundu 2000).

Use of FEA in Nonwoven Materials

With development of the finite element method and an increasing capability of computers, there are still a few works on nonwovens using this method. As it was presented in Section 2.5.1, Bais-Singh and his colleagues employed in their simulation the "layers theory" using FEA code in 1995, which let them, incorporate nonuniform deformation (Bais-Singh, S., Biggers, S.B.JR. and Goswami, B.C. 1998, Bais-Singh, S. and Goswami, B.C. 1995). Later, they used the model to predict the

biaxial tensile deformation behaviour of the nonwoven material (Bais-Singh, S. and Goswami, B.C. 1998). The work successfully introduced the fibres' orientation distribution into the model, and described the nonuniform deformation, which was under compressive strain due to the boundary conditions of a tensile test and material's low stiffness. But in their theory some parameters, such as shear stiffness and the Poisson's ratio of the lamina, are hard to measure. And the model only has the capability to describe the nonuniform deformation caused by boundary conditions. It ignores the nonunifrom deformation resulted from the nonuniform microstructure of the material. Therefore, it is hard to get a good understanding of the nonuniform deformation mechanism of the nonwovens.

In 1997, Adanur and Liao reported their FEA model, which assumed that the fibres that make up the fabric were bound together at nodal points of the mesh of finite elements, and within each finite element the fabric is made up of a number of fibre layers (Liao, Adanur 1997). Later they introduced the effect of fibre curl to describe the nonlinear behaviour at the initial deformation stage (Adanur, S. and Liao, T. 1999). Based on their model, failure analysis also had been done with introduction of a fibre failure criterion (Liao, Adanur 1999a). The advantages of this model are that it is possible to define different material properties at different elements, and it is not necessary to know the fabric's Poisson's ratio values before calculation. Although the model is announced to successfully match the experiment, it still cannot reflect essential features of the nonunifrom deformation of nonwoven materials such as nonuniform density and reorientation of fibres.

In the previous numerical models, the works focused on the nonwovens, which have fibres bonded by the binders between fibres. Therefore, their models cannot be used to simulate the thermally bonded nonwovens, which have visible bond points through the fabrics. In 2004, Mueller and Kochmann suggested their model to simulate thermally bonded nonwovens (Mueller, D.H. and Kochmann, M. 2004). Solid elements are used to represent bond points and the connections between the bonded area are modelled using link elements (Figure 2.23).
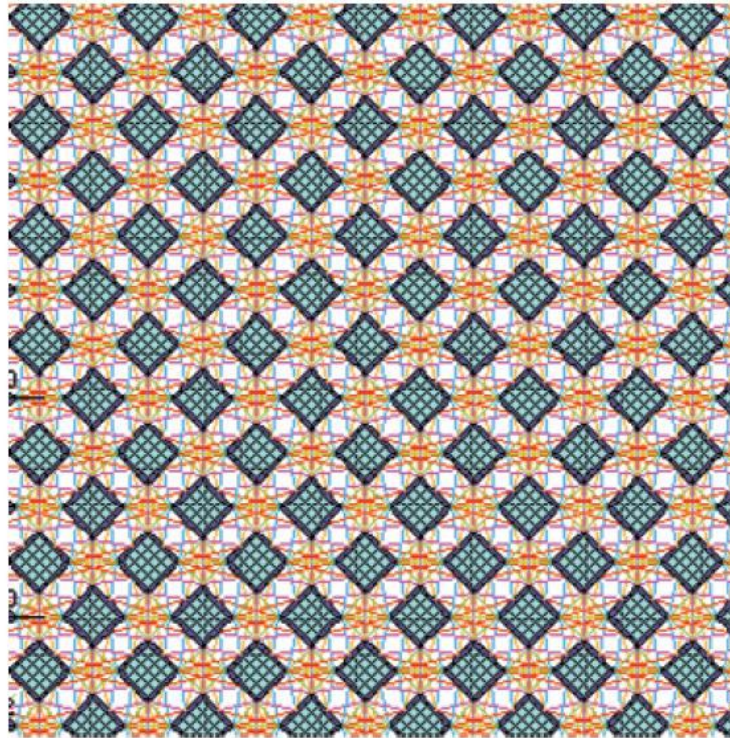
Figure 2.23: FE model of a thermally bonded nonwoven with square bond points (Mueller, D.H. and Kochmann, M. 2004)

To introduce ODF of fibres, which brings geometric nonlinearity into the model, each base cell consists of 22 fibre bundles with different orientations. The bond points are composed of two regions: well bonded zone and boundary zone. The boundary zone describes partly bonded and deformed fibres (Figure 2.24). The model is the first discontinuous FE model to simulate thermally bonded nonwoven fabrics and for the first time brings a method to describe the deformation mechanism of nonwovens in terms of the microstructure of the material. And because of its discontinuous structure, the model could cover the nonlinear behaviour caused by both the fibres' material properties and their geometric assembly. However, the model is still based on unit cells that mean the model structure is periodic. Therefore, it cannot properly represent ODF, various fibre lengths and material density. Hence, it cannot explain the deformation mechanism of thermally bonded nonwovens properly.
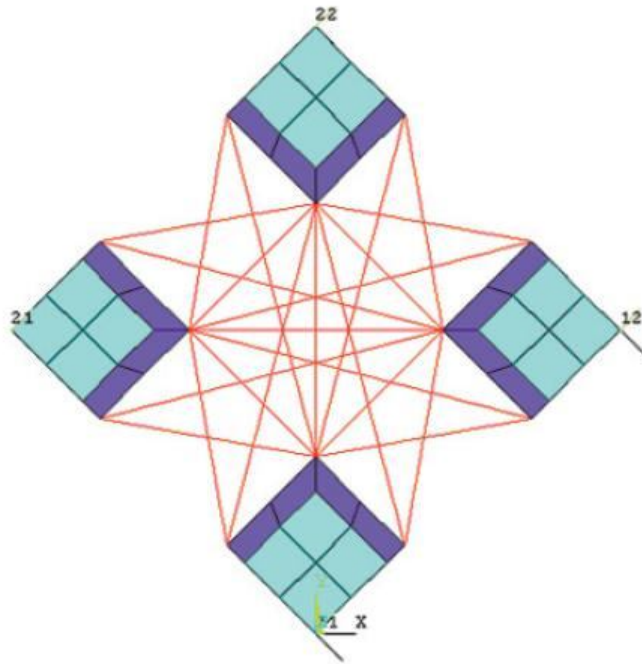
Figure 2.24: Base cell with bond points, boundary area and connecting fibres (Mueller, D.H. and Kochmann, M. 2004)

Another discontinuous model was published in 2005 by Limem and Warner (Limem, S. and Warner, S.B. 2005). To model adhesive point-bonded spunbond fabrics, they developed a truss-based model (Figure 2.25).
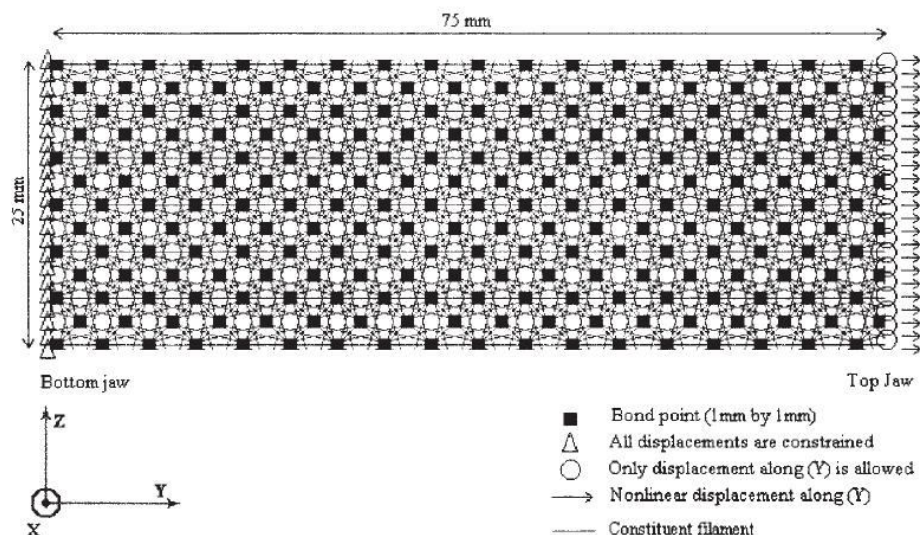
Figure 2.25: Geometry model of spunbond nonwoven fabric (Limem, S. and Warner, S.B. 2005)

The basic structure of the model is composed by eight groups: one group of bond point and seven straight fibre groups corresponding to seven fibre orientation angles covering the angular range from 0° to 180° (Figure 2.26). The bond points are assumed as isotropic and elastic, and failure is caused by rupture of fibres. Similar to the Mueller's model the structure of the model is still periodic, and it is impossible to represent properly the microstructure of nonwovens, which is highly nonuniformed. Although the results of the model are announced to have a good agreement with experimental results, it still cannot help understanding the deformation mechanism of nonwovens.
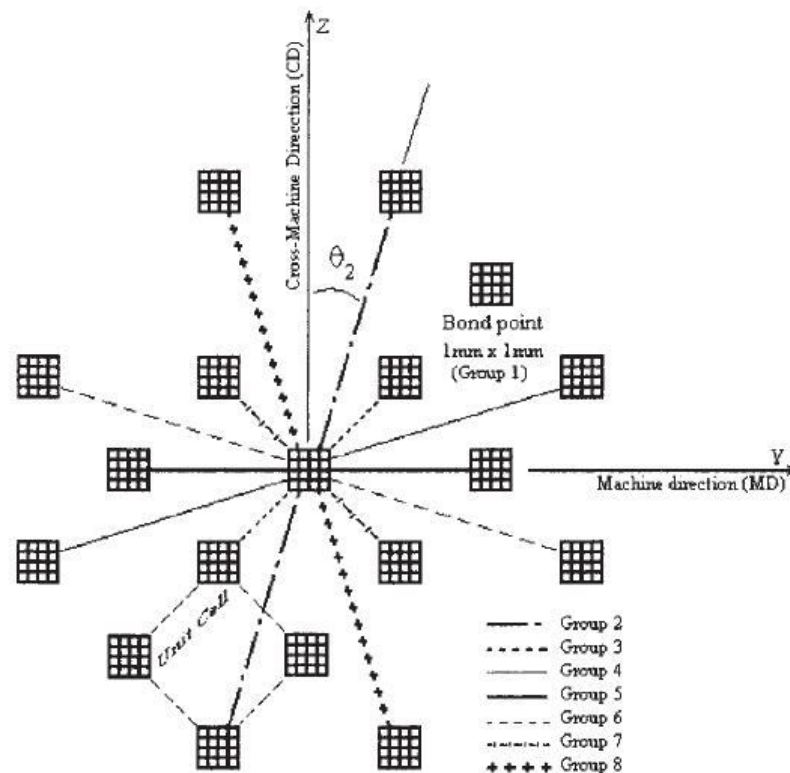
Figure 2.26: Bond point meshing and fibre group distribution (Limem, S. and Warner, S.B. 2005)

Beside the discontinuous models, some work have been done to model random heterogeneous materials using a representative volume element (RVE) in continuous FE models, such as composites and paper, which share a lot of common features with nonwoven materials (Ostoja-Starzewski, M. and Stahl, D.C. 2000, Shan, Gokhale 2002, Gusev 1997, Bronkhorst 2003, Ramasubramanian, M. K. and Wang, Y. 2007). A heterogeneous material is one that is composed of domains of different phases, or

the same material in different states (Torquato 2002). Hence, nonwoven materials could be classified as heterogeneous material, because the material is usually composed by fibres and bonded areas, or unbonded fibres and bonded fibres. The RVE element is widely used to model random heterogeneous materials. An RVE for a volume surrounding a point in a material is a statistically homogeneous representative of the material in the neighbourhood of the point. The concept is only defined in two situations: (1) a unit cell in a periodic microstructure, and (2) statistically representative volume containing a very large (mathematically infinite) set of microscale elements (Ostoja-Starzewski, 2002). For the heterogeneous material, RVE is the bridge which links macro and micro levels of materials description (Silberschemidt, 2005); it is used to represent the various microstructures by elements with various properties. Only a few models could be found to simulate nonwoven materials using RVE. Jacob and his colleagues simulated a compressive behaviour of a nonwoven fabric using RVE (Jacob, K.I., McDowell, D., Tech, G., Aneja, A.P. and Corporation, D. 2003). And in 2006, Engelmayr and Sacks published their model to simulate the flexural behaviour of nonwoven tissues.

The RVE concept is a powerful tool to study heterogeneous materials, and it is also possible to use it for modelling nonwoven materials. However, RVE cannot involve the some features of nonwoven materials, such as fibres' orientation distribution of the overall material due to the periodic structure of RVEs.

Chapter 3 Tensile Behaviour of Low-Density Thermally Bonded Nonwoven Material

3.1 Introduction

As discussed in Chapters 1 and 2, due to the complicated microstructure of nonwoven materials, their tensile behaviour of varies with manufacturing conditions. Therefore, to study the tensile behaviour of a thermally bonded nonwoven material, this study is limited to a thermally bonded nonwoven fabric (polypropylene fibres; density 20 gsm;) produced with a manufacturing speed of 250 m/min and the bonding temperature 146°C. It is a low-density nonwoven, which is generally used for medical and hygiene applications. Due to its low density, it provides a better opportunity for an optical analysis of the microstructure of thermally bonded nonwoven materials. It facilitates a study of the deformation mechanisms of such nonwovens by understanding the effect of its microstructures. To analyse the low-density nonwoven material, tensile tests performed by various researchers. Different test methods are available for nonwoven materials (Mao, Russell et al. 2007a):

- Standard test methods defined by standardizing authorities (e.g. BS EN ISO 13934-1:1999; ASTM D 5035 – 95);
- Test methods established by industrial associations (e.g. ITS 110.4; WSP 110.4; ERT 20.2-89);
- Non-standard test techniques designed for researcher purposes.

The important factors of tensile tests for nonwoven materials are the specimen's dimensions and loading speed. According to the literatures, different researchers follow different test standards in their research. For example, Kim and Pourdeyhimi used samples 25.4 mm (1 inch) wide and with a 101.6 (4 inches) gauge length in their researches and the tests involved a 100 %/min extension rate(Kim, H.S. and Pourdeyhimi, B. 2000, Kim, Pourdeyhimi et al. 2002, Kim, H.S. and Pourdeyhimi, B.

2001c). The shape factor (= gauge length/ width) of their specimens is 4. But Gautier and his colleagues chose a larger specimen (width-150 mm; gauge length-300 mm; shape factor 2) in their study and the test speed is 50 mm/min (Gautier,K.B., Kocher,Ch.W. and Drean, J. 2007). Being a highly nonhomogeneous material, the deformation mechanism of nonwoven material is affected by specimens' dimensions. A few of studies have been done to investigate the effects of the dimensions of nonwoven specimens, e.g. Bais-Singh (1996) analysed the effect of a gauge length and width of nonwoven specimens on the material's tensile behaviour (Bais-Singh, Anandjiwala et al. 1996).

This chapter focuses on the tensile behaviour of the low-density thermally nonwoven materials. Firstly, tensile tests are carried out for the specimens with varying dimensions and shape factors. The tensile's moduli are calculated based on the obtained stress-strain curves. Secondly, according to the analysis of the effect of dimensions on mechanical properties of the nonwoven material, a type of specimen, which is cut with representative dimensions, is chosen for the later studies. Finally, the tensile behaviour of the nonwoven material is analysed employing the results of standard tensile tests and images of the material's microstructure.

3.2 Tensile tests of specimen with varying dimensions

3.2.1 Specimens and analysis method

As well known, due to the specific features of the manufacturing process, the thermally bonded nonwoven material is highly anisotropic. Usually such materials are tested in two principle directions: machine direction (MD) and cross direction (CD) (Russell 2007). And the machine direction/cross direction (MD/CD) ratio of the material is used to represent the material's anisotropy (Wilson 2007). Therefore, strip-shaped specimens were prepared along both MD and CD. To determine representative dimensions for specimens in this research, uniaxial tensile tests were performed on specimens with various lengths and widths. There were two types of strip specimens: (i) specimens with a constant width and a varying length and (ii) specimens with a constant length and a varying width. In Table 3.1, the respective dimensions and shape factors - the ratio of the length to the width- are presented. The respective

shapes of the tested specimens are shown in Table 3.2.

Width (mm)	Length (mm)			
	12.5	25 (=2x12.5)	50 (=4x12.5)	100(=8x12.5)
	Shape factors			
5	2.5	5	10	20
10 (=2x5)	1.25	2.5	5	10
20 (=4x5)	0.625	1.25	2.5	5
40 (=8x5)	0.3125	0.625	1.25	2.5

Table 3.1: Dimensions and shape factors for tested specimen
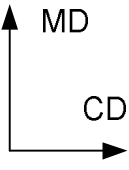
Table 3.2: Shapes of tested specimens for two directions

The equipment for tensile tests was a high-precision Instron Micro Tester 5848 with a 2 kN loading cell (Figure 3.1). Special clamps were manufactured to fix the strip specimens of nonwoven materials (Figure 3.2), which were designed to avoid the slips during the test and the damage of the specimen caused by the clamps. The clamp is formed by two pieces of metal sheets; the internal sides of the metal sheets are stuck with rubber sheets, which used to protect the specimens and generate more friction between specimen and clamp. When the nonwoven specimen is put between the metal sheets, two screws are used to connect the two metal sheets, which make the specimens clamped tightly.

Figure 3.1: Instron Micro Tester 5848

Figure 3.2: Clamps and sample installation

All the specimens were tested using testing speed 25 mm/min. A typical force-elongation plot of the tested nonwoven material (polypropylene fibres; density 20 gsm) is presented in Figure 3.3. There are three stages of the deformation of the nonwoven material: elastic stage, plastic stage and breaking stage. In the elastic stage, the material shortly performs linearly, and then it behaves non-linearly. After the specimen achieves its maximum force, it starts to break, and the breaking stage shows a substantial drop in the force level, which means the material usually, breaks in stages.
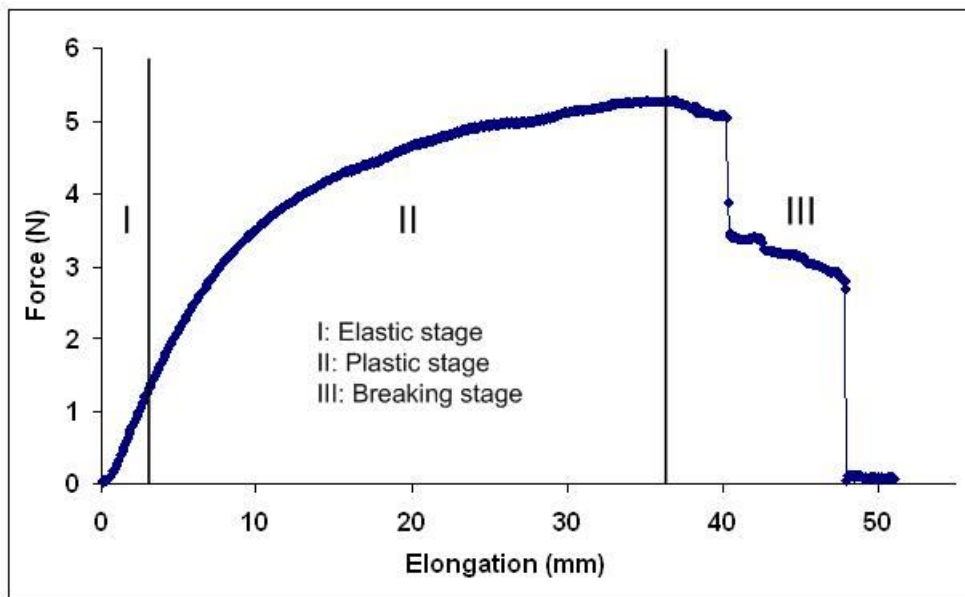
Figure 3.3: Typical force – elongation curve of the thermally bonded nonwoven material (direction: MD; gauge length: 25 mm; width: 20 mm; test speed: 25 mm/min)

Figure 3.4 shows both the engineering strain-stress plot and true strain – stress plot of the nonwoven material. The calculation method is shown as following

$$\sigma_{eng} = \frac{F}{W} \; , \tag{3.1}$$

$$\varepsilon_{eng} = \frac{l - l_0}{l_0} = \frac{l}{l_0} - 1 \; , \tag{3.2}$$

$$\varepsilon_{true} = \ln(1 + \varepsilon_{eng}) \; , \tag{3.3}$$

60

$$\sigma_{true} = \sigma_{eng}(1 + \varepsilon_{eng}) \ ,$$

(3.4)

Where

σ_{eng} is the engineering stress, expressed in *N/mm*, as is traditional for nonwoven material;

F is the force acting over the area *A* of the cross section of the specimen, expressed in *N*;

W is the initial width of the, expressed in *mm*;

l is the deformed length of the specimen, expressed in *mm*;

l_0 is the initial length of the specimen, expressed in *mm*;

ε_{eng} is the engineering strain;

σ_{true} is the true stress, expressed in *N/mm*;

ε_{true} is the true strain;
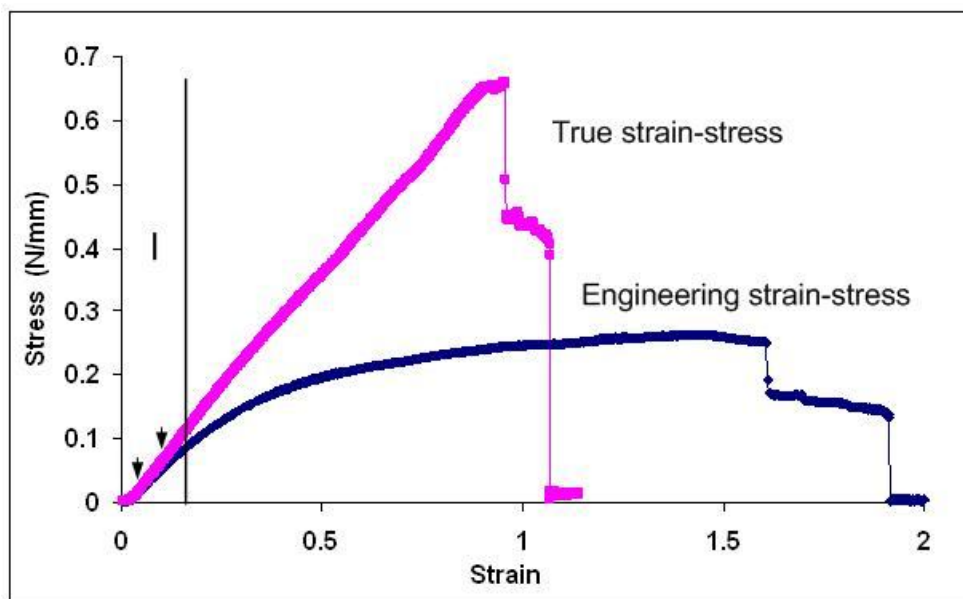
Figure 3.4: Comparison of true strain-stress curve and engineering stress-strain curve (Direction of the specimen: MD; gauge length: 25 mm; width: 20 mm; test speed: 25 mm/min)

In theory, the approach based on engineering strain/stress assumes that the cross area

61

(width, in case of nonwovens) of the specimen remain constant during the test. Therefore, it is usually used to describe the material exposed to relative small strain, which only has a small change in the cross area of the specimen. But when the material achieves large strains, a notion of true strain/stress is used due to a significant reduction of the cross section (width). However, according to the equations of both two methods, the strain-stress plots are similar in the initial stage. This is also obvious in graphs of our experimental results, as stage I, which is shown in Figure 3.4. Moreover, another difference between the true strain-stress curve and the engineering one is that the former shows almost a linear behaviour for the entire deformation process. It can not reveal the yield point, which indicates the elastic (linear) limit.

Due to the short linear period of the deformation, which is hard to be defined by true strain/stress curve, the tensile modulus was calculated according to the obtained engineering strain-stress plot. The relationship is $E = \dfrac{\Delta\sigma}{\Delta\varepsilon}$, where E is the tensile modulus, expressed in N/mm. The difference in stress $\Delta\sigma$ is calculated within the elastic stage for two strains and $\Delta\varepsilon$ is their difference. Based on the data of our experiments, the material's tensile moduli in both the machine direction and cross direction were determined and are presented in Tables 3.3 and 3.4.

Length (mm)	Width (mm)							
	5		10		20		40	
	Average Modulus (N/mm)	Standard Deviation	Average Modulus (N/mm)	Standard Deviation	Average Modulus (N/mm)	Standard Deviation	Average Modulus (N/mm)	Standard Deviation
12.5	0.99	0.13	1.42	0.15	0.45	0.06	1.22	0.18
25	0.71	0.08	0.68	0.09	0.55	0.04	1.13	0.1
50	0.88	0.06	0.97	0.07	0.75	0.03	0.94	0.09
100	1.38	0.15	1.53	0.07	1.57	0.12	1.74	0.16

Table 3.3: Summarised data for tensile modulus of nonwoven material (MD)

Length (mm)	Width (mm)							
	5		10		20		40	
	Average Modulus (N/mm)	Standard Deviation	Average Modulus (N/mm)	Standard Deviation	Average Modulus (N/mm)	Standard Deviation	Average Modulus (N/mm)	Standard Deviation
12.5	0.034	0.0057	0.042	0.0065	0.031	0.0064	0.048	0.0028
25	0.027	0.0097	0.030	0.0050	0.032	0.0084	0.043	0.0044
50	0.029	0.0065	0.037	0.0056	0.025	0.0031	0.043	0.0043
100	0.042	0.0050	0.080	0.0070	0.082	0.0058	0.0723	0.0035

Table 3.4: Summarised data for tensile modulus of nonwoven material (CD)

3.2.2 Effect of sample's length

To investigate the length effect, specimens of a nonwoven fabric with four different lengths – 12.5 mm, 25 mm, 50 mm and 100 mm – were tested. Specimens were cut along both MD and CD.

The results obtained for the machine direction are presented in Figure 3.5. For the specimens with the width 5 mm and 10 mm the average moduli considerately decrease with an increase in the gage length from 12.5 mm to 25 mm. The differences are 39.1% and 52.1%, respectively. The shape factor increases from 1.25 to 2.5 and 2.5 to 5, respectively. It shows that the material properties of the specimens with relative smaller width are not stable and cannot represent properly the mechanical properties of this kind of material. For specimens with the width is 20 mm and 40 mm, the change in the average moduli is smaller, when the gage length increases from 12.5 mm to 25 mm the differences are 22.2% and 7.3%. The changes of the shape factor are from 0.625 to 1.25 and 0.3125 to 0.626, respectively. An explanation for this phenomenon could be as follows: in MD, when the shape factor of specimens is smaller than 1, which means the length of the specimen is smaller than its width, the average moduli are closer to each other even while the length of the specimen changes. If we treat the modulus obtained for the specimen with the shape factor below 1, it can be considered as the initial modulus of the nonwoven material. We can deduce that the initial modulus of the nonwoven material is independent of the length change. And it could be assumed that the specimens with the shape factor smaller than 1 cannot represent the material properties of the nonwoven material. When the

specimen's length increases from 25 mm to 100 mm, the average modulus increases. There is only one exception - the specimen with the width of 40 mm with the length increasing from 25 mm to 50 mm the average modulus decreases (the shape factor increases from 0.625 to 1.25), which still indicates that the modulus is an initial one. The highest magnitudes of the average modulus are always obtained for the specimen's length specimen 100 mm, which means that specimens at the large-length scale generally have a more stable and better material is performance. For the specimens with the smallest length (12.5 mm), the obtained modulus is relatively high and not consistent. It shows, that when the shape factor of the specimen is smaller than 1, the effect of the specimen's width is evident. In this case, the obtained modulus is the initial one of the specimen and it cannot represent the material behaviour of the nonwoven fabric. For the specimens with 25 mm and 50 mm length, when the specimen's shape factor is larger than 1, the moduli are consistent, as shown by the circle in Figure 3.5.
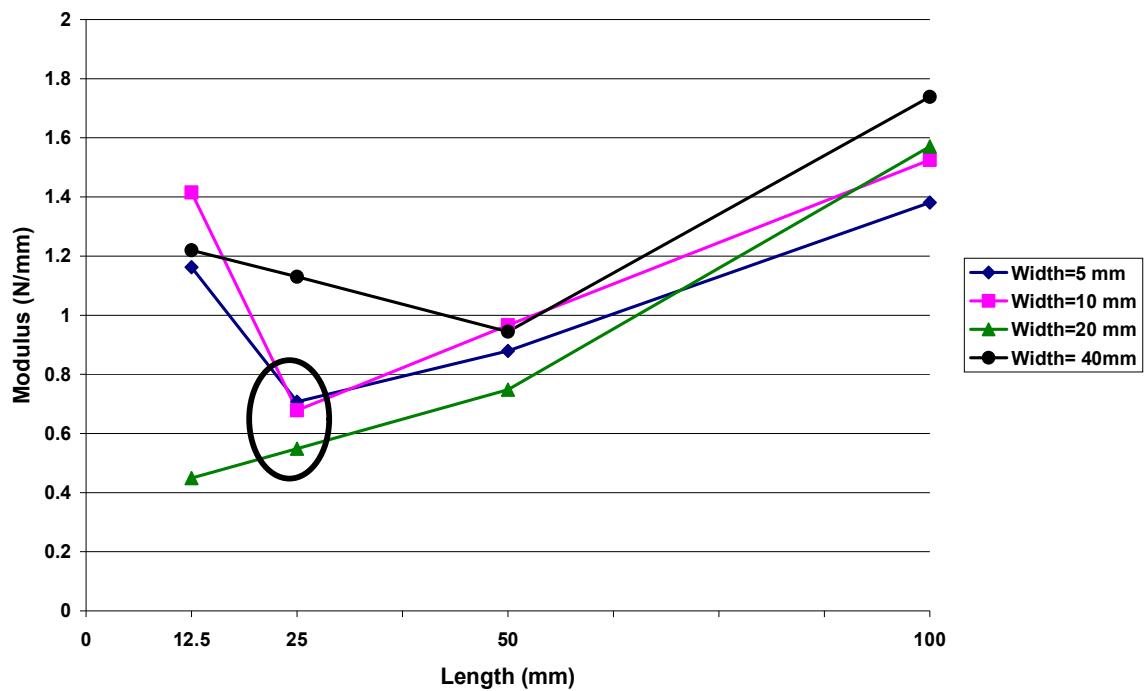
Figure 3.5: Effect of gage length on tensile modulus (MD)

For the cross direction (Figure 3.6), when the specimen's length increases from 12.5 mm to 25 mm, the average moduli of specimens with relatively smaller widths (5 mm, 10 mm) decrease by 19.5% and 30.0%. The shape factors increase from 2.5 to 5 and

1.25 to 2.5, respectively. The moduli of the specimens with widths 20 mm and 40 mm change by 3.9 % and 11.1%, respectively. The shape factors increase in this case from 0.625 to 1.25 and 0.3125 to 0.625. This phenomena once more confirm the conclusion that the effect the gage length is smaller when the specimen's shape factor is smaller than 1. But when the shape factor is bigger than 1, the modulus changes at a larger scale and the effect of the length becomes more important. When the specimen's length increases to 100 mm, the average modulus increases significantly, e.g. when the specimen's width is 20 mm, the modulus increase by 222.7 %, which is the largest increase. Similar to the results obtained for MD, the specimens with a large length (e.g. 100 mm) have higher moduli. The only exception is the specimen with the smallest width (5 mm), which cannot represent the material behaviour due to its excessive large shape factor (20). For the specimens, which have the shape factor bigger than 1, the moduli obtained from the specimens with 25 mm length are consistent, as shown by the circle in Figure 3.6.
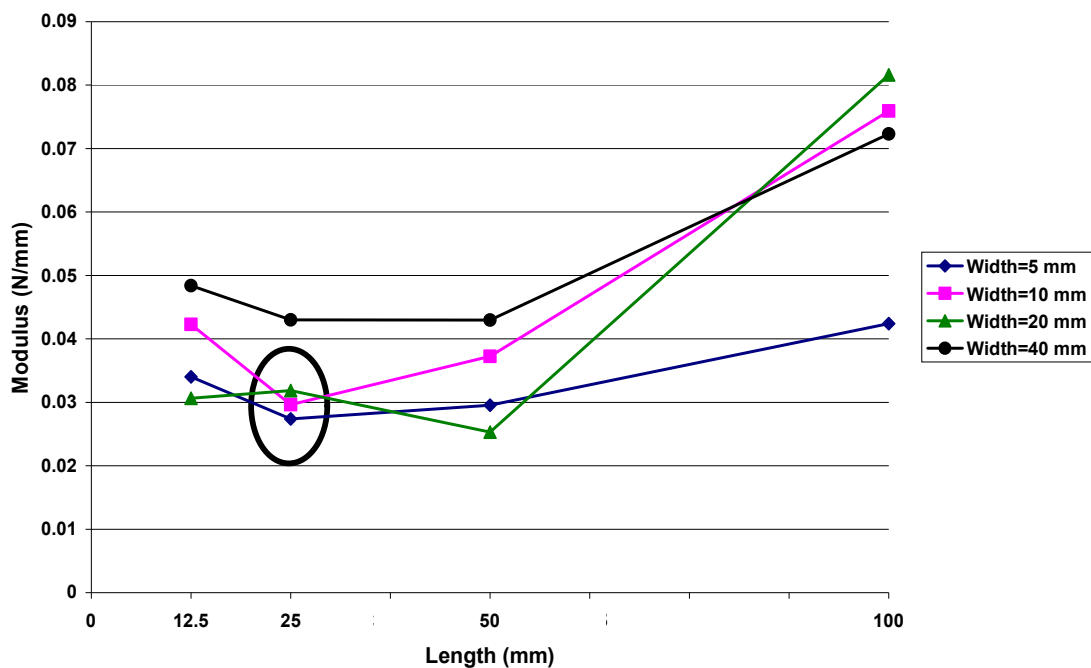
Figure 3.6: Effect of gage length on tensile modulus (CD)

3.2.3 Effect of width

To investigate the width effect, specimens of a nonwoven fabric with four different widths – 5 mm, 10 mm, 20 mm and 40 mm – were tested. Specimens were cut along

MD and CD.

In machine direction, for the specimen's length of 50 mm and 100 mm, similar average moduli were obtained for the entire range of width (Figure 3.7). It means the specimens with a relatively large width have a more stable material performance than the specimens with smaller widths. The shape factors decrease from 10 to 2.5 and from 20 to 5. And in a combination with the results of the analysis of the length effect, it is possible to deduce that the specimens with large dimensions show stable material properties since the effects of features of the material's microstructures are more fully represented in the tested volume. But when the length of the specimen is 12.5 mm and 25 mm, big changes of average moduli were obtained. The average modulus of specimens with the 12.5 mm length at first declines (by 68.3%) and then increases (by 171.8%) when the width increases from 10 mm to 40 mm. The shape factor decreases from 1.25 to 0.3125. For the specimens with the 25 mm length, the average modulus increases by 100.6 % with the width increasing form 20 mm to 40 mm. The shape factor changes from 1.25 to 0.625. The results indicate that the change of the width affects the material properties significantly, when the shape factor of the specimen decreases from the magnitude above 1 to the one below 1. This phenomenon is just opposite to the effect of length. Another insight of the analysis is that it confirms once more that the specimens with a relatively large width have similar moduli, except the specimens with the largest length (100 mm), which have much larger moduli. The phenomenon demonstrates that the large width brings a more stable material performance of the specimens. Similar results were also obtained for the specimens with a 20 mm width as shown by the circle in Figure 3.7. For the specimens with relatively smaller widths, 10 mm and 5 mm, higher moduli and larger scatter were obtained, which means that the specimens with smaller widths do not show stable material behaviour and may not reflect a real deformation mechanism of the material.
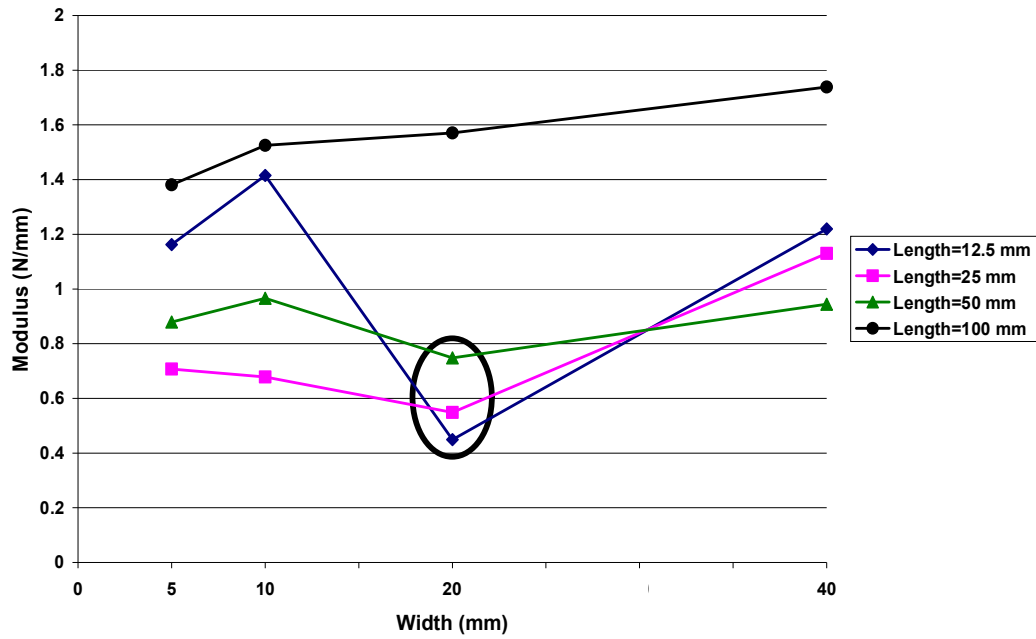
Figure 3.7: Effect of width on tensile modulus (MD)

For the cross direction (Figure 3.8), the specimens with a 100 mm length have similar average moduli for the level of width 10 mm, 20 mm and 40 mm, the smallest average modulus was obtained when the width was 5 mm, which was 79.1% lower than the average modulus obtained for specimens with a 10 mm width. The shape factor is 20, which is highest in all the specimens. The phenomenon shows again that the specimens with large length have stable and better material performance, except the specimen with the smallest width (5 mm). For specimens with length 12.5 mm, 25 mm and 50 mm, the magnitudes of average moduli have very low magnitudes close to each other. Although there are variations as the width changes, the similar average moduli were obtained due to the poor mechanical performance.
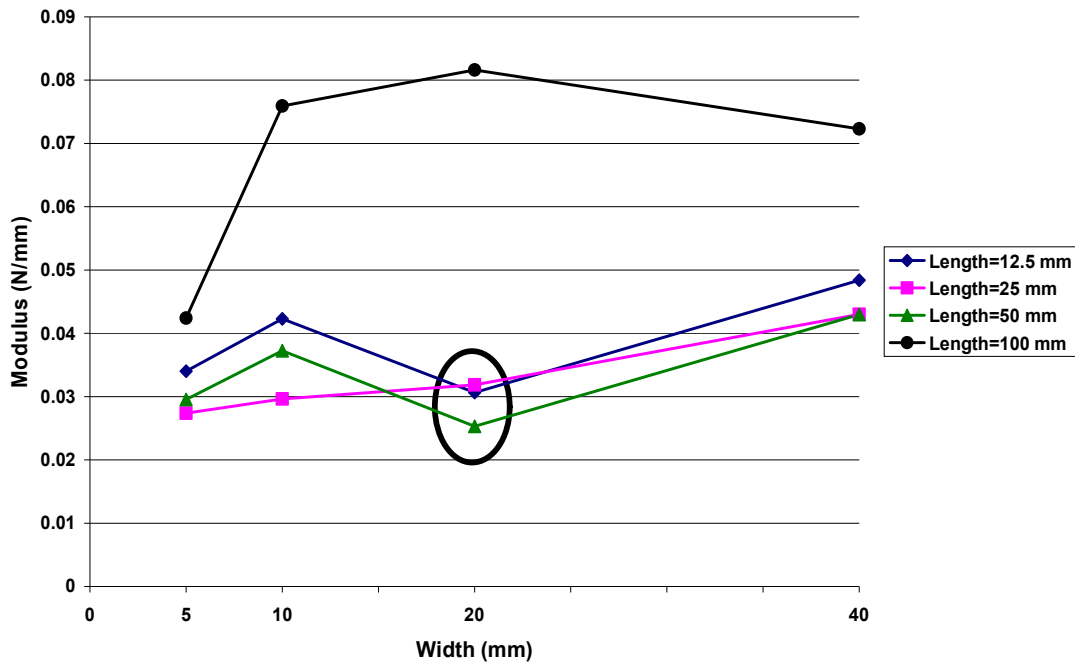
Figure 3.8: Effect of width on tensile modulus (CD)

According to the above analysis, it is apparent that the specimen's dimensions affect the material properties significantly. Although the material performs with a high extent of variability due to its nonhomogeneous and discontinuous microstructure, the analysis still indicate some trends for the effects of material's dimensions on its mechanical properties.

- For the specimens with a relatively small width the material performs unstably and the obtained results show a big scatter. Therefore, these specimens would not represent the material properties of the nonwoven material. But for the specimens with a relatively large width, the consistent results could be obtained.

- For the specimens with larger lengths, generally, the material properties are improved and the material performs stably. But when the length of the specimen decreases to a certain level, the material start to behave unstably.

- When the specimen's shape factor is smaller than 1, which means the length of

68

the specimen is larger than its width, the length effect is not significant, but the effect of width plays a more important role. However, the moduli obtained from these specimens are initial moduli, which cannot describe the real material properties of the nonwoven material.

In summary, the specimen's dimensions affect the material behaviour distinctly. The specimens with smaller dimensions do not behave stably. For the specimens with large dimensions, although the experiment results are consistent, the effect of material's microstructure is hard to study in the specimens making the analysis more complicated. Therefore, according to the above experiment results, in the next stage of the research, specimens with dimensions as 25 mm gauge length and 20 mm width are prepared to be studied in both experimental and numerical analysis.

3.3 Deformation mechanisms of low-density thermally bonded nonwoven material

According to the literature and the analysis in previous section, it is evident that the deformation mechanisms of nonwoven material are affected by its microstructure. For the low-density thermally bonded nonwoven material, the effect of its microstructure is more significant. First, due to the manufacturing process, it is clear that the nonwoven material includes two components: a fibrous web and bonding points. Rectangles, forming a regular pattern in Figure 3.9 (a), are bonding points and other parts of nonwoven forms the fibrous web. Figure 3.9 (b) shows a bonding point, which is formed by partially melted and compressed fibres. As a result of this thermal process the areas of bonding points are much stiffer than the areas occupied by the fibrous web since the fibres in these points are glued together and their relative movements that are responsible for high stretching ability of the fibrous network are severely restricted. Besides, the two components microstructure, which could strongly affect the strain/stress distribution in the nonwoven material during its extension, the randomly discontinuous microstructure of the fabric may cause randomly nonhomogenous local strain/stress transformations in the material. Therefore, to understand the deformation mechanism of the low-density thermally bonded

69

nonwoven material, the results of tensile tests should be analysed by combining with the image analysis of its microstructure.
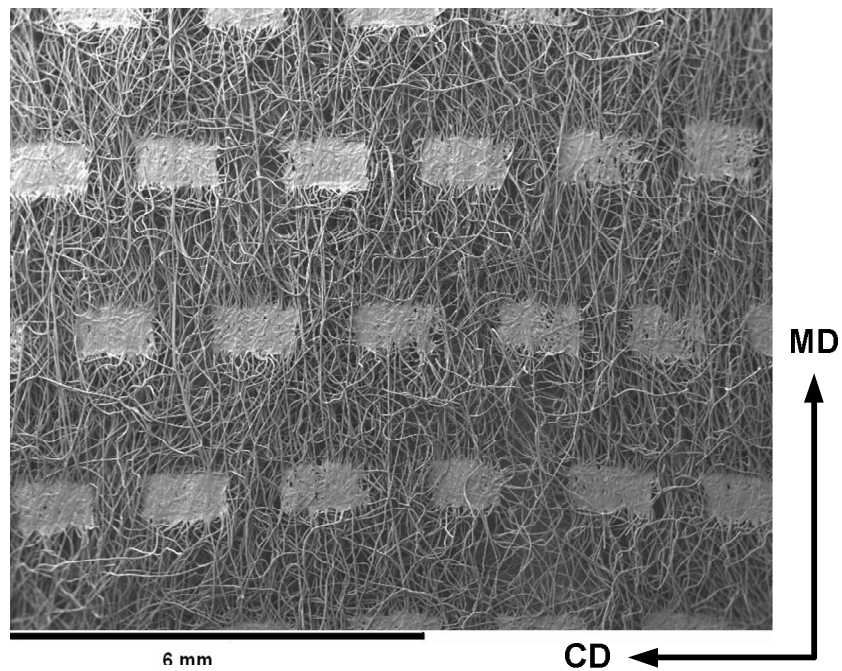
(a)
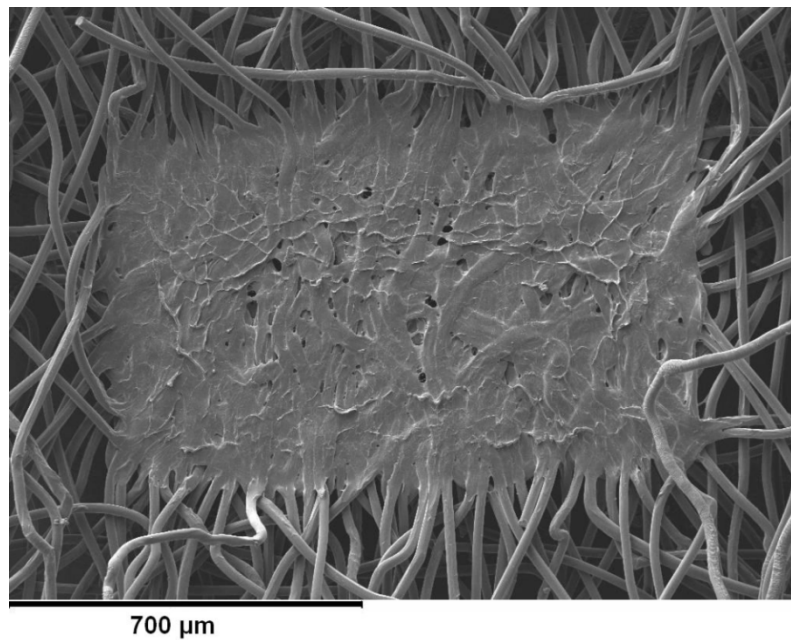
(b)

Figure 3.9: Two-component microstructure of low-density thermally bonded nonwoven material (SEM picture); (a): bonding lines and fibrous network, (b): details of bond points

Tensile tests were carried out. The specimens, which were used in the experiments, were cut with 60 mm length (gauge length: 25mm) and 20 mm width, and the test speed was 25 mm/min. True stresses and strains are used to describe the material's deformation, which is a highly nonlinear behaviour with a large strain level. And the images of the specimens were captured by scanning electron microscopy (SEM) and the Thermoelasic Stress Analysis System.

Table 3.5 shows the material's tensile modulus, its maximum strength and the strain level at maximum strength obtained for strip specimens with the chosen gauge length and width in both the machine direction and cross direction (Figure 3.10).

	Machine Direction (MD)		Cross Direction (CD)	
	Magnitude	Standard Deviation	Magnitude	Standard Deviation
Average Modulus (N/mm)	0.55	0.04	0.032	0.0084
Maximum Strength (N/mm)	0.90	0.11	0.133	0.032
Strain at the Maximum Strength (%)	105.29	5.31	124.54	4.37

Table 3.5: Summarised data for tensile tests of nonwoven (25 mm x 20 mm)
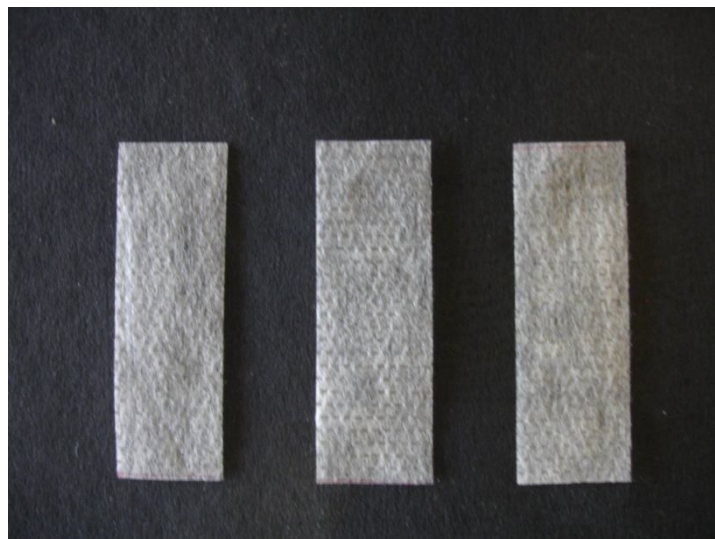
Figure 3.10: Shape of strip specimens with 60 mm length (gauge length 25 mm) and 20 mm width

The different material performances between MD specimen and CD specimen are shown in Figure 3.11, the maximum strength and tensile modulus of the material in machine direction is much higher than these in cross direction, which means the nonwoven material is highly anisotropic.

As shown in Figure 3.11, the MD specimen behaves almost bi-linearly; two trend lines are drawn to fit the stress-strain curve at its elastic and plastic stages, which describes the deformational behaviour of the nonwoven material. At the breaking stage, the stress drops in two stages, which presents the failure mechanism of the material.
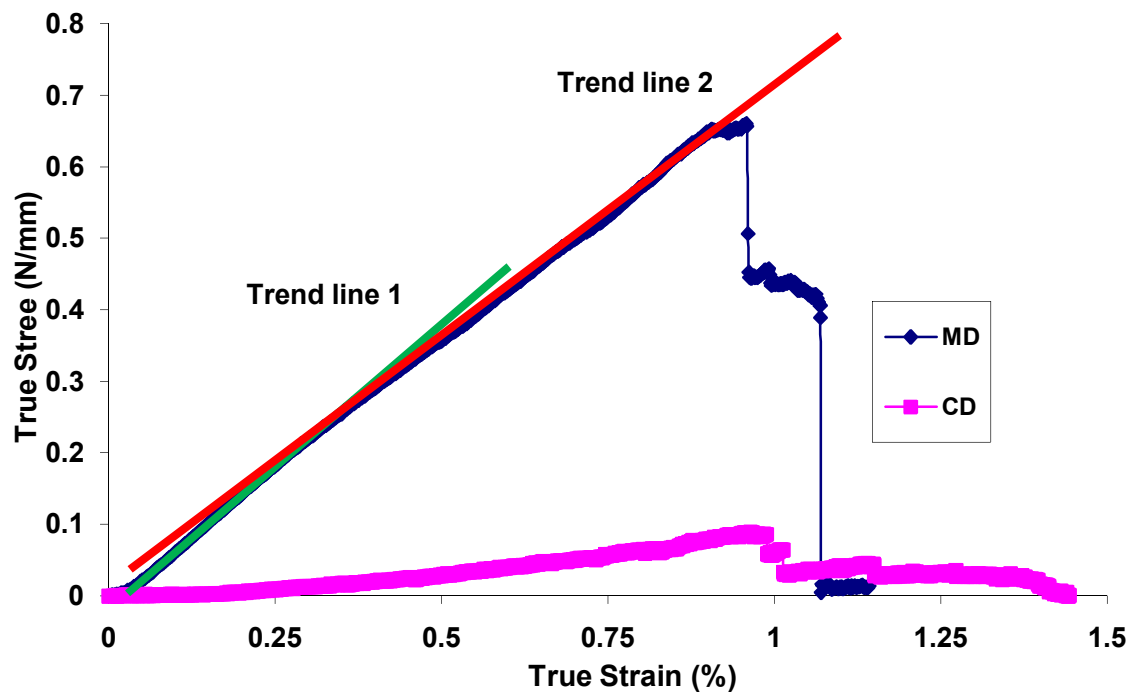
Figure 3.11: Comparison of typical stress-strain relationships of thermally bonded nonwoven material in machine direction and cross direction

To investigate deformation mechanisms of the nonwoven material by understanding the material's microstructure, Thermoelastic Stress Analysis System was used to record the procedure of the tensile test. The system was combined of an Instron Microtester for tensile tests, an infrared camera (CMT384SM) for detecting the change in the specimen's temperature and a computer for signal processing. The

system provides the stress distribution of the specimen during the tensile test. Moreover the SEM images were captured from deformed specimens after tests to reveal the rearrangement of the microstructure of the specimens caused by the external extension.

For the machine direction, at the initial stage of the tensile deformation (shown in Figure 3.12), a specimen presents a clear striped system, which is formed by strips of bonding points with intermediate strips of the fibre network. As shown in Figure 3.13, the width of bond points is larger than its height, and spaces between bond points are relatively narrow (about 1 mm) so when bond points form a straight line, the local material properties vary significantly between the specimen's bonding lines and the surrounding network. At the initial stage of the deformation, the "striped system" performs stably and linearly, which is represented by trend line 1 in Figure 3.11.

But in the nonwoven sheet, there are always areas with a lower density as compared to other areas, due to smaller numbers of fibres being assembled in such areas during the manufacturing process (Figure 3.14). The weaker areas are always the reason for the stress concentrations in tension and cause breaking.
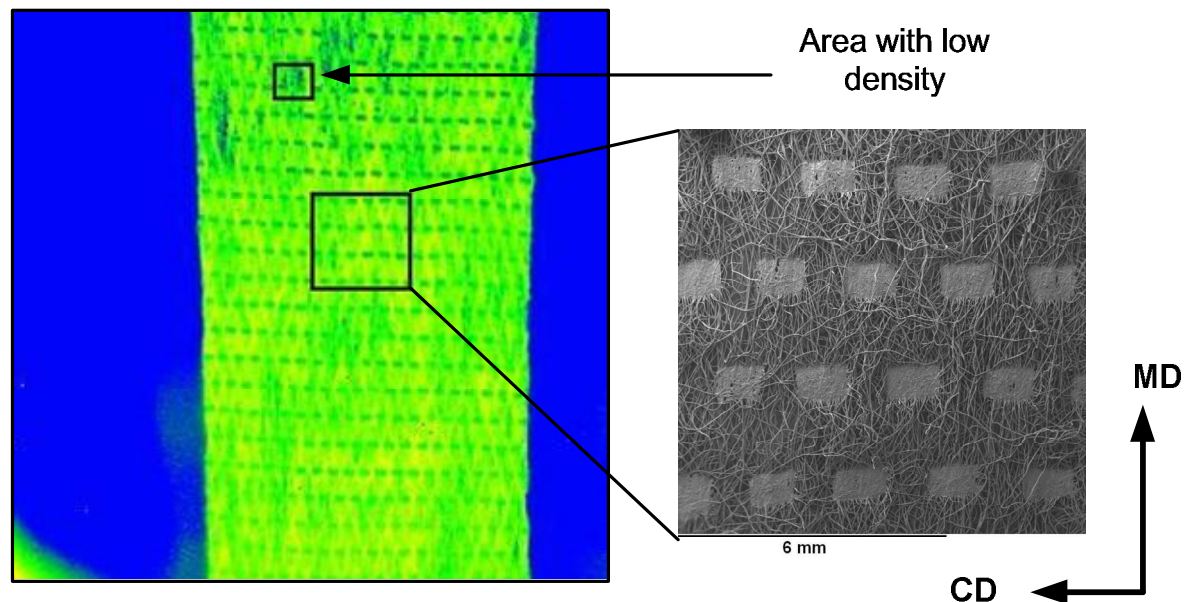
Figure 3.12: Initial stage of tensile behaviour (MD), (strain: 15 %)
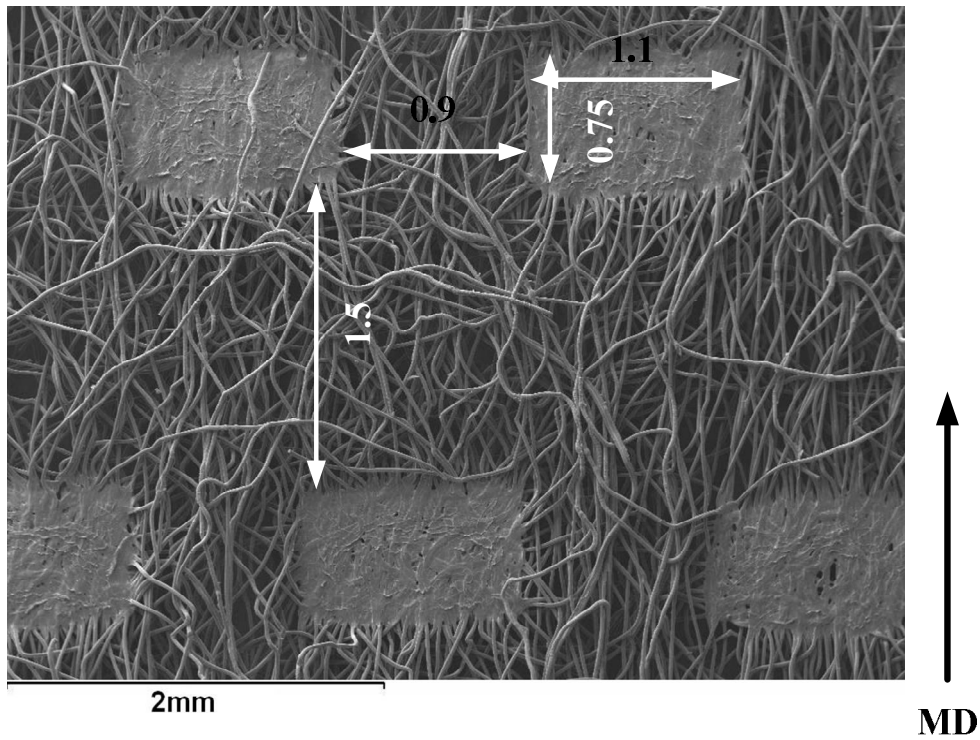
Figure 3.13: Dimensions of bond points and spacing between them
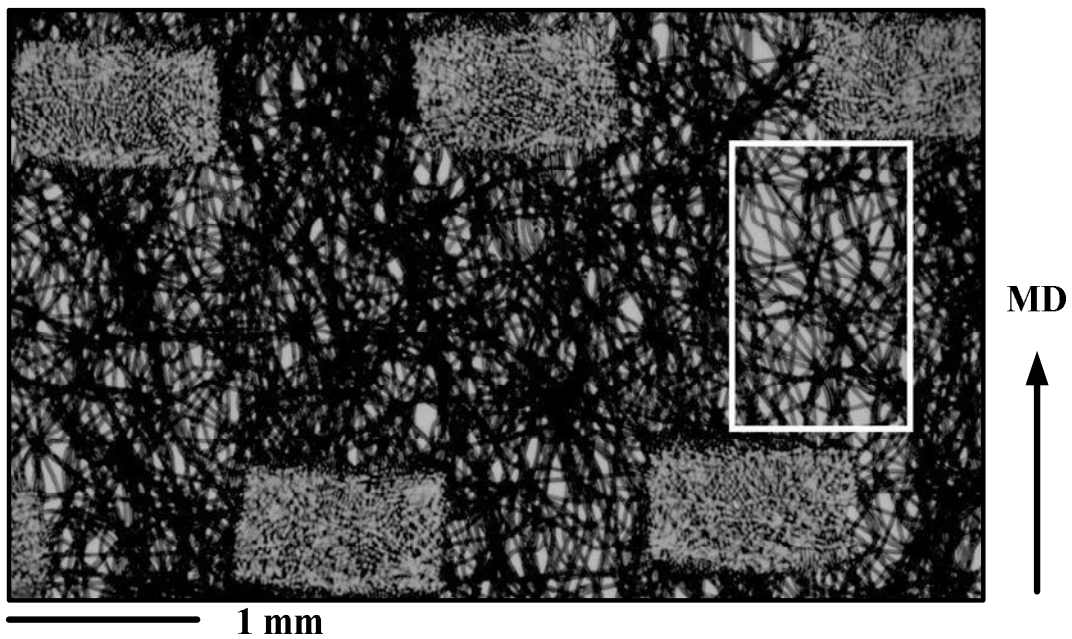
Figure 3.14: Nonuniform density of the nonwoven material; the area with lower density is marked with the rectangle

Figure 3.15 shows deformation of the strip system at an advanced stage of the process of tension. The strips of bond points are distorted due to the different local level of

stress transferred from neighbouring areas. Although, within a single strip of bond points, the spaces between bond points are narrow, the fibrous areas within the spaces still have significantly lower stiffness comparing with the bond points. When the deformation of the whole specimen achieves the advanced stage, stresses can concentrate at the areas with low density. Due to the low density, the stiffness of these areas is even lower than that of other fibrous areas with more fibres. The concentrated stress transfers from one low-density area to another, generating shear stress in the specimen and causing distortion of the strips of bond points. The change of the deformation mechanism of the nonwoven material is responsible for the bi-linear character of the strain-stress relationship as Figure 3.11. When the shear stress is generated in the specimen, the slope of the strain-stress curve diminishes, resulting in the second portion of the linear behaviour, with the trend line 2.
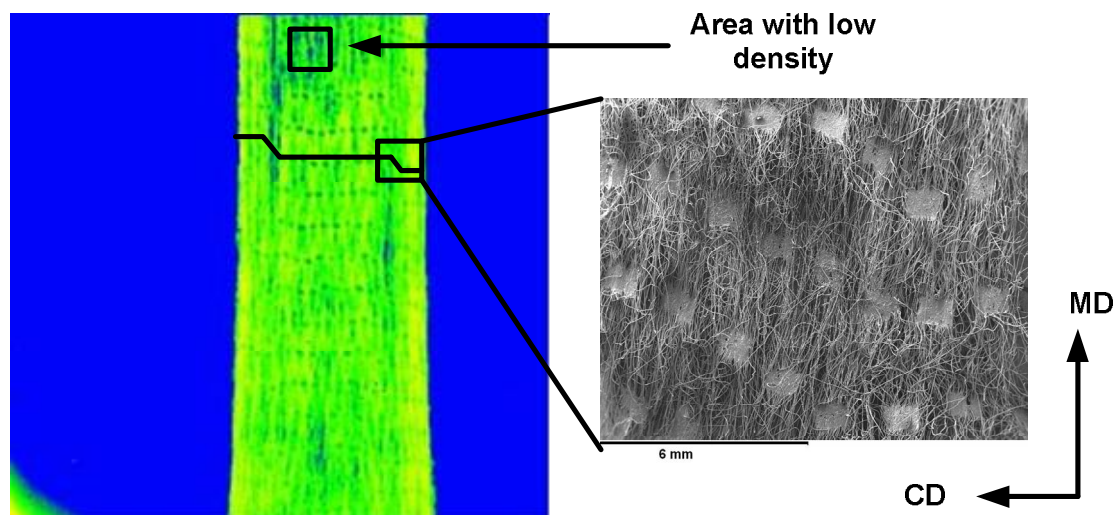
Figure 3.15: Advanced deformation stage of layered system (MD), (strain: 75%)

When the specimen is approaching its maximum strength, the material starts to break (shown in Figure 3.16), beginning from the areas with lower density. With further tensile stretching, the creaks are driven by the shear stress and transfer through the specimen and link other weak areas into a macroscopic defect. With microscopic defects, the stress of the specimen can still stay at a relatively stable level. As shown in (Figure 3.11), there is a small platform around the maximum strength of the specimen. When the material finally achieves its maximum strength, the final rupture

of the specimen starts.
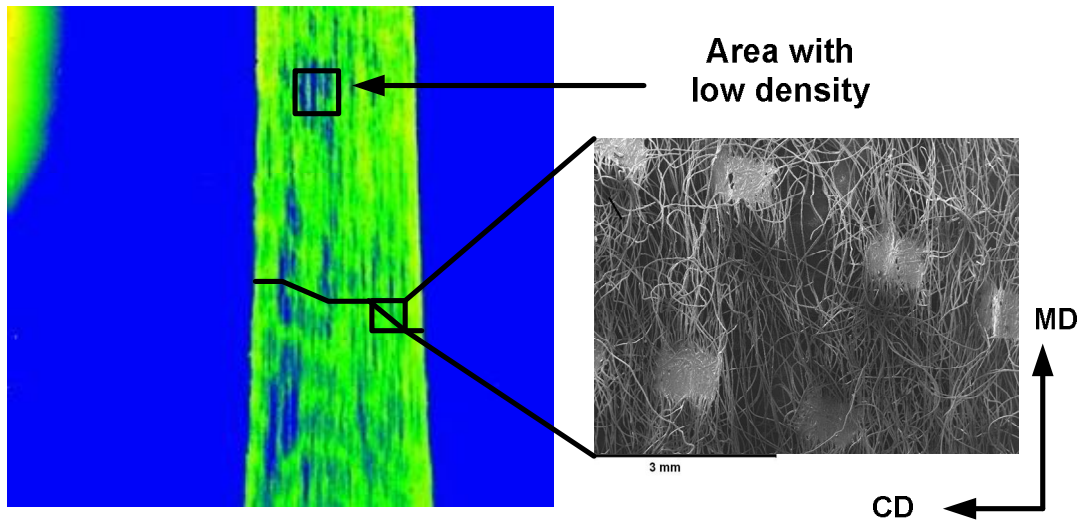
Figure 3.16: Shear stress transition through weak areas of nonwoven material (MD), (strain: 125%)

The failure mechanism of the nonwoven material is governed by both the internal shear stress and external tensile stress. The rupture could start at different locations, such as the lateral boundaries of the specimen or its central area (Figure 3.17). Besides, a nonuniformed strain distribution caused by the boundary conditions of the experiment, the location of the rupture is determined by the location of low-density areas and the character of transfer of the shear stress.
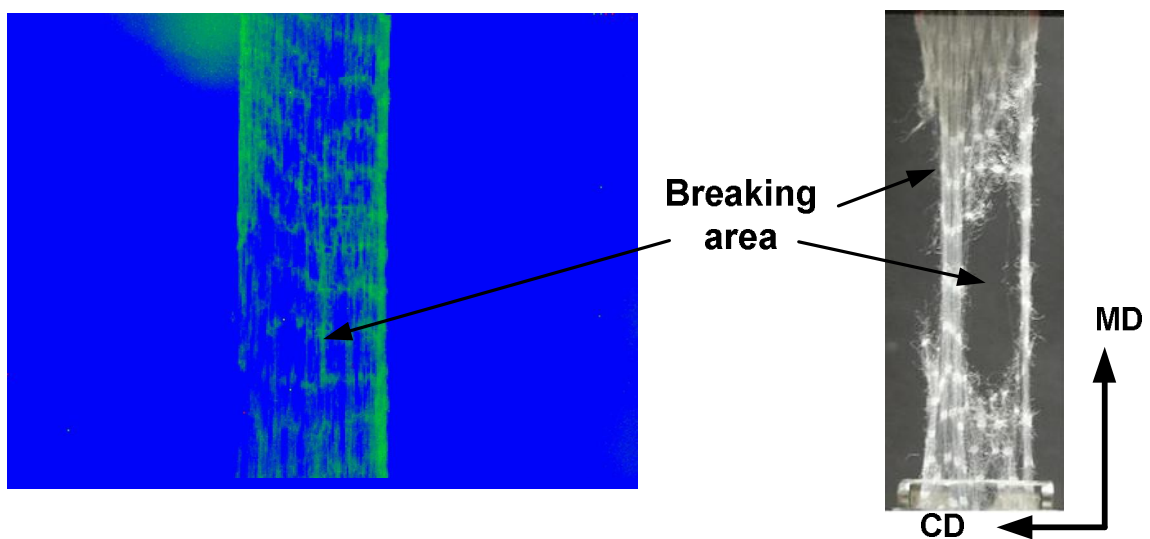
Figure 3.17: Breaking point of nonwoven material (MD), (strain: 141%)

In cross direction the strain-stress curve of the specimens shows a highly nonlinear behaviour before its rupture. But it is still possible to simplify the nonlinear behaviour of the specimen to a triple-linear behaviour as shown in Figure 3.18. These three trend lines are used to present different stages of the deformation.
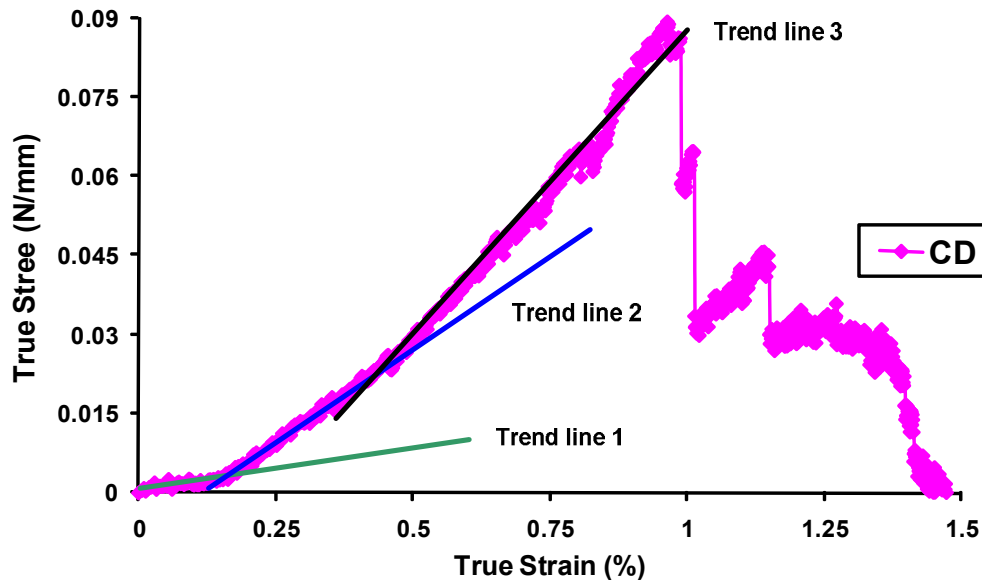
Figure 3.18: Typical stress-strain relationship of thermally bonded nonwoven material in cross direction

According to the results of tensile tests and the image analysis, in the cross direction, the deformation mechanism of elastic extension is more complicated, and it can be divided into three main stages.

At the initial stage of tension, the slope of the strain-stress curve is low, which is due to the pure fibre-net strips along the cross direction as shown in Figure 3.19. The fibre-net strip consists of curly fibres with friction between fibres. Therefore, the fibre-net strips have really low stiffness, and the stiffness is mainly contributed by the stretching of fibres. Moreover, due to the spacing arrangement of the bond points, the space between two neighbouring bond points along the cross direction is the narrowest space between any two bond points. Therefore, it is easy to deduce that the fibres connecting two neighbouring bond points along cross direction are easier to be stretches and start to carry the load earlier than other fibres. However, the number of the fibres connecting two neighbouring bond points along the cross direction

represents only a small part of the total number. It causes the initial stiffness (presented by trend line 1) of the specimen at this stage to be lower than the stiffness (presented by trend line 2 and 3) at more advanced stages of the material's deformation (shown in Figure 3.18). Therefore, at the initial stage, the deformation mechanism of CD specimens is mainly governed by the straightening of curly fibres, release of entangled fibres and the initial deformation of fibres between two neighbouring bond points along the cross direction.
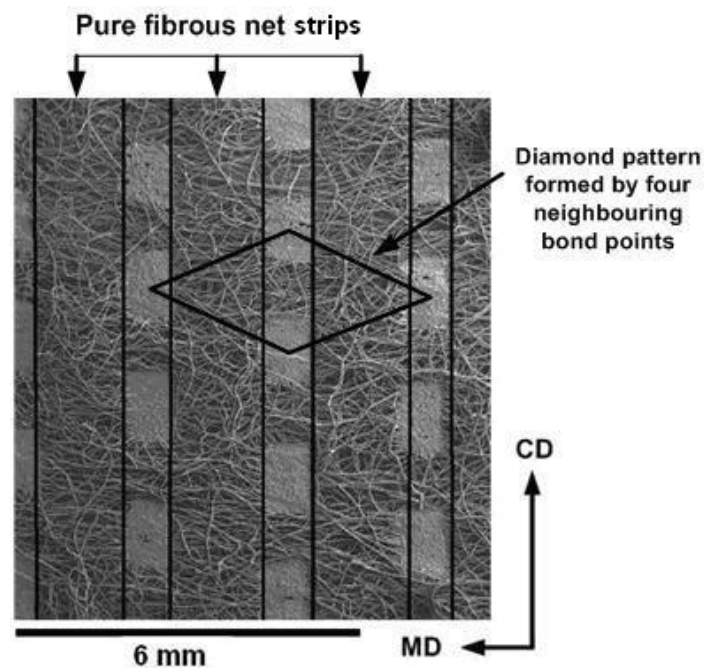
Figure 3.19: Fibrous net strips along cross direction

With further extension, four neighbouring bond points form a diamond pattern (shown in Figure 3.20). The fibres, which are connecting two neighbouring bond points along the cross direction start to carry more load due to the larger external extension. Moreover, the diamond pattern becomes a basis for load bearing, and the stress also transfers along the boundaries of the diamonds. At the end of this stage, the fibres between two neighbouring bond points along the cross direction start to break. The diamond pattern begins to contract rapidly, and holes appear inside the diamond patterns in the areas with low density of fibres. This deformation stage is presented by trend line 2 in Figure 3.18.
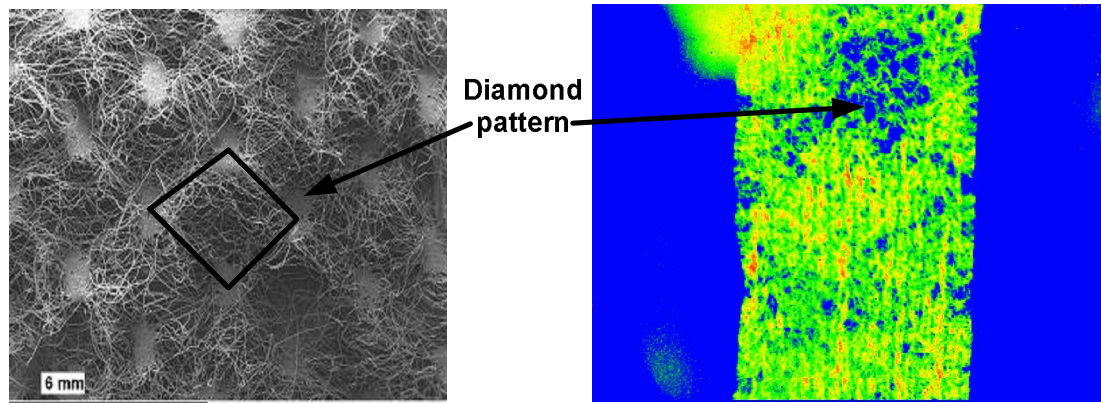
Figure 3.20: Diamond pattern during initial extension along cross direction (strain: 30 %)

At the following stage of the deformation process, the boundaries of diamond shapes are rearranged by longitudinal tensile stretching and lateral contraction. Their boundaries will align along the tensile direction and linked by the bonding points. In the image obtained with the infrared camera (Figure 3.21), the orange pattern shows that the boundaries of diamond patterns are reoriented to the direction along the loading direction (cross direction) and carry the load. This is shown schematically in Figure 3.22. At this stage, more fibres are arranged along the loading direction due to the reorientation caused by external extension. Therefore, the material becomes stiffer, which is presented by trend line 3 (Figure 3.18).
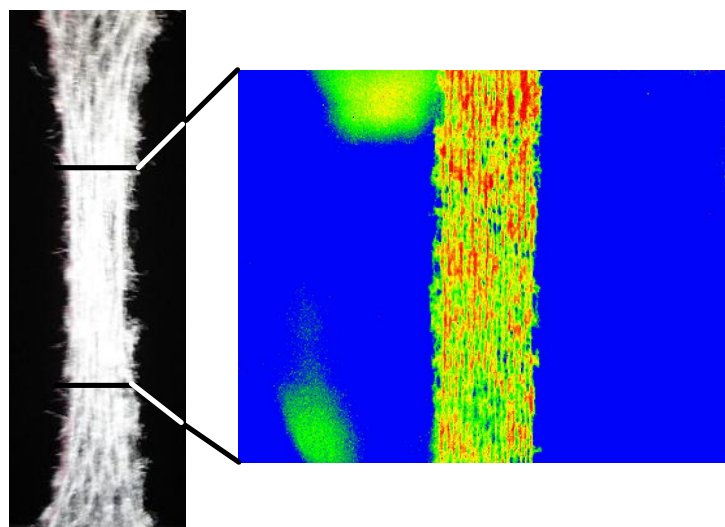
Figure 3.21: Second tensile stage of deformation in cross direction (strain: 80%)
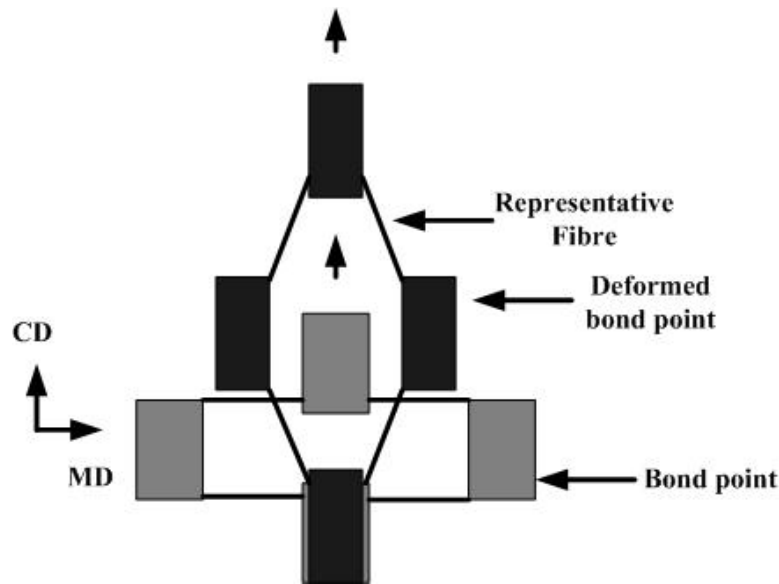
Figure 3.22: Transformation of diamond pattern at advanced stage of tensile test

When the material starts to break, the initial breaking points are often found on a boundary of bonding points, which is the stress-concentration area at the third stage of the tensile behaviour of CD specimens. As shown in Figure 3.23, the rupture of the material usually develops in stages due to the material's partial rupture, which is the reason for the drops in the stress on the strain-stress curve. At the breaking stage, the deformation mechanism of the material is dominated by the tension of bundles of fibres along the loading direction and shear stress transferring from one damage area to another one.
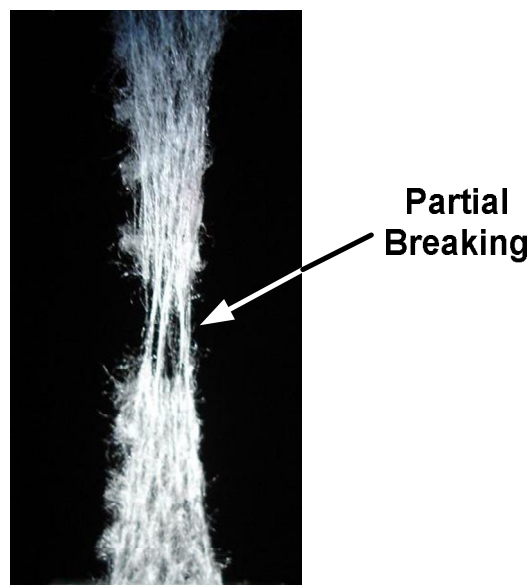
Figure 3.23: The finial (breaking) tensile stage of the specimen in cross direction

3.4 Discussions and conclusions

The tensile behaviour of the low density thermally bonded nonwoven material is defined to by different factors linked to properties of single fibres, properties of bond points and the microstructure of the material, especially the pattern and character of bonding points, fibres' orientation distribution functions (ODF), their density, the presence of curved fibres and entangled fibrous structure. According to the results of standard tensile tests, it is possible to analyse their effect on the overall material behaviour qualitatively.

- The type of ODF is controlled by the manufacturing process. The orientation distribution determines the proportion of fibres along the loading direction and their angle with regard to the loading direction. The amount (proportion) of fibres, capable to carry external loading, affects the fabric properties significantly. The apparent different material properties for the machine and cross direction are mainly due to it. The effect of ODF influences the material performance during the entire extension behaviour.

- The layout of bonding points and their properties are also determined during the manufacturing process. Since the set of bonding points is the stiffest component in the material and they connect the fibres in it they affect the overall material properties significantly and also contribute to the differences between the machine and cross direction. In machine direction, bond points forms the striped system, the stress transfers from a strip of bond points to a strip of fibrous network at the initial stage of the extension. And at the advanced stage of the extension, shear stress, which starts from low-density areas, transfer through strips due to the horizontal space (gap) between neighbouring bond points. In cross direction, four neighbouring bond points form a diamond pattern, with the short fibres between two neighbouring bond points starting to deform along the cross direction. When these fibres start to rupture, the diamond pattern contracts rapidly, and the long fibres along the boundaries of the diamond pattern start to carry the load. Moreover, the bond

points also constrain the overall lateral contraction since they are stiffer than the fibrous network.

- The properties of a single fibre forming the studied nonwoven and fibre density dominate the overall fabric properties during the entire extension process except the initial stage, because the fibres are the basic load carriers in the material. Stiffer fibres and their higher density will result in better mechanical properties of the overall material. The existence of curled fibres and the entangled fibre structure causes the nonlinear character of the material properties at the initial stage of the extension. Its effect becomes weaker at the advanced stages of the extension process.

Chapter 4 Continuous Finite Element Model of Low-Density Thermally Bonded Nonwoven Material

4.1 Introduction

As reviewed in Chapter 2, considerable efforts have been done to study the thermally bonded nonwoven fabrics using numerical simulations. Basically, there are two types of models differing by their treatments of material's structure: continuous model and discontinuous model. The continuous model treats the bonded nonwoven material as a kind of two-phase composite material. By ignoring voids within the material, the fibrous network of the material is treated as a continuous component in contrast to the bonding points. The method is based on the classic theory of composite materials. And there are some studies (Bais-Singh, S., Biggers, S.B.JR. and Goswami, B.C. 1998, Bais-Singh, S. and Goswami, B.C. 1998, Liao, Adanur 1997, Demirci 2008, Adanur, Liao 1998), which announce to describe successfully the mechanical performance of nonwoven materials, especially for the nonwovens with relatively high densities. In this chapter, continuous models are developed for the low-density thermally bonded nonwoven material and tested for both its machine direction (MD) and the cross direction (CD) of the material. These models are developed to investigate their capabilities to describe the deformation mechanism of the material and the effect of bond points on the overall material performance.

4.2 Material model for continuous finite element simulations

When the nonwoven material is analysed at macro-scale, the material is assumed to be a two phases composite material. The two phases are thermally bond points and a fibrous network. According to the experimental results, the phase of bond points is apparently stiffer than the phase of the fibrous network. Therefore, the immediate hypothesis is that the material properties of the nonwoven could be described using the classic composite theory shown in Figure 4.1. The central dark area in Figure 4a,

which usually represents fibres or other reinforcing material in composites, can be used to describe the bond points of the nonwoven material. And the other area, which usually represents a matrix of the composite, can be treated as a fibrous network for the nonwovens. Another assumption for the method is that both phases (bond point and fibrous net) of the nonwoven material are treated as continuous materials.
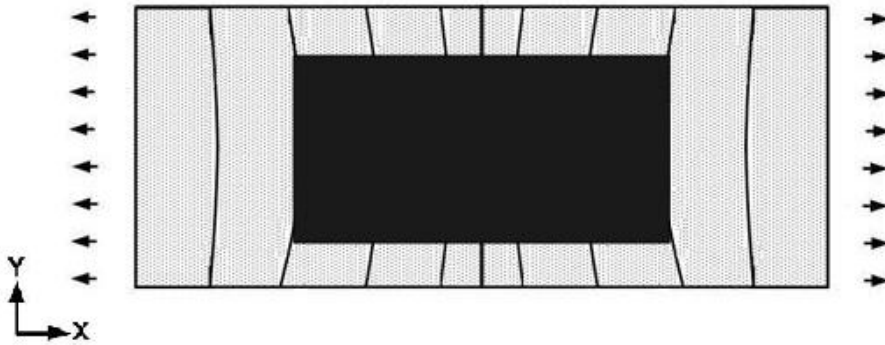
(a)
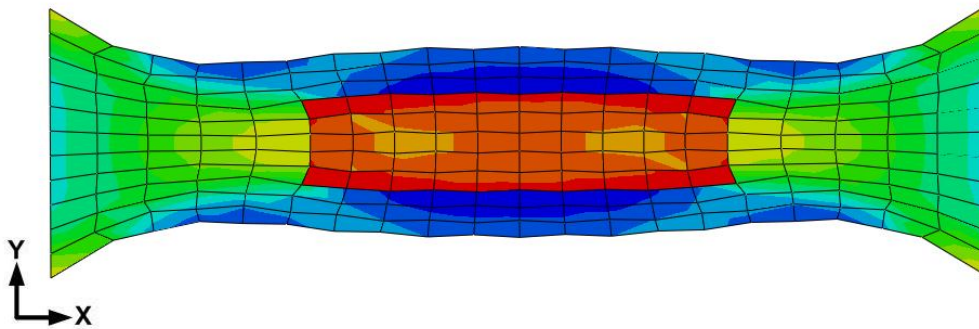
(b)

Figure 4.1: Two-component structure of composite material: (a) theoretical model; (b) numerical simulation

According to observations during the experiments, the studied nonwoven material performs as a striped system during its extension. Because the width of bonding points is larger than their height, and the spaces between the bonding points are relatively narrow (about 0.7 mm) so when the bonding points are arranged as a straight line, the local material properties vary significantly between specimen's

bonding lines and a surrounding network. To describe the striped system and its effect on the material behaviours of the overall material, the overall elastic modulus of the fabric can be presented as follows:

For the machine direction (MD), the striped structure and its representative element are shown in Figure 4.2. The relationship between the elastic modulus of the overall fabric and the elastic modulus of the two components (bond points and fibrous network) of the fabric is presented in the following form:

$$E_{FM} = \frac{E_{fM} E_{BM}}{V_f E_{BM} + V_B E_{fM}} \,, \tag{4.1}$$

$$E_{BM} = E_{bM} v_b + E_{fM} V_B (1 - v_b) \,, \tag{4.2}$$

where E_{FM} is the effective modulus in machine direction, E_{fM} is the MD modulus of the fibrous network, E_{BM} is the MD modulus of the bond layer, E_{bM} is the modulus of the bond points in machine direction, V_F is the volume ratio of the fibrous network in the fabric, V_B is volume ratio of bond strips in the fabric, v_b is the volume ratio of bond points in the bond layer.
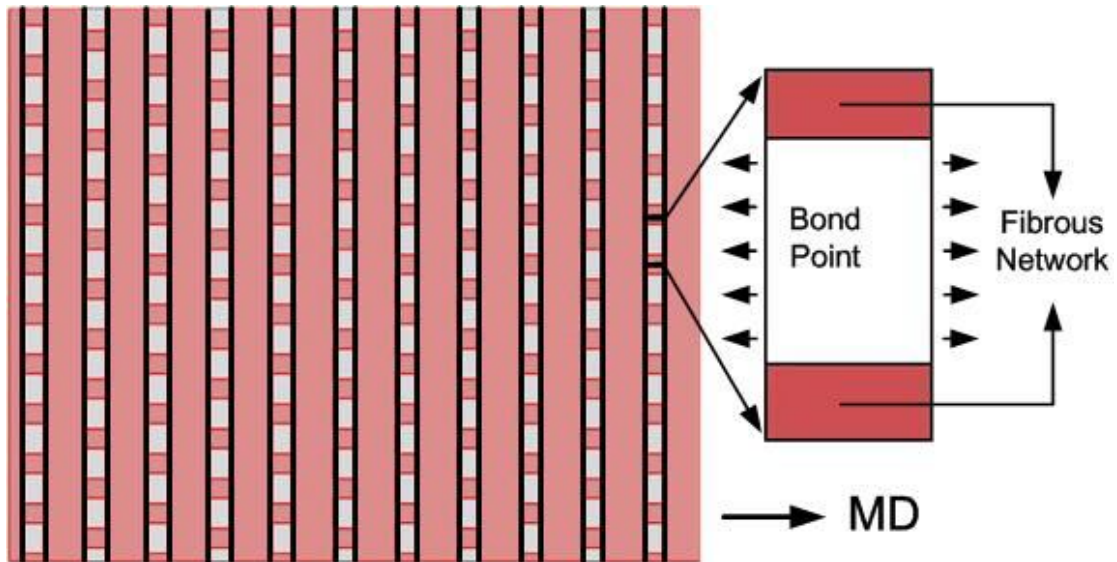
Figure 4.2: Mechanics of material idealization of thermally bonded nonwoven material loaded in machine direction (MD)

For cross direction, the striped structure and its representative element are shown in Figure 4.3. The equations describing the relationship between the elastic modulus of bond points, fibrous network and the overall material are presented as following:

$$E_{FC} = V_F E_{fC} + V_B E_{B_1},$$ (4.3)

$$E_{BC} = \frac{E_{bC} E_{fC}}{V_b E_{bC} + E_{fC} V_B (1 - V_b)},$$ (4.4)

where E_{FC} is the longitudinal modulus of the whole fabric, E_{fC} is the longitudinal modulus of the fibrous network, E_{BC} is the longitudinal modulus of the bond strip, E_{bC} is the longitudinal modulus of the bond points.
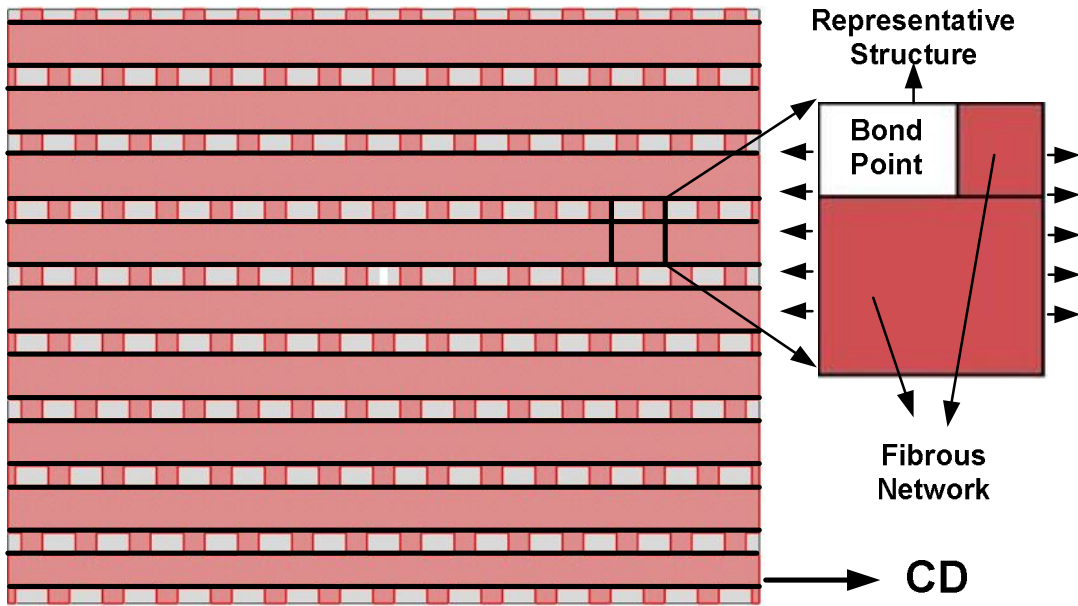
Figure 4.3: Mechanics of material idealization of thermally bonded nonwoven material loaded in cross direction (CD)

As determined in Chapter 3, the dimensions 25 mm x 20 mm will be used in numerical simulations. According to the experiment results the magnitudes 5.5 MPa and 0.32 MPa were used in the model as elastic moduli of the nonwoven material in machine and cross directions, respectively. However, there are some essential parameters missing for these models. According to the literature, there still no

researches, investigating the material properties of bond points, such research is complicated, for the low-density nonwoven material as fibres inside the bond points are partially melted and connected to the surrounding fibrous network. The sample preparation is difficult since cutting the single bond point will lead to a "pulling out" behaviour to the fibres. In practice, it can damage the specimen due to its poor stiffness. Moreover, the dimensions of the bond point are 1.1 mm x 0.75 mm, being too small to be tested even with the Micro Tester system. Other parameters, which are hard to determine by experiments, are the Poisson's ratio and shear moduli of bond points and the fibrous network. It is mainly due to the low compression and shear stiffness of the nonwovens. From the Petterson and Backer's pioneering work (Backer, S. and Petterson, D. R. 1960), it is obvious that the Poisson's ratio and shear moduli of the nonwoven are hard to obtain by both experimental and numerical methods. Therefore, researchers started to look for methods allowing them to avoid the use of these parameters as the input information into their models or just use provisional values for them (Kim 2004a, Bais-Singh, S., Biggers, S.B.JR. and Goswami, B.C. 1998, Adanur, S. and Liao, T. 1999). Still, a well-received method has not been established. Hence, in this chapter, the continuous model is used only for a qualitative analysis of the effect of bonding points, and the input parameters of the model are determined as following:

- Since it is hard to measure the material properties of bond points and fibrous, the material properties of these two components in both MD and CD are calculated using equations 4.1-4.4. And the elastic moduli of bond points are assumed as five times higher than the moduli of the fibrous network in both two principle directions.

- According to the literature survey, there is currently no method, which can properly measure the shear moduli and Poisson's ratios of the low-density fibrous network and bond points of the nonwoven material. Therefore, for the bond points, the shear moduli and Poisson's ratios are assumed to be equal to those of the solid polypropylene (PP). For the fibrous network, due to its low compression stiffness, the Poisson's ratio is assigned a reasonable low value,

and the shear moduli are calculated using $G = \dfrac{E}{2(1+v)}$ by assuming the material as isotropic.

4.3 Geometric model of thermally bonded nonwoven material and boundary conditions

According to experimental results, the nonwoven material is a dimension-dependent and shape-dependent material. In this analysis the models for both machine direction and cross directions were developed using the same dimensions and a constant shape factor. As the analysis in Chapter 3, the dimensions of the specimens in the model were chosen 25 mm x 20 mm as their length and width, respectively, for models for (Figure 4.4) both the machine and cross directions. The shape factor is 1.25. The geometry models are defined in *x-y* plane. The thickness of the bond points and fibrous net are 0.02 mm and 0.2 mm respectively, these magnitudes are according to the measurement of real nonwoven material using beam callipers.
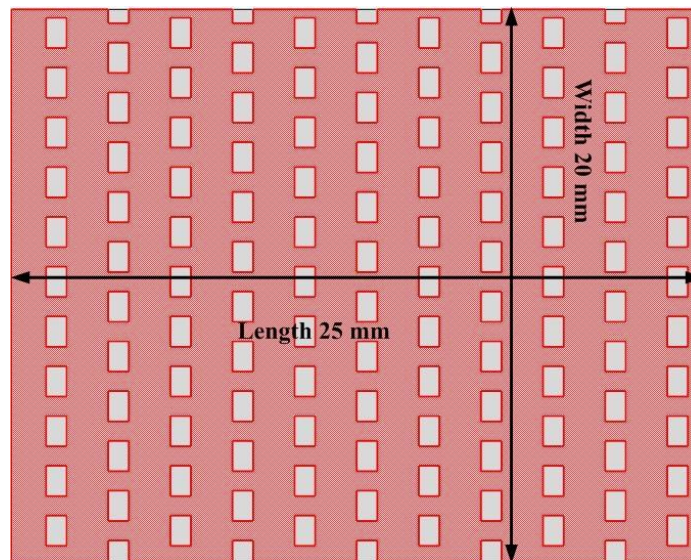
(a)
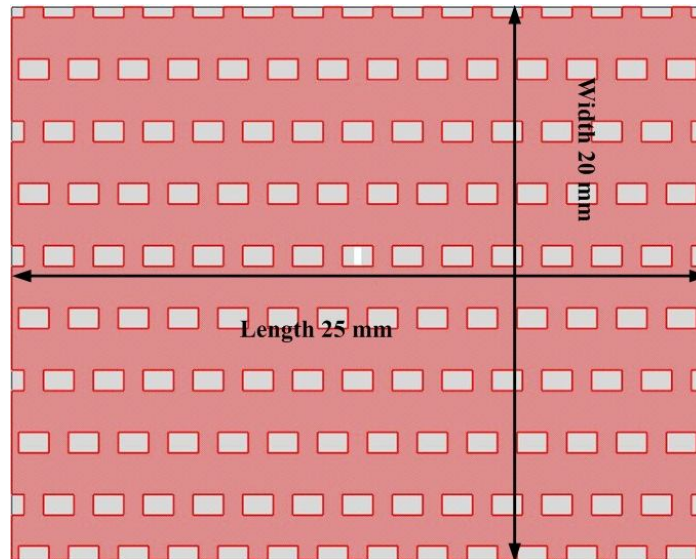
(b)

Figure 4.4: Geometry of continuous model: (a) CD; (b) MD

The dimensions of each bonding point are (width) 0.75 mm x (length) 1.1 mm. The spacing arrangement of bonding points is shown in Figure 4.5, and the respective magnitudes are given in Table 4.1.

Bond shape	Width (mm)	Height (mm)	Gap width in CD (mm)	Gap length in MD (mm)	CD overlap (mm)
Rectangle	1.1	0.75	0.7	1.5	0.2

Table 4.1: Geometry data for bonding points of nonwoven material
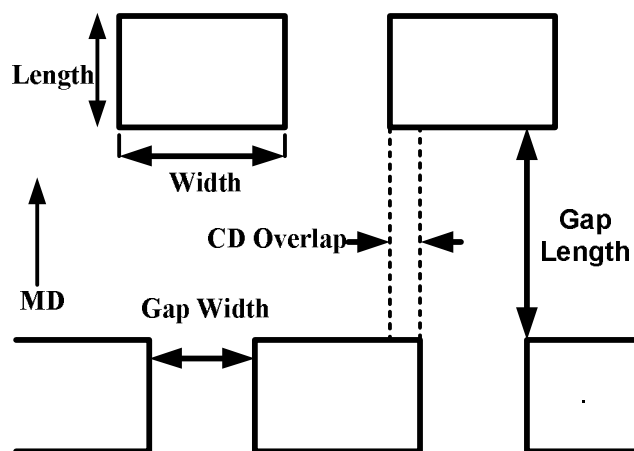
Figure 4.5: Layout of bonding points in nonwoven material

89

The boundary conditions of the model are shown in Figure 4.6. One boundary of the geometry model, which is perpendicular to the loading direction was set as "ENCASTRE" (U1= U2 = U3 = UR1 = UR2 = UR3 = 0), constraining all the degrees of freedom of the boundary to simulate the fixed jaw of the testing machine. Another vertical boundary of the model was set as "XASYMM" (U2 = U3 = UR1 = 0) and "U1 = 40". The boundaries, which are parallel to the loading direction were set as "ZSYMM" (U3=UR1=UR2=0). The setting is to simulate the loading conditions of the specimen in tensile tests.
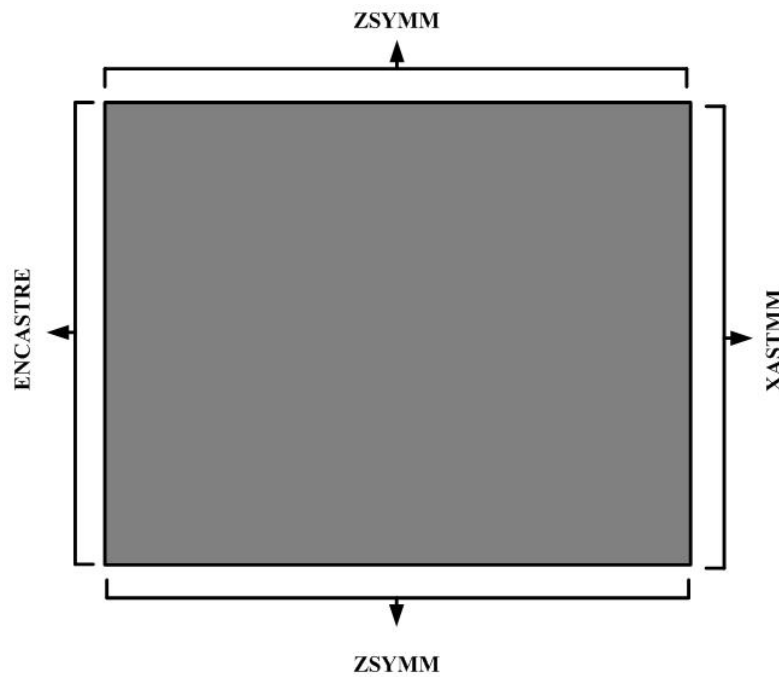
Figure 4.6: Boundary and loading conditions of continuous model

Since bonding points in the model are not arranged symmetrically (Figure 4.5), the meshing based on rectangular element causes their distortion around bonding areas in the model. Hence, triangular elements are chosen for the model. The real fabric is a very thin material, and thickness of the bonding points is even smaller than that of the fibrous areas. Therefore, the ABAQUS quadratic triangle element STRI65 was used to simulate the fibrous web, and the quadratic quadrilateral element S8R5 was used to model the bonding points (ABAQUS 2001) (Figure 4.7). Thickness of those two types of elements is determined by the experimental results: 0.02 mm for bond points and 0.2 mm for fibrous network. But these elements still have their limitations in

representing this low-density nonwoven material; for instance, they are not appropriate to simulate the material's behaviour at high strain levels.

(a)
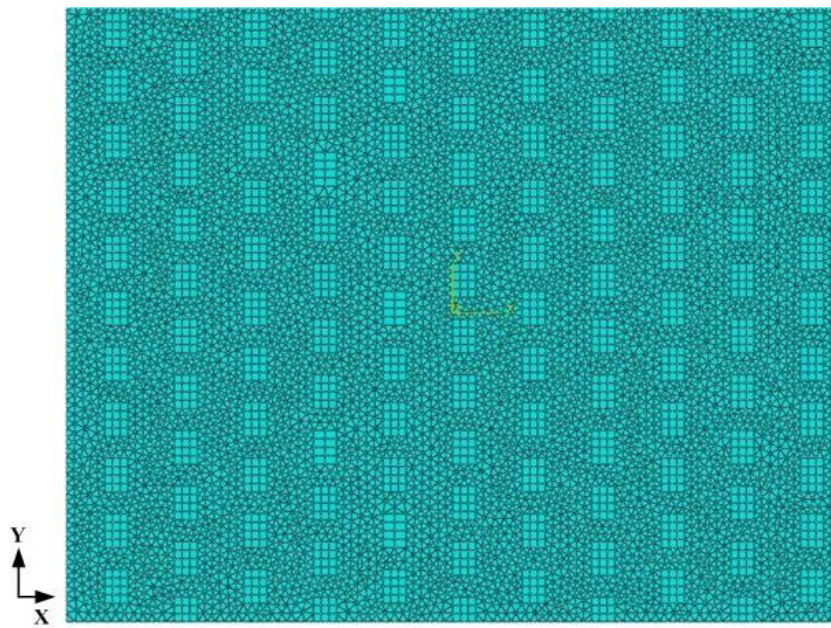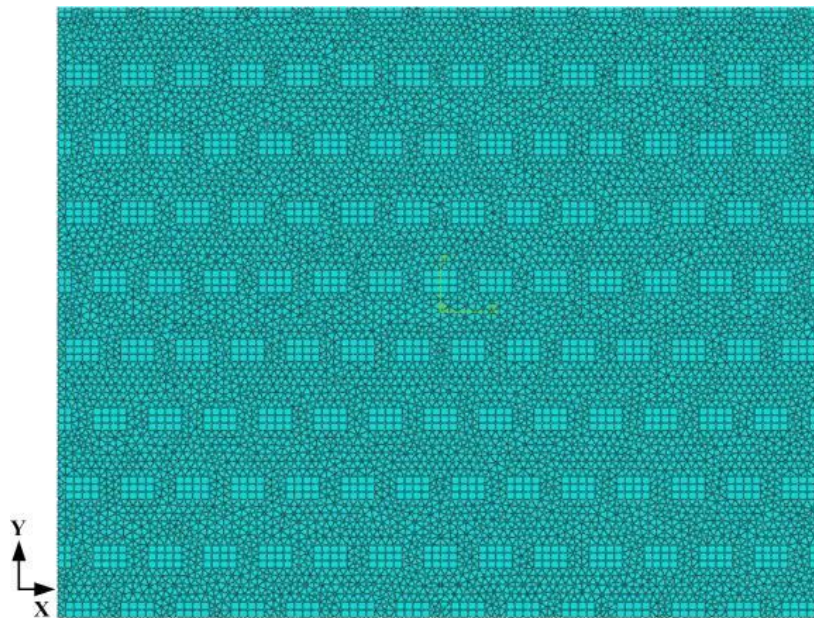
(b)

Figure 4.7: Undeformed continuous finite element models: (a) machine direction; (b) cross direction

4.4 Results of continuous models

The results of finite element simulations for both MD and CD models are shown in terms of Von Mises stress in Figure 4.8 for the axial tension in the x direction. The ranges of scales for the models are different due to the significant different mechanical performances. Different stress distributions are the apparent results of simulations, which are due to the different arrangements of bonding points along two principle directions in the nonwoven. In machine direction, the model clearly presented a striped system, which was formed by lines of bonding points with intermediate stripes of fibrous web. According to the obtained results, the line of bonding points carries a higher stress level due to their higher stiffness. And the area of fibrous network was characterised by a uniform and relatively low stress. In cross direction, the stress distribution was more complicated; the stress in the area of fibrous web is not uniform as for the model in machine direction. Due to the pattern of bonding points, four neighbouring points formed a diamond pattern, which acted as a basic load-carrying unit in the material. During the deformation the stress transfers along the boundaries of the diamond patterns. The obtained results match the experimental observation well.

Another result of the simulations is the different necking behaviours at high strain for two principle directions, which also match our experimental observations. For stretching in machine direction, necking of the specimen is much smaller than the one in cross direction due to restricted contraction of stripes in lateral direction, linked to a combination of small gap width and high stiffness of bond points. In the CD model, the overall lateral contraction is mainly defined by low stiffness of the fibrous network that occupies the gap length, as shown in Figure 4.5.
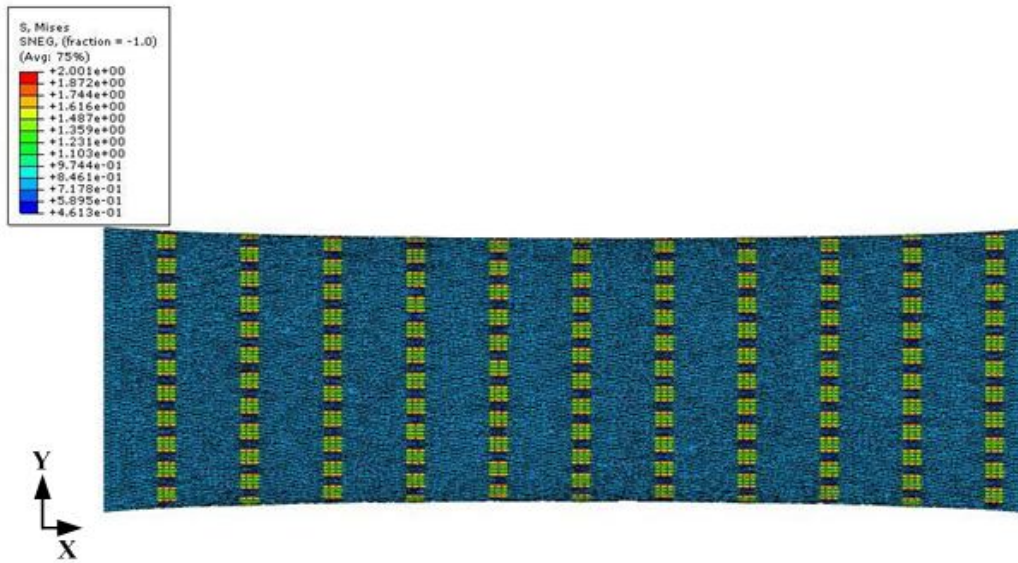
(a)
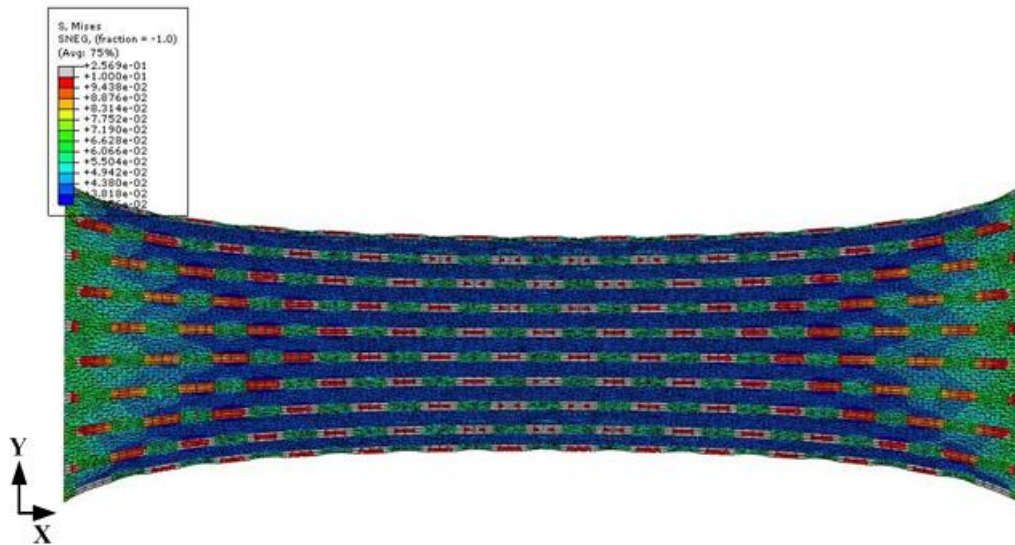
(b)

Figure 4.8: Results of continuous finite element models: (a) machine direction; (b) cross direction (strain 160 %)

As a result of the varying necking behaviour, different stress distributions in bond points and areas around them are demonstrated in Figure 4.9; for both models the figure focuses on the central areas of the models. For the model in machine direction

(Figure. 4.9a), the bond points are compressed due to the lateral contraction, and the areas between two bond points along the *y* direction experience relatively lower stresses compared with other areas of the fibrous network. Besides these areas, the fibrous network has a uniform stress distribution. Figure 4.9b shows the detailed stress distribution for the model in cross direction. It is apparent that the bond points are compressed to a higher level along the *y* direction and stretched to a larger deformation in the loading direction *x*, compared with the performance in MD model. A higher stress concentration is obtained in the areas between two neighbouring bond points along loading direction, especially inside the diamond patterns. And the stresses along the boundaries of the diamond patterns have lower magnitudes and are more uniformly distributed. Due to the higher stiffness of the bond points, the results could be used to improve the material properties of the nonwoven material in certain directions by adjusting the material properties and arrangement of bond points.

(a)

94
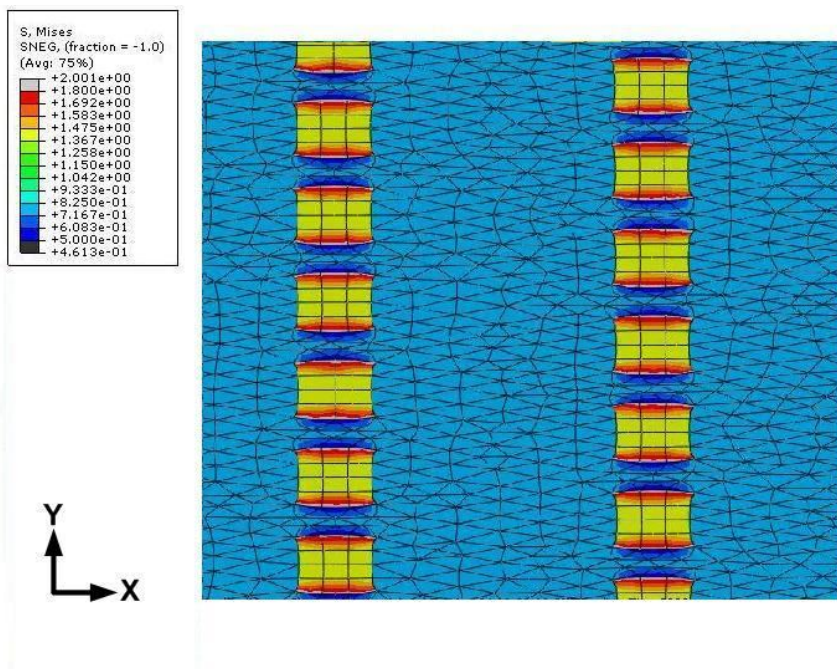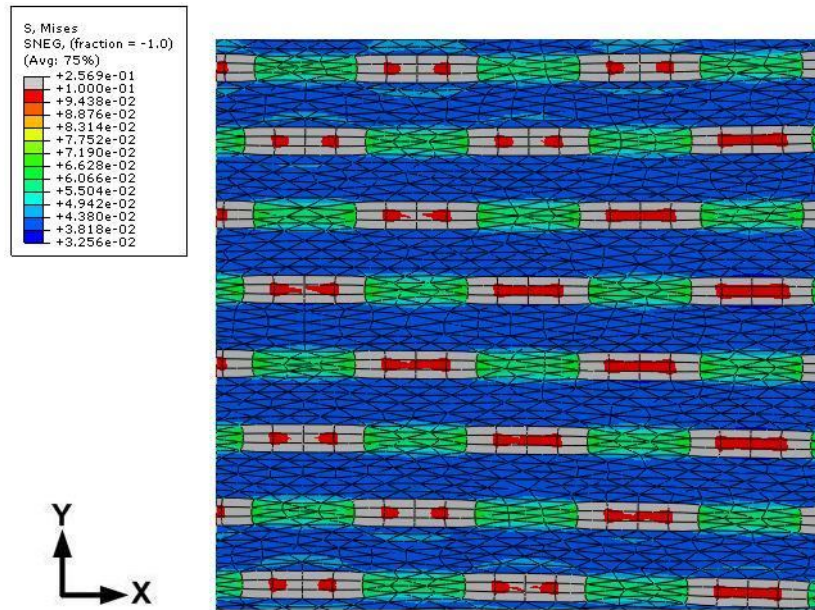
(b)

Figure 4.9: Detailed stress distribution of the continuous models: (a) MD; (b) CD

The results for stress-strain relations obtained in simulations with the continuous FE models, which describe the anisotropic material properties of the nonwoven material, are presented in Figure 4.10. The stresses are averaged over the smallest width of the specimens. The obtained anisotropic mechanical performances match our experiment results.
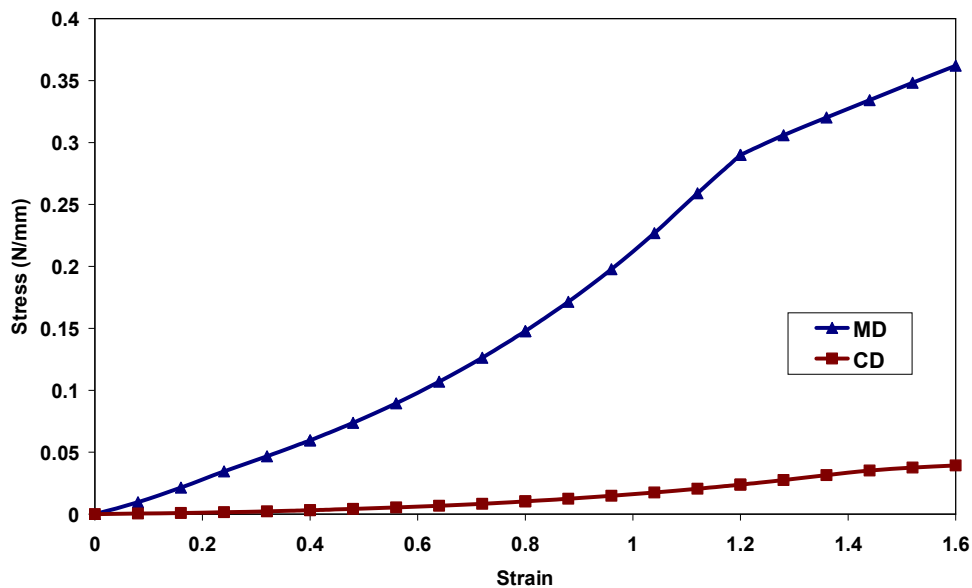
Figure 4.10: Calculated stress-strain relationships for MD and CD (continuous FE model)

Figure 4.11a shows a comparison between the results of the simulation and experimental studies. For loading in machine direction it shows a slower stress increase at initial stages of stretching than in experiments, which results in different shapes of two stress/strain curves. However, the experimental and calculated curves have an intersection at approximate 112% strain. It means that the model predicts relatively higher level of load observed in experiments. The differences in deformations are due to the underestimation of the real stresses by the material models in the FE simulations. There are mainly two reasons, which cause the deflection: first, the material model, which is represented by Equation 4.1 and 4.2, is developed based on the well-known "rule of mixtures" (Clarke, Suresh et al. 1996). It tends to underestimate stresses compared with the real material. For the Equation 4.1, the model assumes that the bond strips and the strips of fibrous network adjacent to the bond strip have equal stress. The principle of the equal stress model is shown in Figure 4.12a, which represents a section of the model along cross direction including one strip of bond points and one strip of fibrous network. The stresses of strip of bond points σ_B, strip of fibrous network σ_f and the overall material σ is equal to each others: $\sigma = \sigma_B = \sigma_f$. And for Equation 4.2, the assumption is of an equal strain, which means within a bond strip the bond points and the fibrous network neighbouring to the bond points experience the same level of strain during the extension process. As shown in Figure 4.12 b, the strain levels for bond points ε_b, fibrous network ε_f and the overall material ε is same: $\varepsilon = \varepsilon_b = \varepsilon_f$. In reality, the bond strips have much higher stress than the strips of fibrous network due to their higher stiffness, contradicting the assumption of equal stress. And within a bond strip the bond points only achieve a smaller strain level than their neighbouring fibrous network, which is also in contrast to the assumption of equal strain. Therefore, the model tends to underestimate the modulus (Clarke, Suresh et al. 1996). Second, the microstructure of nonwovens is much more complicated than that of composite materials, which the "rule of mixture" is supposed to represent. The nonuniform stress/strain distribution in nonwovens is not only caused by the different material properties of bond points and fibrous network, but also caused by the material's discontinuous microstructure and its uneven density. Therefore, the highly

nonuniform stress/strain distributions of the material lead to a high level of distortion of elements, causing the difference between the calculated and measured results.

Due to the similar reasons considered for the model in machine direction, the results of numerical simulations in cross direction show a difference from the experimental result. Up to strain 130% of the calculated stress is underestimated compared with the measured result. And when the strain level is higher than 130%, the results of simulation exhibit a somewhat higher magnitude than the experimental results since there is no criterion for local fibre breaking in the numerical model.
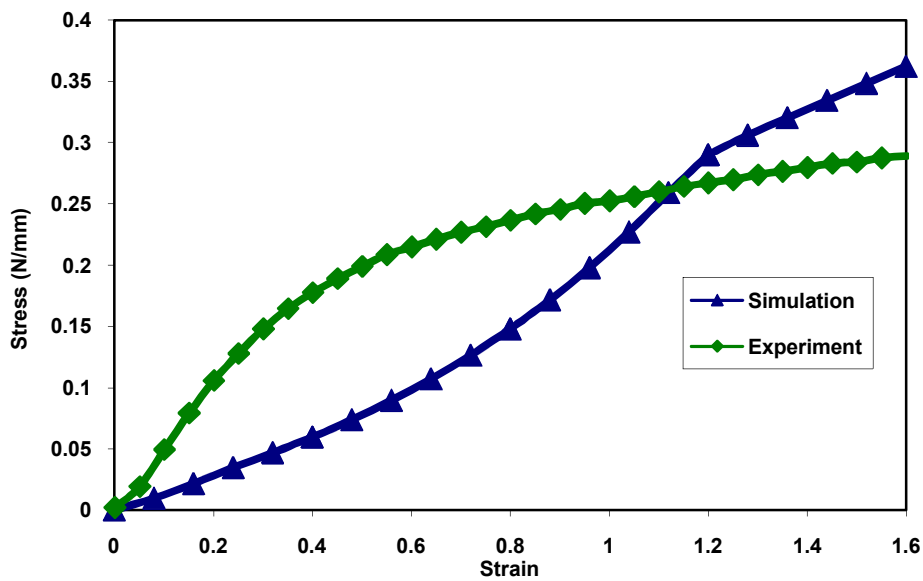
(a)
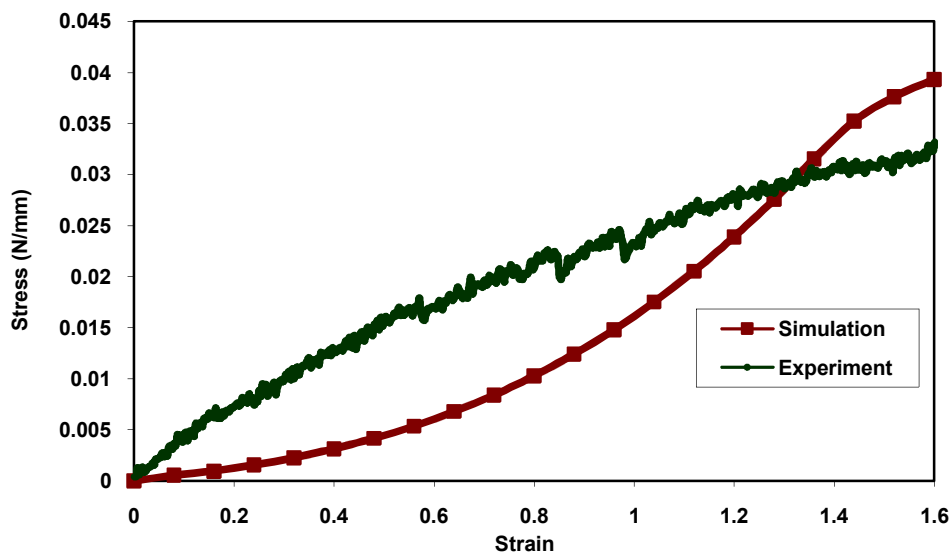
(b)

Figure 4.11: Comparison of experimental results and results of simulations: (a) MD; (b) CD

(a)

(b)
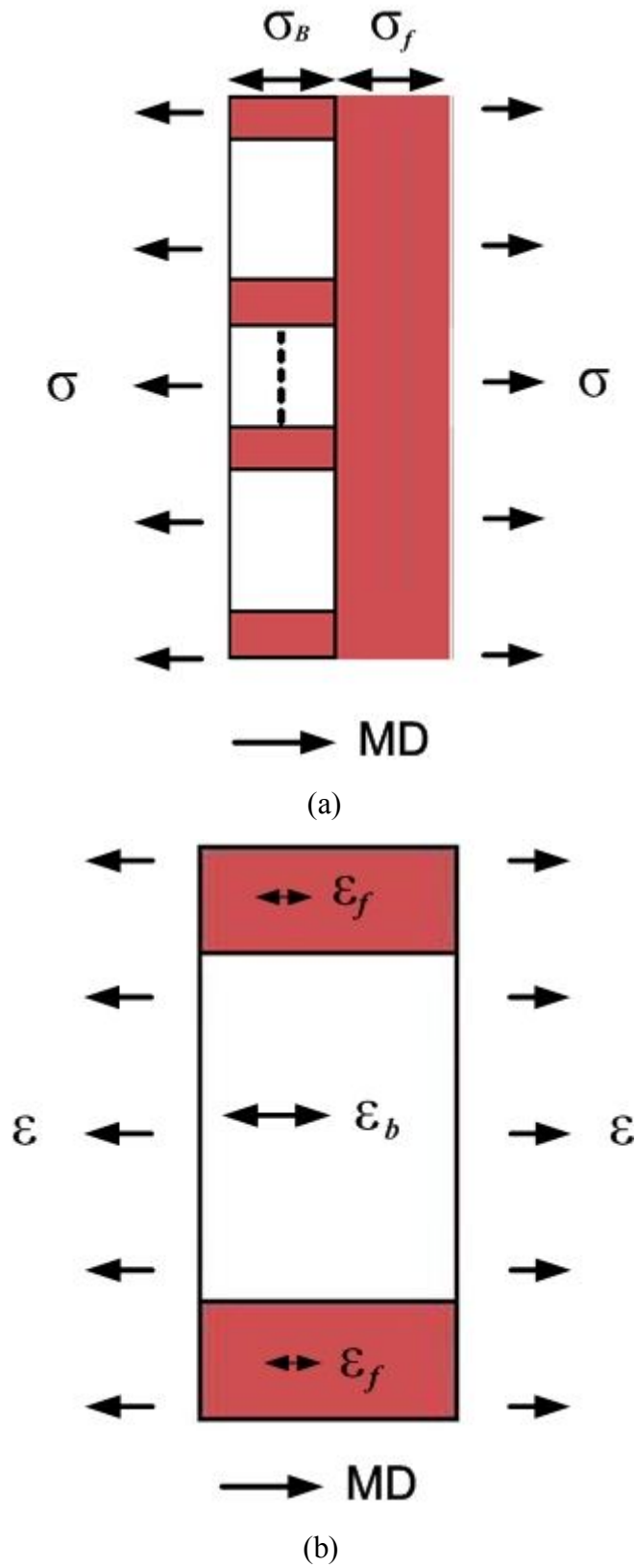
Figure 4.12: Theory models for continuous FE simulation: (a) equal stress model; (b) equal strain model

4.5 Discussions and conclusions

Continuous FE models were developed to simulate the tensile behaviours of the low density thermally bonded nonwoven material for its both two principle directions: MD and CD. The models treat the material as a two-component material. The fibrous network and thermally bonded areas were introduced into the model according to their apparently different material properties. And the capability of the models was studied by comparing the results of simulations and experimental studies. The obtained results follow:

The continuous models present different deformation mechanisms of the material in its machine and cross directions; it is caused by the material's geometry features and different material properties of the material components. The implemented geometry features are the density, shape, size, thickness and spacing of bond points that continuous models can properly reflect. But the microstructure of the fibrous network cannot be introduced into such models. For the MD model, the deformation mechanism of the material is based on a strips system, with the higher stress carried by the strips formed by bond points, and the phenomena match the experimental observation. For the CD model, four neighbouring bond points forms a diamond pattern, as a basic load carrier; the area within the pattern present a zone of higher stress concentration than its boundaries. These phenomena were also observed in experiments. And the distinct necking effects for the material are described for its two principle directions. Moreover, the models also reproduce the anisotropic mechanical performance of the material.

However, due to the continuous nature of the models, they could not adequately reflect the discontinuous and nonuniform microstructure of the nonwoven material. So the character of obtained stress/stain relationships cannot match the measured ones, although at relatively high strain levels, the calculated results have common points with measured results. A lower increment of stresses displayed at initial deformation stages in calculated results; the curves have a concave shape for both two principle directions, which is different from the convex curves obtained from experiments. There are three main reasons for these deflections. First, it is caused by the nature of the material models that tend to underestimate the stress. Second, the discontinuous

and nonuniform microstructure of the material result in a seriously nonuniform strain/stress distribution during the extension. Not accounting for this enlarges the difference caused by the inadequate material models. Finally, the model needs the precise knowledge of the input parameters for both bond points and the fibrous network, which are hard to be measured experimentally. And the provisional values used in present models can also cause the difference in results. Therefore, the approach of continuous FE model does not have the potential to describe the low density thermally bonded nonwoven material quantitatively due to its continuous nature, although there are some successful studies for high-density nonwovens, where the effect of microstructure is less pronounced.

Although the continuous FE model could not be used to simulate the low-density thermally bonded nonwoven material quantitatively, it still could help to analyse the effects of bonding features (density, shape, size, and spacing) on the overall properties of the fabric and deformation mechanisms. And the results of simulations with the model proved that the effect of microstructure cannot be ignored for such low-density nonwoven materials. Therefore, the discontinuity and nonuniformity of the material should be carefully investigated and an advanced model should be developed with account for the effects of the material's microstructure.

Chapter 5 Effect of Microstructure

5.1 Introduction

In previous chapter the continuous FE models were presented to describe the tensile behaviour of the low-density thermally point bonded nonwoven material. The models are successfully described the features of the two-component nonwoven material, consisting of bond points and the fibrous network. The effects of bond points, which are stiffer than another component of the material – the fibrous network - were analysed.

Although the continuous models could simulate the studies material by introduction of some of its features, there are still some properties of the material that cannot be described by them. According to our experimental results, the mechanical properties of the nonwoven material are determined by both the material properties of single fibres and microstructure of the materials, which cannot be directly introduced into the continuous model. Obviously, the discontinuity and nonuniformity of the material, which are characteristic for the low-density of the nonwoven material, significantly affect its material properties and deformation mechanisms. Therefore, the approach of continuous FE models is not suitable to describe the material properties of low-density nonwoven materials due to its continuous nature. In this chapter, the effects of microstructure of the low-density nonwoven material on the overall material properties of fabric will be investigated by using various image capture systems and numerical methods. First, the microstructure of the low-density thermally bonded nonwoven material will be investigated using a micro x-ray computed tomography (CT) system, which could provide a more detailed morphology of the material's discontinuous and nonuniform microstructure. Then the effects of the material's discontinuous and nonuniform microstructure on strain and stress distribution of the material are analysed using experimental and numerical methods, respectively. After the determination of the significantly effects of material's microstructure on overall mechanical properties of the low-density nonwoven material, the fibres orientation

distribution function (ODF) and tensile behaviour of fibres are investigated, which are important effective factors of the mechanical performance of the material and are supposed to be used in further advanced finite element analysis.

5.2 Microstructure of low-density thermally bonded nonwoven material

In Chapter 3 the microstructure of the nonwoven material was demonstrated with a series of by scanning electron microscope (SEM) images. The images provide an immediate impression of the two-component structure of the nonwoven material. According to geometry information obtained from these SEM images, continuous FE models were developed as presented in Chapter 4. However, the two-component structure cannot describe the microstructure of the low-density nonwoven material properly. Due to the manufacturing process of the material and its low density, the microstructure of the material is assumed to be discontinuous and nonuniform. The microscopic images obtained from a micro x-ray CT system provide full three-dimensional information that can be used to develop the assumptions for the discontinuous model. The micro CT system is shown in Figure 5.1.

Figure 5.1: Micro X-Ray Computed Tomography system

The micro CT system requires that the specimen is fixed in front of the x-ray source vertically and fixed at the bottom by the grip. However, due to the low bending stiffness of the nonwoven material, it is hard to fix the position of the specimen within the CT system. Therefore, the specimens were attached to a hard paper-board, which had a window as a measurement area to expose the nonwoven material for scanning. The prepared specimen is shown in Figure 5.2.
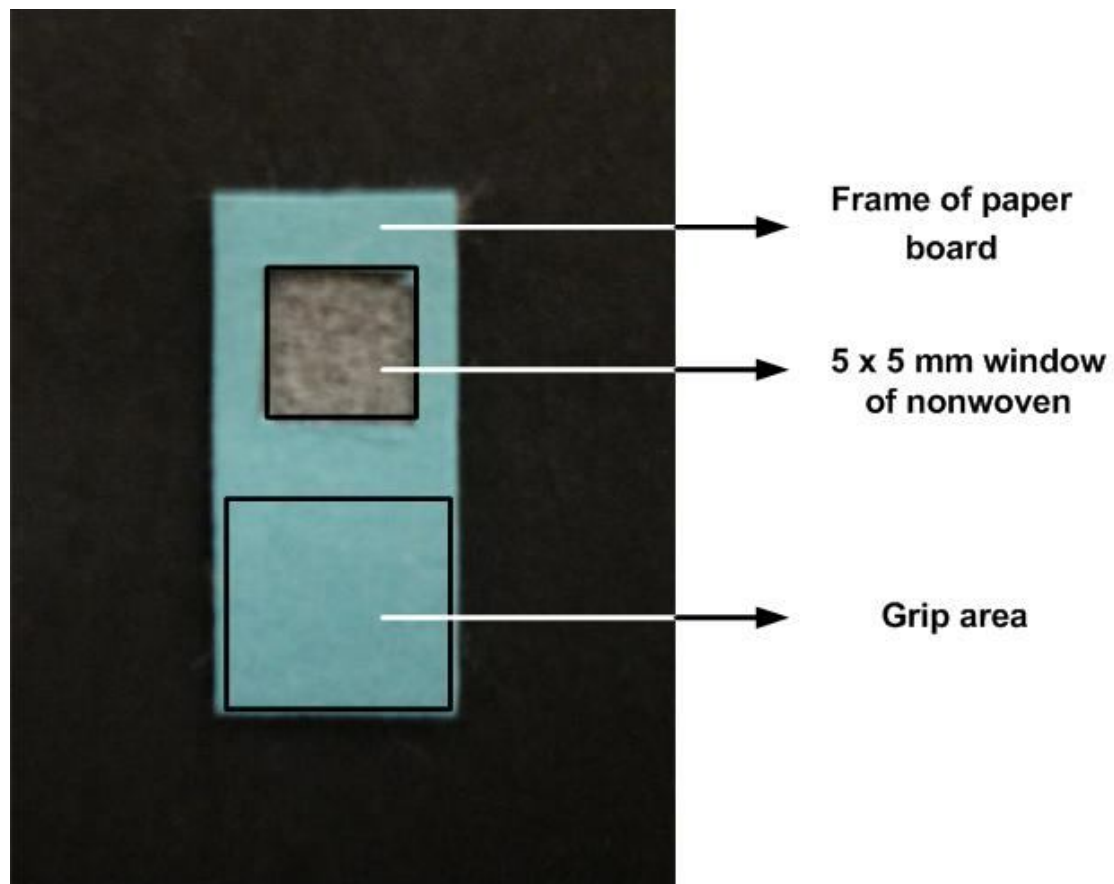
Figure 5.2: Specimen prepared for micro CT scan

Figure 5.3 shows the in-plan microstructure of the nonwoven material. Apparently, voids areas are randomly located throughout the material, which determines the highly nonuniform and discontinuous microstructure of the low density nonwoven material.
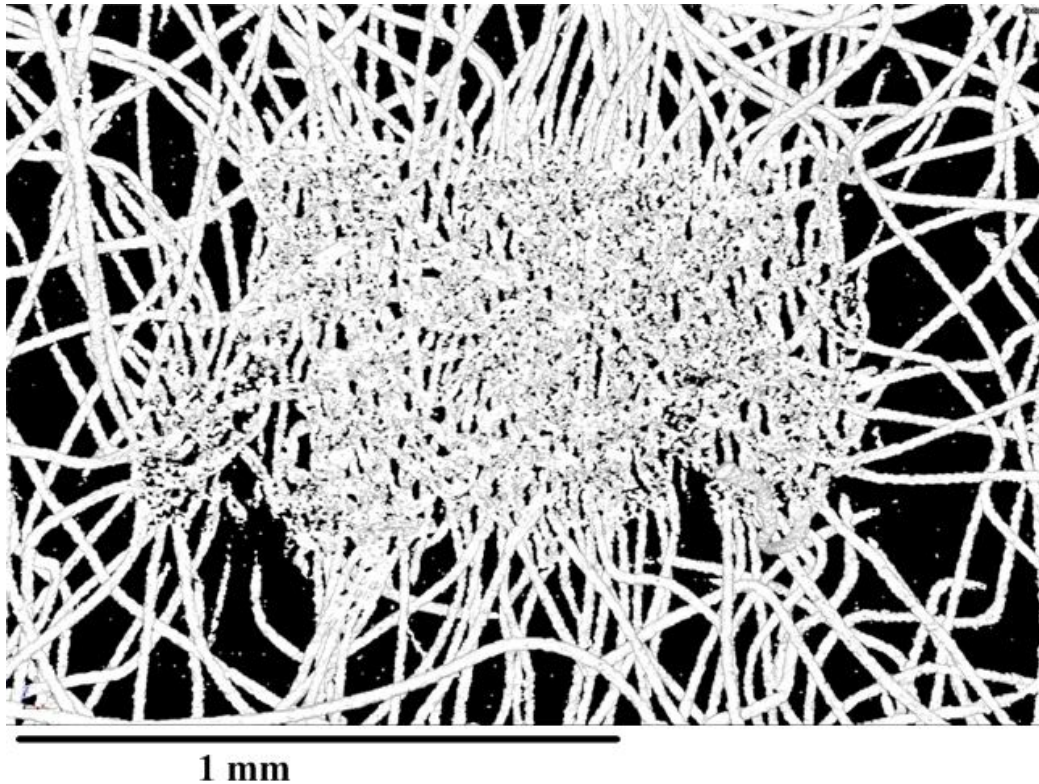
Figure 5.3: X-ray micro CT image of microsturcture of low-density thermally bonded nonwoven material

The micro x-ray CT system also provides the geometry information in three dimensions by digital "slicing" in any arbitrary plane. This non-destructive approach provides information for a non-disturbed microstructure as compared to a physical cutting. Figure 5.4 shows the microstructure of the material for a through-thickness cross-section. Different thicknesses of the bonded area (bond point) and unbonded area (fibrous network) are measured using image processing software. According to the image, the bonded area has lower thickness than the unbonded area. This is linked to the manufacturing process: the bonded area is formed by melted and compressed fibres that later solidify. The measured average thickness of the area is 0.02 mm, and this magnitude could be used for future experimental and numerical studies. For the unbonded area, the measured average thickness is 0.18 mm. However, the magnitude cannot be used for mechanical calculations due to its unbonded nature. According to the original definition of true stress/strain, the volume of the specimen should be constant. But the unbonded area is formed by loosely assembled fibres, with spaces

104

between them. When the unbonded area is stretched, its loose structure is compressed, the volume of the material changes, contradicting to the original definition.
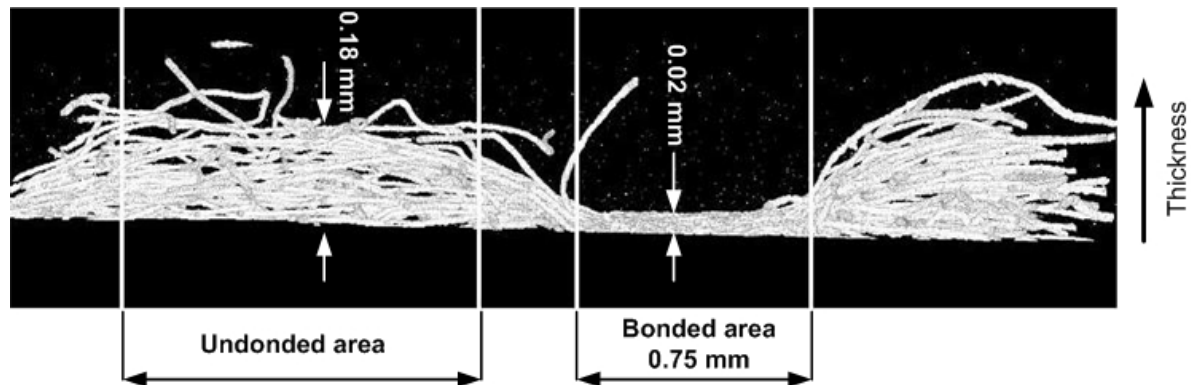
Figure 5.4: Microstructure of through-thickness cross-section area of low-density thermally bonded nonwoven material

5.3 Nonuniform strain distribution in low-density thermally point bonded nonwoven material

Based on the images obtained with the micro x-ray CT system, the microstructure of the low-density nonwoven material can be defined as highly discontinuous and nonuniform. It is easy to conclude that such as microstructure could cause a nonuniform strain distribution in the material, even for uniform external loading conditions. To analyze the nonuniform deformation mechanism of the material, a new series of tensile tests was carried out coupled with image analysis. The testing area of the specimens was 25 mm × 20 mm; the testing speed was 25 mm/min. Three types of marks were prepared for those specimens: highlighted bond points, orthogonal (4 mm x 4 mm) mesh formed by axial and transverse straight lines and randomly highlighted points, which are shown as Figure 5.5. For the specimens with highlighted bond points and orthogonal mesh, the marks were drawn by pen with black ink. For the specimens with randomly highlighted points, the marks were painted by spraying black ink on the specimens.

(a)   (b)   (c)
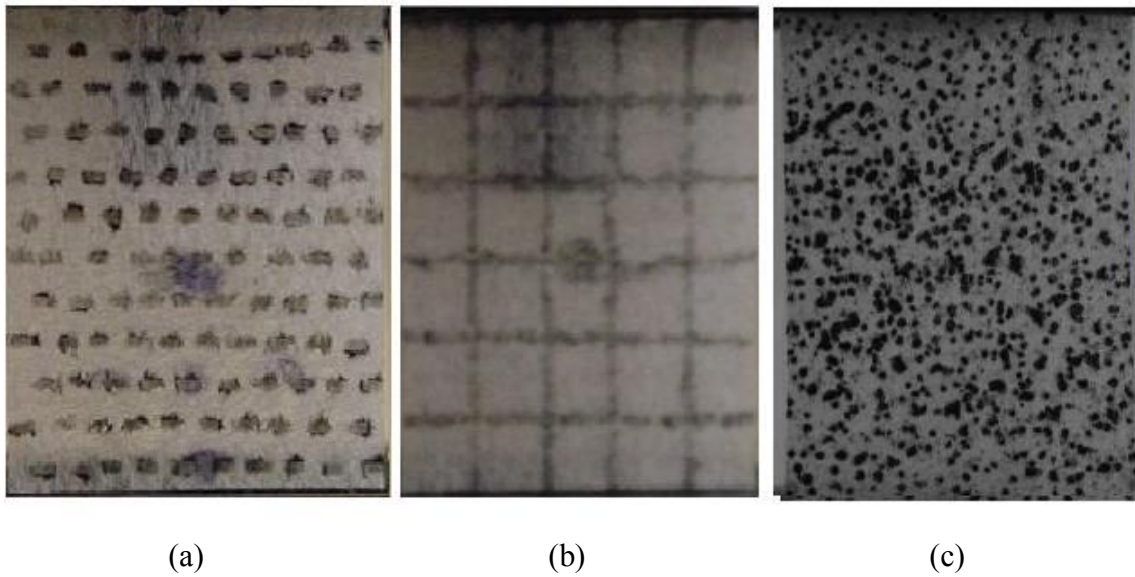
Figure 5.5: Specimens of nonwoven material used for image analysis: (a) specimen with highlighted bond points; (b) specimen with orthogonal mesh; (c) specimen with random points

The specimens with highlighted bond points and the orthogonal mesh were tested in both machine direction (MD) and cross direction (CD). Pictures were captured with the digital camera when the strain of the specimen was 0%, 20%, 40%, 60% and 80%. INSTRON Micro-Tester 5848 was used for the tensile tests; the specimens were extended using one fixed end and one moving end. Therefore, during the experiment, the height of the camera was controlled to keep the focus point targeting at the central point of the specimen to perform measurements. The specimens with randomly highlighted points were analyzed with the ARAMIS system (Figure5.6), which is an optical 3D deformation analysis system for measuring deformation and strain during loading of complex materials and geometries. During the tensile test, two serious of pictures were captured by two high-speed digital cameras and the pictures were analysed by an image analysis program provided with the system. Then strain distribution of the tested specimen was calculated for increasing strain levels.
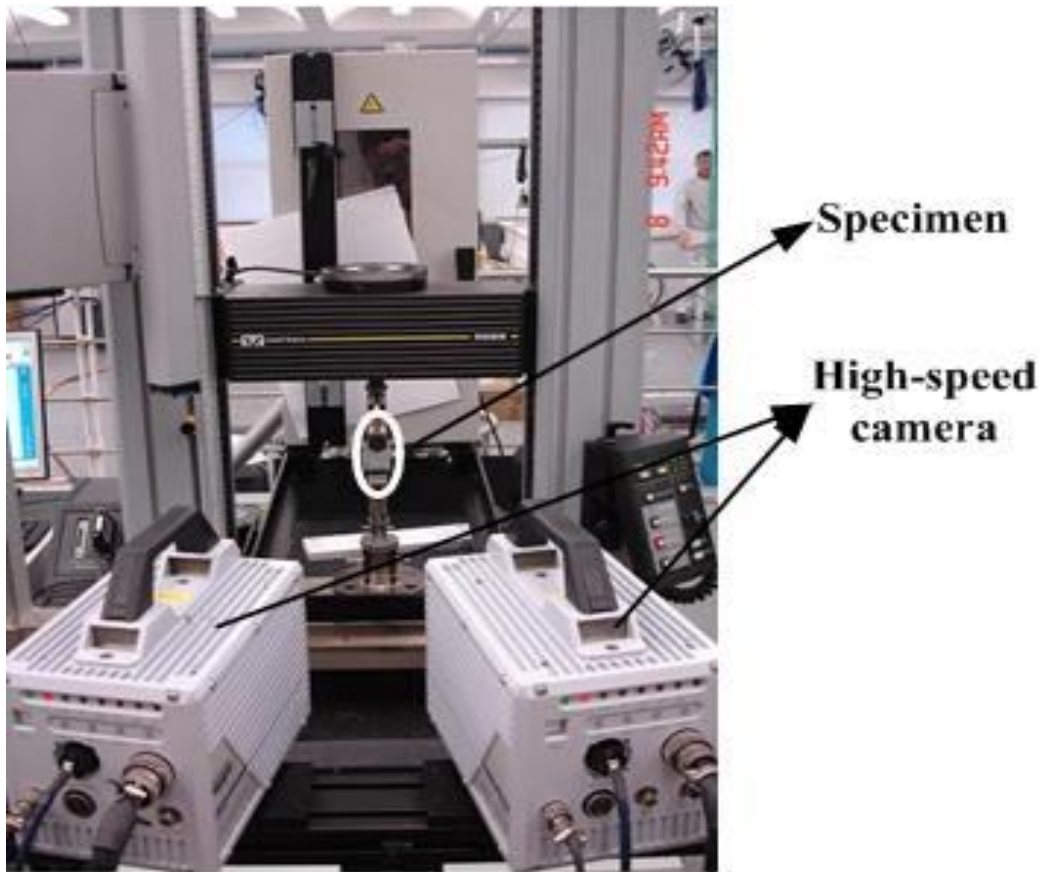
Figure 5.6: ARAMIS system and INSTRON tester

Figure 5.7 shows a specimen with highlighted bond points tested in machine direction. For the undeformed specimen (Figure 5.7a), the bond points forms nearly straight lines in the horizontal direction; these lines are parallel to each other. During the deformation, the straight lines start to distort. With each increment of deformation, the level of distortion increases. Moreover, the resulting distortion is not symmetric for the loading direction and differs from line to line. Five specimens were tested under same conditions, and the obtained distortion varies from specimen to specimen. The observed process vividly displays that the material deforms nonuniformly due to its discontinuous structure.

<center>(a)   (b)   (c)   (d)   (e)</center>

Figure 5.7: MD specimens with highlighted bond points: (a): non-deformed specimen; (b) specimen under 20% strain; (c) specimen under 40% strain; (d) specimen under 60% strain; (e) specimen under 80% strain.

The MD specimen with an initially rectangular mesh is shown in Figure 5.8. During the deformation, the axial lines show the similar distortion as in the specimen with highlighted bond points, the lines distort and the character of the distortion varies from line to line. But these tests also demonstrate another feature of the material's deformation mechanism. As shown in Figure 5.8, the axial lines of the rectangular mesh show symmetric necking with increasing extension along the machine direction. It means that the material can still have a symmetric necking behaviour, even in a case of discontinuous microstructure.

Figure 5.8: MD specimens with rectangular mesh: (a) non-deformed specimen; (b) specimen under 20% strain; (c) specimen under 40% strain; (d): specimen under 60% strain; (e) specimen under 80% strain

Figure 5.9 presents analysis of the results obtained for an MD specimen with the ARAMIS system, which gives strain distribution mapping for the deformed material. The pictures for strain level s of 0%, 20%, 40% and 60% were collected to compare with each other to demonstrate the change of the strain distribution. To calculate the instantaneous strain of the specimen, the ARAMIS analysis system masks the material as reference points. Figure 5.9b displays the masked specimen with 0% strain, with a blue colour corresponding to the uniform state. In the specimen exposed to strain of 20 %, the material in the boundary area near grips has larger strains about 60%, which are shown in red in Figure 5.9c. It is due to the constrained boundary condition applied by the grips. And other areas of the specimen, away from the grips, are still practically under uniform strain. When the specimen achieves overall strain of 40% (Figure 5.9d), the strain in the central parts of the specimen is distributed nonuniformly and apparently is not affected by bond points, which are located in the material regularly. In the specimen at 60% strain, the strain nonuniformity achieves a higher level, with the areas with high levels of strain located in the material randomly.

The phenomena means that the nonuniform deformation mechanism of the material is not only caused by the boundary conditions of the specimen and the bond points, which are formed by a stiffer material and causing stress concentration, but also resulted from the random discontinuous fibrous network and its random density distribution.

Figure 5.9: Results obtained with ARAMIS system for MD: (a) non-deformed specimen; (b) masked specimen under 0% strain; (c) specimen under 20% strain; (d) specimen under 40% strain; (e) specimen under 60% strain

The next step of the study was to analyse deformation in cross direction. In the specimen with highlighted bond points, the lines formed by bond points are along the loading direction in this case. Figure 5.10a shows the undeformed specimen, with the bond points of the specimen not being fully symmetric. Therefore, when the specimen is at 20% strain (Figure 5.10b) the necking of the overall material is also not symmetric. But the lines formed by bond points are distorted symmetrically with regard to the cross direction. This means the symmetry of the material deformation does not depend on the overall shape of the material; it depends on the arrangement of bond points of the material.
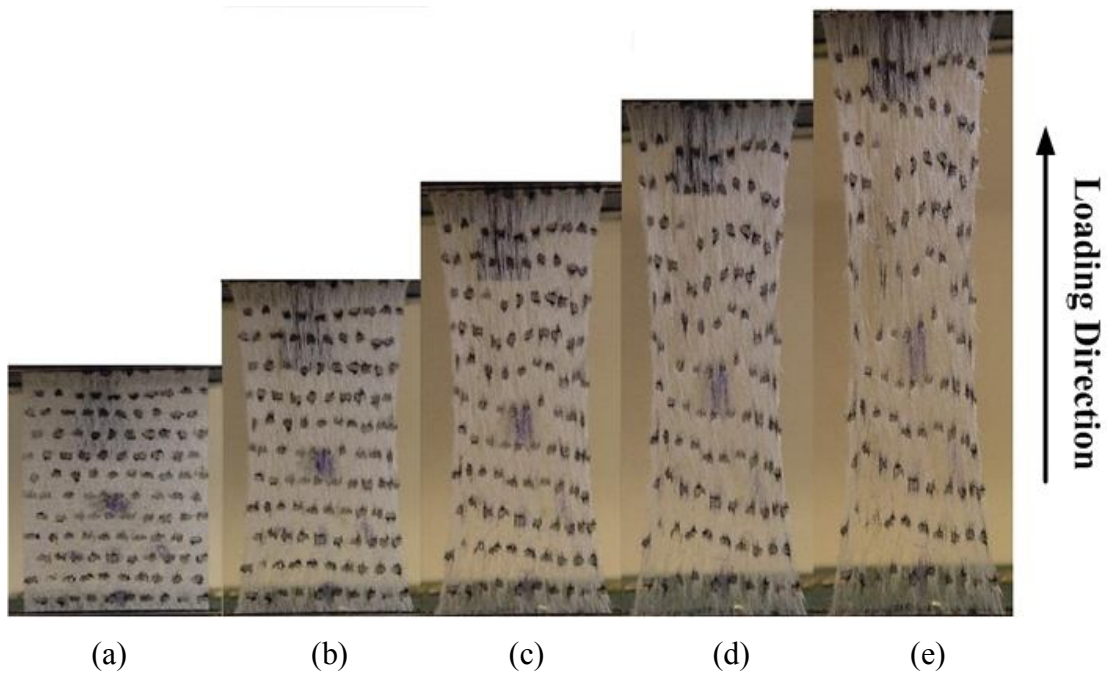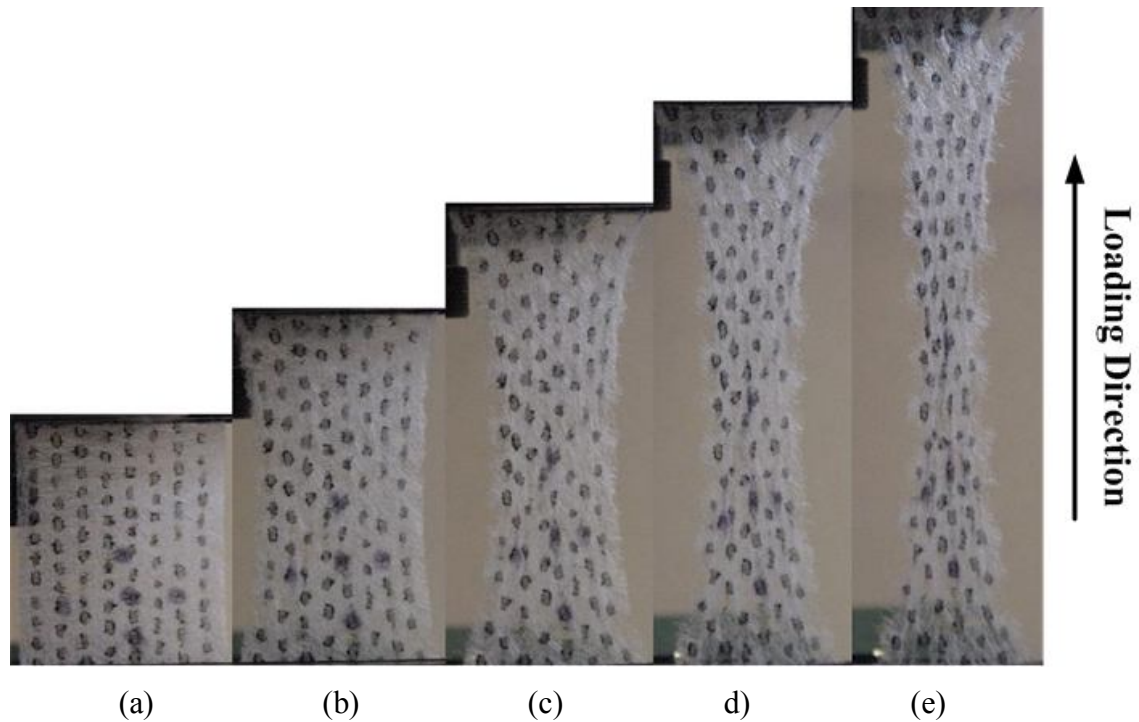
Figure 5.10: CD specimens with highlighted bond points: (a) non-deformed specimen; (b) specimen under 20% strain; (c) specimen under 40% strain; (d) specimen under 60% strain; (e): specimen under 80% strain

In a CD specimen with an orthogonal mesh (Figure 5.11), the axial straight lines, parallel to the loading direction start to distort during the deformation of the material due to the necking effect. This necking is generally symmetric with regard to the middle line of bond points. The transverse lines of the rectangular mesh distort taking a waving shape, which is due to the staggered arrangement of lines of bond points along loading direction. When the overall strain increases to 40%, the area with a relatively lower density starts to fail (Figure 5.11c). With the increase in the deformation, the breaking area develops and will cause the final rupture. Actually, in most of the tensile tests, the rupture of the material usually starts from the areas with low density.
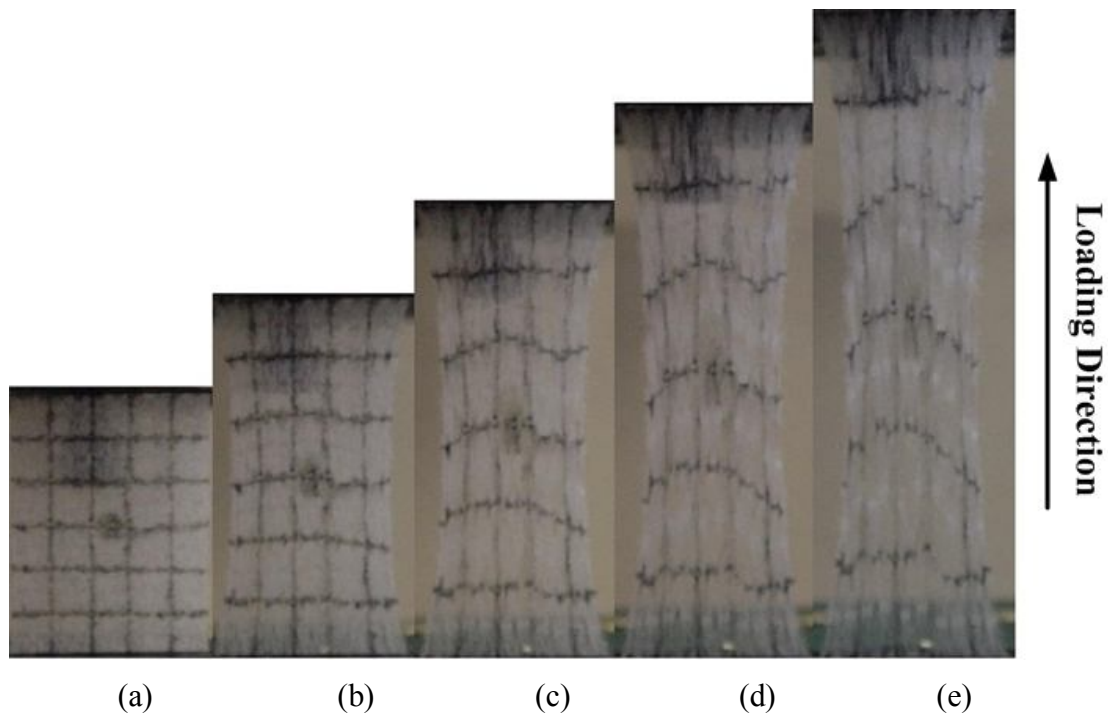
111
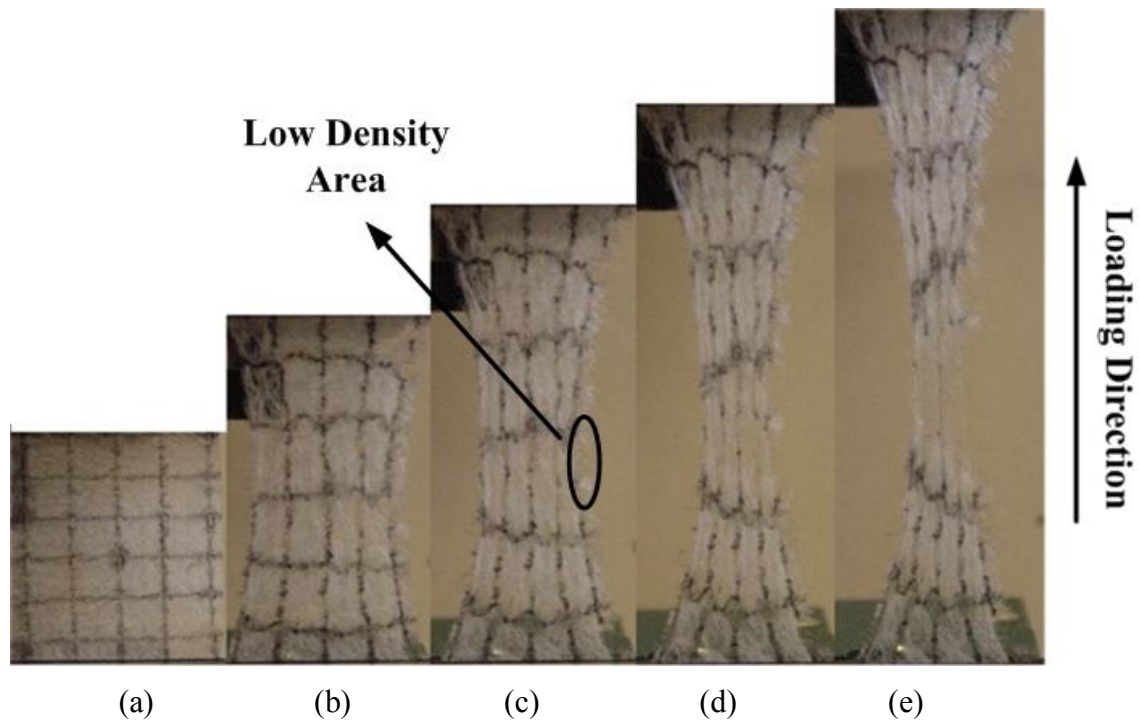
Figure 5.11: CD specimen with orthogonal mesh: (a) non-deformed specimen; (b) specimen under 20% strain; (c) specimen under 40% strain; (d) specimen under 60% strain; (e) specimen under 80% strain

Figure 5.12 demonstrates results of tests performed with the ARAMIS system for a CD specimen. A highly nonuniform strain distribution was obtained for the specimen under 20% strain. It means that the specimen stretched in the cross direction, the strains are distributed more nonuniformly than in the specimen (see Figure 5.9) MD, and large local deformations happen in some areas even at the very early stages of extension. When the specimen is under the overall strain of 40%, some areas of the material start to achieve 60% strain (red area). And for the overall specimen's deformation of 60%, some areas of the material still have low strain levels (green and yellow areas). Those phenomena demonstrate that the material has a random, nonuniform deformation mechanism. And the level of its nonuniformity in cross direction is higher than in machine direction, which matches the simulation results of the continuous FE models presented in the previous chapter.
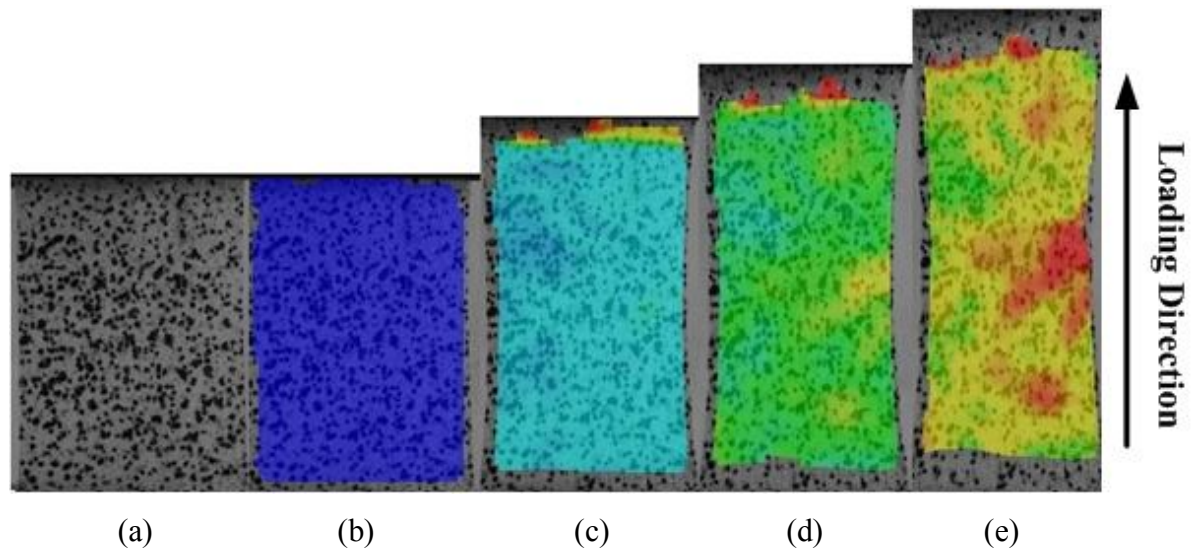
112
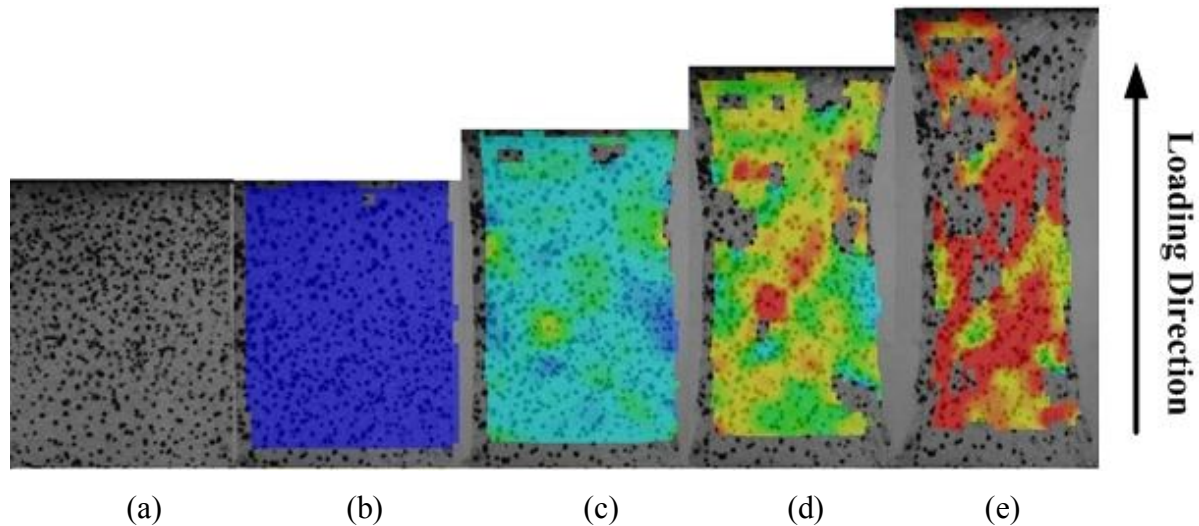
Figure 5.12: Results obtained with ARAMIS system for CD: (a) non-deformed specimen; (b) masked specimen under 0% strain; (c) specimen under 20% strain; (d) specimen under 40% strain; (e) specimen under 60% strain

According to the strain distribution studies, the reasons for the nonuniform strain distribution of the nonwoven material can be summarized in the following way: First, the nonuniform strain distribution of the material is caused by the boundary conditions of the material, which is the same as in any uniform material. Second, it is resulted from the arrangement of bond points. The stiffness of bond points is higher than that of the fibrous network, which usually causes stress concentration. Therefore, the arrangement and shape of bond points affect the deformation mechanism of the material. Finally, the nonuniform strain distribution is also caused by the discontinuous structure of the fibrous network. Such network has a nonuniform density distribution, which leads to a nonuniform strain distribution during the deformation. And the areas with apparently low density usually cause a local failure causing the final rupture of the overall material at higher strain levels.

5.4 Effects of voids

According to our previous experimental analysis (Section 5.2), the traditional stress calculation method is unsuitable for a low-density nonwoven material. Due to its discontinuous structure of loosely arranged fibres, the volume of the material will

reduce with the increase in the external load, and this is contradicts to the standard definition of the stress calculation methods. Therefore, a new method was developed to account for the discontinuous microstructure of the material. First, to avoid the effect of void areas in the material, the initial effective cross area was calculated using an image analysis program. The picture of the microstructure of the nonwoven material (Figure 5.13a) was captured by applying a background light to the specimen to obtain a clear contrast between the material and voids. The black areas are the fibrous network and white areas are voids and bond points. Out of these three components shown in the picture only, the fibrous network and the bond points can really carry load, and they are defined as an effective area. To calculate the proportion of the effective area to overall area accurately, the picture was converted into one in Figure 5.13b using the MATLAB programme. Two operations were used to achieve that: first the bond points are converted into pure black area. Then, the overall picture is converted to black and white picture using the gray level threshold of 100. In the obtained picture (Figure 5.13b), the black area is the effective area and the white areas represent voids. Then the percentage of the black area as a part of the overall area was calculated. It is equal to 88.01% for Figure 5.13b. Six images were captured for different areas of a big fabric, and the results are shown in Table 5.1; the average level for the effective area is 81.68 %.

(a)

114
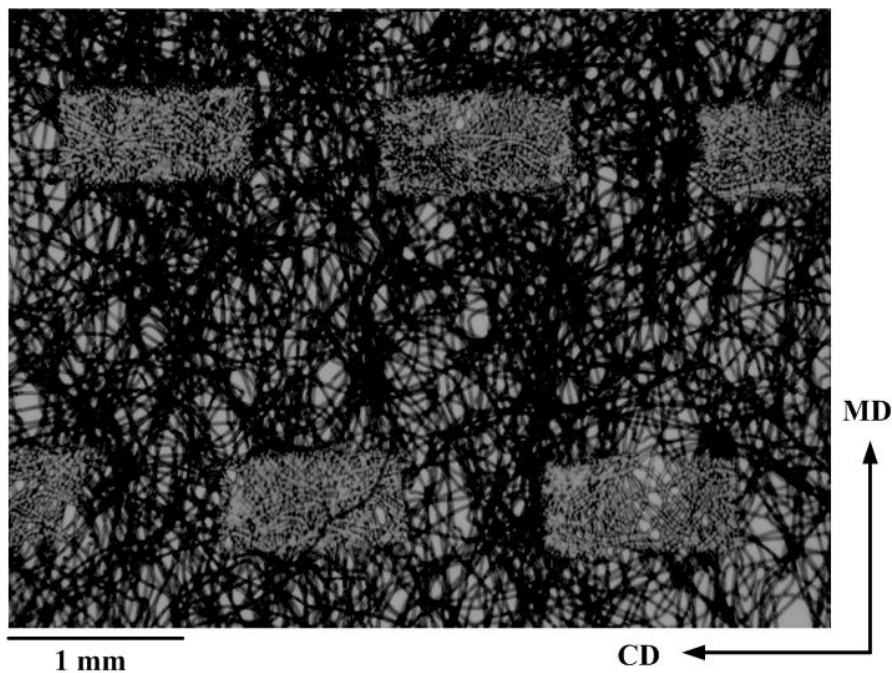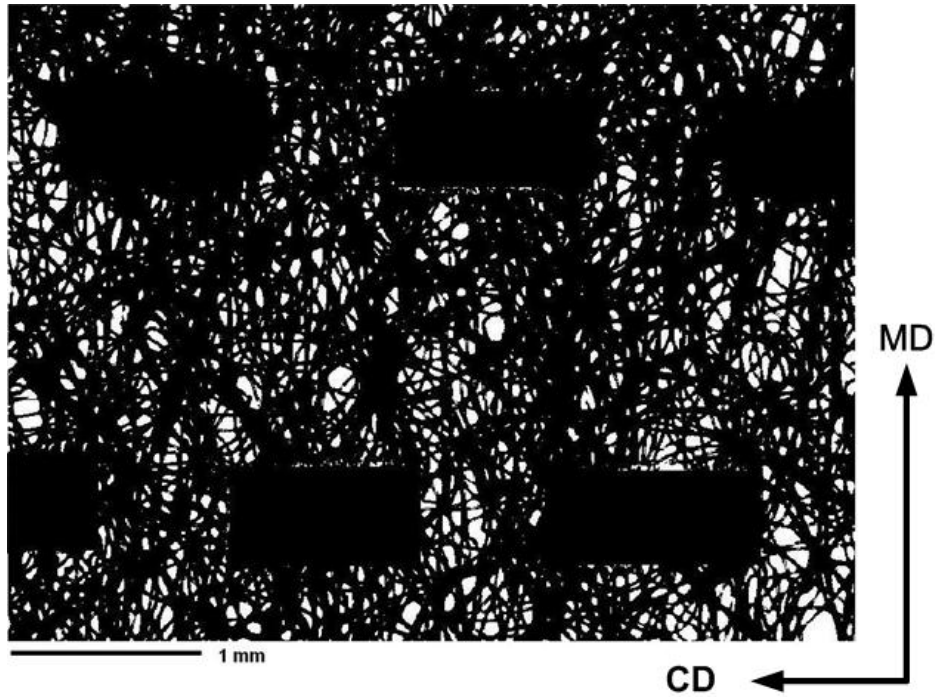
(b)

Figure 5.13: Microscopic images of nonwoven material: (a) original picture; (b) black and white picture converted with threshold 100

Sample	1	2	3	4	5	6	Average	Standard Deviation
Percentage (%)	88.01	83.62	78.20	82.61	86.24	71.40	81.68	6.05

Table 5.1: Results of density analysis of nonwoven material

Then, the thickness of the fabric was assumed to be constant. And the effective area of the material is represented using an average effective width $\overline{W}_{Eff}$ in our calculation. The relationship between $\overline{W}_{Eff}$ and the fabric's width W_{Fabric} is

$$P = \frac{A_{Eff}}{A_{Fabric}} = \frac{\overline{W}_{Eff}}{W_{Fabric}} ,$$
(5.1)

where P is the ratio of the effective area of the material A_{Eff} to its overall area A_{Fabric}. Then the effective stress of the material could be calculated using the relationship:

115

$$\sigma_{Eff} = \frac{F}{W_{Eff}} = K_\sigma \sigma_{eng} \text{ and } \sigma_{True} = K_\sigma \sigma_{Eng} (1 + \varepsilon_{Eng}), \qquad (5.2)$$

where

F is the reaction force;

K_σ is stress renormalization factor, $K_\sigma = \dfrac{1}{P}$;

σ_{Eng} is the engineering stress;

σ_{True} is the true stress;

ε_{Eng} is the engineering strain.

5.5 Orientation distribution of fibres

Due to the discontinuous microstructure of the nonwoven material and its low density (20 gsm), its mechanical properties are determined not only by the mechanical properties of single fibres and bonding points but also by the arrangement of fibres and bonding points. Hence, the orientation distribution becomes one of the major research interests. At present, two methods are mainly used by the researchers to calculate the orientation distribution function (ODF), Fourier Transform (FT) and Hough Transform (HT).

In this project, the low-density thermally bonded nonwoven material is studied with an optical microscopic system (Figure 5.14) provided by NCRC of North Carolina State University to obtain images for analysis. Six images were obtained for different positions of the nonwoven sheet for our calculation of ODF; the sample image is shown in Figure 5.15.
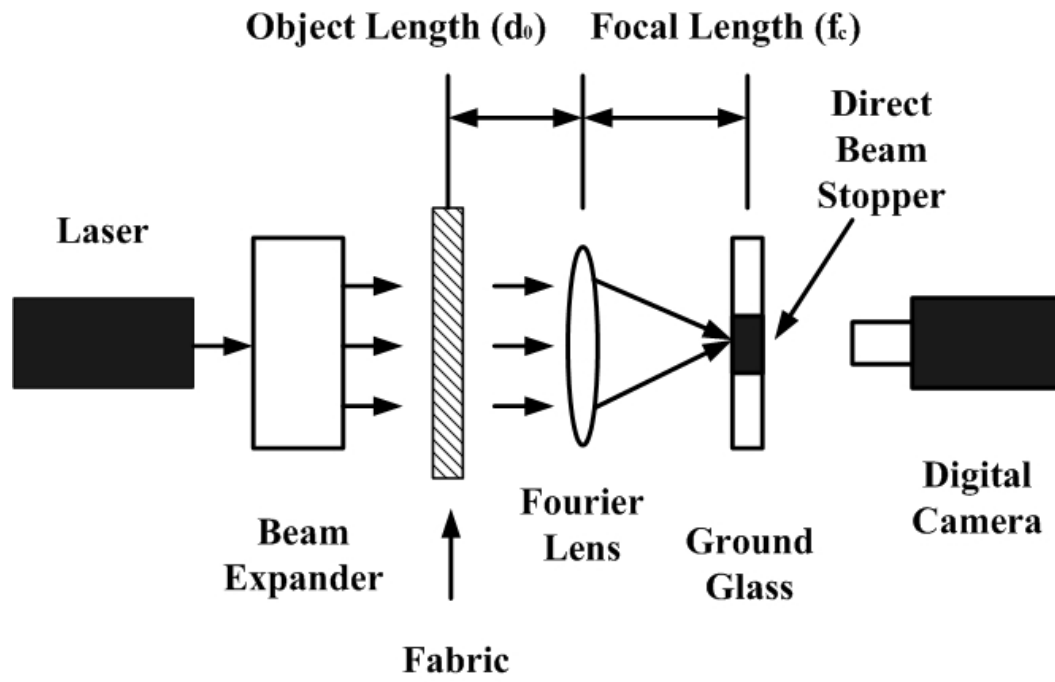
Figure 5.14: Schematic of image capture system (Jeddi, A.A., Kim, H.S. and Pourdeyhimi, B. 2001)
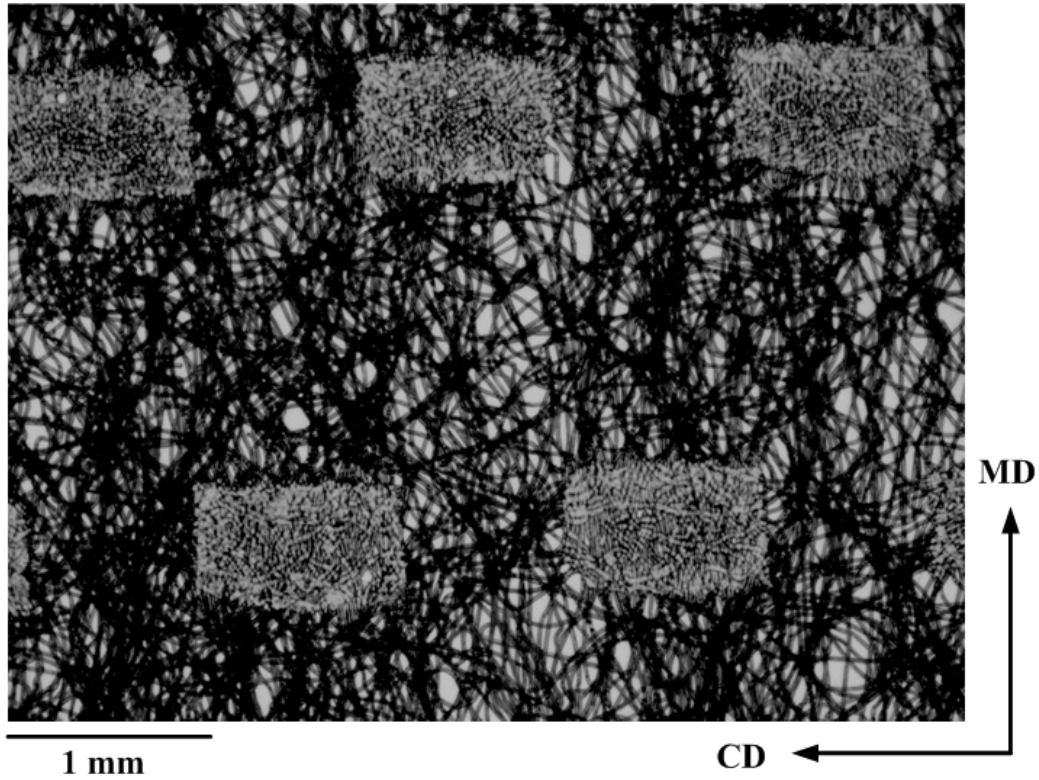
Figure 5.15: Sample image of nonwoven material used for ODF analysis

Then the images were analysed using the Fourier Transform method. In two dimensions, the direct Fourier Transform is given as:

$$F_f(u,v) = \int_{-\infty}^{+\infty}\int_{-\infty}^{+\infty} f(x,y)\exp[-j2\pi(ux+vy)]dxdy \quad , \tag{5.3}$$

where $f(x, y)$ is the image and $F(u, v)$ is its transform, u refers to the frequency along the x direction, and v represents the frequency along the y-axis.

The results of the analysis are given in Tables 5.2 − 5.3 and Figure 5.16. The fibre orientation distribution in the material is nearly symmetric with the highest frequency (7.04 %) obtained for 90°, which is the machine direction. That means that the material has more fibres along the machine direction than other directions due to the manufacturing process. The lowest frequency (4.08 %) was obtained for 0°, which is the cross direction of the material. Another feature reflected in the results is the frequency increase with the angle approaching 90° (MD). The results provide a direct evidence to explain the anisotropic material properties of the nonwoven material. And it is easy to determine the stiffest direction of the material – its machine direction- due to a higher portion of fibres along it (or close to it).

Angle of fibre orientation (degree)	0	10	20	30	40	50	60	70	80
Average frequency (%)	4.08	4.58	4.72	4.70	5.20	5.30	5.78	6.30	6.81
Standard deviation	0.35	0.29	0.26	0.20	0.19	0.29	0.26	0.22	0.35
Angle of fibre orientation (degree)	90	100	110	120	130	140	150	160	170
Average Frequency (%)	7.04	6.94	6.58	6.16	5.84	5.34	4.88	4.80	4.08
Standard deviation	0.25	0.38	0.34	0.35	0.28	0.22	0.18	0.18	0.24

Table 5.2: Orientation distribution of the nonwoven material

	1	2	3	4	5	6
Dominant Angle (degree)	96.61	101.85	102.56	95.60	97.60	95.98
Standard Deviation	5.10	5.03	5.07	5.08	5.10	5.00

Table 5.3: Dominant angle of thermally bonded nonwoven material
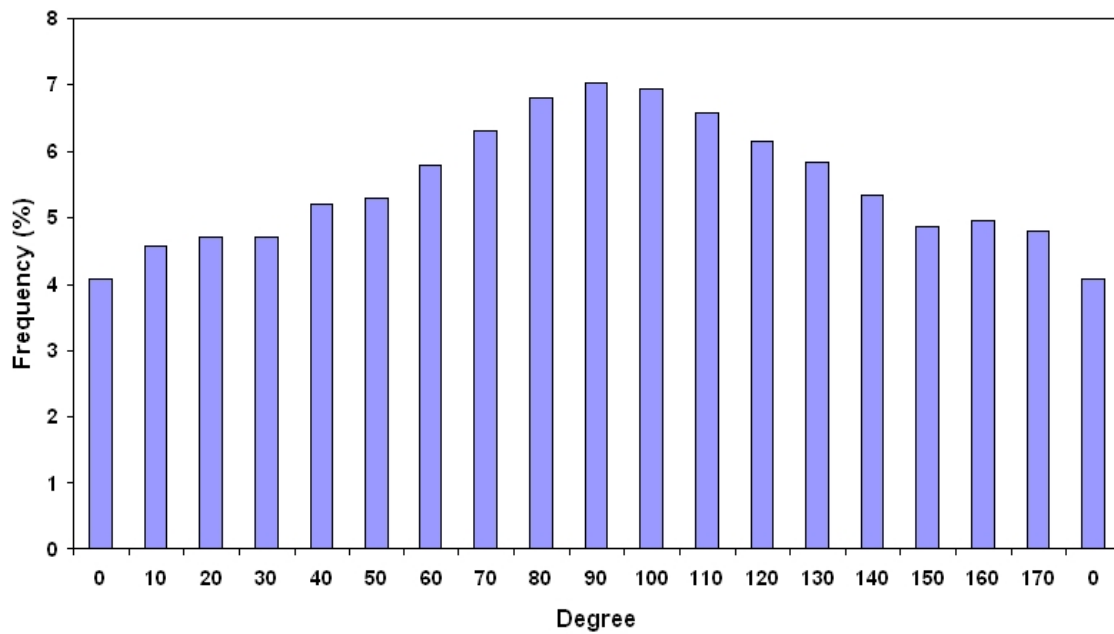
Figure 5.16: Average ODF obtained from images with ten degree interval range (0° corresponds to CD)

According to the measured average orientation distribution function for the fibrous network, the anisotropic ratio R of the randomly fibrous network is determined by the following equation [5.4]

$$R = \frac{\sum_{i=0}^{17}|f(\alpha_i)sin\alpha_i|}{\sum_{i=0}^{17}|f(\alpha_i)cos\alpha_i|} \, ,$$
(5.4)

where α_i is the representative direction of fibres relative to cross direction of the material, and its magnitude is equal to $10\,i$ (in degrees) with i being an integer

between 0 to 17. $f(\alpha_i)$ is the frequency of fibres along the direction α_i. Based on the measurements the magnitude of R is 1.16.

5.6 Material properties of polypropylene fibre

According to results of the previous research, properties of low-density nonwoven materials are determined by features of its microstructure. The microstructure of the nonwoven material is formed my fibres, which are randomly assembled. Therefore, the mechanical properties of the overall nonwoven material are determined by the properties of fibre at a large extent. Tensile tests have been performed to determine the properties of single fibres. And the obtained results will be used as input parameters for the future analysis of the mechanical properties of the nonwoven material.

The specimens of the experiments are free polypropylene fibres obtained from the nonwoven fabric; the length of the specimens is 30 mm. The tests were performed using Instron MicroTester 5848 with a 5 N loading cell. Three different testing speeds were chosen for the tests - 12.5 mm/min, 25 mm/min and 50 mm/min-, which are the same to the testing speeds used in the tensile tests of fabric; six specimens were tested for each testing speed.

To calculate the stress of the fibres, the diameter of fibres need to be measured. However it is hard to determine the diameter of fibres using traditional tools. In this research, the diameter of the PP fibres was measured using image analysis approach. Using SEM images of the nonwoven material, the diameter of fibres were determined according to the magnification of the overall image; the results are shown as Figure 5.17. The average diameter of fibres obtained by those measurements is 0.02 mm.

Unit: mm
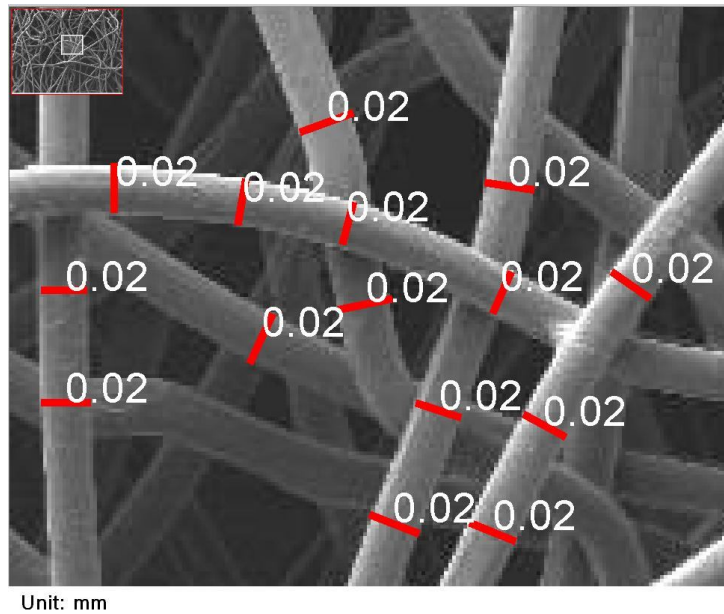
Figure 5.17: Measurements of the diameter of polypropylene fibres

A typical tensile behaviour of the PP fibres, which is obtained from tensile tests, is shown in Figure 5.18. This behaviour is highly nonlinear. To simplify it, the stress/strain curve could be divided into three stages according to the slope of the curve. They are defined as initial stage (I in Figure 5.18), second stage (II) and third stage (III).
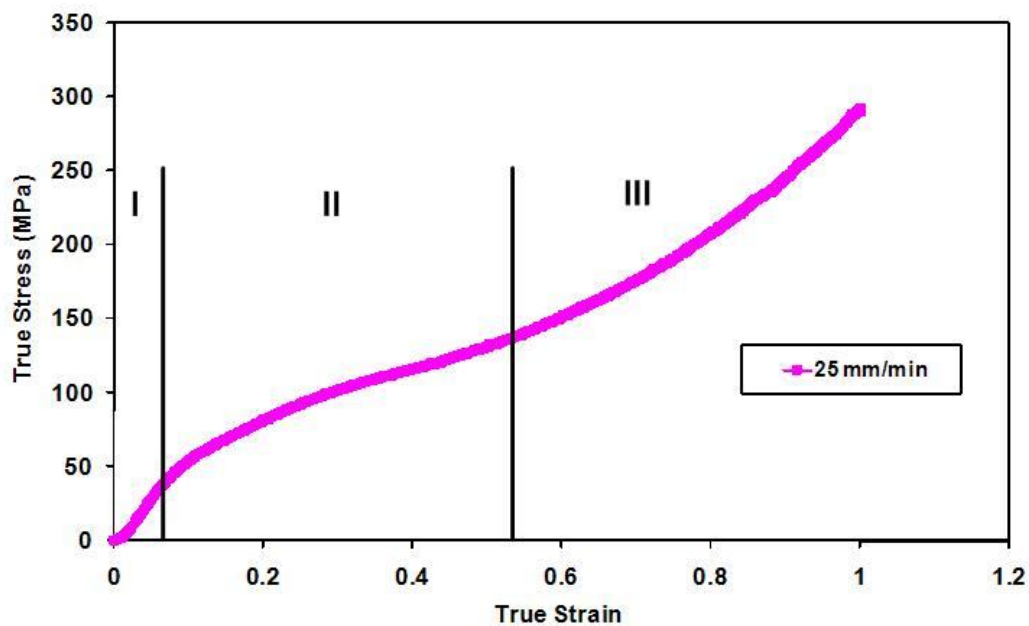
Figure 5.18: Typical stress-strain relationship of PP fibre

The studied fibres demonstrate strain-rate sensitivity; Figure 5.19 shows their mechanical behaviour for different testing speeds using 12.5 m/min, 25mm/min and 50mm/min, which are same to the testing speeds used in the tensile test of fabric. For fibres, they correspond to strain rates of 0.00694 1/s, 0.0138 1/s and 0.0278 1/s, respectively. The specimens tested with different testing speeds show different mechanical behaviours. It is a very important factor for the overall material properties of the nonwoven material, and is one of the reasons for the rate-dependent properties of nonwoven fabric.
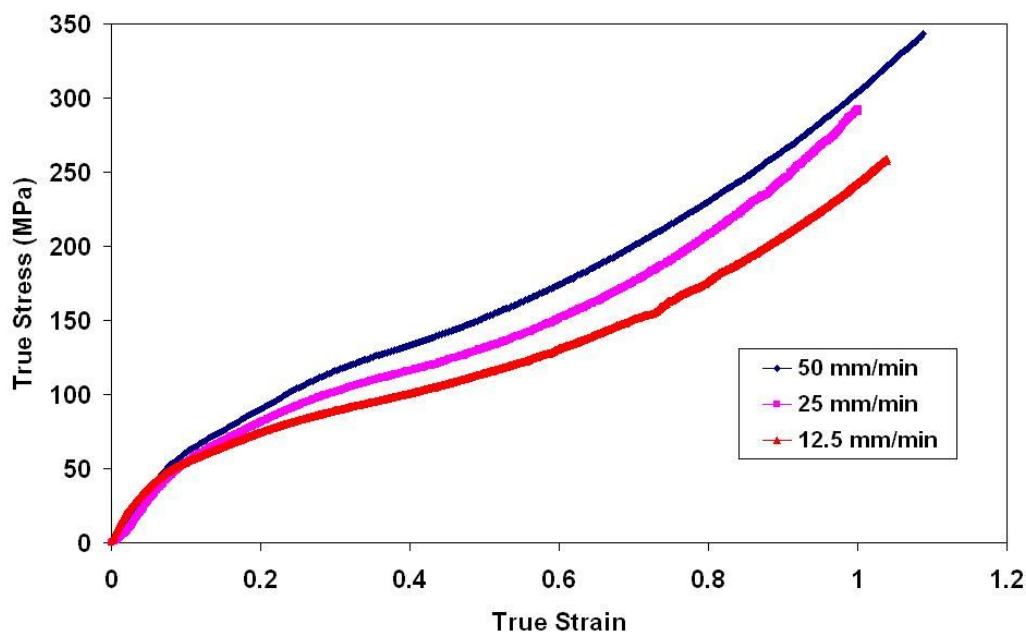
Figure 5.19: Typical tensile behaviours of PP fibre at different test speeds

Due to the highly nonlinear material behaviour of fibres, it is not easy to describe their material properties. Therefore, the initial, second and third stages of the material behaviours are approximated by linear behaviours with different levels of moduli, and the results are used to analyses the different mechanical behaviours of the specimens under different loading speeds. The moduli were calculated and the results are summarized as Figures 5.20, 5.21 and 5.22. The standard deviation is used to indicate the dispersion of the results.

With the increase in the test speed from 12.5 mm/min to 25 mm/min, the initial average modulus decreases (Figure 5.20). Its magnitude for the fibres tested at 12.5

mm/min is 10.9% higher than the one for the fibres tested at 25 mm/min. And when the fibres are tested at 50 mm/min, the obtained average modulus has a similar magnitude to the one tested at 25 mm/min. With consideration of stress/strain relationships shown in Figure 5.19, for the initial stage, the fibres demonstrate a similar mechanical behaviour under different loading speeds. At this stage, the fibres achieve similar stress levels and have similar moduli.
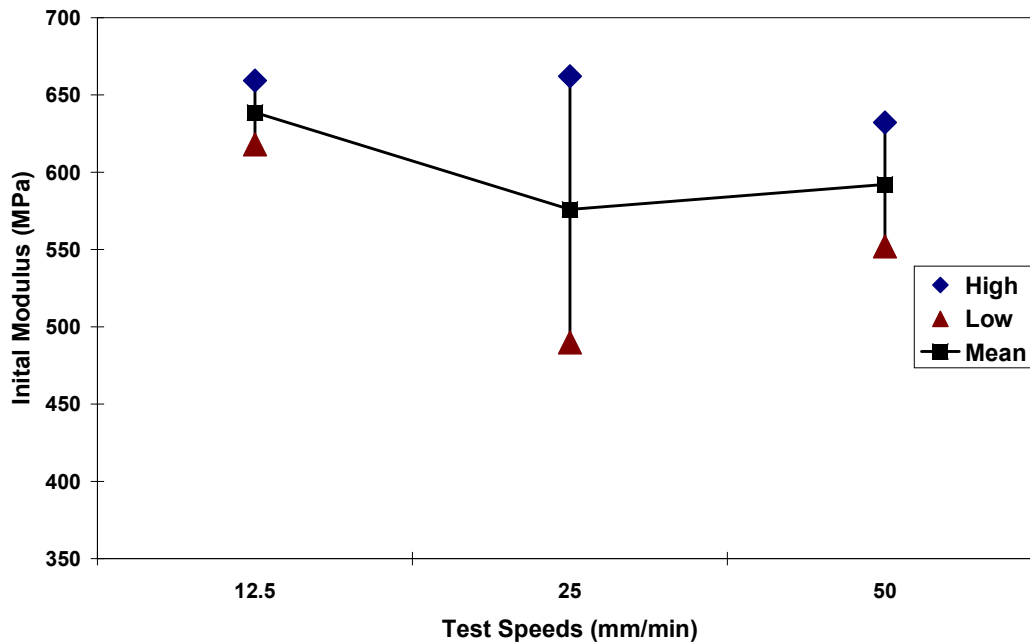
Figure 5.20: Effect of test speed on initial tensile modulus of PP fibres

At the second stage of the deformation, the fibres show a higher nonlinear behaviour. A higher loading speed causes an accelerated higher stress growth at the beginning of this stage, and then the stress increases mildly with the strain increase during the rest period of the stage (Figure 5.19). The second-stage moduli were calculated for this period of the deformation stage, and the magnitudes are similar to each other. The highest magnitude was obtained for the fibre tested at 50 mm/min (Fig. 5.21). It is 10.7% higher than the lowest magnitude, which was obtained for the fibre tested at 12.5 mm/min. Considering the stress/strain relationship in Figure 5.19, it is obvious that the rate-dependent mechanical performances occur at the beginning of second stage of the deformation.
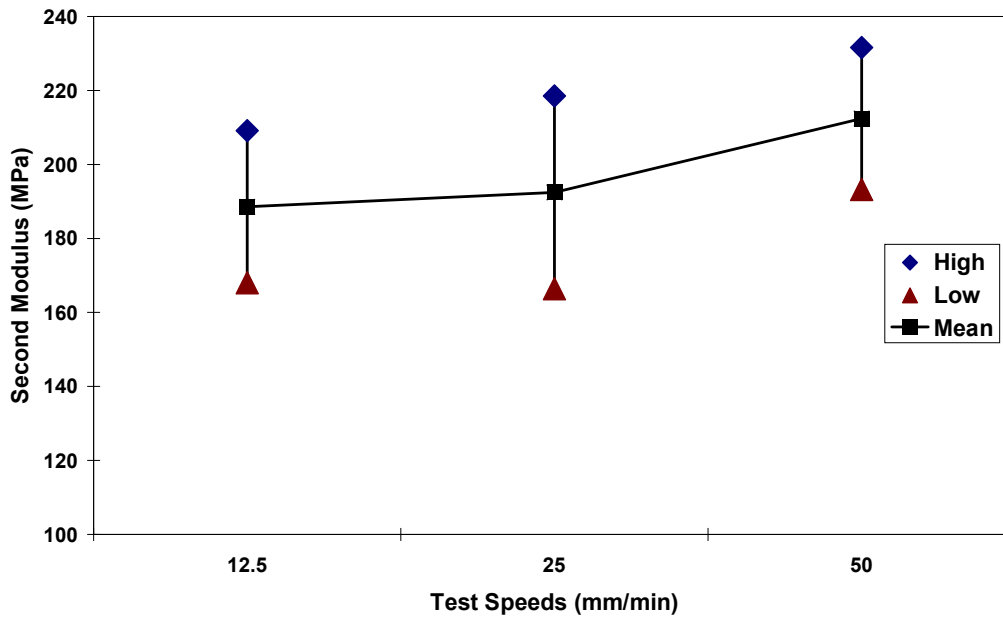
Figure 5.21: Effect of test speed on tensile modulus of second stage for PP fibres

The third-stage moduli were calculated, when the fibres achieved a higher strain level (higher than 55%). The highest modulus was obtained for the fibres tested at 25 mm/min. It is 45% higher than the lowest modulus obtained for the specimens tested at 12.5 mm/min. Similar magnitudes were obtained for moduli for the fibres tested at 12.5 mm/min and 25 mm/min.
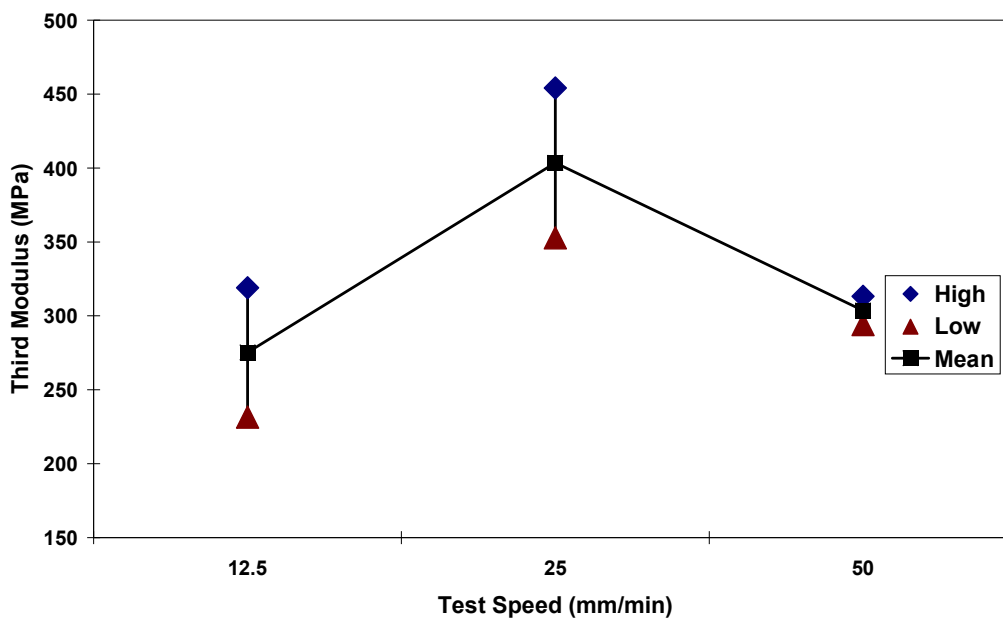
Figure 5.22: Effect of test speed on tensile modulus of third stage for PP fibres

124

Based on the results of the experiments, it was determined that the tensile behaviour of PP fibres is highly nonlinear and rate-dependent. However, at the initial stage of the deformation the tensile behaviour of the fibres is practically not sensitive to the loading speed, and similar performances were obtained. When the deformation transits to the second stage, the mechanical performance of fibres shows its rate-dependent character. Specimens under higher loading speed achieve higher stresses and their moduli are higher. With the further increase in the strain, at the third stage of the deformation, the fibres continue to behave rate-dependent and the moduli show a large scatter for the specimens at different loading speeds.

5.7 Conclusions

In this chapter, the low density nonwoven fabric is investigated using various testing methods to explore its features at micro-scale, and the effects of the discontinuous and nonuniform microstructure are analysed. Tensile tests were implemented for polypropylene fibres to investigate their rate-dependent mechanical properties. According to the obtained results, the significance of material's microstructure for the low-density nonwoven material can be summarised as follows:

1. The microstructure of the low-density nonwoven material was investigated using optical microscopy with a background light source and the x-ray micro CT system. The results show a highly discontinuous and nonuniform microstructure of the nonwoven material. Therefore, the assumption of the previous chapter, that the material is composed with two components: fibrous network and bond points should be modified as there are three different main phases within the material: bond points, fibrous network and void areas. Due to the low density of the material, there are significant void areas randomly located within the fibrous network. And the void areas are supposed to affect the overall material properties significantly. One immediate effect is that the traditional stress calculation method is not suitable for this material. Therefore, it brings to a conclusion that the finite element model based on the continuous microstructure as suggested in the previous chapter cannot properly describe the material properties of the low-density nonwoven fabric.

2. Using image analysis methods, the nonuniform strain distribution of the specimens, which were loaded by tension, was determined. There are three main reasons, which cause the nonuniform strain distribution: First, the boundary conditions of tensile test results in a macroscopically nonuniform strain distribution. Second, the bond points of the fabric, which are much stiffer than the fibrous network, contribute to the nonuniform strain distribution in the specimens. Third, the material's discontinuous and nonuniform microstructure causes the nonuniform strain distribution in the nonwoven material as a main factor. The results emphasize again that the mechanical performance of the low-density nonwoven material is highly determined by the features of its discontinuous and nonuniform microstructure. And the further numerical modelling should account for this information.

3. At microscale, the randomly assembled fibres are one of the most import features of the material's microstructure, which determines the discontinuity and nonuniformity of the material and affects material properties significantly. Therefore, the orientation distribution function (ODF) of the fibrous network was measured using the image analysis system and the developed program. Although the fibres are arranged randomly during the manufacturing process, there are still preferred directions along which there are more fibres compared to other direction. More fibres aligned along one certain direction cause better mechanical properties in this direction. Therefore, the measured ODF provides important information to understand the anisotropic mechanical performance of the material. Moreover, the mechanical properties of the fibres were investigated using single-fibre tensile tests. According to the microstructure of the material, fibres are main load carrier of the material, and their nonlinear and rate-dependent material properties result in overall nonlinear and rate-dependent material properties of the nonwoven. Therefore, the ODF and the material properties of fibres play an important role on the material properties of the nonwoven material and this information should be introduced into numerical models.

Chapter 6 Discontinuous Finite Element Model for Low Density Thermally Bonded Nonwoven Material

6.1 Introduction

In Chapter 4, continuous finite element models were developed to simulate the mechanical properties of the low-density thermally bonded nonwoven material. However, due to their continuous nature, the models cannot describe the material properties properly. The discontinuous and nonuniform microstructure of the material was studies in Chapter 5. The results of experiments and image analysis revealed that the microstructure of the material affects the mechanical properties of the nonwoven material significantly. Hence, the nonwoven material should be treated as a kind of three-phase material when accounting for the features of its microstructure. The three features are bond points, fibrous network and voids. To develop advanced numerical models for the low-density nonwoven material, the features of the material's microstructure should be introduced into them. In this chapter, the geometry structure of the low density nonwoven material is introduced numerically then advanced discontinuous FE models are developed and analysed with an account for the discontinuous microstructure of the material.

6.2 Simulation of loose fibrous network

As discussed in previous chapters, one of the drawbacks of the continuous finite element model in studying of low-density nonwovens is that the model cannot involve the discontinuous microstructure of the material in the analysis. Such discontinuity of the material is mainly determined by its discontinuous fibrous network, which is formed by randomly arranged fibres. Due to the low density of the material, void areas locate throughout the fibrous network, and affect the overall mechanical properties significantly. Therefore, to develop an advanced finite element model with

an account for the discontinuity of the material, the random and discontinuous fibrous network has to be generated numerically.

Geometric information for the fibrous web is the fibre diameter, fibre orientation distribution and curvature feature of fibres. According to the experimental results, the fibre orientation distribution is one of the most important factors, which determines the material's anisotropy and discontinuity. And the fibrous network forms the matrix in nonwoven that contains bond points. Therefore, it is assumed that the fibres are straight and arranged according to the orientation distributions. The orientation distribution of the studied fabric could be measured using the method presented at Chapter 5. To generate the random fibrous network, a program was developed using the Python programming language to describe the continuous random fibrous assembly according to the orientation distribution.
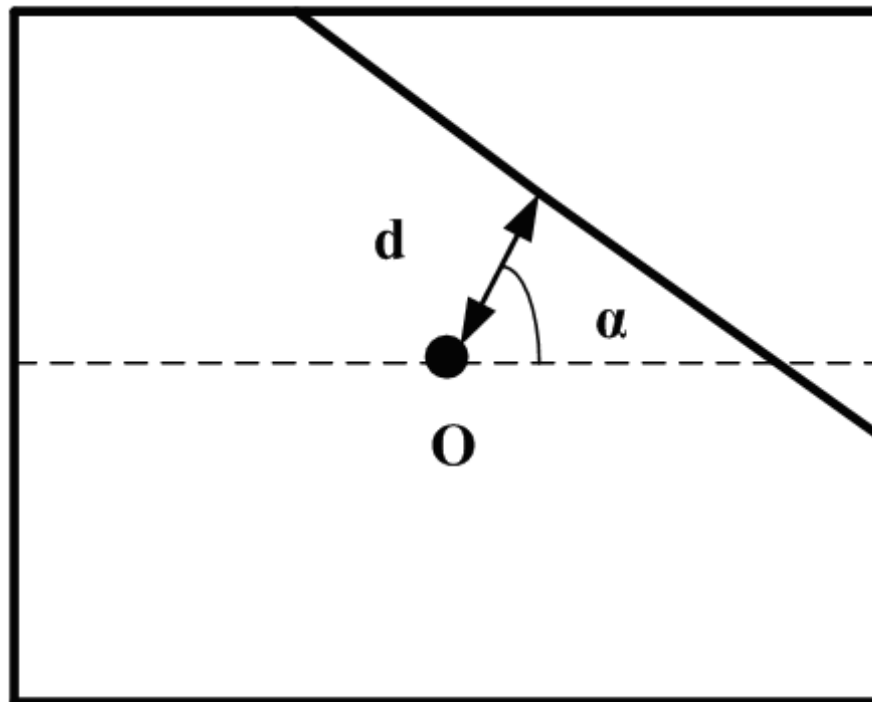
Figure 6.1: Scheme for algorithm used to model random distribution of fibres

In that algorithm, to generate one fibre, a point O (Figure 6.1) is located as the centre point of a sheet area first, then an angle α is defined according to the orientation distribution of the fibre. From the point O, a segment with a slope α to the horizontal

line and a random length *d* is generated using random functions. Finally, a line, perpendicular to this segment and intersecting it at the end point, opposite to O, is generated throughout the sheet area. By repeating this method, a fibrous network with continuous fibres was generated according to the experimentally measured orientation distribution of fibres.

Figure 6.2 demonstrates some sample images of the geometric simulation with different fibre orientation distributions, fibre densities and diameters of fibres. Using the developed program, it is possible to generate a fibrous network with different orientation distributions. Figure 6.2a shows a network consisting of fibres at 0° and 90°, while Figure 6.2b presents an image of a network with a random fibre's orientation distribution. Also, the program could generate fibrous networks with different density of fibres. Figure 6.2c presents an image, which is generated with two times higher density than the network shown in Figure 6.2b. Moreover, the fibrous network can be also generated using fibres with different diameters. Figure 6.2d presents a network, which is constituted by fibres with a smaller diameter than other networks.
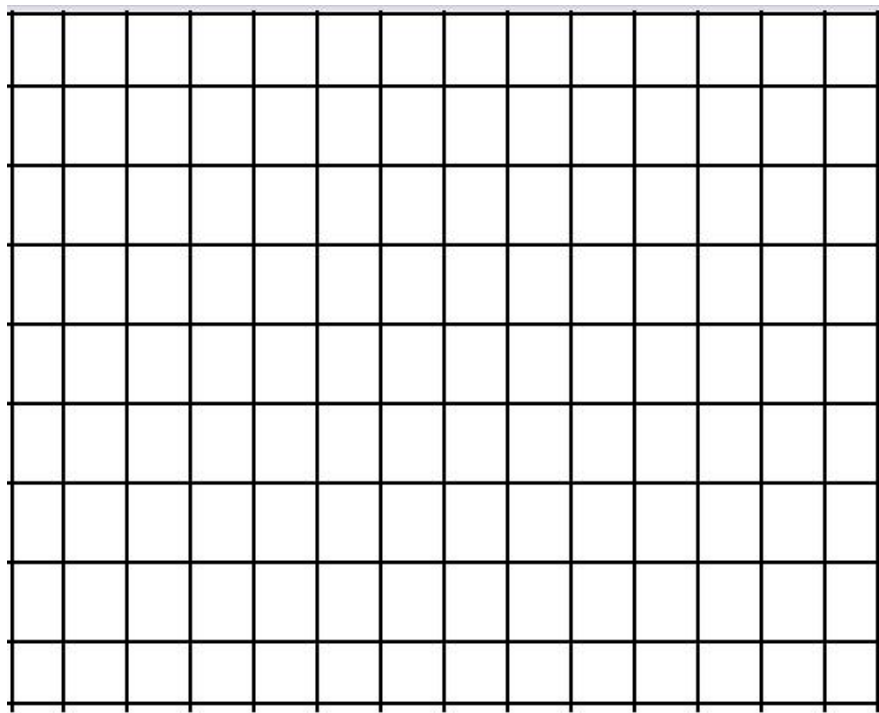
(a)
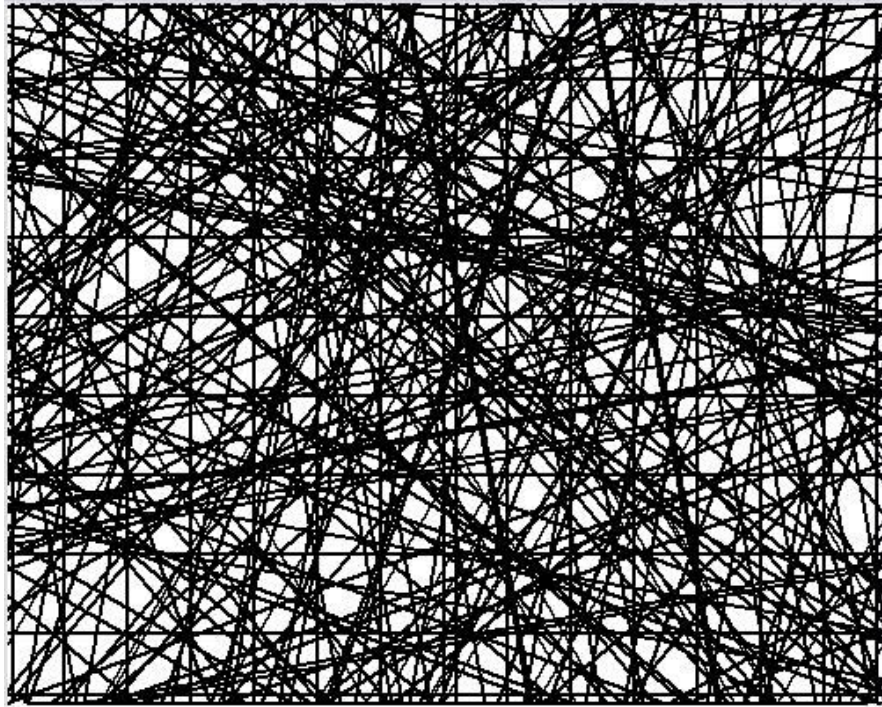
(b)
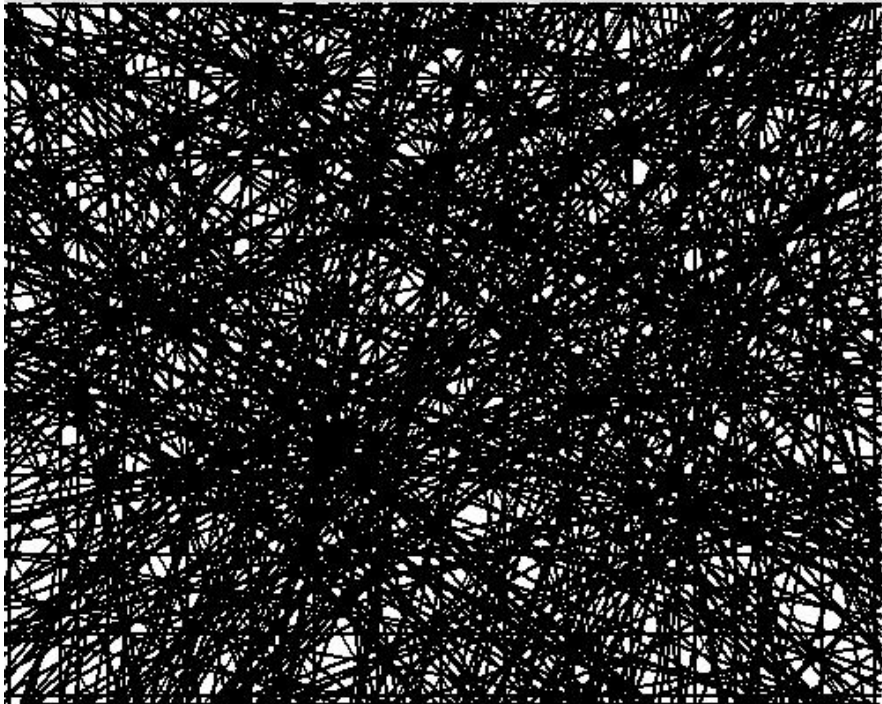
(c)
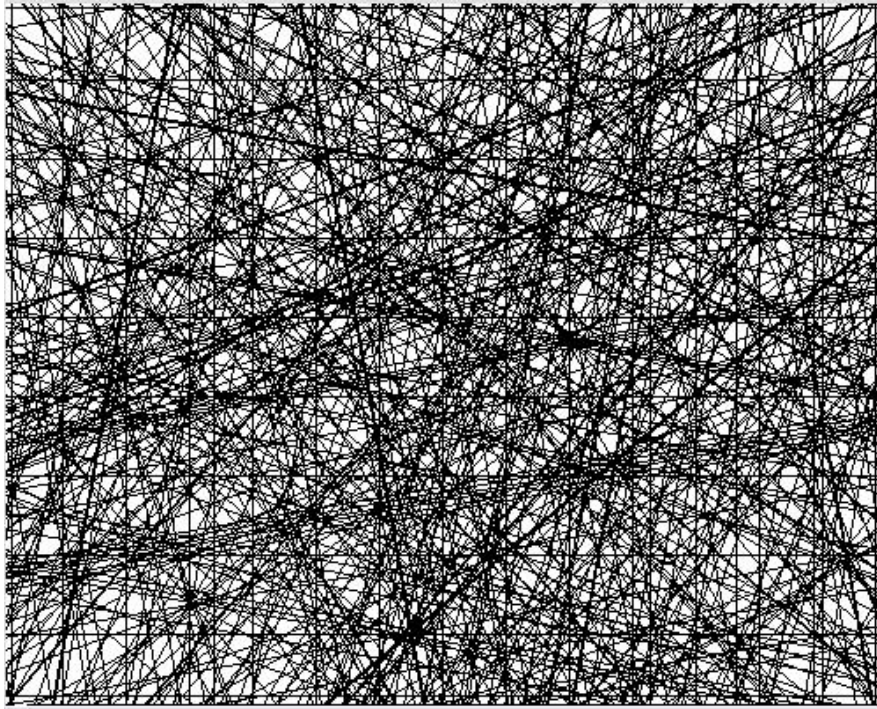
(d)

Figure 6.2: Geometry simulations of fibrous networks of nonwoven materials: (a) network with 0° and 90° fibres (diameter of fibres: 2 pixels); (b) network with 245 fibres and random fibre distribution (diameter of fibres: 2 pixels); (c) network with 490 fibres and random fibre distribution (diameter of fibres: 2 pixels); (d) network with 490 fibres and random fibre distribution (diameter of fibres: 1 pixels)

6.3 Development of discontinuous finite-element models

After the development of the random fibrous network, it became possible to develop discontinuous finite-element (FE) models to simulate the effects of microstructure of the low-density thermally bonded nonwoven material, which is characterized by the three-phase (bonded areas, fibres and voids) microstructure of the material.

6.3.1 Geometry and mesh of discontinuous finite-element models

To introduce the fibrous network generated by the Python programme to the finite-element software, the fibrous network was developed according to orientation distribution function measured for the real fabric. All the fibres were modelled

131

straight neglecting the effect of their curvature in order to reduce the computational cost and the risk of dissociation. Then the coordinates of the end points of the line were calculated and transformed into the format, which could be read by the ABAQUS software. After editing the ABAQUS input file, the geometry of the discontinuous model was generated with the finite-element analysis software (Figure 6.3a). The dimensions of the fibrous web is 25 mm x 20 mm. Due to the large number of fibres, forming the real nonwoven material, it is not practical and efficient to introduce the exact number of fibres into the discontinuous model. The trusses of the geometry part of the FE model are representative fibres, which represent a certain number of fibres having close directions.
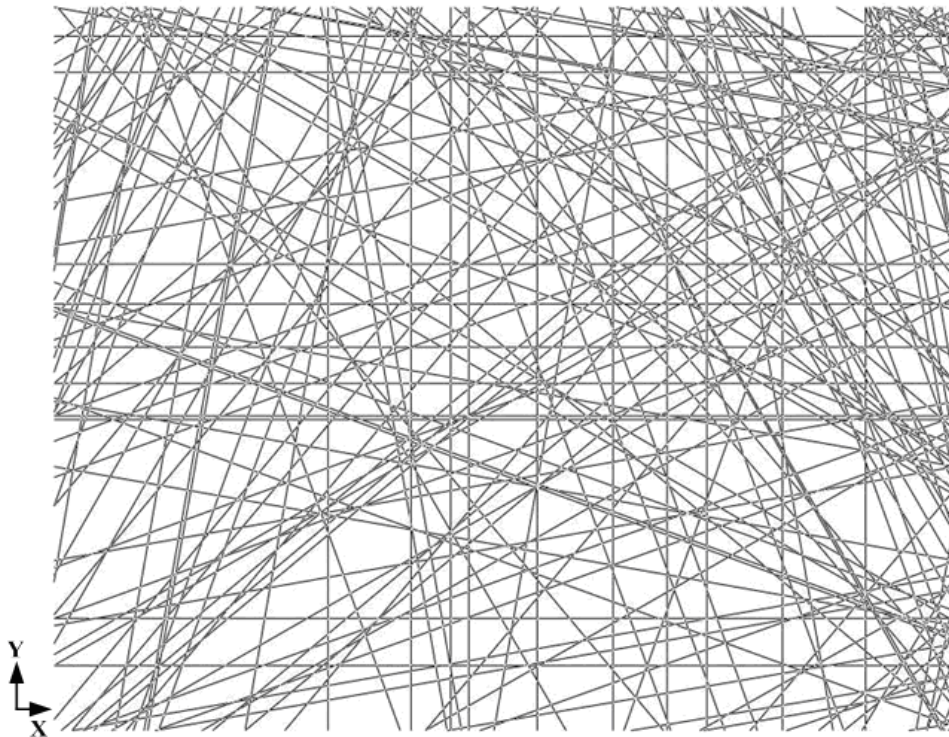
(a)
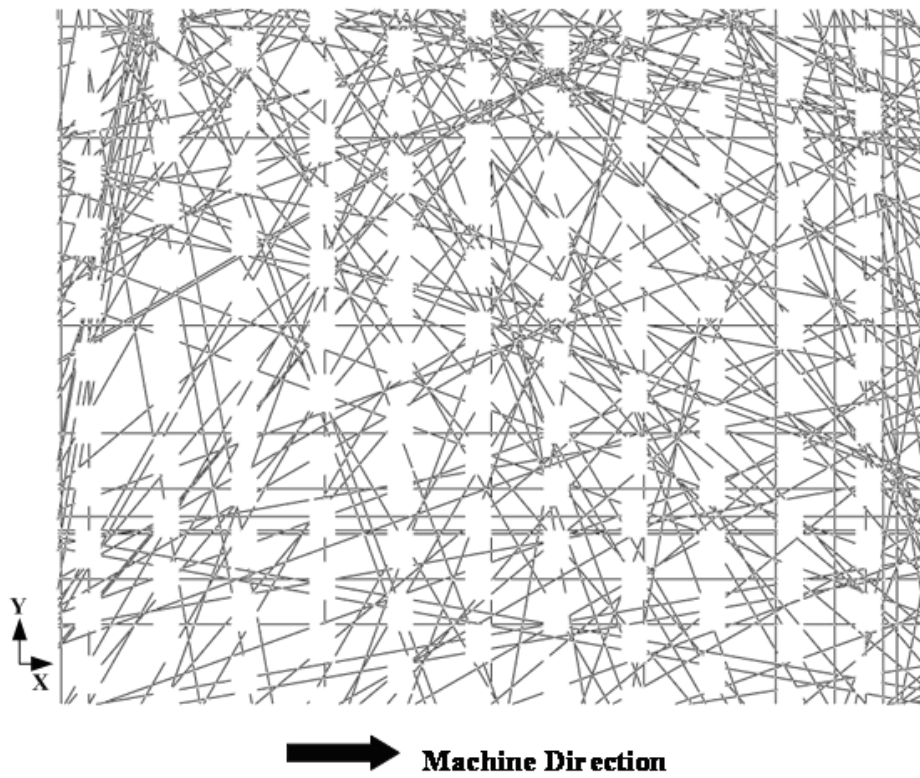
(b)
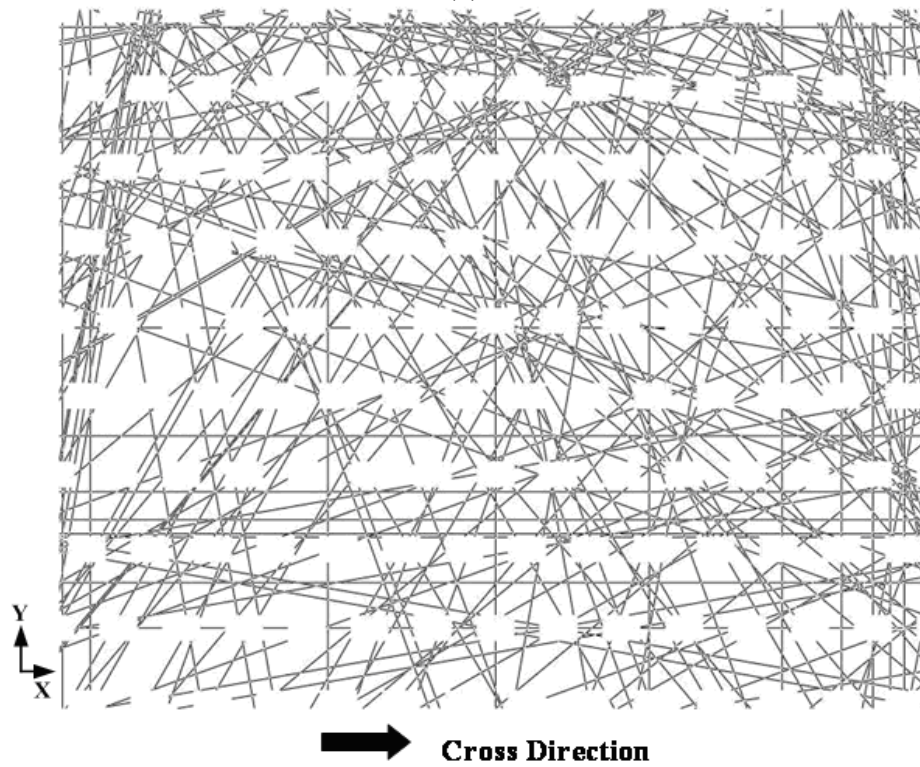
(c)

Figure 6.3: Fibrous network of discontinuous model (a) and geometry models of divided fibrous network: machine direction (b) and cross direction (c)

133

To introduce the geometric information of bonding points into FE simulations, the geometric model of the fibrous network should be divided into areas to leave the space for the bonding points since overlapping elements cause problems during meshing. The coordinates of the bonding points were used to divide the continuous fibres into parts within the geometry model of the fibrous network; the resulting geometry models for MD and CD are shown in Figures 6.3b and 6.3c, respectively. Then the geometry of bonding points was used as input into the ABAQUS software according to the measurement data obtained for the real material. And each bonding point was divided into two areas - the central area and the external area (0.05 mm wide) along the perimeter of the points – to leave the possibility of combining elements of the fibres and bonding points. Moreover, the thicknesses of both the fibrous web and the bond points of present models were chosen as constant at 0.02 mm.

The meshing process of the discontinuous model was carried out in two steps. First, the fibrous network was meshed using truss elements (T2D2) in order to avoid the ABAQUS software generating nodes automatically in the overlapping points of fibres to stop sliding of fibres. Then, the bonding points were meshed using shell elements of ABAQUS (Figure 6.4). The external areas of the bonding points were meshed first using shell element S3 with spacing between nodes 0.05 mm. At the next stage, additional nodes were defined along the boundaries of bonding points so that to coincide with the nodes of truss elements, connected to the boundaries. So there were common nodes shared by both the shell elements and the truss elements, which gave the possibility to transfer load and displacements from fibres to bonding points. The internal areas of bonding points then were meshed according to the location of the shared nodes with the external mesh using shell element S4R.
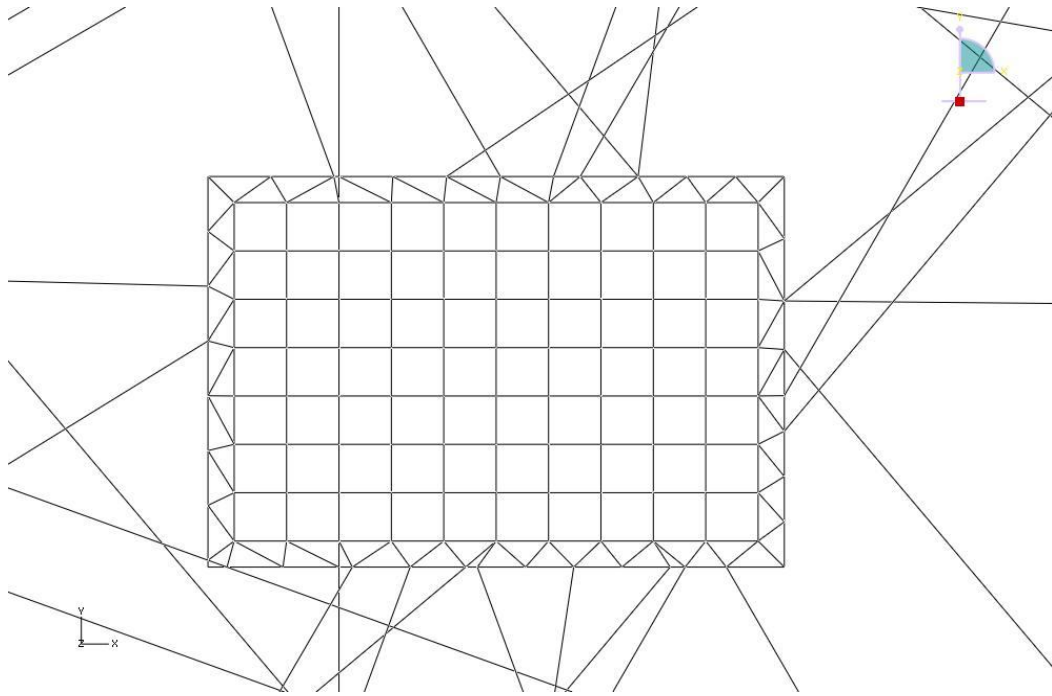
Figure 6.4: Meshed details for discontinuous model

To the author's knowledge, there are only two discontinuous finite element models in literature used to simulate nonwoven materials. Comparing the mesh details of our model with those in the Mueller's model (Mueller, D.H. and Kochmann, M. 2004) it is easy to find out that the fibres in present models (Figure 6.5) were generated randomly and not periodically. Besides, finer meshes were generated in present model for the bonding points – as compared with 8 elements per point in (Mueller, D.H. and Kochmann, M. 2004) so that to connect more fibres to them. Therefore, present models have the capability to simulate the mechanical properties due to the nonuniformity of the material as well as to better represent the mechanical behaviour of bonding points.
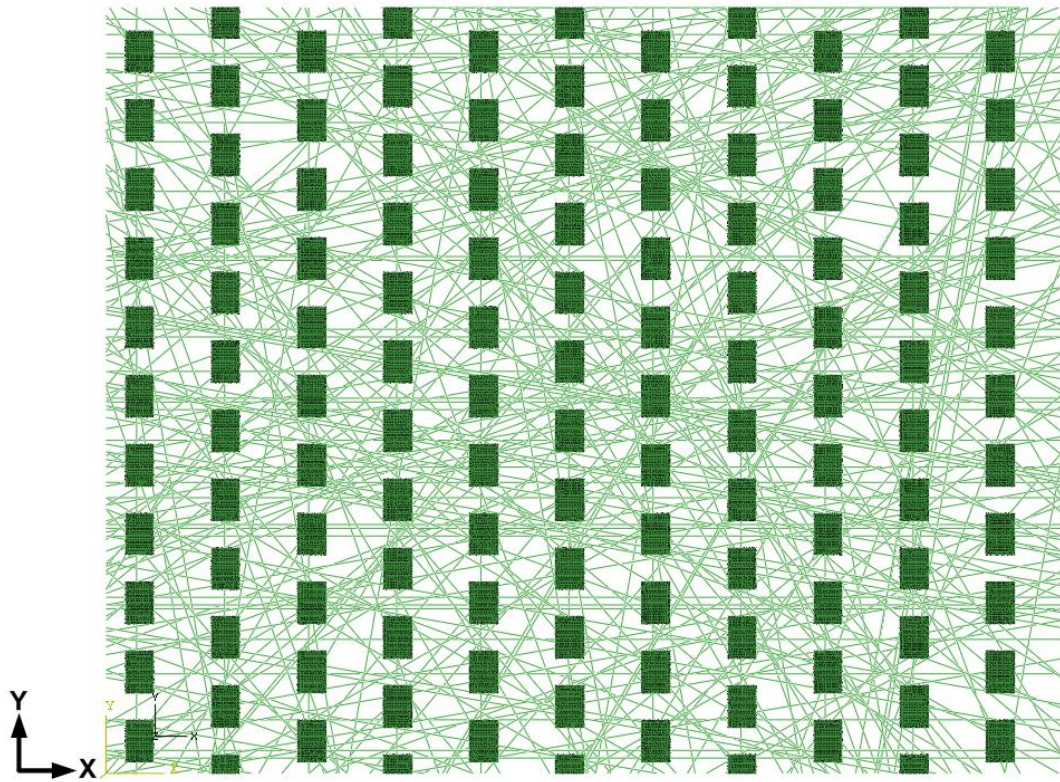
(a)
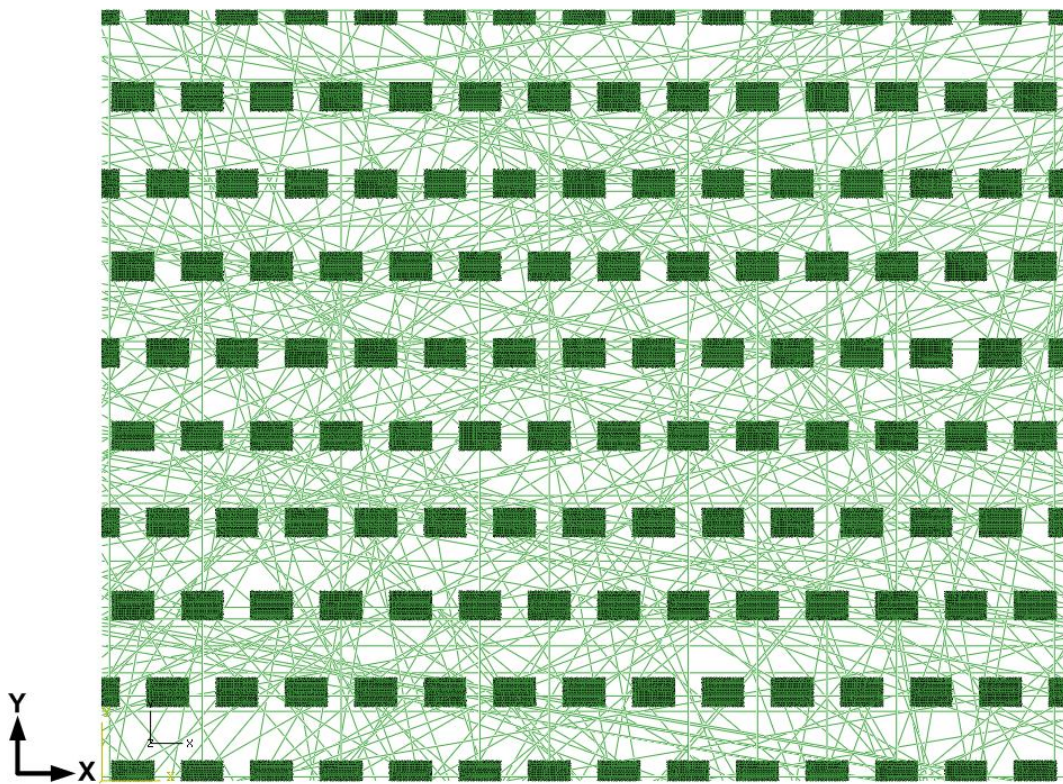
(b)

Figure 6.5: Discontinuous FE models: (a) machine direction; (b) cross direction

6.3.2 Material properties for discontinuous FE models

Theoretically, it is possible to introduce a real number of fibres into the discontinuous model. However, to reduce the computation time, representative fibres were used in the discontinuous FE model. Therefore, to introduce real material properties of single fibres into the discontinuous model, it is essential to determine how many fibres of the modelled nonwoven correspond to one representative fibre in the model. Then the material properties of the representative fibres could be determined according to the relationship between the numbers of representative fibres and real ones. To generate the geometry part with proper numbers of representative fibres, the fibre density of the real nonwoven material have to be determined first. For the real nonwoven material, the average number of fibres n within a certain area A_{fabric} is calculated as follows:

$$n = \frac{\rho_{fabric} \times A_{fabric}}{\bar{l} \times \bar{a}_{fibre} \times \rho_{fibre}} \, , \tag{6.1}$$

where ρ_{fabric} is the density of the nonwoven material, its specific unit is gram per square meters (gsm), $\bar{a}_{fibre}$ is the average cross-sectional area of fibres, ρ_{fibre} is the density of polypropylene fibres, $\bar{l}$ is the average length of the fibres within the area A_{fabric}.

To determine the value of $\bar{l}$, the Python programme, which was used to generate the random fibrous web for the discontinuous model, was modified and used to simulate results of the manufacturing process, when the staple fibres are assembled on the transfer belt to form a random fibrous web. In the simulation, the arrangement of fibres was according to the measured orientation distribution function of the real material. The programme defined a web with area 25 mm × 20 mm and includes 245 trusses. The length of each truss within the web was calculated according to their coordinates, and the average magnitudes were determined for each realization. The results in Table 6.1 demonstrate that the average lengths did not deviate much from the global average of 20.42 mm and that magnitude was used in Eq. 6.1.

Sample	1	2	3	4	5	6	Average value
Average length of fibres (mm)	20.18	20.09	19.98	21.16	20.69	20.40	20.42

Table 6.1: Average length of fibres for different statistical realizations of random fibrous web

The ratio γ of the number of the trusses n' in the discontinuous model to the number of fibres in the real material n can be introduced in the following way:

$$\gamma = \frac{n'}{n},$$
(6.2)

where n' is measured for the same A_{fabric}. Therefore, the input effective modulus of the lines within the discontinuous model is calculated for the elastic stage as

$$E_{\text{effctive}} = \frac{1}{\gamma} E_{\text{fibre}}.$$
(6.3)

The loading conditions used in the discontinuous FE model were to simulate a tensile test with a constant test speed. But due to the microstructure of the nonwoven material, which is formed by fibres along different orientations, the loading conditions of the fibres differ according to their relative orientations and locations. Figure 6.6 presents the extension mechanism of a fibre within the nonwoven material, which has original length L and oriented at angle θ to the cross direction. When the fibre is stretched by the external loading force along the machine direction (MD), it demonstrates two types of behaviour: first, it is extended along its own axis. Second, it is reoriented towards the loading direction. Obviously, since the fibres of the nonwoven are assembled randomly with different original angles θ, even when the overall material is extended uniformly with a constant rate, different fibres are stretched with different extension rates along their own axes.
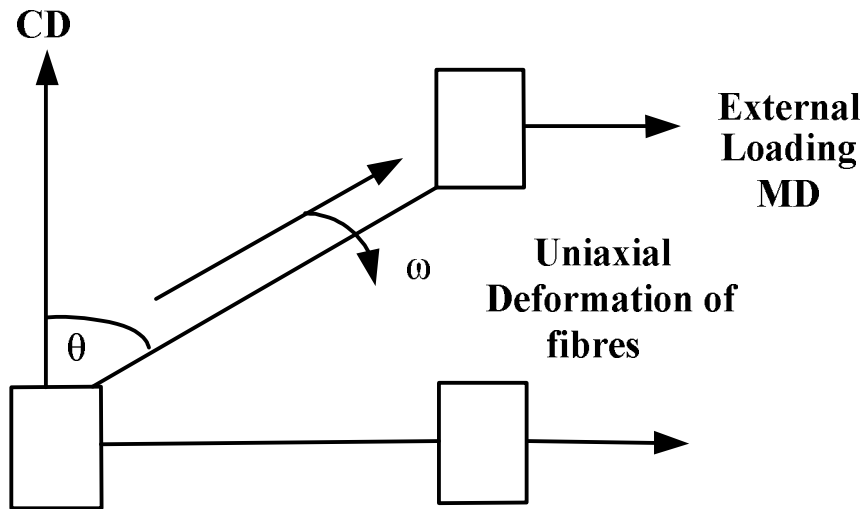
Figure 6.6: Extension mechanism of fibre within nonwoven fabric

Therefore, the rate-dependent mechanical properties of the polypropylene fibres have to be considered before they are introduced into the discontinuous FE model. Figure 6.7 shows the measured tensile behaviour of polypropylene fibres (length: 30 mm) under different testing rates: 50 mm/min, 25 mm/min and 12.5 mm/min. It is clear that the mechanical performance of fibres is highly nonlinear and rate-dependent. However, during the initial stage (I) of the deformation, fibres behave in a similar way and linearly under different testing rates. Moreover, due to the discontinuous microstructure of the material, which is basically formed by loosely arranged fibres, the material's deformation is mainly caused by the rearrangement of fibrous structure rather than direct stretching. Therefore, the most fibres within the material always have significantly lower levels of strain than the one of the overall material. Hence, the initial modulus of the fibre is used in the discontinuous model to simulate the initial tensile behaviour of the nonwoven material since fibre properties are independent of the extension rate at the initial stage and the fibres are mainly at a low strain level. For the bond points, approximate elastic material properties were employed, assuming them to be stiffer than the fibres. Their chosen modulus was five times higher than that of the fibres. The Poisson's ratio of polypropylene 0.42 is used in the model for both fibres and bond points.

139
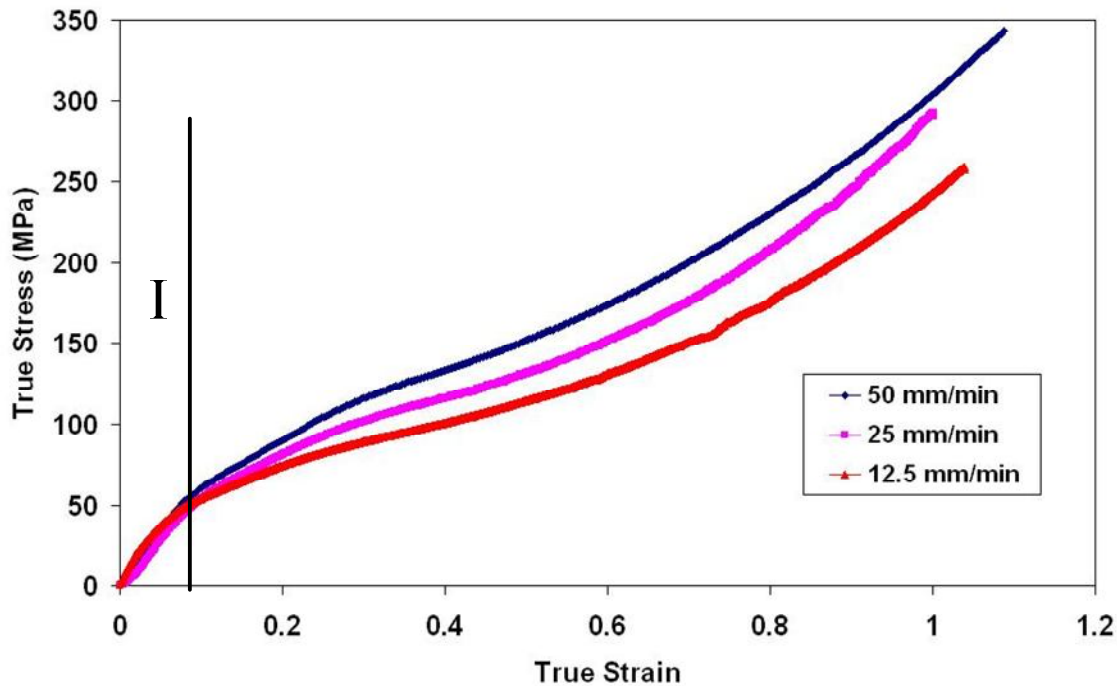
Figure 6.7: Tensile behaviours of polypropylene fibres at different test rates

6.3.3 Analysis of discontinuous models

To describe the tensile behaviours of the nonwoven material in its two principle directions - MD and CD - and analyze the effects of the orientation distribution and arrangement of bond points, twelve models with various arrangements of bond points and orientation distributions were developed. Three different fibrous webs (Figure 6.8) were generated according to three different orientation distribution functions and 245 fibres were used in all three different fibrous webs. To ensure that most of the fibres connect to the bond points and avoid unconnected areas, 20 of the 245 lines were generated with designed locations according to the different arrangements of bond points as shown in Figure 6.2a. For OD1 distribution, the highest frequency of fibres occurs for 90°, the ratio of anisotropy is 1.16, which is calculated based on the orientation distribution of fibres as presented in the previous chapter; a distribution with the largest number of fibres assembled along 0° (loading direction), is denoted OD2, which is an inverted OD1 and the ratio of anisotropy is 0.86. And it represents the original ODF of real fabric. OD3 is designed by assigning more fibres along 0° than in OD2, and its ratio of anisotropy is 1.43.

140
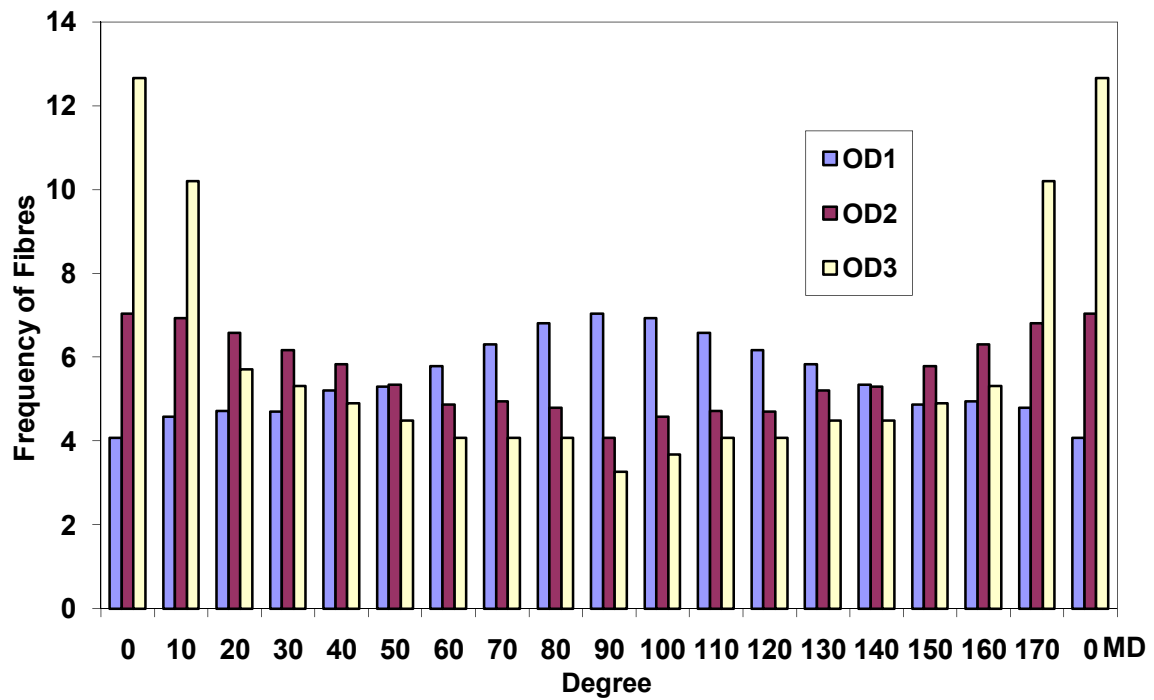
Figure 6.8: Orientation distributions used in discontinuous models.

Four different arrangements of bond points – staggered MD, staggered CD, lined MD and lined CD - were suggested for modelling; they are shown as Figure 6.9. The dimensions of bond points for all four arrangements are the same, according to those of the real nonwoven material. For the staggered MD arrangement, the staggered strips of bond points, which are formed by lines of bond points, are perpendicular to the loading direction. It was used to simulate the arrangements of bond points for MD specimens of the real nonwoven. The staggered CD simulated the arrangement of bond points for CD specimens of the real material. The arrangement of lined MD and the arrangement lined CD have strips of bond points arranged without staggering.
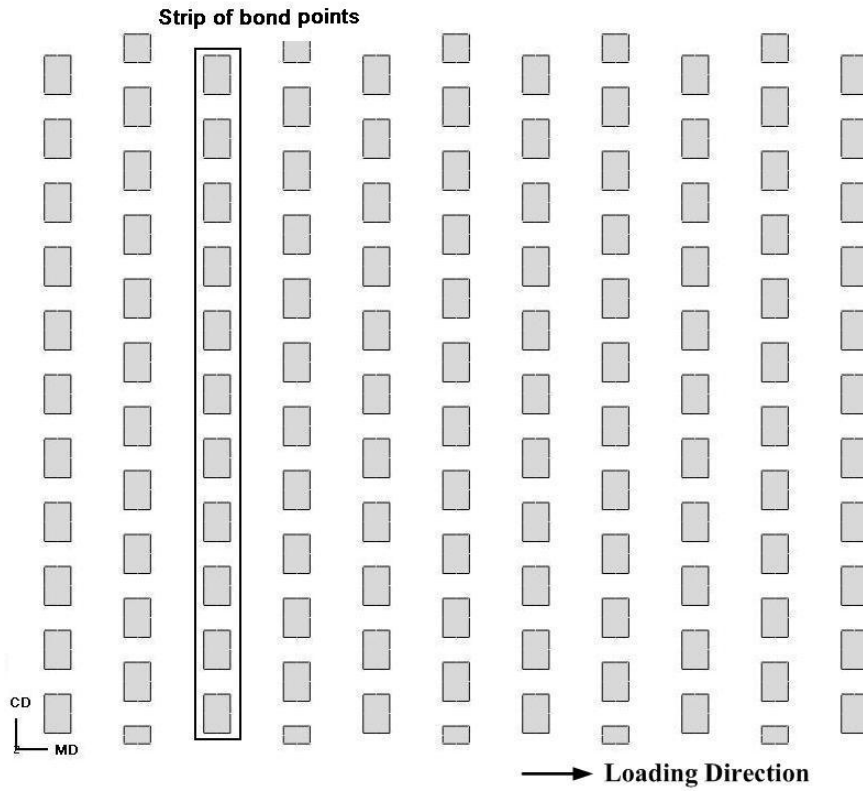
(a)
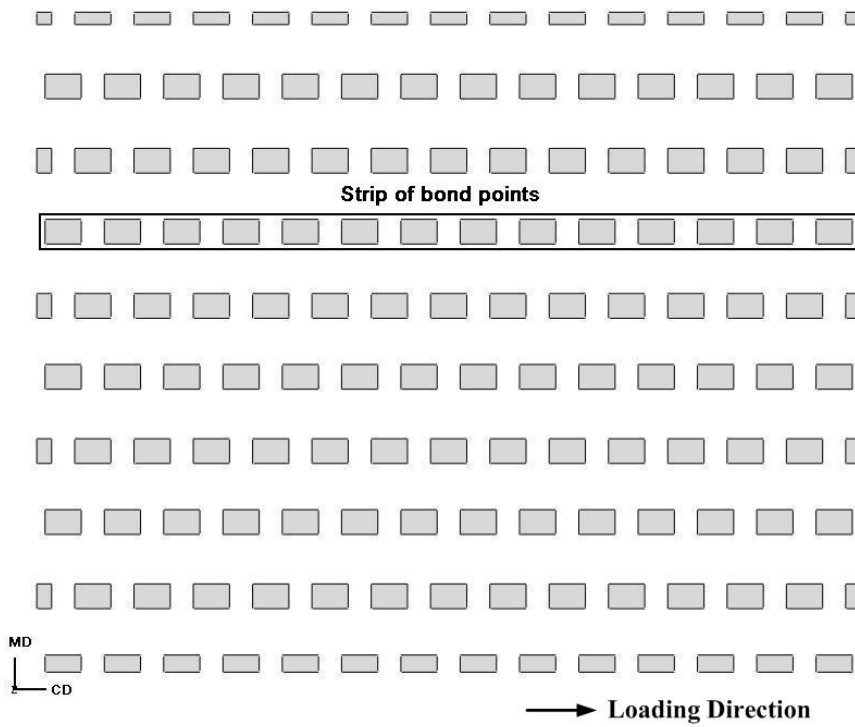
(b)
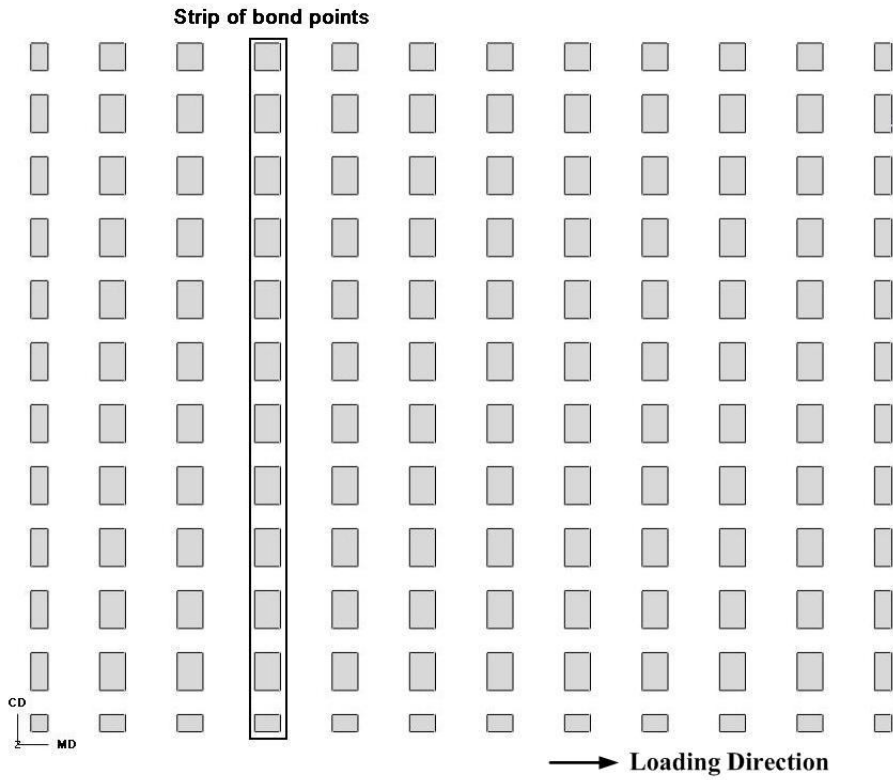
(c)
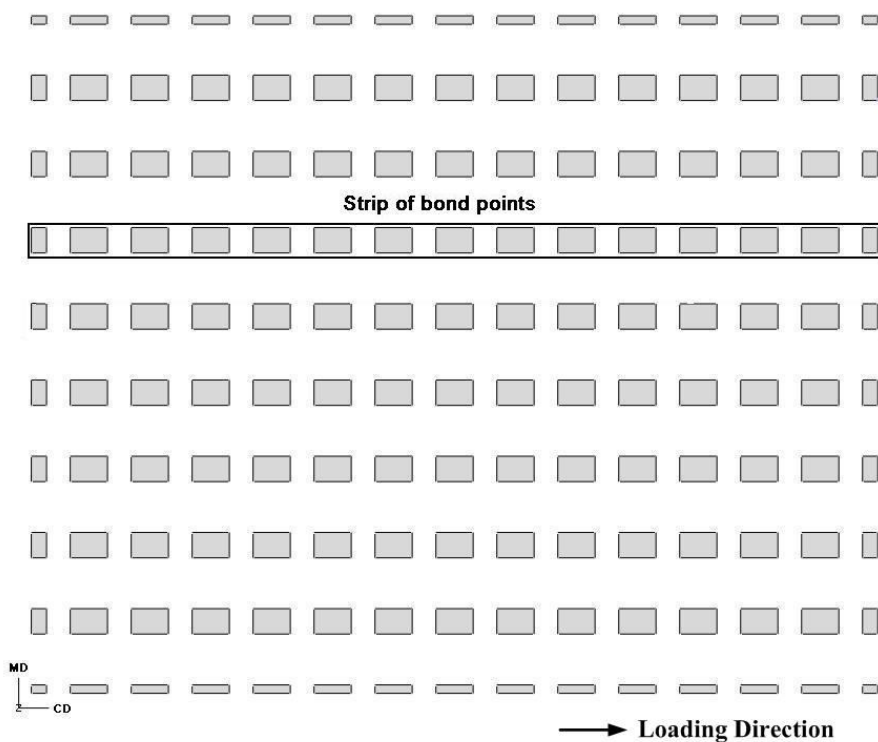
(d)

Figure 6.9: Arrangement of bond points used in discontinuous models: (a) staggered MD; (b) staggered CD; (c) lined MD; (d) lined CD.

143

Twelve discontinuous models were developed based on the three types of fibres orientation distributions and four arrangements of bond points: (i) OD1/Staggered MD; (ii) OD2/Staggered MD; (iii) OD3/Staggered MD; (iv) OD1/Staggered CD; (v) OD2/Staggered CD; (vi) OD3/Staggered CD; (vii) OD1/Lined MD; (viii) OD2/Lined MD; (ix) OD3/Lined MD; (x) OD1/Lined CD and (xi) OD2/Lined CD; (xii) OD3/Lined CD. The scheme of the geometry model for discontinuous FE models is demonstrated in Figure 6.10.
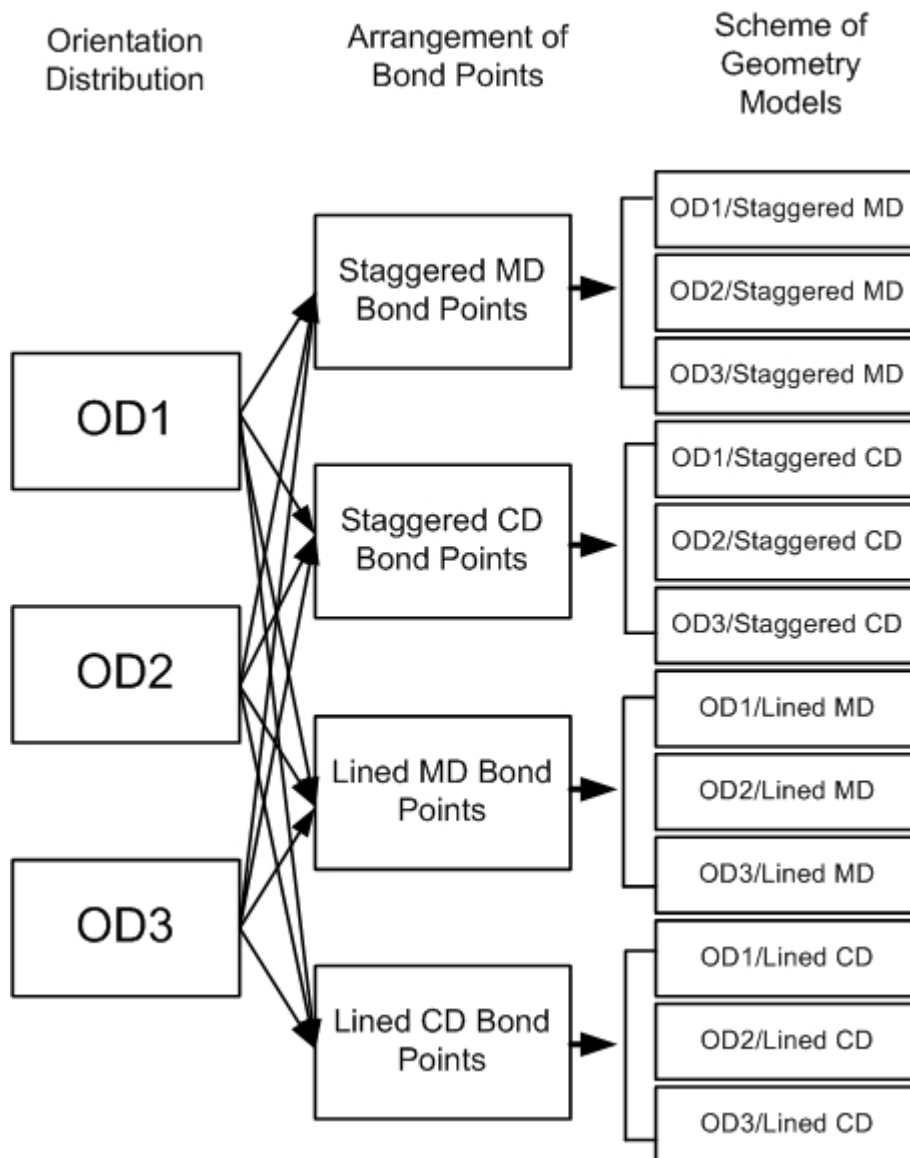
Figure 6.10: Scheme of geometry models for discontinuous FE models

The model OD2/Staggered MD was developed to simulate the tensile behaviour of the real nonwoven material in machine direction. To describe the tensile behaviour in cross direction, the model OD1/Staggered CD was used. Other models are used to investigate the effects of the fibres' orientation and arrangement of bond points by comparing with two models representing the studied real nonwoven. To simulate the tensile behaviours of the nonwoven fabric in two principle directions, the boundary conditions of the models were applied as following: one edge, perpendicular to the loading direction, was fixed as "ENCASTRE". All the degrees of freedom of the nodes located at this boundary were constrained. This boundary condition corresponds to fixture of the specimen in a grip in the test. A uniform displacement (15 mm) in x direction was applied to the opposite boundary of the models to simulate the static tensile deformation.

The obtained results for discontinuous FE models are presented in Figures 6.11 and 6.12. However, due to the complex structures of the models and relatively high deformation level in the simulations, the elements within the models were distorted and rotated to a large degree, especially for the shell elements connected with truss elements. It made the convergence of the developed models very difficult, and simulations terminated at different strain levels. As is obvious from Figures 6.11 and 6.12, all the models accounting for the random and discontinuous microstructure of the nonwoven material demonstrate the nonuniform stress/strain distributions.

The effect of arrangement of bond points on the deformation mechanism of the material is apparent. The models with the staggered MD and lined MD arrangements of bond points deform as a stripped system formed by lines of bond points with intermediate layers of a fibrous web. The fibres assembled at the corners of the models, which are the ends of the necking curvature, had a higher strain level and stress concentration due to the used type of boundary conditions. But most of the fibres participated in the load transfer, and the stress/strain distribution is relatively uniform for different fibres. For the models with the staggered CD arrangements of bond points the deformation behaviour was based on a generation of the diamond patterns, formed by four neighbouring bond points. Apart of the fibres, located at the corners of the specimens, fibres connecting two neighbouring bond points along the loading direction carry higher stresses even at relatively low overall strain levels, due

to their orientation and smaller initial length. It is therefore can be anticipated that these fibres tend to rupture at early stages of the deformation process in the real test. This makes the diamond patterns the basic load carrier, with the load transferred by the boundaries of diamond-shaped cells. The models with lined CD bond points tended to deform as a strip system. However, the bond points could not properly form the strips due to relatively large spaces between two neighbouring bond points along the y direction.

(a)

(b)

(c)

(d)

(e)

(f)

(g)

(h)

(i)

(j)

(k)

(l)
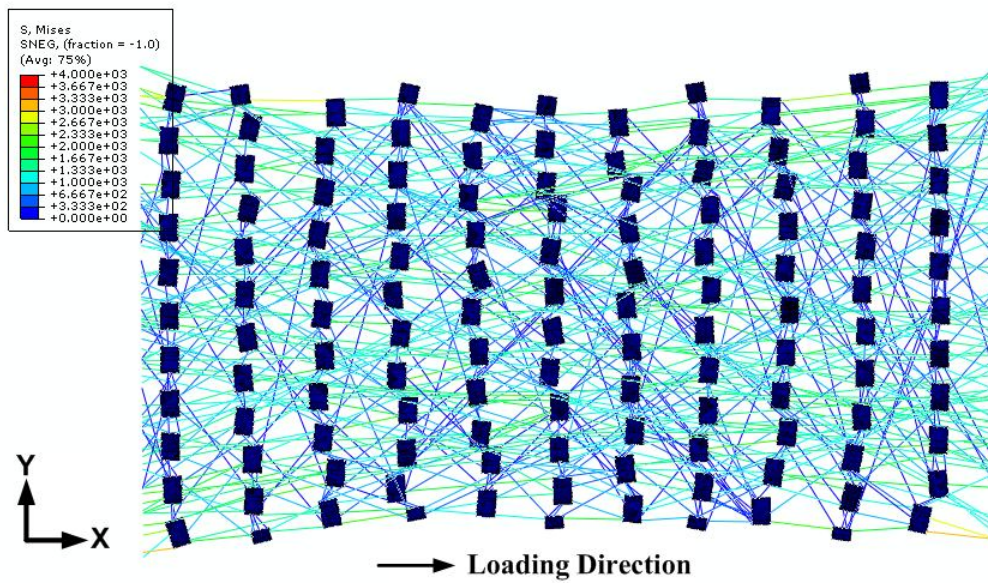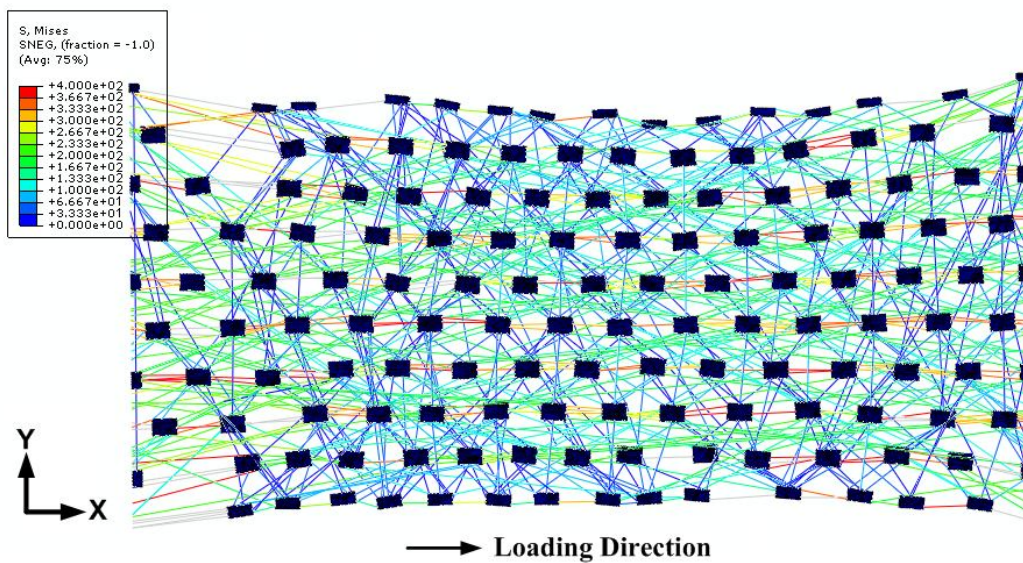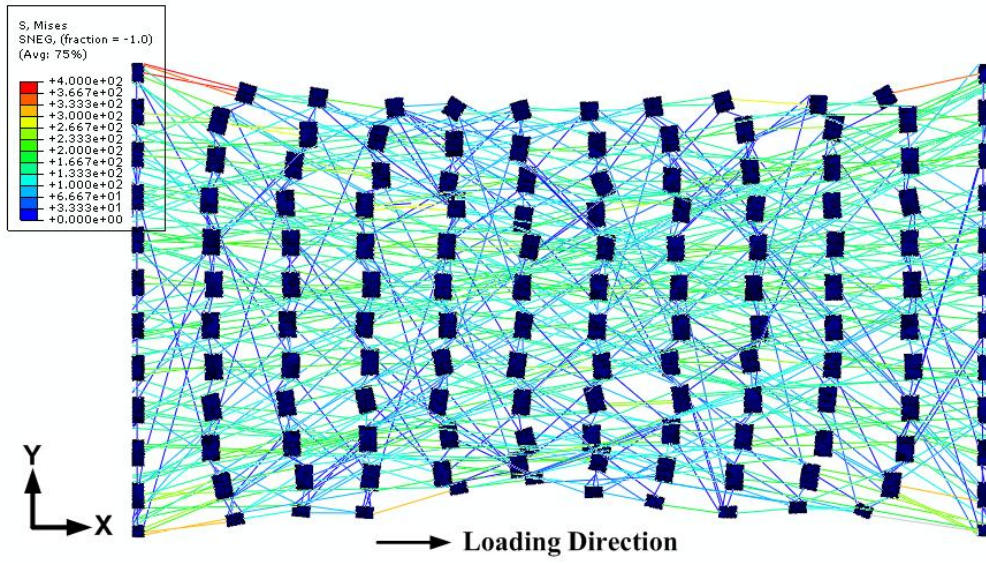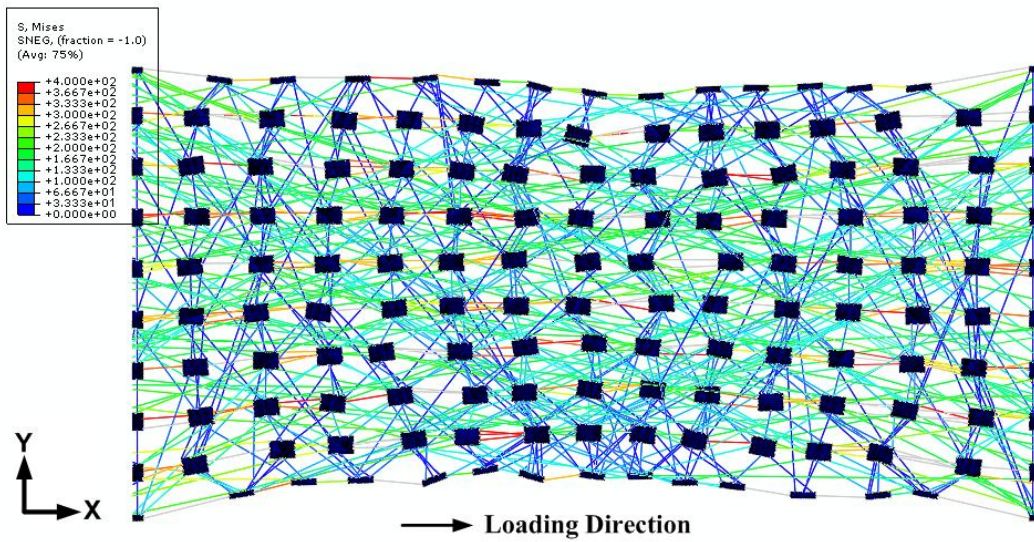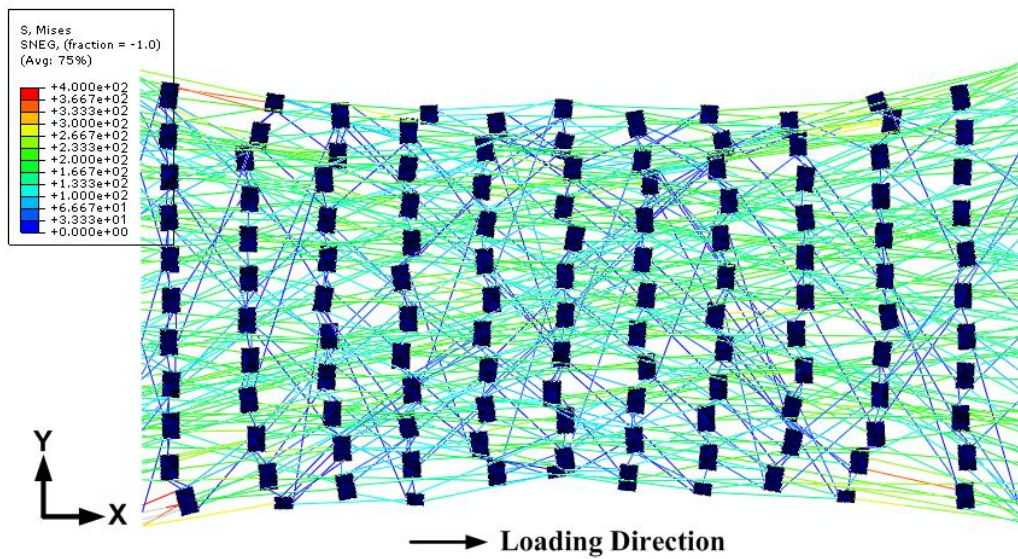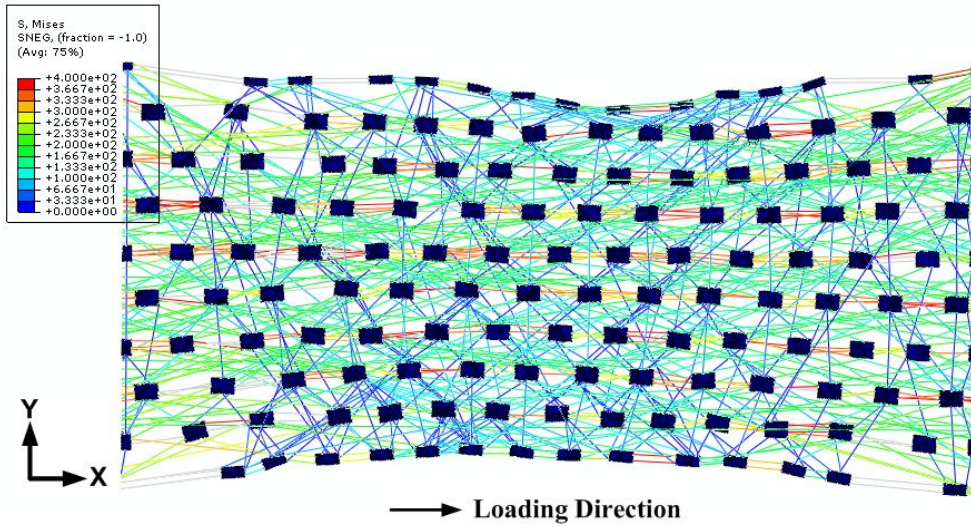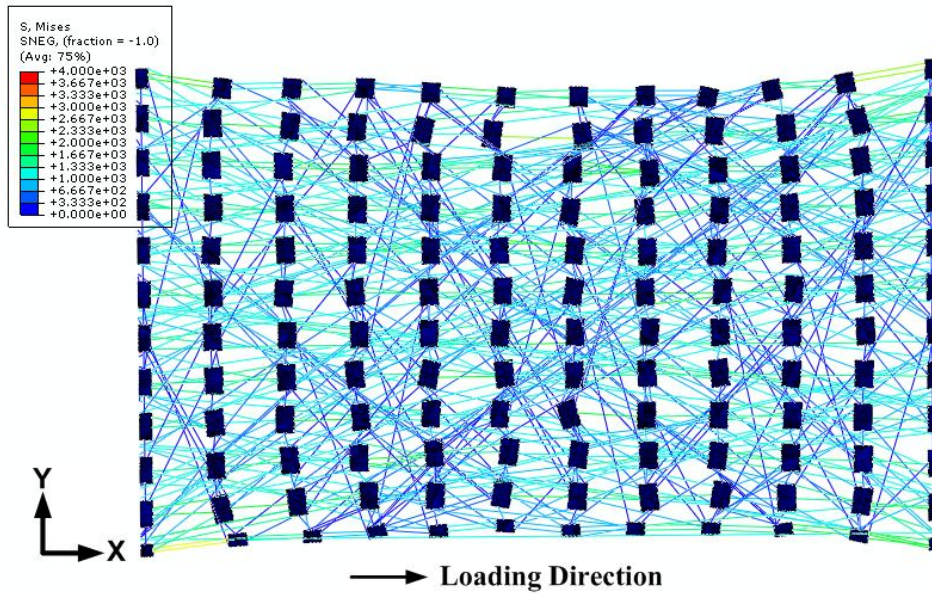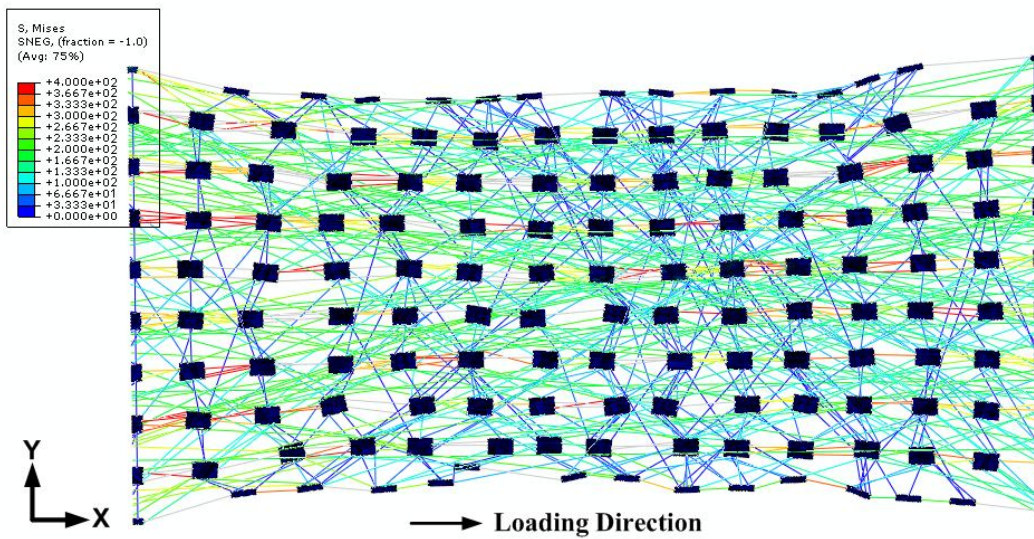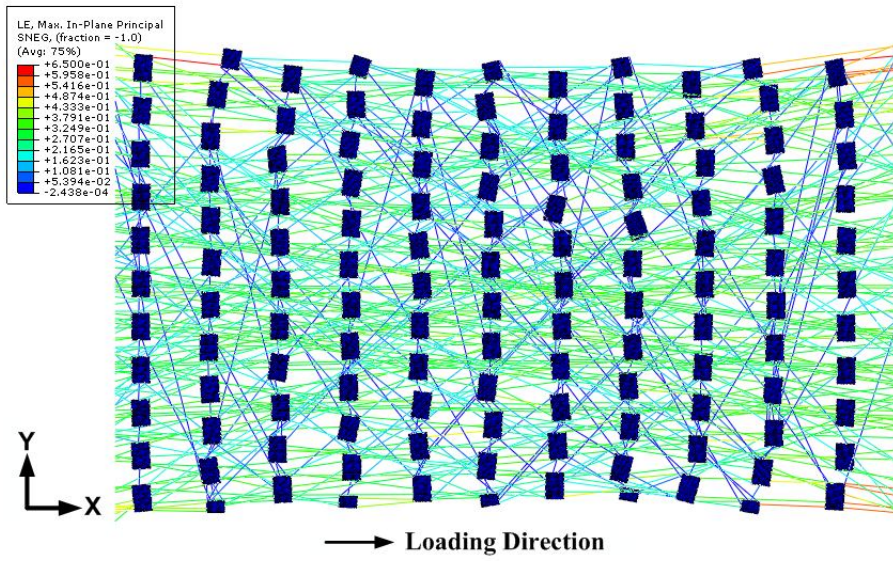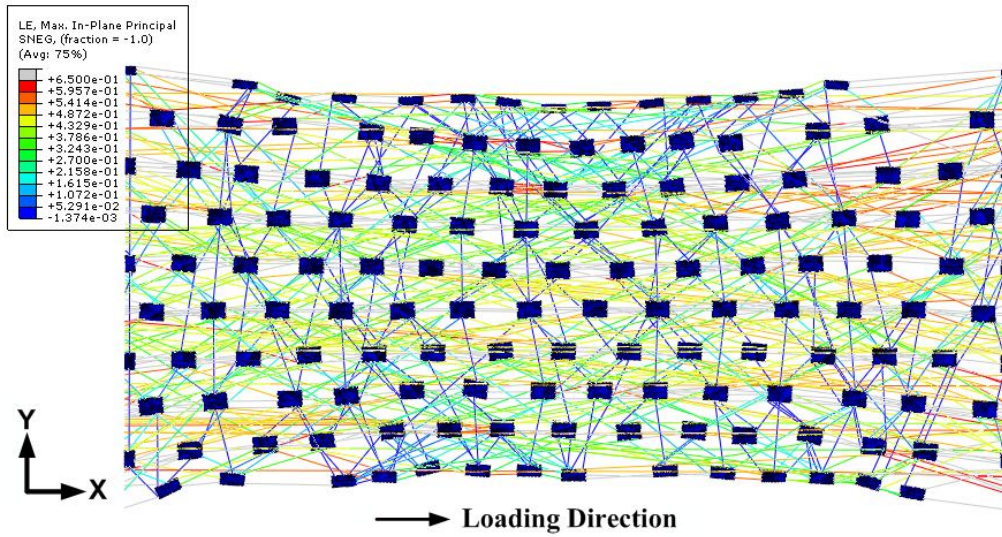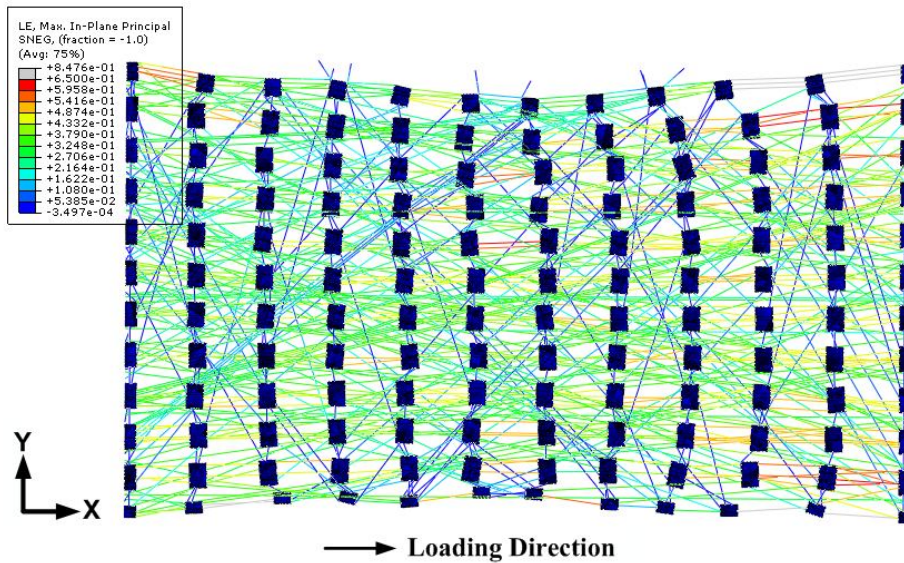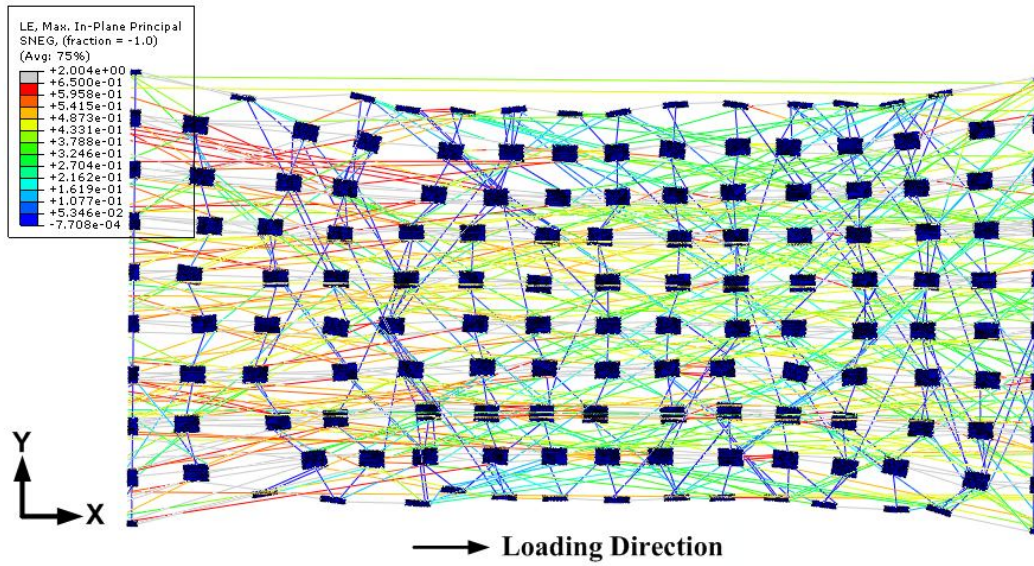
Figure 6.11: Stress distribution in deformed discontinuous FE models of nonwoven material: (a) OD1/Staggered MD (Strain: 39.6%); (b) OD1/Staggered CD (Strain: 60%); (c) OD1/Lined MD (Strain: 38.4%); (d) OD1/Lined CD (Strain: 60%); (e) OD2/Staggered MD (Strain: 49.8%); (f) OD2/Staggered CD (Strain: 60%); (g) OD2/Lined MD (Strain: 36.2%); (h) OD2/Lined CD (Strain: 60%); (i) OD3/Staggered MD (Strain: 30%); (j) OD3/ Staggered CD (Strain: 60%); (k) OD3/Lined MD (Strain: 36%); (l) OD3/Lined CD (Strain: 60%).

(a)

(b)

(c)

(d)

(e)
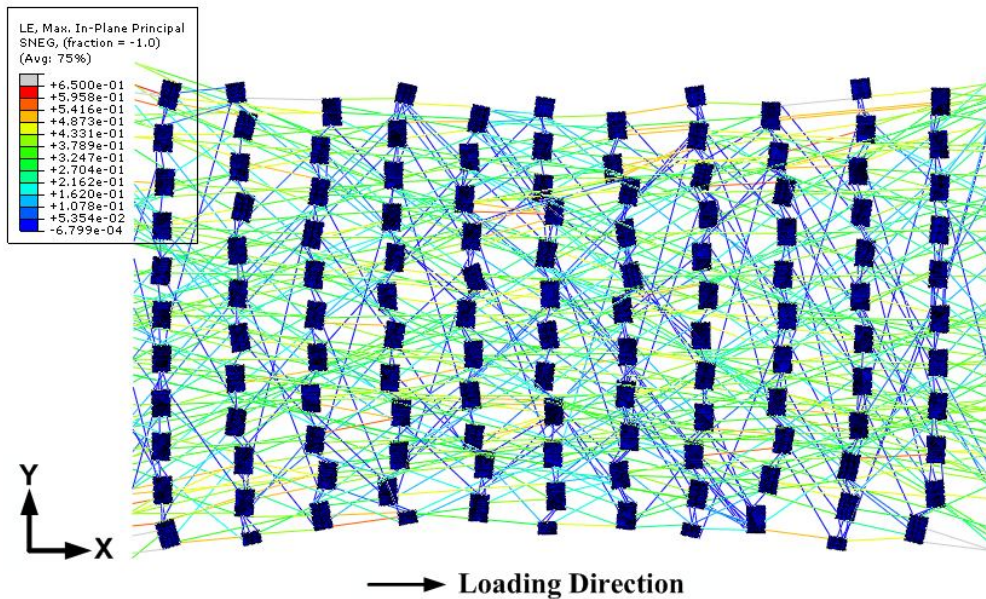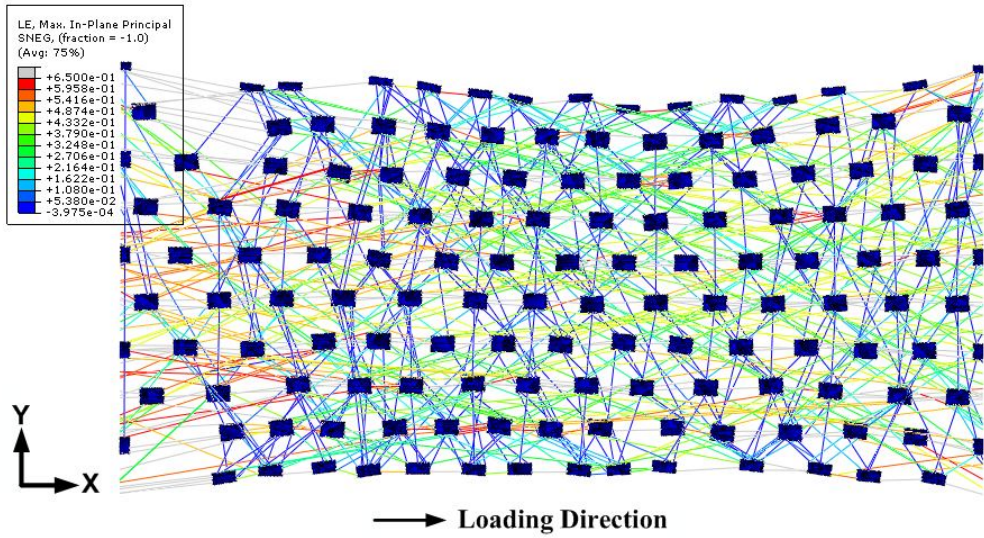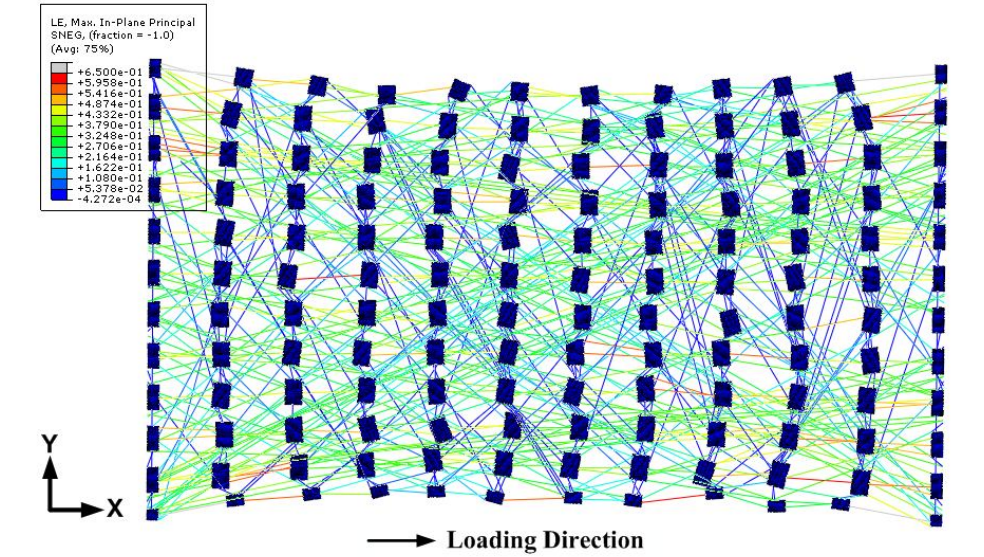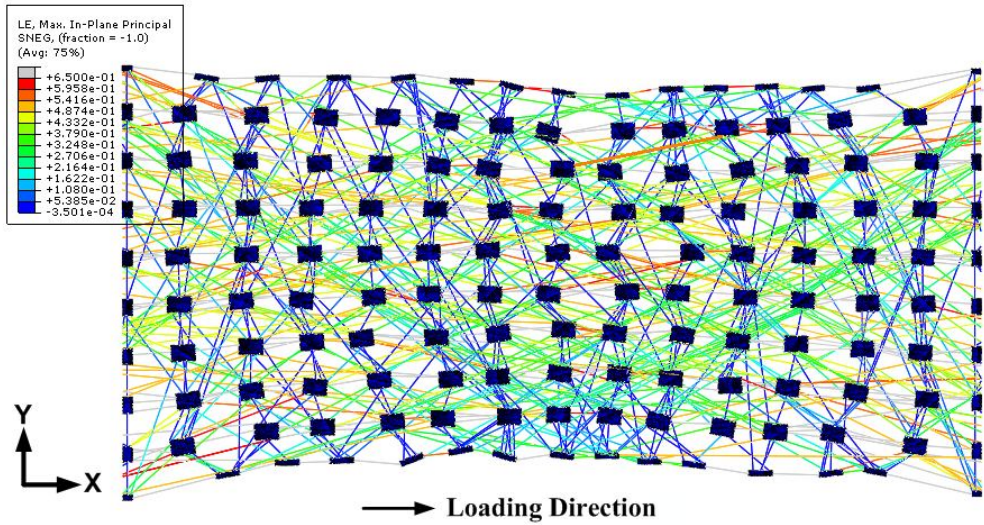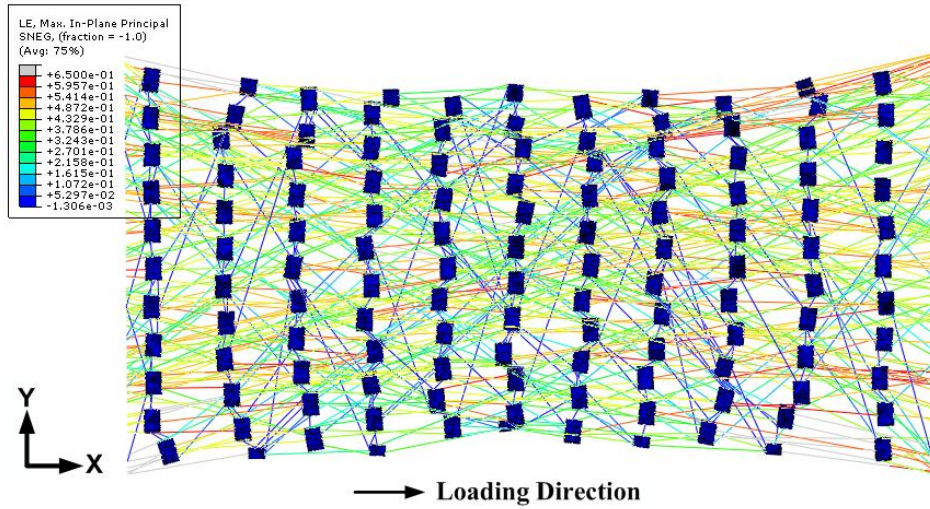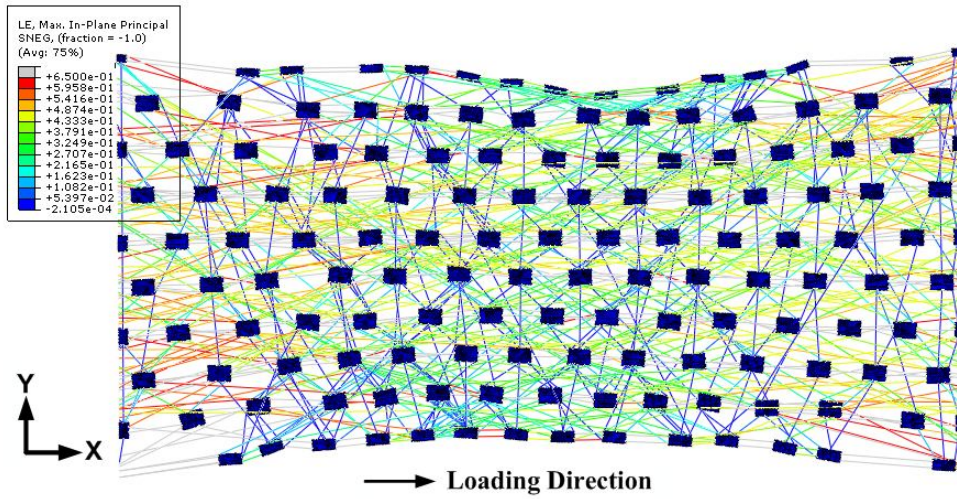
(f)
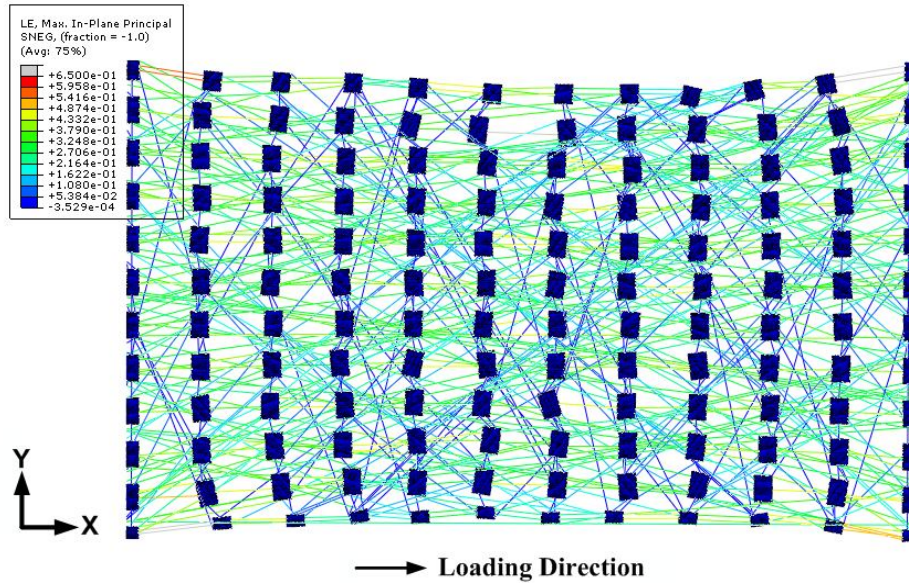
(g)
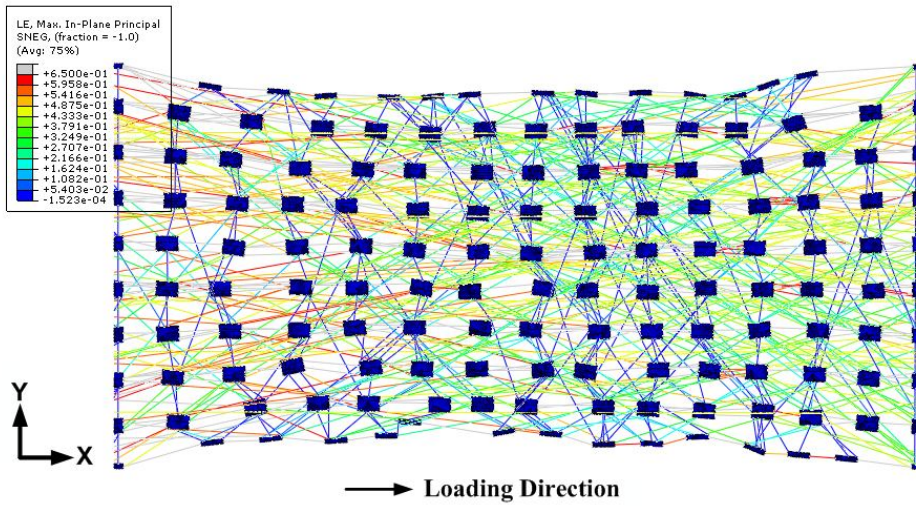
(h)
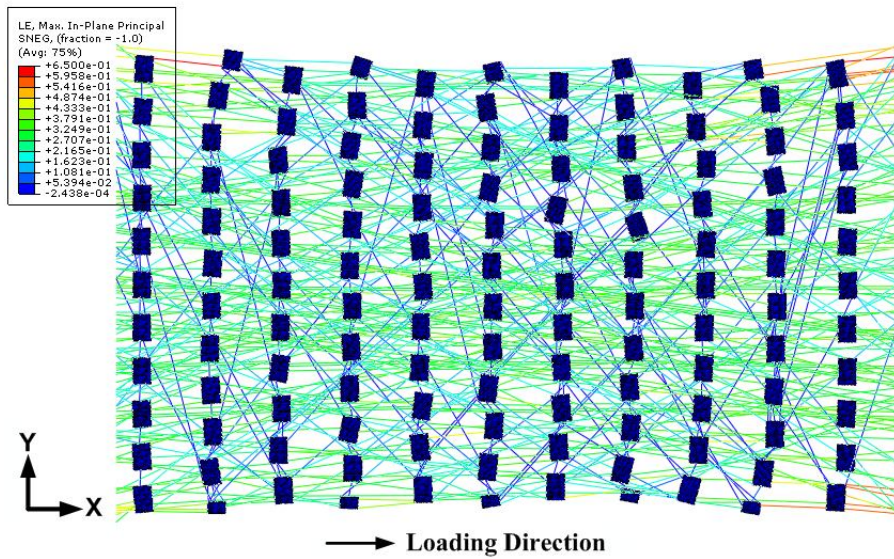
(i)
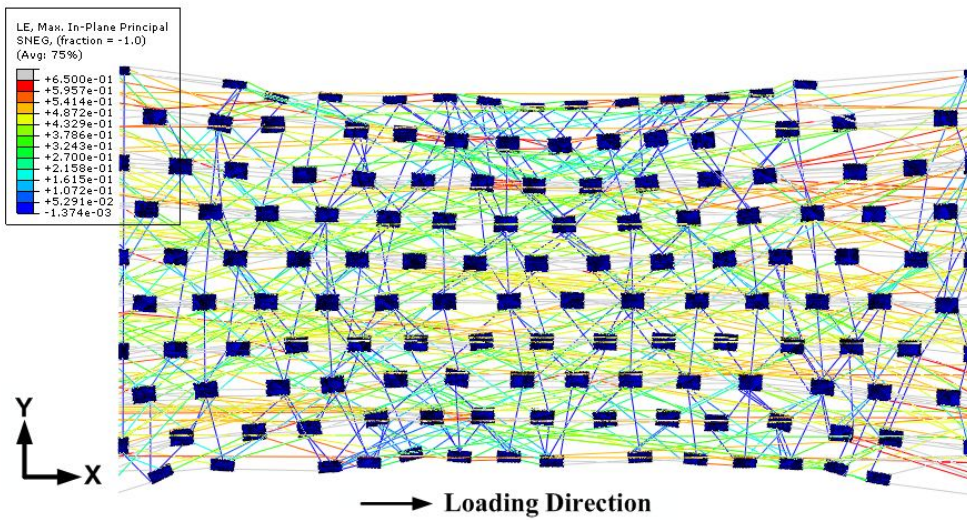
(j)
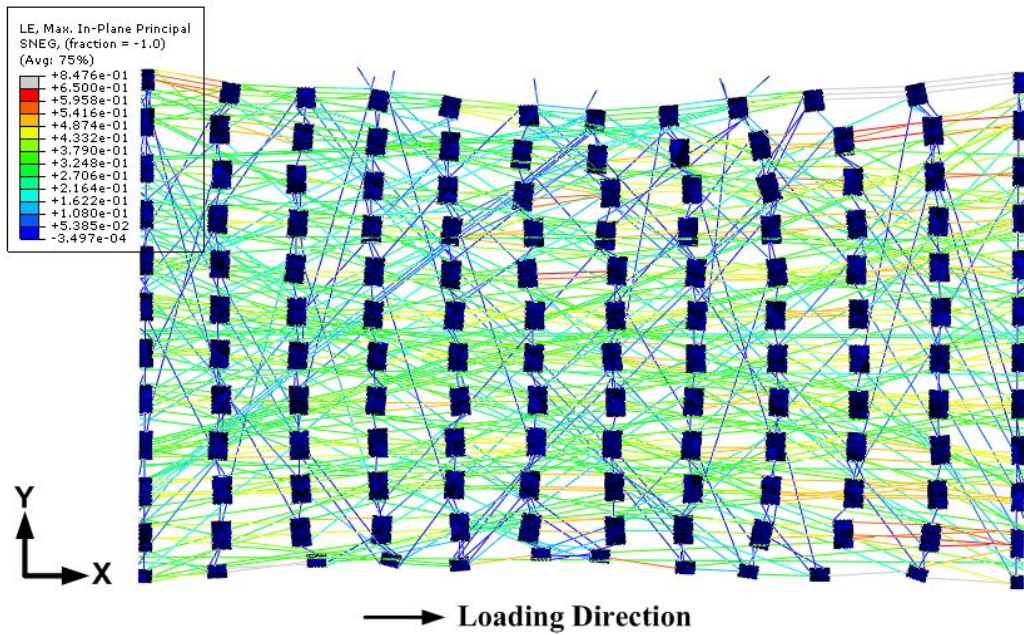
(k)
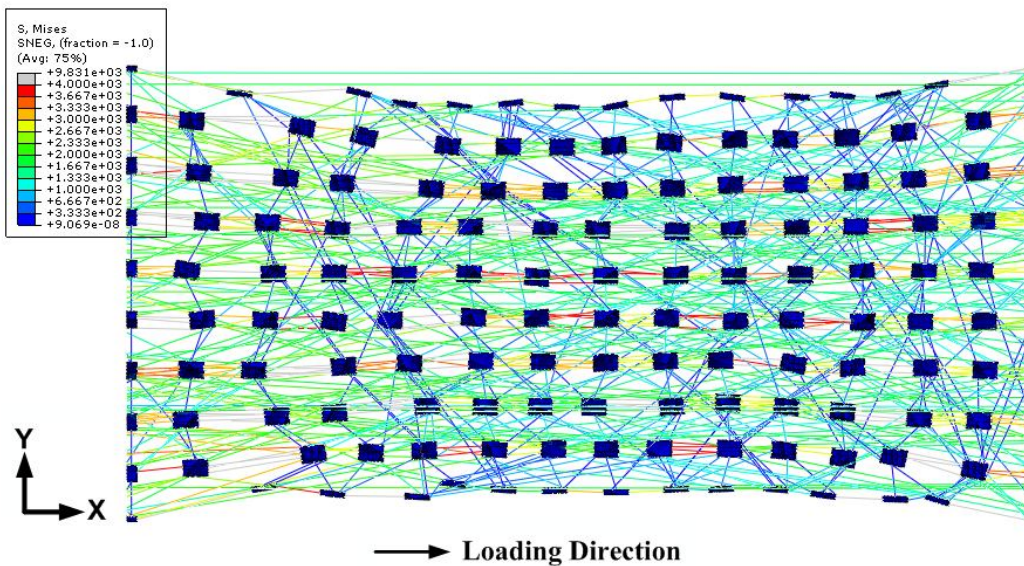
(l)

Figure 6.12: Strain distribution in deformed discontinuous FE models of nonwoven material: (a) OD1/Staggered MD (Strain: 39%); (b) OD1/Staggered CD (Strain: 60%); (c) OD1/Lined MD (Strain: 36%); (d) OD1/Lined CD (Strain: 60%); (e) OD2/Staggered MD (Strain: 48%); (f) OD2/Staggered CD (Strain: 60%); (g) OD2/Lined MD (Strain: 30%); (h) OD2/Lined CD (Strain: 60%); (i) OD3/Staggered MD (Strain: 30%); (j) OD3/ Staggered CD (Strain: 60%); (k) OD3/Lined MD (Strain: 36%); (l) OD3/Lined CD (Strain: 60%).

Since all the fibres in the nonwoven fabric are assumed to have same mechanical properties, the strain of fibres mainly determines their stress. And as shown in Figure 6.11 and 6.12, the fibres in the deformed fabric are at different strain levels; this finding agrees with the results of experimental ARIMIS analysis presented in the previous chapter. Fibres in different locations and with different directions, some of the fibres are at lower strain levels than that of the overall material, while, some of them are at higher strain levels. The phenomenon is essential to understand the nonuniform mechanical performance of the material and provides important information for the analysis of its failure mechanism. Figures 6.13 and 6.14 demonstrate quantitatively the strain distribution of fibres in the deformed FE models, when the overall models are under different strain levels. And Table 6.2 and 6.3 reveal the magnitudes of average strains of the fibres for the analysed FE models.

Figure 6.13 shows the nonuniform strain distributions for the models with staggered and lined MD bond points. It clearly demonstrates nonunifrom fibres' strain distributions for all the models. For example, when the overall strain of the model - OD1/Staggered MD - is 10%, the maximum strain for the fibres in the model is 26.1% and the minimum strain of fibres is -10.2% (i.e. in compression). And with the increase in the overall strain, the distribution changes and its nonuniformity increase. When the overall strain of the model is 39.6%, the maximum strain for the fires is 82.7% and the minimum strain is -27.2%. Although the fibres in the model have different levels of strain, most of the fibres are still at similar strain levels. As shown in Figure 6.13a, when the model is at 10% strain, the peak frequency of the distribution locates within the range between 0% and 10% strain and the average magnitude is 5.2% (Table 6.2), which means most of the fibres are at this strain level. However, there are still some fibres are at higher strain level up to 30 % and 23.1 % of them are compressed and have negative strain. The standard deviation of average strain of fibres is 6 %. It is because that the fibres locate at the corners of the model tend to have extreme strain levels due to the effect of lateral contraction. The fibres, which are aligned perpendicular to the loading direction, are normally compressed and have negative strain during the overall deformation due to the lateral contraction. When the overall strain of model increases to 20%, the peak of the distribution apparently decreases by 38.5% and moves to strain range between 10% and 20%. The average strain of fibres is 10.3 %, nearly half of the overall one. But, there are still a

large number (23.2%) of fibres are under the strain level between 0% and 10%, and 22.2 % of fibres are compressed. The standard deviation of the average strain increases to 11.1%, which means the nonuniformity of the fibres' strain distribution, becomes much higher. When the overall strain of the model achieves 30%, the peak of the strain distribution is within the range between 20% and 30%. The peak frequency of the distribution decrease by 16.5 % and the average strain of the fibres is 15.3%, which is smaller than the overall strain of the model. It is because the elongation of the model is not only due to the elongation of fibres but also caused by the re-construction of the microstructure of the model, which is resulted from the reorientation of the fibres. The standard deviation of the strain of fibres achieves to 15.8%, meaning that the nonuniformity of the strain distribution increase to a higher level. Finally, when the overall model deforms to 39.6% strain, the peak frequency of the distribution is between 30% and 40 % and decreased by 6.8 %. The average strain of fibres is 20% and the standard deviation is 19.7%. The compressed fibres are 20.2% of the total number. The phenomena means for the model with random fibrous structure, the strain of most of fibres increases with the increase of overall model (Figure 6.15a). As well, the nonuniformity of the strain distribution also increases, when the strain of overall material achieves a higher strain level. As shown in Figure 6.15b, the standard deviation, which indicates the nonuniformity of the strain distribution, increases with the increase of overall strain. However, the average strain of fibres is smaller than the overall strain of specimen, when the overall strain achieves a higher strain level (Figure 6.15a). Moreover, although the proportion of compressed fibres slightly decreases with the increase in the overall strain, it basically stays at a similar lever. It means the number of compressed fibres is generally determined by the original microstructure of the material and it does not change significantly with the increasing overall strain of fabric, when the overall strain is not extremely high.

As shown in Figure 6.13a and 6.13b, for the models with fibres' orientation distributions OD2 and OD3, similar phenomena are obtained to the model with orientation distribution OD1. With the increase in the overall strain, the strain of fibres and the nonuniformity of the fibres' strain distribution increase. And the proportion of compressed fibres does not change apparently with the increase of overall strain. However, as shown in the Table 6.2a, at the same overall strain levels,

the average strains of fibres increase, when the orientation distribution of the model change from OD1 to OD2. And for the model with orientation distribution OD3, the average strains of fibres increase to a higher level, when the overall strains of models are at same strain level. As shown in Figure 6.8, from OD1 to OD3, the frequency of fibres along or close to loading direction increases. It means that fibres in these models can achieve higher strains, when the models have fibrous network with more fibres along or close to the loading direction. And, as shown in Table 6.2a, the standard deviations of strains of the models keep at a similar level. That means the nonunifromity of the models is not affected apparently by the changing of orientation distributions. Moreover, the average proportions of compressed fibres for the model with OD2 and OD3 orientation distribution are 14.8% and 14.4% respectively, which are lower than the magnitude for the model with OD1 orientation distribution. The finding is easy to explain as: when the number of fibres within the fabric is a constant, more fibres along or close to the loading direction means that a smaller numbers of the fibres are affected by lateral contraction and be compressed during the deformation.

For the models with the lined MD arrangement of bond points, the obtained results reveal similar phenomena to the results for the models with the staggered MD arrangement. However, due to the different arrangements of bond points, there are inflections for the strain distribution curves at fibres' strain range between 10% and 20%, when the overall strain achieve a relatively higher level (> 30 %). For instance, for the model OD1/Staggered MD, when the overall strain is 30%, 15.9% fibres are within the strain range between 0 % and 10%, 17.8% fibres are within the strain range from 10 % to 20 % and the peak frequency is 24.8%. But for the model OD1/Lined MD, the magnitudes are 18.3%, 15.2% and 23%, respectively. It means that the lined MD arrangement results in a fibres' strain distribution with a higher percentage of fibres are under a lower strain level, while a higher percentage of fibres are under an extremely high strain level. Actually, when the overall strain is 30%, only 1.8% fibres in model OD1/Staggered MD are with strain higher than 40 %, but there are 3.7 % fibres in model OD1/ Lined MD, which have a higher risk to rupture. Moreover, the differences in the standard deviation of the strain of fibres also prove the phenomena (see Table 6.2 and Figure 6.15b). For the same overall strain levels, the models with

the lined MD arrangement of bond points have higher deviations compared to the models with the staggered MD arrangement.

(a)

(b)

(c)

(d)

159
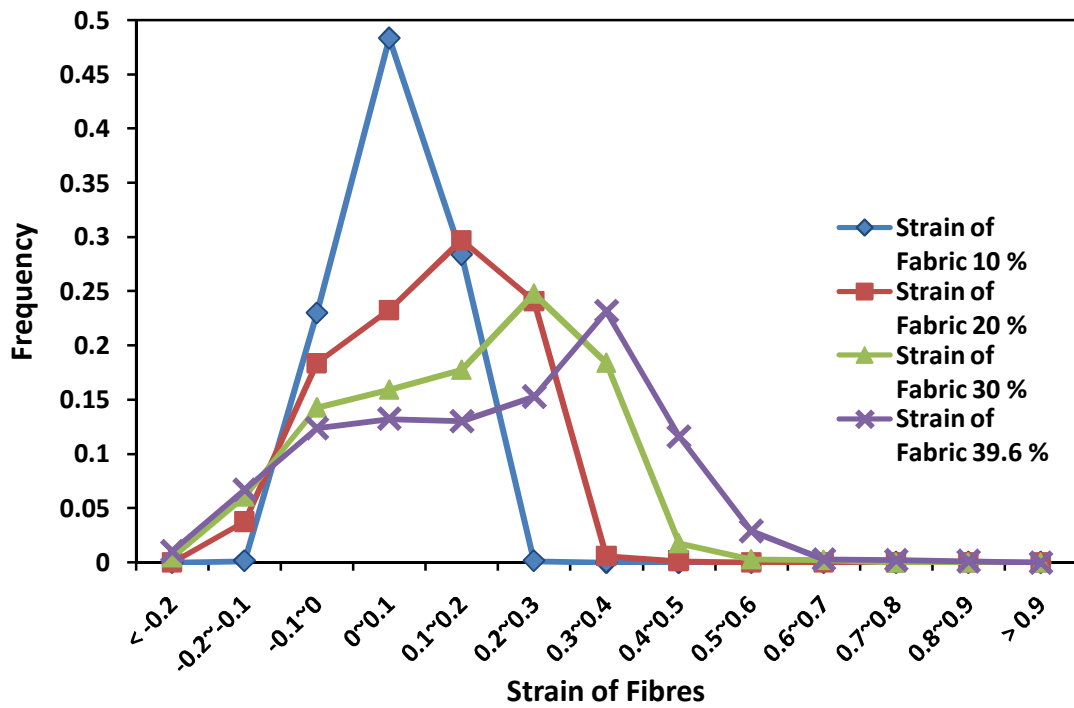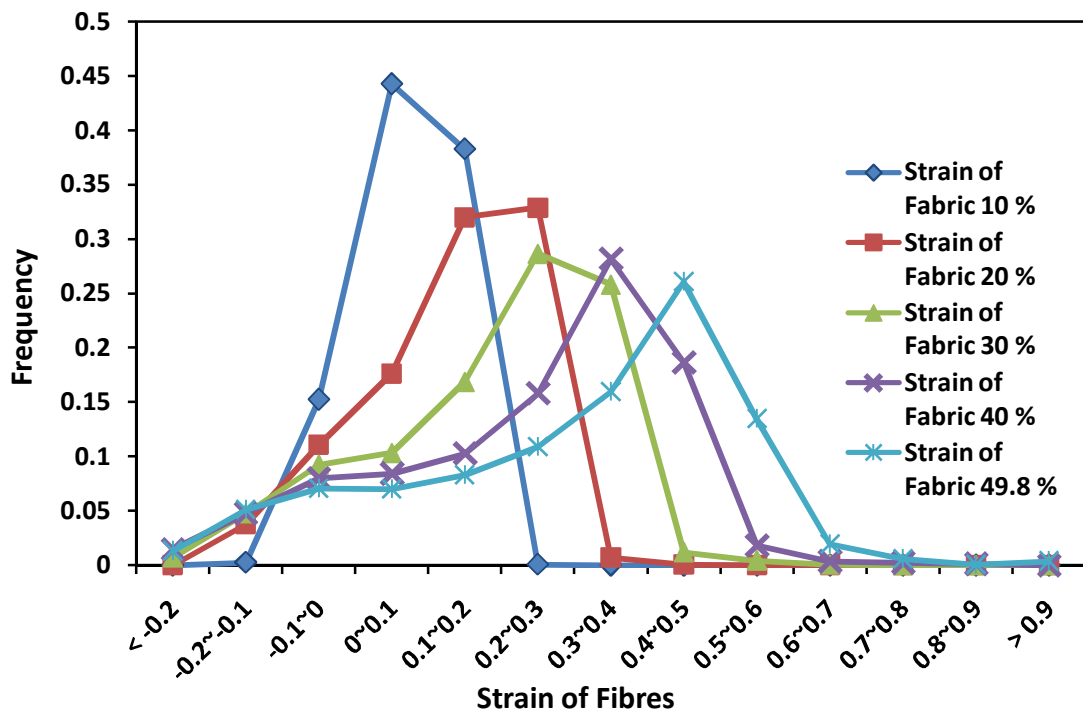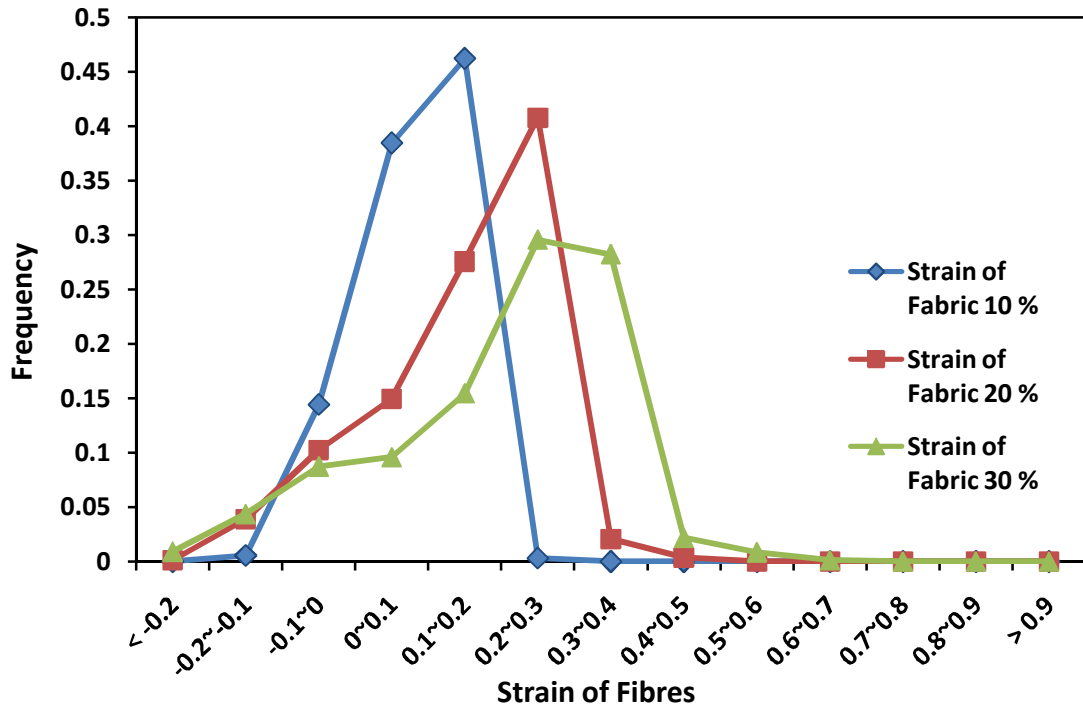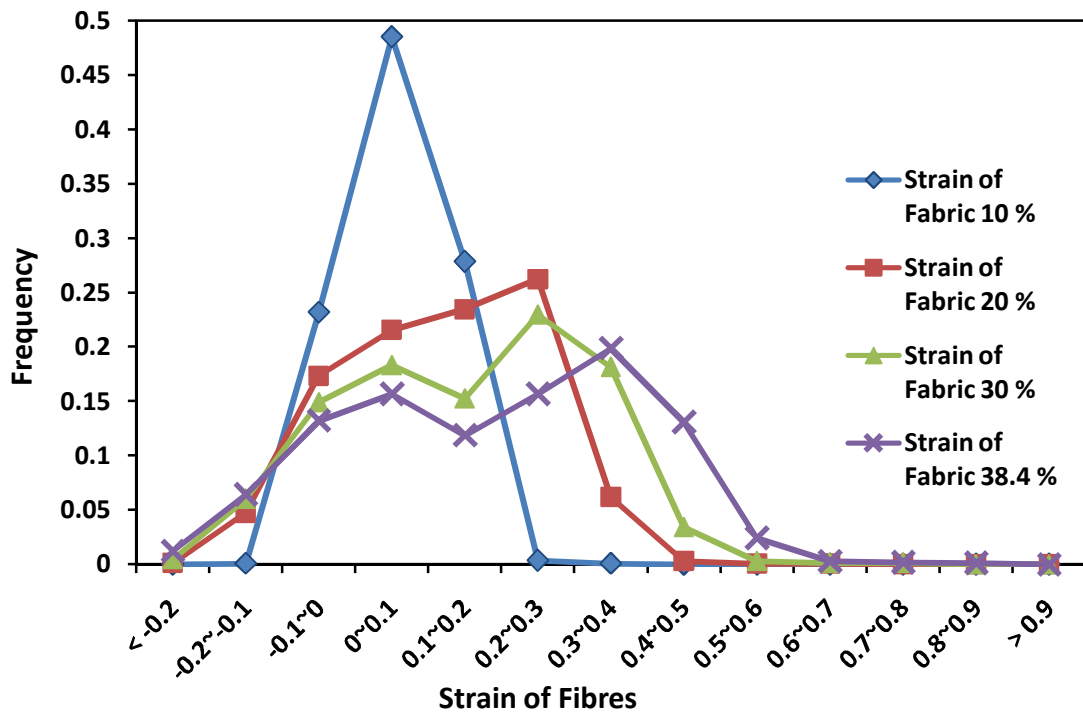
(e)

(f)

Figure 6.13: Distribution of strain of fibres for models: (a) OD1/Staggered MD; (b) OD2/Staggered MD; (c) OD3/Staggered MD; (d) OD1/Lined MD; (e) OD2/Lined MD; (f) OD3/Lined MD

Strain of Fabric (%)	OD1/Staggered MD		Strain of Fabric (%)	OD2/Staggered MD		Strain of Fabric (%)	OD3/Staggered MD	
	Average Strain of Fibres (%)	Standard Deviation (%)		Average Strain of Fibres (%)	Standard Deviation (%)		Average Strain of Fibres (%)	Standard Deviation (%)
10	5.2	6.0	10	6.6	5.8	10	7.5	6.2
20	10.3	11.1	20	13.0	10.8	20	14.6	11.5
30	15.3	15.8	30	19.0	15.2	30	20.3	15.4
39.6	20.0	19.7	40	24.8	19.0	_	_	_
_	_	_	49.8	30.3	22.3	_	_	_

(a)

Strain of Fabric (%)	OD1/Lined MD		Strain of Fabric (%)	OD2/Lined MD		Strain of Fabric (%)	OD3/Lined MD	
	Average Strain of Fibres (%)	Standard Deviation (%)		Average Strain of Fibres (%)	Standard Deviation (%)		Average Strain of Fibres (%)	Standard Deviation (%)
10	5.4	6.4	10	7.4	7.4	10	7.5	6.6
20	11.9	13.3	20	12.8	12.1	20	16.2	13.4
30	15.4	16.6	30	18.2	16.4	30	21.0	17.0
38	19.0	19.9	36	21.6	19.0	38	25.1	19.8

(b)

Table 6.2: Summarised results of average strain of fibres for models with staggered (a), and lined (b) MD arrangements of bond points

For the models with staggered and lined CD arrangements of bond points, the fibres' strain distributions are shown in Figure 6.14. The results show the models with CD – staggered CD and lined CD- arrangements of bond points have obvious different fibres' strain distribution from the models with MD – staggered MD and lined MD - arrangement of bond points. When the strain level of fibres increases with the increase in the overall strain of the model, the peak frequency of the fibres' strain tends to be at a lower level. For instance, when the overall strain of the model - OD1/Staggered CD - is 30%, there are 19.7% fibres are at the strain range from 0% to 10%, 16% of fibres

are at the strain range from 10% to 20% and 17.9% fibres are with 20% to 30% strain. But for the model OD1/Staggered MD, the magnitudes are 15.9%, 17.8% and 24.8%, which have a higher frequency for the higher strain level. However, for the model with the CD arrangements of bond points, the frequency of fibres at extremely high strain is higher than the one in the model with MD arrangements. For example, for model OD1/Staggered CD, when the overall strain is 30%, there are 8% fibres at strain range from 40% to 50% and 6.3% fibres are at 50% to 60%. The magnitudes for the model with the staggered MD are 1.8% and 0.28%. Therefore, the average strains of fibres for the models with CD arrangements of bond points are generally higher than the ones for the models with MD arrangements of bond points, which are shown as Figure 6.15a. Although they are still lower than the overall strain of fabric, the fibres in the models with CD arrangements tend to have strain close to the overall strain. Because the diamond patterns are basic load carrier for the models with CD arrangements of bond points, and the boundaries of the diamond patterns will reoriented along the loading direction during the extension, which caused a higher fraction of fibres have strains closed to the overall strain. Besides, the nonuniformity level of models with CD arrangements is much higher than the one for the models with MD arrangements. As revealed by the analysis, the standard deviations of strain of fibres for the models with CD arrangements of bond points is generally higher than the ones for the models with MD arrangements of bond points (Figure 6.15b). The phenomena means the fibres in the models with CD arrangements have a higher risk to achieve extremely higher strain levels than the ones in the models with MD arrangements. The above phenomena occur in all the models with staggered or lined CD arrangements of bond points, although the models with staggered CD arrangement of bond points have slightly smaller average strains of fibres than the models with lined CD arrangement. Moreover, the effect of the fibres' orientation distribution on the distribution of strain for the models with CD arrangements of bond points is similar to that for the models with MD arrangements. When more fibres are assigned along or close to the loading direction, the peak frequency tend to move towards to higher strain level and the average strain is also higher, which means the more fibres effectively carry higher load and contribute the increase of the overall strain.
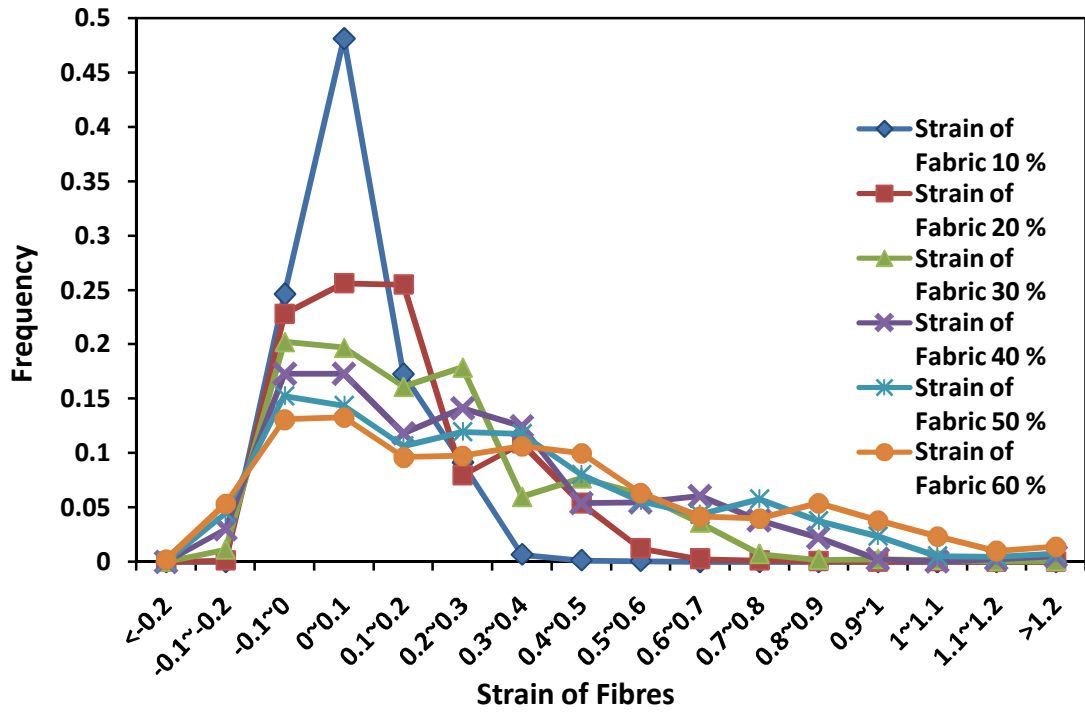
(a)
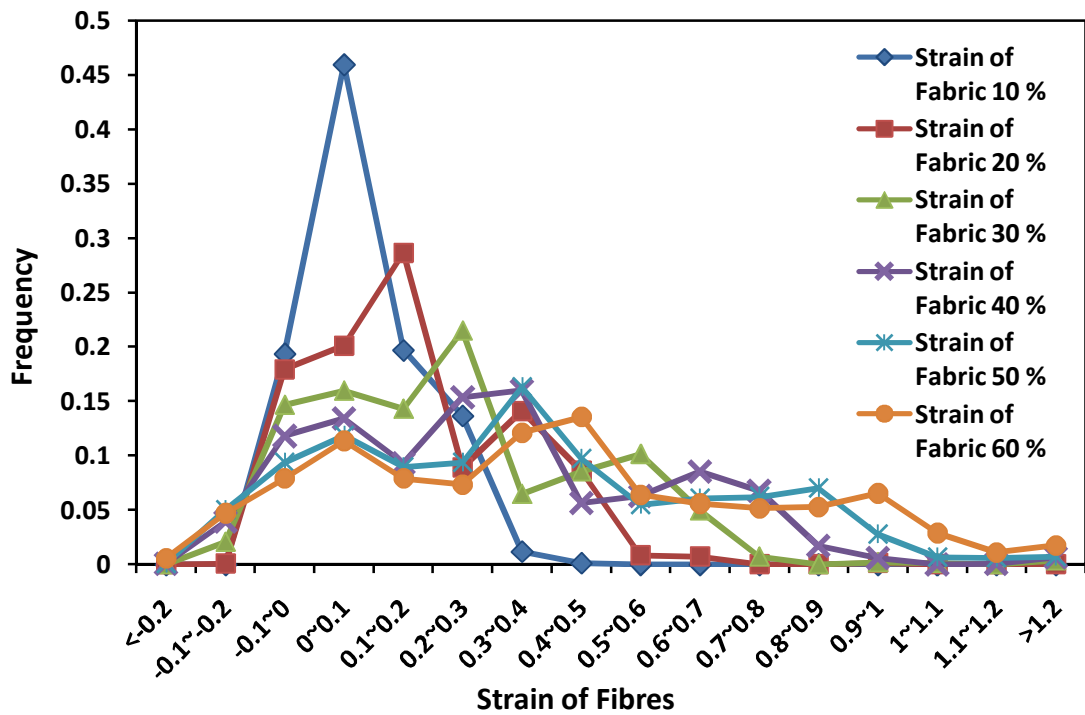
(b)
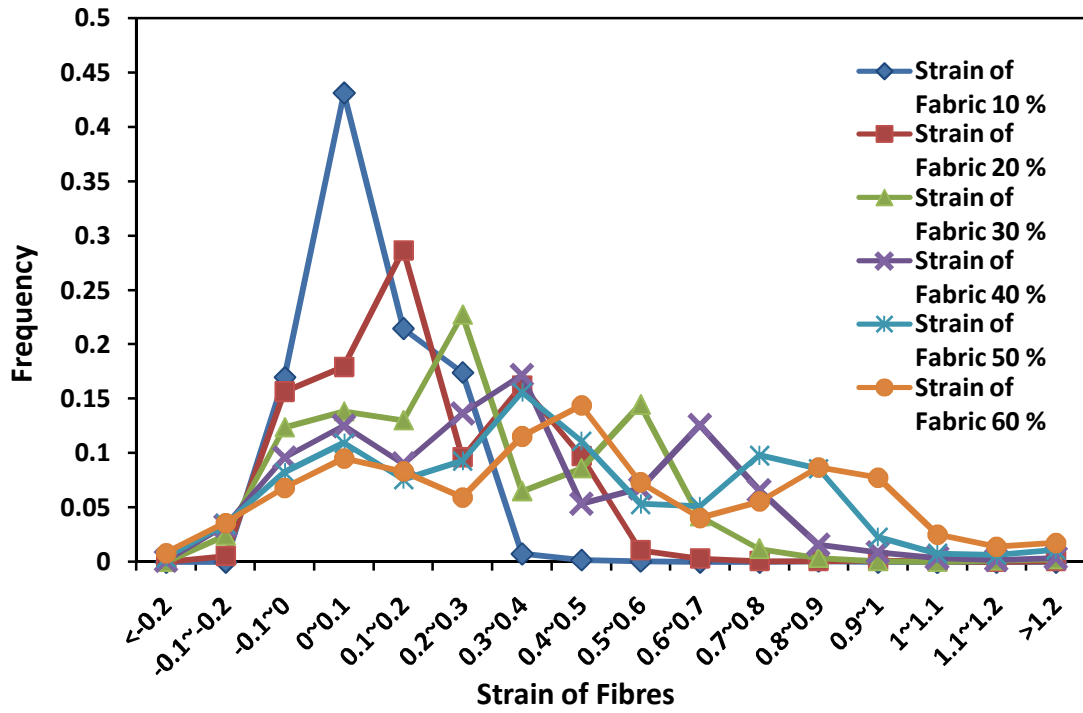
(c)
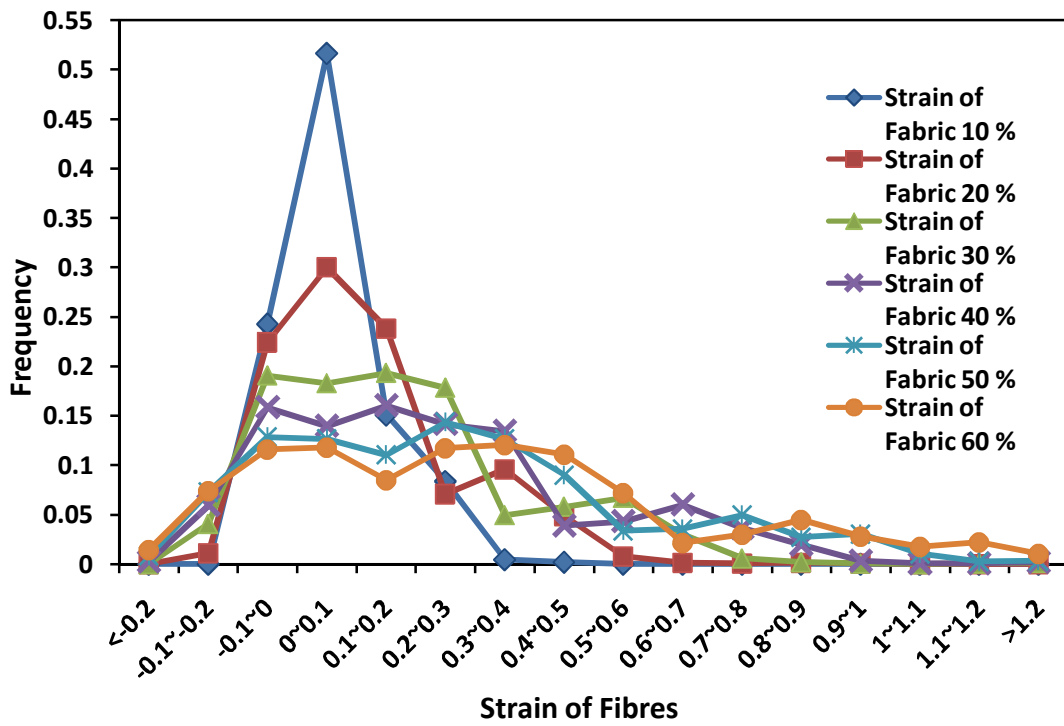
(d)
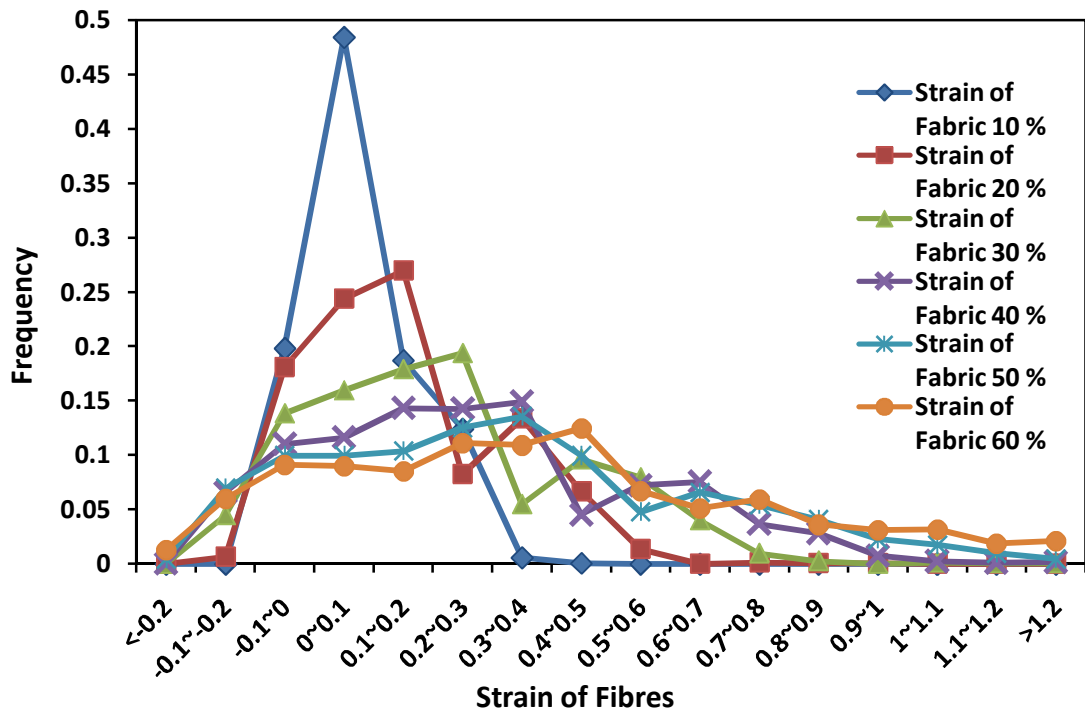
(e)
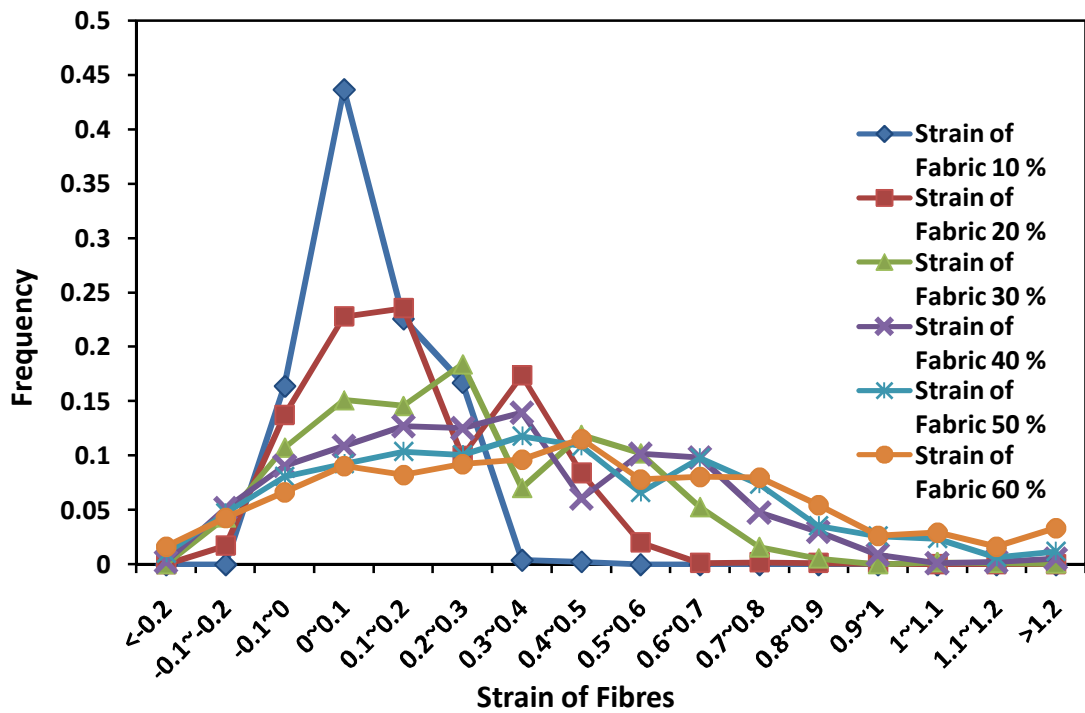
(f)

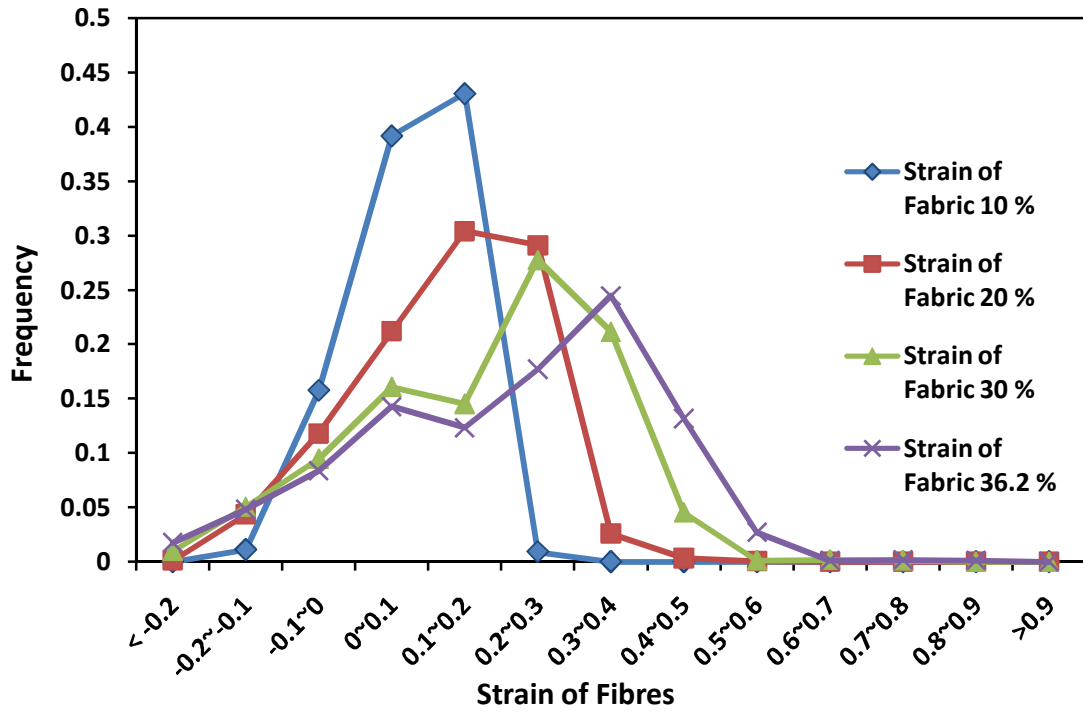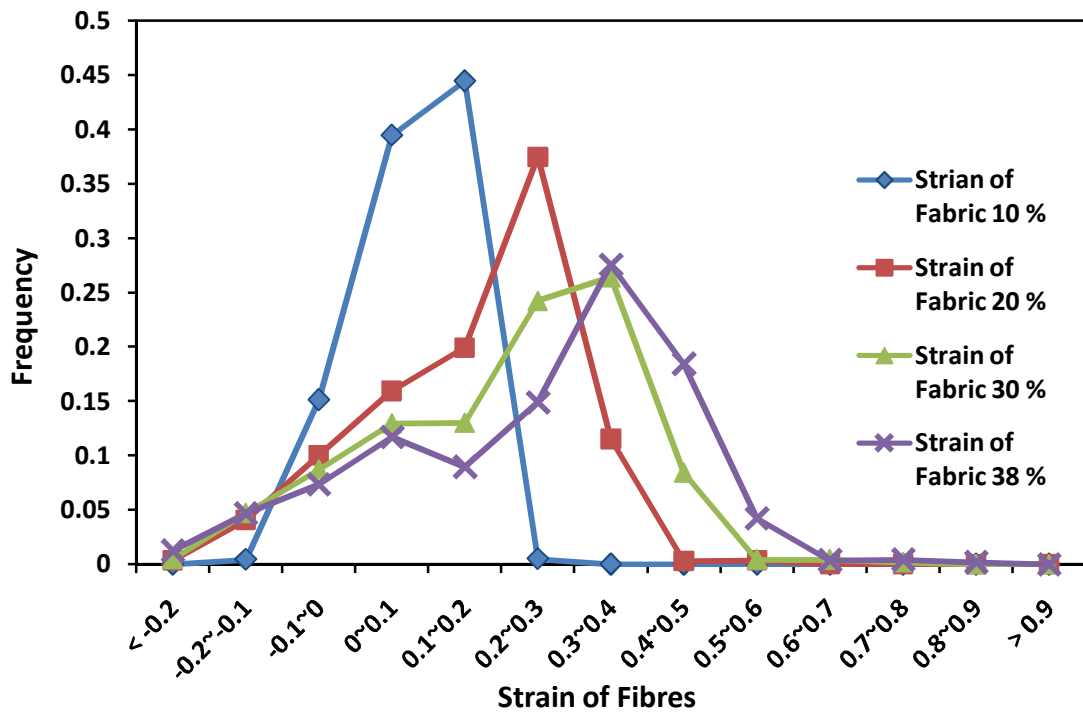Figure 6.14: Distribution of strain of fibres for models: Distribution of strain of fibres for models: (a) OD1/Staggered CD; (b) OD2/ Staggered CD; (c) OD3/ Staggered CD ; (d) OD1/Lined CD; (e) OD2/ Lined CD; (f) OD3/ Lined CD

Strain of Fabric (%)	OD1/Staggered CD		Strain of Fabric (%)	OD2/Staggered CD		Strain of Fabric (%)	OD3/Staggered CD	
	Average Strain of Fibres (%)	Standard Deviation (%)		Average Strain of Fibres (%)	Standard Deviation (%)		Average Strain of Fibres (%)	Standard Deviation (%)
10	7.0	8.5	10	8.7	9.0	10	9.7	9.4
20	13.4	15.7	20	16.5	16.4	20	18.3	17.0
30	19.4	21.8	30	23.6	23.1	30	26	23.3
40	24.9	28.0	40	30	29.2	40	33.1	28.7
50	29.9	33.2	50	36	34.0	50	39.6	33.4
60	34.5	37.7	60	41.5	38.3	60	45.5	37.8

(a)

Strain of Fabric (%)	OD1/Lined CD		Strain of Fabric (%)	OD2/ Lined CD		Strain of Fabric (%)	OD3/ Lined CD	
	Average Strain of Fibres (%)	Standard Deviation (%)		Average Strain of Fibres (%)	Standard Deviation (%)		Average Strain of Fibres (%)	Standard Deviation (%)
10	6.3	8.3	10	7.8	8.8	10	9.4	9.3
20	12.1	15.2	20	15.0	16.0	20	17.8	16.9
30	17.5	21.1	30	21.5	22.2	30	25.2	23.3
40	22.6	26.2	40	27.4	27.5	40	31.9	28.8
50	27.3	30.8	50	32.9	32.2	50	38.0	33.6
60	31.7	34.9	60	37.9	36.6	60	43.4	38.0

(b)

Table 6.3: Summarised results of average strain of fibres for models with staggered (a) and lined (b) CD arrangements of bond points
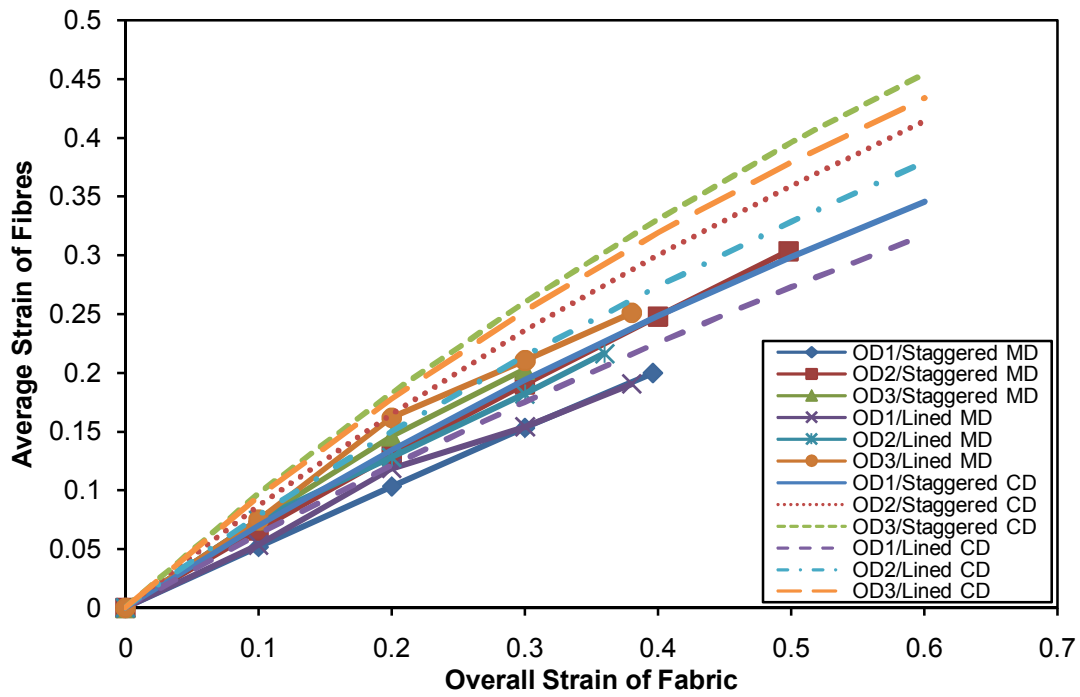
(a)
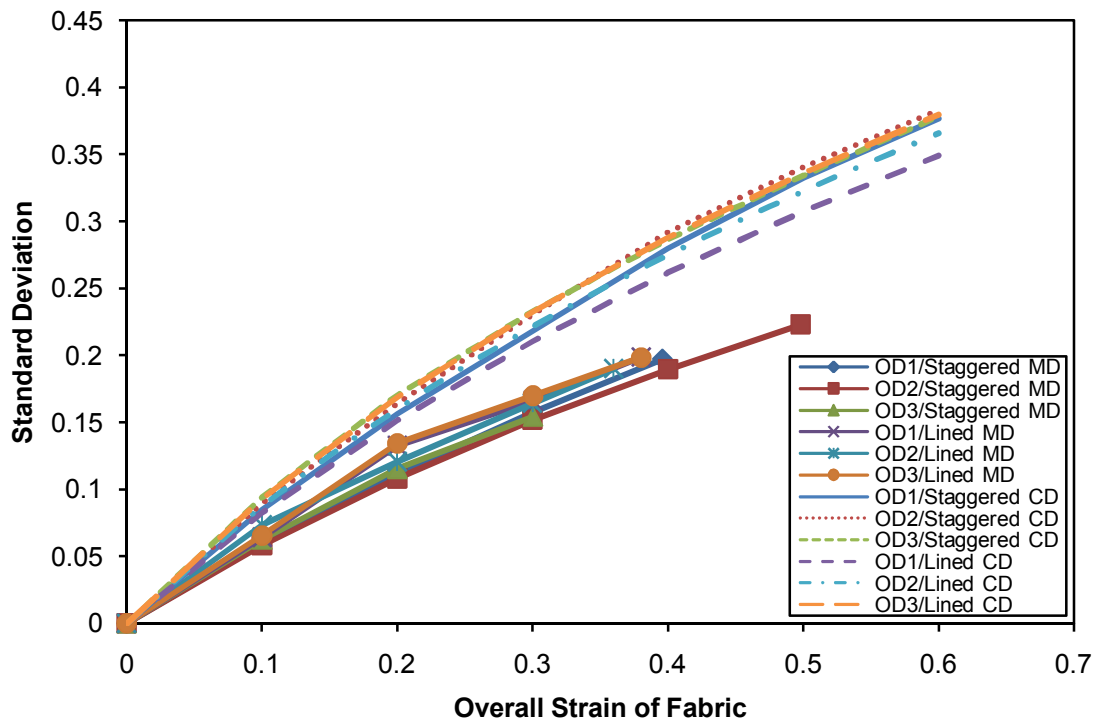
(b)

Figure 6.15: Summarised average strains (a) and their standard deviations of fibres of discontinuous models

Effects of ODF and arrangement of bond points

To analyze the effects of the arrangement of bond points and ODF on the overall mechanical performance of the fabric, models with the same orientation distribution and four different arrangements of bond points were compared with each other. Four models -OD1/Staggered MD, OD1/Staggered CD, OD1/Lined MD and OD1/Lined CD, which have the same fibre orientation distribution OD1-, demonstrated a similar material performance (Figure 6.16a). And similar phenomena were obtained for eight other models as shown in Figures 6.16b and 6.16c. The models with the same fibres' orientation distribution demonstrated a similar material behaviour, even when they had different arrangements of bond points. Although the differences were small, there was still a noticeable trend: the models with Staggered/Lined CD arrangements of bond points had a higher response force than the ones with Staggered/Lined MD arrangements, when the models have the same ODF. Let's note that all the different arrangements of bond points had the same proportions of bonded areas determined by the spacing between the bond points. It results in similar numbers of fibres connected to bond points and carrying the load. Therefore, the arrangement of bond points did not affect the mechanical response of the nonwoven material significantly during their initial stage. But this effect would become more significant when the fibres within the material achieve their plastic/breaking stage. As demonstrated in simulation results, the different arrangements of bond points resulted in different deformation mechanisms in the nonwoven material. And the different deformation mechanisms lead to different stress/strain distributions in the material. In the local areas of the material, the fibres, which are basic load carriers, have different mechanical behaviours depending on their length and orientation. Therefore, when the overall material achieves a higher strain level, the different levels of the overall mechanical response are obtained.
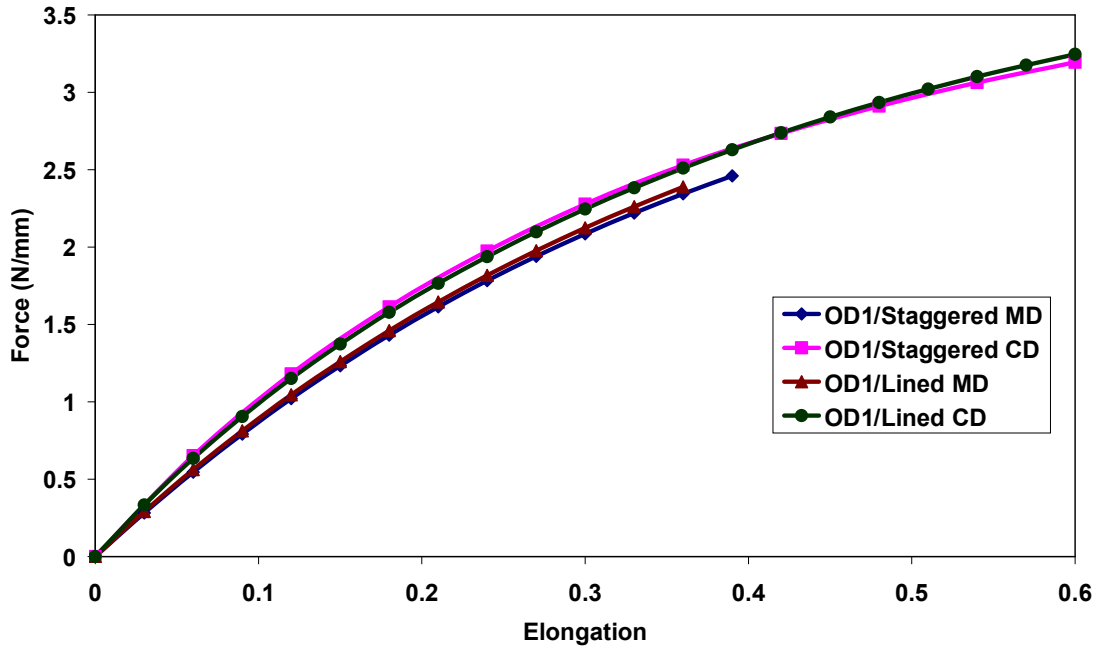
(a)
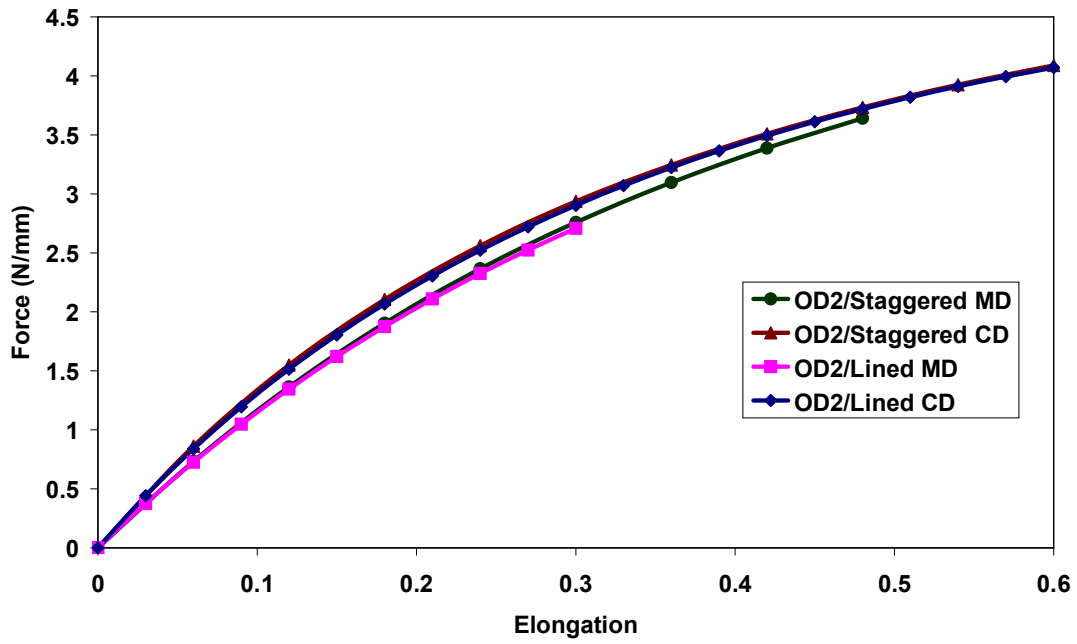
(b)
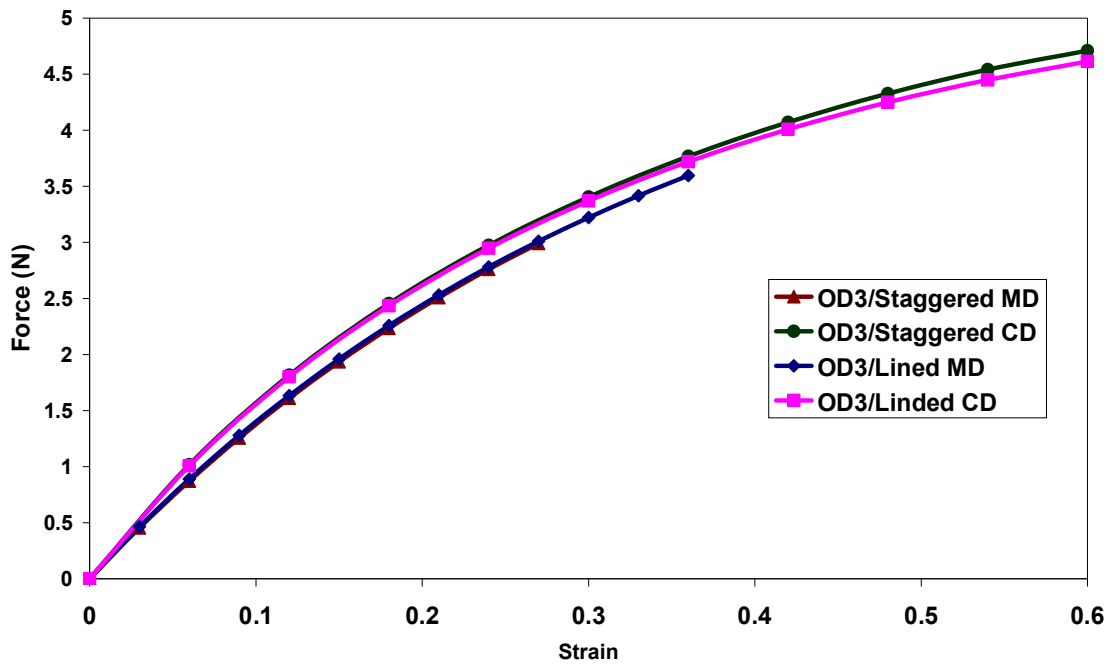
(c)

Figure 6.16: Results of FEA simulations for discontinuous models with various orientation distribution: (a) OD1; (b) OD2; (c) OD3

To investigate the effect of orientation distributions of fibres, the force-strain relationships of models with the same arrangement of bond points but different orientation distributions of fibres are shown in Figure 6.17. There are three different orientation distributions: OD1, OD2 and OD3 (see Figures 6.8). With geometric anisotropic ratios 0.86, 1.16 and 1.43, respectively. For the models with the same arrangement of bond points, the obtained reaction force (RF) increases evidently with the increase of the anisotropic ratio, caused by the change of orientation distribution form OD1 to OD3. A similar result was obtained for the models with the staggered CD arrangement of bond points. For the models with the lined arrangements of bond point - Lined MD and Lined CD - the trends were similar to those for the models with staggered bond points. The obtained results demonstrate that the fibres' orientation distribution has a significant effect on the overall mechanical properties of the material. With the increase in the ratio of anisotropy, which leads to more fibres being aligned along the loading direction, the reaction force of the overall structure increases and a better mechanical performance were obtained in that direction.
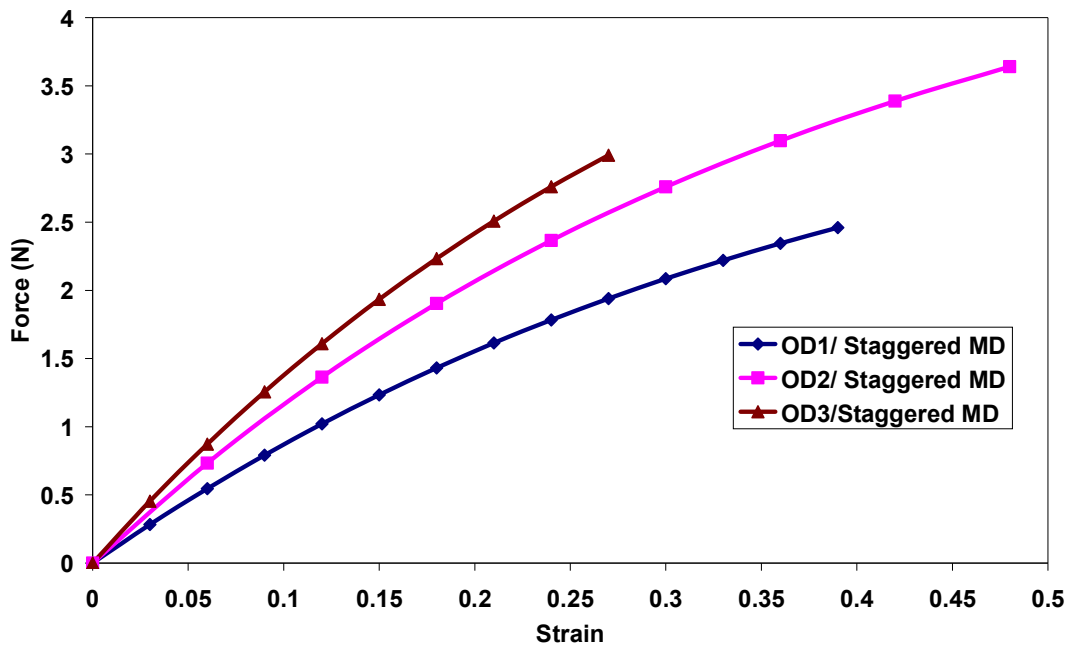
(a)
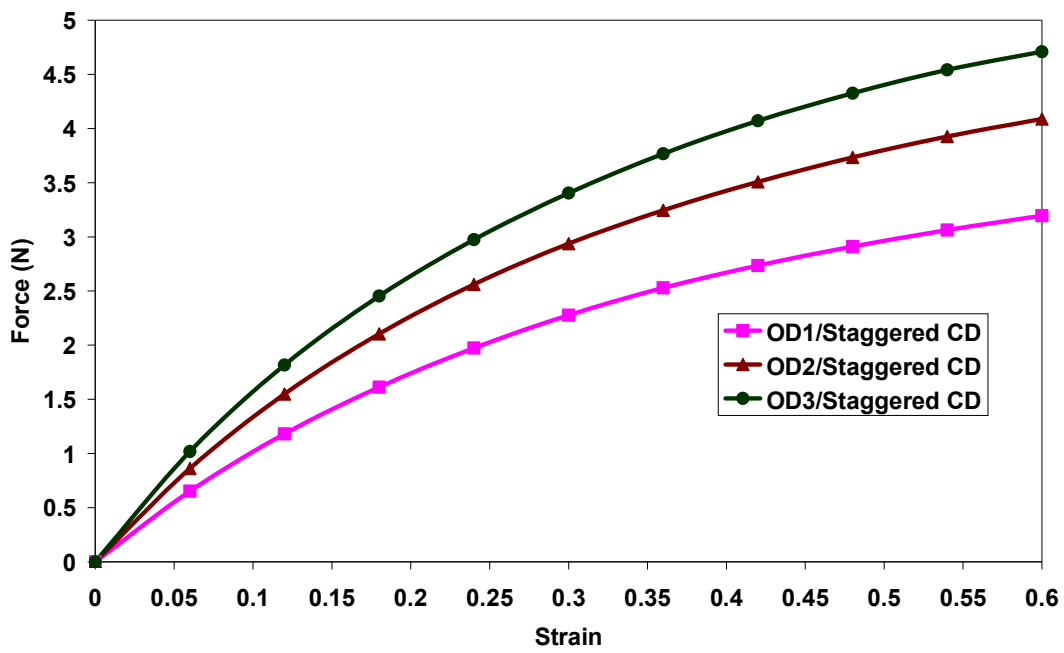
(b)
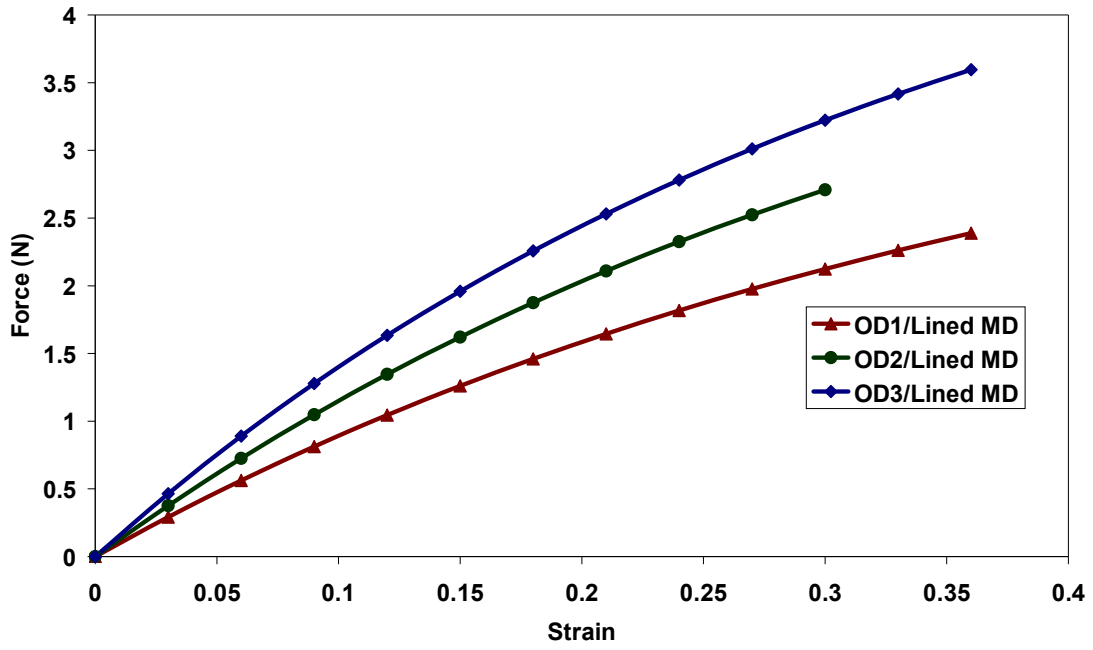
(c)
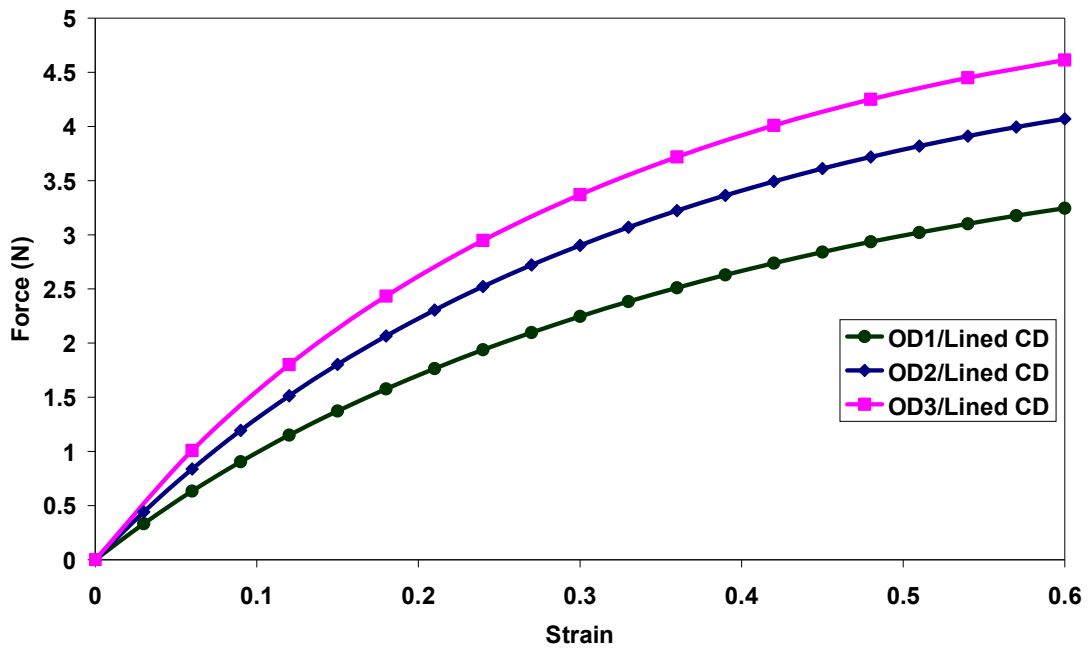
(d)

Figure 6.17: Results of FEA simulations for discontinuous models with same arrangement of bond points: (a) staggered MD arrangement; (b) staggered CD arrangement; (c) lined MD arrangement; (d) lined CD arrangement

172

6.4 Discussion and conclusions

In this chapter, numerical models for the discontinuous random fibrous network were developed according to the orientation distribution function of the low-density thermally bonded nonwoven material. Based on the geometry models, a finite element approach was developed to simulate mechanical properties of the nonwoven material by direct introduction of its discontinuous structure (density, discontinuity, nonuniformity, orientation distribution of fibres, properties of fibres). The material's effective modulus was calculated according to the measured material properties of polypropylene fibres, forming the nonwoven, and implemented into the discontinuous finite element model. Using the finite-element approach, twelve discontinuous models were developed to investigate the effects of the material's geometry features – the arrangement of bond points and random discontinuous fibrous network - on the overall performance of the material, and the obtained results were analysed with regard to the studied features. The detailed results follow:

1. The discontinuous structure of the low-density nonwoven material was generated numerically and used to develop the discontinuous FE models. The geometric nature of the discontinuous models provided advantages in the finite-element analysis compared to the continuous FE models presented in Chapter 5. Firstly, the discontinuous structure of the FE models has the capability to describe the nonuniformity of the low-density nonwoven material. And it also accounts for the effect of volume reduction, which occurs in real experiments but cannot be described in continuous FE models. Secondly, to determine the material properties for the finite-element analysis, the discontinuous models only require the material properties of fibres and bond points, which are easier to measure using physical experiments. Finally, it is possible to use the discontinuous FE models to simulate the anisotropic mechanical performance of the nonwoven material by changing the orientation distribution of fibres.

2. Twelve discontinuous FEA models with different orientation distributions and arrangements of bond points were analysed. The results revealed that the material's discontinuous structure did affect its mechanical properties. The

random fibrous structure resulted in the highly nonlinear material's behaviour even when the fibres had linear properties. It means that the nonlinearity of the nonwoven material was not only caused by the nonlinear material properties of fibres, but also was resulted from the discontinuous microstructure of the material. Besides, the material's random fibrous microstructure is also one of the reasons for the large strain in the material, is determined both by the elongation of the fibres and the reconstruction of the material's microstructure. And the effect of the type of fibres' orientation distribution was due to the changing proportion of fibres along, or close to, the loading direction, which determines the anisotropic material properties of the material and its nonuniformity. A larger fraction of such fibres leads to a higher mechanical overall response of the specimen in this direction. The result is important for design of a nonwoven material with a preferred loading direction. Moreover, the different arrangements of bond points led to different stress/strain relationships of the material, caused by different mechanisms of deformation of the fibrous network. The MD – lined and staggered -arrangement of bond points results in a more uniform strain distribution than the CD –lined and staggered- arrangement of bond point. That means that for the real specimens with CD arrangement of bond points, the fibres in the material have more risk to under a much higher strain level, which may lead to a local failure.

Chapter 7 Conclusions and Future Work

7.1 Conclusions and discussions

This thesis is focused on the deformation mechanisms of a low-density thermally bonded nonwoven material (polypropylene fibres; density 20 gsm) with account for the effects of material's microstructure. To analyse the mechanical properties of the material, various studies were carried out both experimentally and numerically. The experimental work was performed at both macro-scale and micro-scale. At macro-scale, the tensile tests were implemented under varying loading conditions and specimens of different shape and dimensions were tested, coupled with image analysis. At the micro-scale, features of the material's microstructure were determined and their effects on overall mechanical properties of the nonwoven material were established. Due to the complex microstructure of the nonwoven material, it is difficult to study its mechanical properties only by experimental methods. Therefore, two types of FE models were developed to describe the tensile behaviour of the material. The first type - continuous FE models - was used to validate capability of the classic theory to describe the low-density nonwoven material. And the effects of stiffer bond points on nonuniform stress distributions in the deformed material were analysed using such models. The second type - discontinuous models - was developed to provide information on the effect of the material's discontinuous and nonuniform microstructure on the mechanical properties of overall material, which is the first FE model of nonwovens involving the random fibrous network of the material. The effects of orientation distribution of fibres and the arrangement of bond points are summarised based on the results of simulations with finite-element models. The specific novelty and main findings include:

- Due to the various test standards available for nonwoven materials, tensile tests were carried out using specimens with varying dimensions and shape factors to analyse the effects of dimensions on mechanical properties of the nonwoven material in its machine and cross directions. And representative dimensions of the specimen were determined for the low-density thermally

bonded nonwoven material. The obtained results demonstrate that the specimen's dimensions do affect the mechanical properties of the nonwoven material significantly.

1) For the specimens with a relatively small width the material performs unstably and the obtained results show a large scatter.

2) For the specimens with larger lengths, generally, the material properties are improved and the material performs stably. But when the length of the specimen decreases to a certain level, the material start to behave unstably.

3) For the specimens with a shape factor smaller than 1, the length effect is not significant, but the effect of width plays a more important role. However, the moduli obtained for those specimens are initial moduli, which cannot fully describe the real material properties of the nonwoven material. Therefore, according to the analysis of the size-dependent mechanical properties of the nonwoven material, representative dimensions of specimen, which were used in the thesis, were determined as 25 mm for the gauge length and 20 mm for the width.

- Standard tensile tests were perfomed to investigate the deformation mechanisms of the nonwoven material in both machine and cross directions. Additionally, Thermoelastic Stress Analysis (TSA) system was used to record the process. The results show that the material properties of the material are highly anisotropic, which is caused by both the fibres' orientation distribution and arrangement of bond points. Especially, the material has apparently different material properties in its two principle directions: MD and CD. The material can achieve really high strain levels, more than 100%. Besides, according to the results obtained with the TAS system, the deformation mechanism of the material is affected by the arrangement of bond points and the nonuniform microstructure of the material. For the machine direction, the specimen presents clearly a "striped system", which is formed by strips of bonding points with intermediate strips of the fibre network. At the initial stage of the deformation, the striped system behaves stably and linearly. When the specimen achieves an advanced strain level, the strips of bond starts to

176

distort; it is caused by the nonuniform structure of the material. The stress concentrates at the areas with a low local density, and transfers from one low-density area to another, generating shear stress in the specimen. Finally, a micro-failure occurs staring from a low-density area, and the creak propagates though the specimen forming a macroscopic defect. For the cross direction, due to the arrangement of bond points, the initial stage of deformation is governed by stretching curly fibres in fibre-net strips along the loading direction and the initial deformation of fibres between two neighbouring bond points. With further extension, four neighbouring bond points form a diamond pattern. And the fibres connecting two neighbouring bond points along the cross direction mainly carry the load until they start to break, which forms holes inside the formed diamond patterns. At this stage, the diamond pattern begins to contract rapidly with the increase of strain. The boundaries of diamond shapes are rearranged to align along the loading direction by longitudinal tensile stretching and lateral contraction. Finally, an initial breaking point is usually found on a boundary of a bonding point, which develops in rupture.

- Continuous FE models were developed to simulate the tensile behaviours of the nonwoven material by treating the fabric as a two-component material. The models can generally reflect the different deformation mechanisms in both machine and cross directions, caused by the different arrangement of bond points. However, due to the differences between the results of simulation and experiments, the models prove that the nonuniform microstructure of material plays a very important role in the mechanical performance of the material, which cannot be ignored in both experimental and numerical analysis.

- To investigate the effects of the material's nonuniform microstructure, various image analysis methods were used to study the nonwoven. From the images obtained with CT scanning, the nonwoven was determined as a three-component material, which is composed by bond points, the fibrous network and void areas. The nonuniform microstructure was determined to be the main effective factor, which causes nonuniform strain distributions in the material. Moreover, due to the findings, the traditional stress calculation method cannot

be used to analyses this nonwoven material. The void areas are compressed during the extension and cause a reduction of the overall volume of the material; this contradicts to the theory of the traditional stress calculation method. To avoid the effects of the void areas on the stress calculation method, a novel method was suggested. After determining the principle effects of the microstructure of the material, the fibres' orientation distribution and material properties of fibres were measured, which are fundamental features for developing discontinuous finite element models.

- According to the experimental results and analysis of the continuous models, discontinuous finite-element models were developed to simulate the mechanical properties of the nonwoven material. The models emphasised the effects of nonuniform and discontinuous microstructure of the material by treating the material as a three-component none, consisting of bond points, fibrous network and void areas. To generate the discontinuous structure for the discontinuous models, a program was developed using the Python programming language to describe the random fibrous assembly with capability of introducing different fibre orientation distributions, fibre densities and diameters of fibres. Based on the simulation of the random fibrous network, the discontinuous FE models were developed to analyse effects of the material's microstructure on the overall material properties of the nonwoven material. To introduce the real material properties of single fires, a calculation method was suggested for the relationship between the numbers of representative fibres and real ones. In total, three different fibres' orientation distributions and four different arrangements of bond points were introduced into the discontinuous FE models to investigate the effects of the microstructure on the overall mechanical properties and deformation mechanisms. The obtained results demonstrate:

1) The random fibrous structure resulted in the highly nonlinear material's behaviour even when the fibres had linear properties. That means that the nonlinearity of the nonwoven material was not only caused by the nonlinear material properties of fibres, but also resulted from its discontinuous microstructure. Moreover, the random microstructure also

178

leads to a large deformation of the overall material. Therefore, it determines that the elongation of the material is linked to both the elongation of fibres and the reconstruction of the microstructure of the material.

2) The different arrangements of bond points lead to different deformation mechanisms. At macro-scale, the MD arrangements of bond points usually bring on a "strip system", with the stress transfer from a strip of bond points to a strip of the fibrous network. But for the specimens with CD bond points, "diamond pattern" plays an important role in the deformation. The fibres within the diamond patterns, which are along or close to the loading direction, tend to have higher stresses and have a higher risk of failure. However, the fibres along the boundaries of diamond patterns have a similar stress level and they become the basic load carrier after the breaking of the fibres inside the diamond patterns. At micro-scale, the strain/stress distributions of the fibres are apparently different due to the different arrangements of bond points. The MD arrangements of bond points cause more uniform strain distributions than the CD arrangements. Therefore, the fibres within the specimens with CD bond points have a higher risk to experience extremely high strains, which normally results in local failure and leads to final rupture.

3) The fibres' orientation distribution is one of the most important effective factors for the anisotropic material properties of the nonwoven material. More fibres aligned along or close to the loading direction cause a higher overall mechanical performance of the specimen in this direction.

7.1.1 Summary of deformation mechanism of low-density thermally bonded nonwoven material

According to the presented results of experimental and numerical works, the effective factors of deformation mechanisms of the low-density thermally bonded nonwoven material are determined as follows:

The mechanical behaviours of the nonwoven material are determined by both its microstructual features and the loading conditions. During the manufacturing process, the bonding information, the global orientation distribution function of fibres, the global fibre density, the principle directions and the properties of fibres are determined (Figure 7.1). However, due to the size- and shape- dependent mechanical properties of the nonwoven material, when it is cut from a big sheet into smaller specimens with different shapes for specific applications, the features of local microstructure of the specimens may be different from the ones of the global material (except for the bonding information and properties of fibres, which are the same). Moreover, the mechanical performance of the nonwoven material is also dependent of the loading conditions, which is due to the rate-dependent mechanical properties of the fibres. Therefore, it is possible to summarise that the deformation mechanisms of the low-density nonwoven specimen are rather complex and determined by its fibre density, material properties of fibres, orientation distribution of fibres, information of bond points as well as the principle direction of the overall material and loading conditions.

In detail the effects of the material's microstructure on mechanical properties of the low-density nonwoven materials are summarised as following:

- The nonwoven material is made by bonding fibres. The material properties of fibres affect the deformation mechanism of nonwoven material significantly. Fibres with better mechanical properties result in higher mechanical properties of nonwoven specimens. And it is reasonable to deduce that more fibres within the nonwoven material lead to its better mechanical performance, which means that a higher fibre density results in a stronger nonwoven material. However, the fibres in the nonwoven material are arranged randomly, having orientations with regard to the principle directions. The random structure causes geometrical nonlinearity for the material, and the orientation distribution of fibres becomes important to the mechanical performance of the material in certain loading directions. More fibres, aligned along or close to the loading direction, result in a better overall mechanical performance of the material. Moreover, since the density of fibres also determines the discontinuity of the microstructure of the material, a discontinuous

microstructure results in a different mechanical properties of the material if compared with a continuous material.

- Bond points of thermally bonded nonwoven material are another basic component of the material; they are formed by partially melted and compressed fibres and connect the fibres of the materials. The bond points are much stiffer than the fibrous network. In a thermally bonded nonwoven material without bond points, the fibres would only be hold together by friction between fibres. Therefore, the ratio of bonded areas to the material's overall area affects the mechanical properties of the nonwoven material. Higher percentage of bond points results in higher stiffness of the material due to the higher stiffness of bond points. And more bond points mean that most of fibres are connected to the bond points, contributing to the overall stiffness. Moreover, as presented in Chapter 6, the different arrangements of bond points cause different deformation mechanism. At micro-scale, the phenomena demonstrate as different strain distribution of fibres.
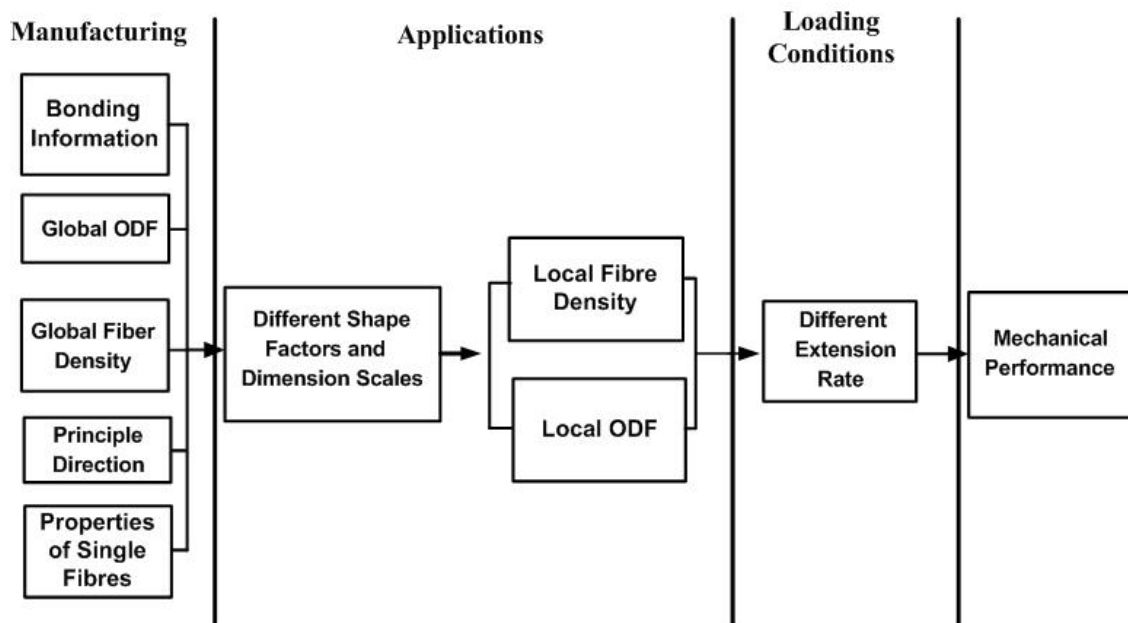
Figure 7.1: Summary of deformation mechanisms of low-density thermally bonded nonwoven material

7.2 Future work

Based on the works in this thesis, the research on mechanical properties of low-density thermally bonded nonwoven material can be further enhanced and extended by the following:

1. Further to the single-fibre tests presented in Chapter 5, single fibres of polypropylene taken from the fabrics should be studied using tensile tester with a high-precision loading cell at various loading. Two types of fibres will be used in the experiments: unbonded fibres and bonded fibres. A rate-dependent tensile modulus and nonlinear behaviour of fibres will be determined for both types of fibres. Besides, the failure criterion of both unbounded and bonded fibres should be determined.

2. Pull-out tests will be performed to pull a fibre out of the fibrous network and bond points, to determine the friction and strength of bonds between fibres. The results could be introduced into the develped discontinuous models presented in Chapter 6.

3. At micro-scale, FEA models could be developed to define the characteristics of the constituent fibres within the nonwoven webs. Both the bonded and unbounded fibres should be simulated. The FEA models should use rate-dependent material models to describe the tensile behaviours of the fibres. Then the models could be introduced into the developed discontinuous FE models as a sub-model to account for the effect of rate-dependant material properties of fibres.

4. The FEA model at meso-scale can be developed to calculate the effective properties of the bond area of thermally bonded nonwoven, which are hard to measure experimentally. The bond points will be investigated with a FE model based on the arrangement and mechanical properties of bonded fibres. The FE model for bonded fibres will be embedded into these models to describe the bonded fibres within the bond points. The geometry features of the FEA model can be obtained from the results of Micro-CT and SEM

studies for the bond points. The tensile behaviour of the bond area will be simulated for the thermally bonded nonwovens. The effective properties of the bond points will be calculated according to the stress/strain curves obtained with the FEA model. Then the calculated effective properties of the bond points could be introduced into present discontinuous FE models.

References

ABAQUS, 2001. Getting Started with ABAQUS/Standard. USA: Hibbitt, Karlsson & Sorensen, Inc.

ADANUR, S. AND LIAO, T., 1999. Fiber Arrangement Characteristics and Their Effects on Nonwoven Tensile Behavior. *Textile Research Journal,* **69**(11), 816-824.

ADANUR, S. and LIAO, T.Y., 1998. Computer Simulation of Mechanical Properties of Nonwoven Geotextiles in Soil-Fabric Interaction. *Textile Research Journal,* **68**(3), 155-162.

ALBRECHT, W., FUCHS, H. and WALTER, K., W., eds, 2003. *Nonwoven Fabrics.* 1st edn. Weinheim, German: WILEY-VCH Verlag Gmbh & Co.

ANDERASSEN, E., MYHRE, O.J., HINRICHSEN, E.L., BRAATHEN, M.D. and HINRICHSEN, E.L., 1995. Relationships Between the Properties of Fibers and Thermally Bonded Nonwoven Fabrics Made of Polypropylene. *Journal of Applied Polymer Science,* **58**(10), 1633-1645.

BACKER, S. AND PETTERSON, D. R., 1960. Some Principles of Nonwoven Fabrics. *Textile Research Journal,* **30**(9), 704-711.

BAIS-SINGH, S. AND GOSWAMI, B.C., 1998. Predicting the Biaxial Tensile Deformation Behavior of Spunbonded Nonwovens. *Textile Research Journal,* **68**(3), 219-227.

BAIS-SINGH, S. AND GOSWAMI, B.C., 1995. Theoretical Determination of the Mechanical Response of Spun-bonded Nonwovens. *Journal of the Textile Institute,* **86**(2), 271-288.

BAIS-SINGH, S., BIGGERS, S.B.JR. AND GOSWAMI, B.C., 1998. Finite Element Modeling of the Nonuniform Deformation of Spun-Bonded Nonwovens. *Textile Research Journal,* **68**(5), 327-342.

BAIS-SINGH, S., ANANDJIWALA, R.D. and GOSWAMI, B.C., 1996. Characterizing Lateral Contraction Behavior of Spunboned Nonwovens During Uniaxial Tensile Deformation. *Textile Research Journal,* **66**(3), 131-140.

BATRA, S., THOMPSON, M., VAUGHN, E. and WADSWORTH, L., eds, 2002. *INDA Nonwovens Glossary.* 1st edn. Raleigh, NC, US: INDA.

BATRA, S.K., 1998. Basics of Nonwoven Fabrics & Technology. 1st edn. Raleigh NC: NCRC.

BATRA, S.K. AND DAVIS, H., 1999. Fiberweb and Nonwoven Production. 1st edn. Raleigh: NCRC Copy Center.

BEIL, N.B. AND ROBERTS, W.W., 2002a. Modeling and Computer Simulation of the Compressional Behavior of Fiber Assemblies Part I: Comparison to van Wyk's Theory. *Textile Research Journal,* **72**(4), 341-351.

BEIL, N.B. AND ROBERTS, W.W., 2002b. Modeling and Computer Simulation of the Compressional Behavior of Fiber Assmblies Part II: Hysteresis, Crimp, and Oirentation Effect. *Textile Research Journal,* **72**(5), 375-382.

BHAT, G.S., JANGALA, P.K. and SPRUIELL, J.E., 2004. Thermal Bonding of Polypropylene Nonwovens: Effect of Bonding Variables on the Structure and Properties of the Fabric. *Journal of Applied Polymer Science,* **92**(6), 3593-3600.

BHAT, G.S. and MALKAN, S.R., 2002. Extruded Continuous Filament Nonwovens: Advance in Scienific Aspect. *Journal of Applied Polymer Science,* **83**(3), 572-585.

BÖHM, H.J., 2004. Modeling the Mechanical Behavior of Short Fibre Reinforced Composites. In: H.J. BÖHM, ed, *Mechanics of Microstructured Material.* First edn. Italy: SpringerWienNewYork, pp. 41-56.

BRITTON, P.N. and SAMPSON, A.J., 1984a. Computer Simulation of the Mechanical Properties of Nonwoven Fabrics Part II: Bond Breaking. *Textile Research Journal,* **54**(1), 1-5.

BRITTON, P.N. and SAMPSON, A.J., 1984b. Computer Simulation of the Mechanical Properties of Nonwoven Fabrics Part III: Fabric Failure. *Textile Research Journal,* **54**(7), 425-428.

BRITTON, P.N. and SAMPSON, A.J., 1983. Computer Simulation of the Mechanical Properties of Nonwoven Fabrics: Part I: The Method. *Textile Research Journal,* **53**(6), 363-368.

BRONKHORST, C.A., 2003. Modelling Paper as A Two-dimensional Elastic-plastic Stochastic Network. *International Journal of Solid Structures,* **40**(20), 5441-5454.

CHAMPION, E.R., 1992. Finite Element Analysis in Manufacturing Engineering: A PC-Based Approach. 1st edn. NY: McGraw-Hill Inc.

CHAND, S., BHAT, G.S., SPRUIELL, J.E. and MALKAN, S., 2001. Structure and Properties of Polypropylene Fibers during Thermal Bonding. *Thermochimica Acta,* **367-68**, 155-160.

CHIDAMBARAM, A., DAVIS, H. and BATRA, S.K., 2000. Strength Loss in Thermally Bonded Polypropylene Fibers. *International Nonwovens Journal,* **9**(3), 27-35.

CLARKE, D.R., SURESH, S. and WARD FRS, I.M., eds, 1996. *An Introduction to Composite Material.* 2nd edn. Cambridge UK: Cambridge University Press.

COX, H.L., 1952. The Elasticity and Strength of Paper and Other Fibrous Material. *British Journal of Applied Physics,* **3**, 72-79.

DANIEL, I.M. AND ISHAI, O., 2006. Engineeing Mechanics of Composite Materials. Second edn. New York: Oxford University Press.

DAVIES, E.R., 2005. Machine Vision. 3rd edn. San Francisco, CA: Elsevier.

DEMIRCI, E., 2008. *Mechanical Properties of Thermally Bonded Bicomponent Fibre Nonwovens: Experimental Study and Micromechanics.* 07-100. Raleigh, US: NCRC.

DESAI, C.S. and KUNDU, T., 2000. Introductory Finite Element Method. 1st edn. Florida, USA: CRC Press LLC.

DHARMADHIKARY, R.K., DAVIS, H., GILMORE, T.F. and BATRA, S.K., 1999. Influence of Fibre Structure on Properties of Thermally Point Bonded Polypropylene Nonwovens. *Textile Research Journal,* **69**(10), 725-734.

DUNLOP, J.I., 1983. Letters to The Editor on the Compression Characteristics of Fibre Masses. *Journal of The Textile Institute,* **74**, 92-97.

EDANA, 09/06, 2008-last update, applications of nonwovens [Homepage of edana], [Online]. Available: http://www.edana.org/Content/Default.asp?PageID=37 [5/14, 2009].

ENGELMAYR JR, G.C. AND SACKS, M.S., 2006. A Structural Model for the Flexural Mechanics of Nonwoven Tissue Engineering Scaffolds. *Journal of Biomechanical Engineering,* **128**, 610-622.

FEDOROVA, N., VERENICH, S. and POURDEYHIMI, B., 2007. Strength Optimization of Thermally Bonded Spunbond Nonwovens. *Jouranl of Engineered Fibers and Fabrics,* **2**(1), 38-48.

GAUTIER,K.B., KOCHER,CH.W. AND DREAN, J., 2007. Anisotropic Mechanical Behavior of Nonwoven Geotextiles Stressed by Uniaxial Tension. *Textile Research Journal,* **77**(1), 20-28.

GHASSEMIEH, E., VERSTEEG, H.K. AND ACAR, M., 2001. Microstructural Analysis of Fiber Segments in Nonwoven Fabrics Using SEM and Image Processing. *International Nonwovens Journal,* **10**(2), 26-31.

GHASSEMIEH, E., ACAR, M. and VERSTEEG, H.K., 2002a. Microstructural Analysis of Non-Woven Fabric using Scanning Electron Microscopy and Image Processing. Part 2: Applicaiton to Hydroentangled Fabric. *Proceedings of the Institution of Mechanical Engineers, Part L: Journal of Materials: Design and Applications,* **216**(4), 211-218.

187

GHASSEMIEH, E., ACAR, M. and VERSTEEG, H.K., 2002b. Microstructural Analysis of Non-Woven Fabrics Using Scanning Electron Microscopy and Image Pocessing. Part 1: Development and Verification of the Method. *Proceedings of the Institution of Mechanical Engineers, Part L: Journal of Materials: Design and Applications,* **216**(3), 199-207.

GILMORE, T., DAVIS, H. and MI, Z., 1993. *Tomographic Approaches to Nonwovens Structure Definition.* S93-8. USA: National Textile Center.

GRINDSTAFF, T.H. AND HANSEN, S.M., 1986. Computer Model for Predicting Point-Bonded Nonwoven Fabric Strength, Part I. *Textile Research Journal,* **56**(6), 389-392.

GUSEV, A.A., 1997. Representative Volume Element Size for Elastic Composites: A Numercial Study. *Journal of the Mechanics and Physics of Solids,* **45**(9), 1449-1459.

HAOMING, R. and BHAT, G.S., 2003. Preparation and Properties of Cotton-Ester Nonwoves. *International Nonwovens Journal,* **12**(2), 53-57.

HEARLE, J.W.S. AND OZSANLAV, V., 1979. Studies of Adhesive-Bonded Non-Woven Fabrics Part III: The Determination of Fibre Orientation and Curl. *Journal of the Textile Institute,* **70**, 487-498.

HEARLE, J.W.S. AND STEVENSON, P.J., 1963. Nonwoven Fabric Studies Part III: The Anisotropy of Nonwoven Fabrics. *Textile Research Journal,* **33**(11), 877-888.

HINE, P.J., LUSTI, H.R. AND GUSEV, A.A., 2002. Numerical simulation of the effects of volume fraction, aspect ratio and fibre length distribution on the elastic and thermoelastic propertied of short fibre composites. *Composites Science and Technology,* **62**, 1445-1453.

HUEBNER, K.H., DEWHIRST, D.L., SMITH, D.E. and BYROM, T.G., 2001. The Finite Element Method for Engineers. 4th edn. New York, USA: John Wiley & Sons, Inc.

JACOB, K.I., MCDOWELL, D., TECH, G., ANEJA, A.P. AND CORPORATION, D., 2003. *Compressive Behavior of Fiber Assemblies.* F02-GT04. Atlanta: National Textile Center.

JEDDI, A.A., KIM, H.S. AND POURDEYHIMI, B., 2001. Measurement of fiber orientation in nonwovens: optical fourier transform. *International Nonwovens Journal,* **10**(3), 10-16.

KAMATH, M.G., DAHIYA, A. AND HEGDE, R.R., April 2004, 2004-last update, thermal bonding of nonwoven fabrics [Homepage of University of Tennessee], [Online]. Available: http://web.utk.edu/~mse/pages/Textiles/Thermal%20Bonding.htm [March/20, 2007].

KIM, H.S., 2004a. Orthotropic Theory for the Prediction of Mechanical Performance in Thermally Point-bonded Nonwoven. *Fiber and Polymers,* **5**(2), 139-144.

KIM, H.S., 2004b. Relationship between Fiber Orientation Distribution Function and Mechanical Anisotropy of Thermally Point-Bonded Nonwovens. *Fiber and Polymers,* **5**(3), 177-181.

KIM, H.S., POURDEYHIMI, B., ABHIRAMAN, A.S. and DESAI, P., 2002. Effect of Bonding Temperature on Load-Deformation Structural Changes in Point-Bonded Nonwoven Fabrics. *Textile Research Journal,* **72**(7), 645-653.

KIM, H.S. AND POURDEYHIMI, B., 2001a. Computational Modeling of Mechanical Performance in Thermally Point Bonded Nonwovens. *Journal of Textile and Appeal, Technology and Management,* **1**(4), 1-7.

KIM, H.S. AND POURDEYHIMI, B., 2001b. Computational Modeling of Mechanical Performance in Thermally Point Bonded Nonwovens. *Journal of Textile and Appeal, Technology and Management,* **1**(4), 1-7.

KIM, H.S. AND POURDEYHIMI, B., 2001c. The Role of Structure on Mechanical Properties of Nonwoven Fabrics. *International Nonwovens Journal,* **10**(2), 32-37.

KIM, H.S. AND POURDEYHIMI, B., 2000. Characterization of Structural Changes in Nonwoven Fabrics During Load-Deformation Experiments. *Journal of Textile and Appeal, Technology and Management,* **1**(1), 1-6.

KIM, H.S., POURDEYHIMI, B. AND ABHIRAMAN, A.S., 2001. Characterizing Structural Changes in Point-Bonded Nonwoven Fabrics During Load-Deformation Experiments. *Textile Research Journal,* **71**(2), 157-163.

KIM, H.S., POURDEYHIMI, B., DESAI, P. and ABHIRAMAN, A.S., 2001. Anisotropy in the Mechanical Properties of Thermally Spot-Bonded Nonwovens: Experimental Observations. *Textile Research Journal,* **71**(11), 965-976.

KOMORI, T. AND ITOH, M., 1994. A Modified Theory of Fiber Contact in General Fiber Assemblies. *Textile Research Journal,* **64**(9), 519-528.

KOMORI, T. AND MAKISHIMA, K., 1978. Numbers of Fiber-to-Fiber Contacts in General Fiber Assemblies. *Textile Research Journal,* **47**(1), 13-17.

KOMORI, T., ITOH, M. AND TAKAKU, A., 1992. A Model Analysis of the Compressibility of Fiber Assemblies. *Textile Research Journal,* **62**(10), 567-574.

KRČMA, R., 1962. Nonwoven Textiles. 1st edn. Manchester: SNTL.

KRUCINSKA, I., JALMUZNA, I. AND ZUREK, W., 2004. Modified Rheological Model for Analysis of Compression of Nonwoven Fabrics. *Textile Research Journal,* **74**(2), 127-133.

KWOK, W.K., CRANE, J.P. and GORRAFA, A., 1988. Polyester Staple for Thermally Bonded Nonwovens. *Nonwovens Industry,* **19**(6), 30-33.

LIAO, T.Y. and ADANUR, S., 1999a. Computerized Failure Analysis of Nonwoven Fabric Based on Fibre Failure Criterion. *Textile Research Journal,* **69**(7), 489-496.

LIAO, T.Y. and ADANUR, S., 1999b. Computerized Failure Analysis of Nonwoven Fabrics Based on Fiber Failure Criterion. *Textile Research Journal,* **69**(7), 489-496.

LIAO, T.Y. and ADANUR, S., 1997. Predicting the Mechanical Properties of Nonwoven Geotextiles with the Finite Element Method. *Textile Research Journal,* **67**(10), 753-760.

LIMEM, S. AND WARNER, S.B., 2005. Adhesive Point-Bonded Spunbond Fabrics. *Textile Research Journal,* **75**(1), 63-72.

MAO, N., RUSSELL, S.J. and POURDEYHIMI, B., 2007a. Characterisation, testing and modelling of nonwoven fabrics. In: S.J. RUSSELL, ed, *Handbook of Nonwovens.* 1st edn. Cambridge, UK: Woodhead Publishing Limites and CRC Press LLC, pp. 401-514.

MAO, N., RUSSELL, S. and POURDEYHIMI, B., 2007b. Characterisation, Testing and Modelling of Nonwoven Fabrics. In: N. MAO, S. RUSSELL and B. POURDEYHIMI, eds, *Handbook of Nonwovens.* 1st edn. Cambridage, UK: Woodhead Publishing, pp. 401-502.

MAO, N. and RUSSELL, S.J., 2003. Modelling of Permeability in Homogeneous Three-Dimension Nonwoven Fabrics. *Textile Research Journal,* **73**(11), 939-944.

MATSUO, T., 1968. *Study on the Mechanical Property of Fiber Assembies*, Tokyo Institute of Technology.

MICHIELSEN, S., POURDEYHIMI, B., AND DESAI, P., 2006. Review of Thermally Point-Bonded Nonwoven: Materials, Processes, and Properties. *Journal of Applied Polymer Science,* **99**, 2489-2496.

MISHAKOV, V. SLUTSKER, G. AND STALEVICH, A., 2006. Modeling the viscoelasticity of nonwoven material with consideration of the irreversible strain component. *Fiber Chemistry,* **38**(1), 50-54.

MUELLER, D.H. AND KOCHMANN, M., 2004. Numerial Modeling of Thermobonded Nonwovens. *International Nonwovens Journal,* **13**(1), 56-62.

OSTOJA-STARZEWSKI, M., 2002a. Lattice models in micromechanics. *Applied Mechanics Reviews,* **55**(1), 35-60.

OSTOJA-STARZEWSKI, M., 2002b. Microstructural Randomness Versus Representative Volume Element in Thermomechanics. *Journal of Applied Mechanics,* **69**, 25-35.

OSTOJA-STARZEWSKI, M. AND STAHL, D.C., 2000. Random Fiber Networks and Special Elastic Orthotropy Of Paper. *Journal of Elasticity,* **60**, 131-149.

PETTERSON, D.R. AND BACKER, S., 1963. Relationship between the Structural Geometry of a Fabric and its Physical Properties. *Textile Research Journal,* **33**(10), 809-816.

POURDEYHIMI, B. AND RAMANATHAN, R, 1996. Measuring Fibre Orientation in Nonwovens Part I: Simulation. *Textile Research Journal,* **66**(11), 713-722.

POURDEYHIMI, B., DENT, R. AND DAVIS, H., 1997. Measuring Fiber Orientation in Nonwovens Part III: Fourier Transform. *Textile Research Journal,* **67**(2), 143-151.

POURDEYHIMI, B., DENT, R., JERBI, A., TANAKA, S. and DESHPANDE, A., 1999. Measuring Fiber Orientation in Nonwovens Part V: Real Webs. *Textile Research Journal,* **69**(3), 185-192.

POURMOHAMMADI, A., 2007. Thermal Bonding. In: A. POURMOHAMMADI, ed, *Handbook of Nonwovens.* 1st edn. Cambridage, UK: Woodhead Publishing, pp. 298-328.

PURDY, A.T., 1983. Developments in Non-woven Fabrics. 1st edn. Manchester UK: Shirley Institute.

RAMASUBRAMANIAN, M. K. AND WANG, Y., 2007. A computational micromechanics constitutive model for the unloading behavior of paper. *International Journal of Solid Structures,* **44**, 7615-7632.

RAWAL, A., 2006. A Modified Micromechanical Model for the Prediction of Tensile Behavior of Nonwoven Structure. *Journal of Industrial Textiles,* **36**(2), 133-149.

RINALDI, A., KRAJCINOVIC, D., PERALTA, P. and LAI, Y.C., 2008. Lattice Models of Polycrystalline Microstructures: A Quantitative Approach. *Mechanics of Materials,* **40**(1-2), 17-36.

RUSSELL, S.J., ed, 2007. *Handbook of Nonwovens.* 1st edn. FL, USA: Woodhead Publishing Limited and CRC PRess LLC.

SHAFFER, B.W., 1964. Stress-Strain Relations of Reinforced Plastics Parallel and Normal to the Internal Filaments. *AIAA Journal,* **2**, 348.

SHAN, Z.H. and GOKHALE, A.M., 2002. Representative Volume Element for Non-uniform Micro-structure. *Computational Materials Science,* **24**(3), 361-379.

SHIMALLA, S.J. and WHITWELL, J.C., 1976. Thermomechanical Behavior of Nonwovens Part I: Responses to Changes in Processing and Post-Bonding Variable. *Textile Research Journal,* **46**(6), 405-417.

SUH, M.W., CHUN, H., BERGER, R.L. and BLOOMFIELD, P., 2010. Distribution of Fiber Intersections in Two-Dimensional Random Fiber Webs- A Basic Geometrical Probability Model. *Textile Research Journal,* **80**(4), 301-311.

TORQUATO, S., 2002. Random Heterogeneous Material. 1st edn. New York, USA: Spring-Verlag, Inc.

VAN WYK, C.M., 1946. Note on The Compressibility of Wool. *Journal of The Textile Institute,* **37**, T285-T292.

WANG, X.Q. and MICHIELSEN, S., 2002. Morphology Gradients in Thermally Point-Bonded Poly (ethylene Terephthalate) Nonwovens. *Textile Research Journal,* **72**(5), 394-398.

WARNER, S.B., 1989. Thermal Bonding of Polypropylene Fibres. *Textile Research Journal,* **59**(3), 151-159.

WILSON, A., 2007. Development of the Nonwovens Industry. In: S.J. RUSSELL, ed, *Handbook of Nonwovens.* 1st edn. Cambridge, UK: Woodhead Publishing Limited, pp. 1-15.

WOOD, E.J., 1990. Application Fourier and Associated Transforms to Pattern Characterization in Textiles. *Textile Research Journal,* **60**(4), 212-220.

XU, B. AND TING, Y., 1995. Measuring Structural Characteristics of Fiber Segments in Nonwoven Fabrics. *Textile Research Journal,* **65**(1), 41-48.

XU, B. and YU, L., 1997. Determining Fibre Oirentation Distribution in Nonwovens with Hough Transform Techniques. *Textile Research Journal,* **67**(8), 563-571.

Publication List

"Finite Element Analysis of Thermally Bonded Nonwoven Material" IACM-ECOOMAS 30 June- 4 July **2008** Congress, Venice, Italy

"Tensile Behaviour of Low Density Thermally Bonded Nonwoven Material": *Journal of Engineered Fibres and Fabrics*, Volume 4, Issue1-**2009**

"2D finite element analysis of thermally bonded nonwoven materials: Continuous and discontinuous models", *Computational Materials Science*. 46 **(2009)** 700-707.

"Finite Element Simulation of Thermally Bonded Nonwoven Materials: Development and Analysis of Discontinuous Model" IWCMM'19 1- 4 September **2009**, Constanta, Romania

"Finite Element Simulation of Low-Density Thermally Bonded Nonwoven Materials: Effects of Orientation Distribution Function and Arrangement of Bond Points" *Computational Materials Science* **in press**